THE UNIVERSITY
of EDINBURGH

THE ROLE OF THE *STRA6* GENE FAMILY IN VERTEBRATE DEVELOPMENT.

NIKI DANIELLE WYATT

PRESENTED FOR THE DEGREE OF DOCTOR OF PHILOSOPHY

THE UNIVERSITY OF EDINBURGH

2012

I HEREBY DECLARE THAT THIS THESIS IS ENTIRELY MY OWN COMPOSITION. THE EXPERIMENTAL WORK DESCRIBED HAS BEEN EXCLUSIVELY PERFORMED BY MYSELF UNLESS OTHERWISE STATED IN THE TEXT. I ALSO DECLARE THAT THE CONTENTS OF THIS THESIS HAVE NOT BEEN SUBMITTED FOR ANY OTHER DEGREE OR PROFESSIONAL QUALIFICATION.

NIKI DANIELLE WYATT

Acknowledgements

I would like to thank my supervisors Professor Robert Hill, Doctor Julia Dorin and Professor David FitzPatrick for all their help, support and suggestions throughout my PhD without you all of this would not have been possible. I would like to thank Paul Devennay and all the staff at the TF for their help in the creation and maintenance of the mouse models described. Thank you to Philippe Gautier for all your help with the bioinformatic analysis of *Stra6.2*. Thank you to Doctor Natalie Reynolds for, not only, showing me the ways of the fish and providing useful suggestions and advice, but also for keeping me sane during the PhD process! Anna Thornburn; you are my PCR hero, the best person to share a cup of tea and a cheese scone with and could keep me laughing for hours with stories of 'the zoo'- Thank you! Thanks to Doctor Laura Lettice and Doctor You Ying Chau for making the office a lovely place to be and getting me through the hard days with a smile! Thanks you to all of C3 and my fellow PhD students who have been there for a laugh, a cry and a beer. I would like to thank my Grandad Frank and Granny Anna; I'm sad that you won't be here to see me finish this journey, but you gave me the love and support I needed to believe in myself. Thank you to my mum, who has given me everything she could to make it possible and telling me to always 'do your best because that is all you can ever do'. Lastly, I would like to thank my husband Stephan for being there at the end of the day to listen to my worries, share in my triumphs and tirelessly support me always.

Abstract

Matthew-Wood syndrome is a rare human birth defect condition defined by the phenotypic constellation of clinical anophthalmia, diaphragmatic hernia, pulmonary hypoplasia and cardiac defects. Matthew-Wood syndrome has a high mortality rate, with most patients dying due to respiratory insufficiency as a consequence of pulmonary hypoplasia, within the first year of life. Mutations within *STRA6* are causative for Matthew-Wood syndrome. STRA6 acts as a retinol transporter for retinol bound to its physiological carrier RBP4 allowing regulated entry of retinol into the cell. A mammalian model for Matthew-Wood syndrome was not found within the literature; however a morpholino knockdown of *stra6* in the zebrafish did show phenotypic features consistent with those observed in human patients. The desire to create a mammalian model of Matthew-Wood syndrome drove the work contained within this thesis.

Stra6-/- mice do not represent a model for Matthew-Wood syndrome with homozygous animals being viable, found in the expected ratio and demonstrating none of the developmental abnormalities observed in human patients. Retinal defects, cataracts and persistent hyperplastic primary vitereous affect the microphthalmic eye of *Stra6-/-* offspring of *Stra6-/-* mothers fed a retinoid-free diet from plug to birth indicating that *Stra6* is required for normal eye development under low-retinoid stress.

The disparity in phenotype between human Matthew-Wood patients and *Stra6-/-* mice may be the result of functional redundancy in the mouse between *Stra6* and its paralogue, *Stra6.2*. *Stra6.2* is well conserved through evolution and is found in diverse species, including the basal eumetazoan *Trichoplax*. *STRA6.2* has become split across its resident chromosome with an associated break in gene synteny, in humans and great apes, causing most of the gene to no longer be transcribed. However a small portion of the gene, representing the final transmembrane domain and the C-terminal intracellular tail of the protein, remains expressed in human.

stra6.2 is required for normal development in the zebrafish with *stra6.2* morphants being phenotypically distinguishable from control injected embryos from the 10-

somite stage by a larger head-tail distance indicating an axial extension defect. *stra6.2* morphants also display microphthalmia, jaw malformation, shortened and curved body axis and retinal lamination defects. *stra6.2* was found to be required to prevent an excess of retinoic acid resulting in an upregulation of retinoic acid-dependent gene expression through an increase in RA synthesis by *Raldh* enzymes in morphants. *Stra6.2-/-* mice are viable and fertile and phenotypically normal, even under retinoid-stress, supporting the notion of functional redundancy. In compound knockouts, normal development and postnatal survival can be maintained by a single copy of *Stra6* in *Stra6+/-;Stra6.2-/-* animals. *Stra6.2* is less able to support normal development and survival with ~50% of *Stra6-/-;Stra6.2+/-* animals dying before weaning or showing reduced growth although the remaining animals are indistinguishable from their littermates. *Stra6* and *Stra6.2* are functionally redundant for development under normal dietary conditions in the mouse and a single copy of either is able to support development in at least 50% of animals.

Stra6-/-;Stra6.2-/- mice were therefore hypothesised to be the logical mouse model of Matthew-Wood syndrome, however these mice die early in gestation between E7.5-E9.5. The early embryonic lethality in *Stra6-/-;Stra6.2-/-* mouse embryos compared to postnatal survival in human Matthew-Wood patients, to which they are the comparable genetic model, could be attributed to the shortened *STRA6.2* remaining within the human genome. The equivalent portion of *Stra6* has validated signalling motifs, which may still be active in STRA6.2, allowing development to proceed in human '*STRA6-/-*' embryos.

Table of contents

Chapter Three: *Stra6* knockout mice as a model for Matthew-Wood syndrome

List of Tables

List of Figures

Abbreviations

9c-RA	9-cis retinoic acid
ADH	alcohol dehydrogenases
BCMO1	beta-carotene mono-oxygenase 1
BCMO2	beta-carotene mono-oxygenase 2
BMP	bone morphogenic protein
CDH	congenital diaphragmatic hernia
cDNA	complementary DNA
CNS	central nervous system
CRBP	cellular retinol binding protein
CYP26	cytochrome P450-family 26
DEAB	diethylaminobenzaldehyde
ERG	electroretinogram
ES, ESC	embryonic stem cell
EtOH	ethanol
FACS	florescent activated cell sorting
FGF	fibroblast growth factor
GCL	ganglion cell layer
GFAP	Glial fibrillary acidic protein
GFP	green fluorescent protein
HPLC	high performance liquid chromatography
I.U.	International Units
ICM	inner cell mass
INL	inner nuclear layer
IPL	inner plexiform layer
JAK	Janus kinase
KO	knockout
KOMP	knockout mouse project
LOD	logarithm (base 10) of odds
LRAT	Lecithin-retinol acyltransferase
mRNA	messenger RNA
NCoA	nuclear co-activator protein
NCoR	nuclear co-repressor protein
NG	nasalacrimal groove
nls	neckless
ntl	no tail
OM	oropharyngeal membrane
ONL	outer nuclear layer
OPL	outer plexiform layer
OPT	optical projection tomography

OS	outer segment
PCR	polymerase chain reaction
PDAC	Pulmonary hypoplasia, Diaphragmatic hernia, Anophthalmia, Cardiac defects
PFA	paraformaldehyde
PHPV	persistent hyperplastic primary vitreous
PPARγ	peroxisome prolferator-activator receptor gamma
PRL	photoreptor layer
RA	retinoic acid
RAL	Retinaldehyde, retinal
RALDH	retinaldehyde dehydrogenase
RAR	retinoic acid receptors
RARE	retinoic acid response element
RBP	retinol binding protein
RDH	Retinol dehydrogenase
RE	Retinyl esters
REH	Retinyl ester hydrolase
ROH	retinol, vitamin-A alcohol
RPE	retinal pigmented epithelium
RPE65	retinal pigmented epithelium-specific 65kDa protein
RT-PCR	reverse transcriptase PCR
RXR	retinoid X receptor
SDR	short-chain dehydrogenases/reductases
SH2	src homology domain 2
shh	sonic hedgehog
SNP	single nucleotide polymorphism
SOCS	suppressor of cytokine signalling
STAT	signal transducer and activator of transcription
STRA	stimulated by retinoic acid
TR	thyroid receptor
VAD	vitamin-A deficiency
WISH	wholemount *in situ* hybridisation
WT	wild type
YFP	yellow fluorescent protein

Chapter One

Introduction

1.0 In the beginning.....

Vitamin A was formally discovered in 1914 by E.V. McCollum as a factor required for the normal growth of rats. His work, inspired by the work of E.B. Hart into the effects of feeding single cereal diets to heifers, noted that rats fed on purified diets of casein, lard, starch and salts would not grow unless these diets were supplemented with ether extracts of butter or egg yolk. These ether extracts he concluded must contain an 'organic complex without which the animals cannot make further increase in body weight' and that it was not a lack of fats responsible for this growth restriction as lard or olive oil were not able to promote growth in the same fashion (McCollum 1913). He later named the 'lipoid' or fat-like substance discovered as fat soluble A in order to distinguish it from the newly discovered vitamin or water soluble B. This discovery has led to the now wide and varied field of research into vitamin A-like molecules or retinoids.

1.1 Retinoids

1.1.1 Chemistry

Retinoids can be defined by three characteristic domains: a β-ionone ring, polyunsaturated chain and polar end group *(*Figure 1.1*)*, although some synthetic retinoids differ from this blueprint with changes made to the β-ionone ring or chain to create 'designer' retinoids for pharmaceutical purposes. The type of polar end group defines the 'natural' retinoids and can exist in several oxidation states from reduced (retinol) to oxidised (retinoic acid) *(*Figure 1.2*)*. Retinoids can also be found in two 'storage' forms which can be enzymatically converted (Figure 1.2). Retinoids are hydrophobic in nature and poorly soluble in water although some solubility is achieved due to self-aggregation into micelles. The double bonds of the chain region result in retinoids being highly labile and susceptible to photodegradation, oxidation and isomerisation. Due to their unstable nature, retinoids are *in vivo* generally protected within hydrophobic pockets of binding proteins (Noy 1999).

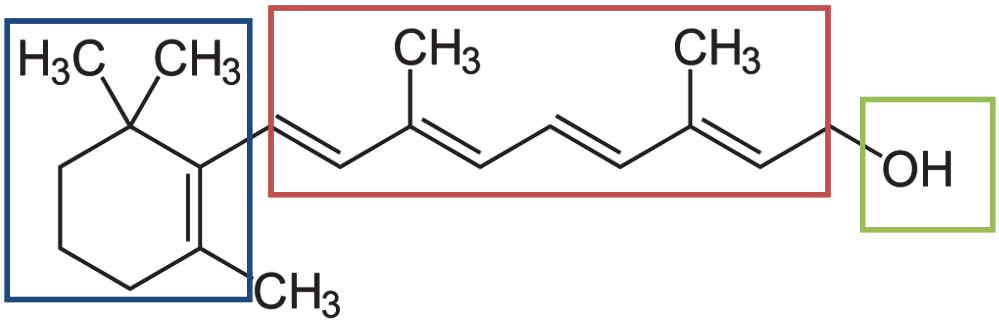

Figure 1.1 Characteristic retinoid domains

Retinoids contain three chemical domains; a β-ionone ring (blue box), a polyunsaturated chain (red box) and a polar end group (green box).

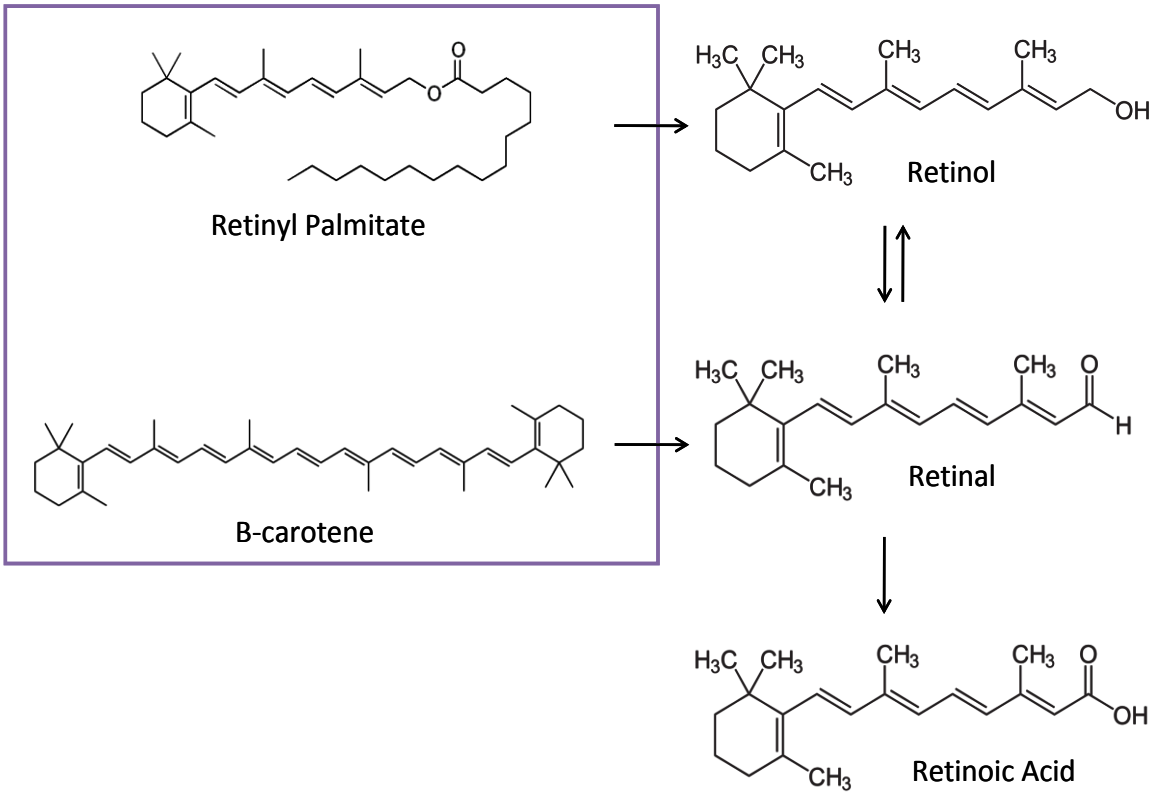

Figure 1.2 Retinoid structure

The chemical structure of the physiologically relevant retinoids is shown. Purple box indicates storage retinoids. Arrows indicate enzymatic conversions of retinoids.

1.1.2 Dietary procurement

Thomas Moore reported in 1930 that carotene fed to vitamin A deficient rats could be taken up by and then detected in the liver of these rats (Moore 1930). This shed light on the observations made by H. Steenbock 10 years earlier that, although most lipid extracts able to maintain growth in rats were generally yellow in colour, colourless ether extracts of liver were also active, providing a paradox to his hypothesis that vitamin A was a yellow pigment (Wolf 2001). Moore concluded that, although it was clear carotene and vitamin A were distinct molecules, carotene was a precursor for vitamin A (Moore 1930).

Retinoids are generally acquired from the diet as either retinyl esters or as provitamin A carotenoids from animal and plant sources respectively *(Fig 2)*. Carotenoids may be absorbed intact, although the extent to which this occurs is species dependent (Lee 1999), alternatively carotenoids can be cleaved to form retinol. Retinyl esters (RE), the main form of vitamin A of animal origin, are converted through the action of various retinyl ester hydrolases to retinol. Retinol within the intestine is taken in by the enterocyte and subject to esterification by lecithin:retinol acyltransferase (LRAT). Carotenoids can be taken up by mucosal cells and cleaved by beta-carotene mono-oxygenase 1 (BCMO1) or beta-carotene mono-oxygenase 2 (BCMO2) (Ambrosio 2011) to form one or two molecules of retinaldehyde respectively, which can then be converted to retinol. Retinol acquired from either carotenoids or retinyl esters is then esterified by LRAT and packaged in chylomicrons which travel in the lymph. These are taken up mainly by the hepatocytes where it can either be hydrolysed to retinol and bound to its specific transporter, retinol binding protein, or transferred to the hepatic stellate cells for storage mainly as retinyl esters (*Fig 3*) (Gottesman 2001; Harrison 2005).

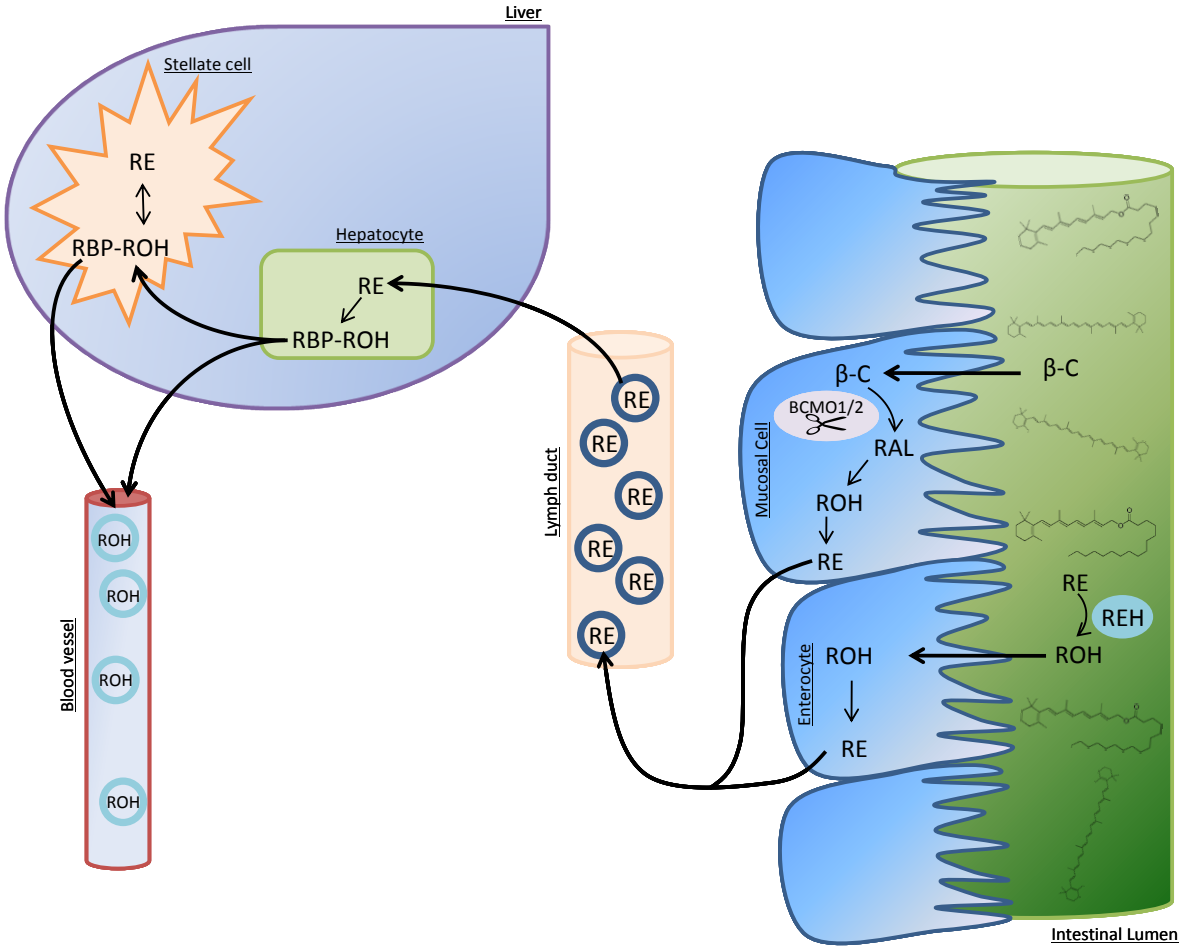

Figure 1.3 Retinoid dietary procurement

Animals procure retinoids from their diet and these must be absorbed, transported and stored to allow appropriate steady levels of retinoids in the body. Beta-carotene (β-C) is absorbed by mucosal cells of the intestine where it is cleaved to form retinal (RAL) which is converted to retinol (ROH) and then to retinyl esters (RE). Retinyl esters are converted into retinol in the intestinal lumen by retinyl ester hydrolase (REH) and then absorbed into the enterocytes where they are esterified back to retinyl esters. Retinyl esters formed from dietary procured retinoids are then packaged into chylomicrons (dark blue circles) and travel in the lymph. Heptocytes within the liver take up these chylomicrons and convert the retinyl esters to retinol which is bound to RBP (RBP-ROH). RBP-ROH (light blue circles) can then be

secreted into the blood for use or transported to stellate cells where it is stored as retinyl esters.

1.1.3 Cellular metabolism

Retinoids, defined as 20 carbon isoprenoids with a beta-ionylidene ring, conjugated double bonded side chain and a terminal functional group, differ in their chemical and biological properties. The metabolism of retinol can be considered as a pathway to the formation of retinoic acid, the most potent retinoid in terms of embryological teratology; however the retinoids have distinct biological roles in addition to their action as intermediates for retinoic acid production.

Retinol can either be esterified by LRAT for storage or oxidised to form retinaldehyde (Figure 1.4). Cytosolic medium-chain alcohol dehydrogenases (ADH) and membrane-bound short-chain dehydrogenase/reductases (SDR) are able to catalyse the oxidation of retinol to retinal. ADHs convert free retinol not bound to cellular retinol binding protein (CRBP-I) and ADH1, 3 & 4 have been shown to be catalytically active *in vitro*. SDRs in contrast only catalyse oxidation when retinol is bound by the chaperone CRBP-I and retinol dehydrogenases (RDH) 1, 5 & 11 have been highlighted as active in this process. SDRs are also able to convert retinal to retinol, specifically within the photoreceptors in order to recycle retinol to the RPE cells. The conversion of retinol to retinal is the rate limiting step in the formation of retinoic acid.

Retinal can function both as an intermediate for retinoic acid production and, in its 11-cis conformation, as a prosthetic group bound to opsins to form the visual pigments. 11-cis retinal is formed within the retinal pigmented epithelium and is transported to the photoreceptor cell. 11-cis retinal is covalently linked to an opsin, a G protein-coupled trasnmembrane receptor, to form the visual pigments. Light induces a photochemical reaction, in which 11-cis retinal is isomerised to all-trans retinal, causing a conformational change in the opsin. The 11-cis retinal must then be replaced from the retinoid cycle and the all-trans retinal formed can be converted to retinol for recycling as described above (Figure 1.5).

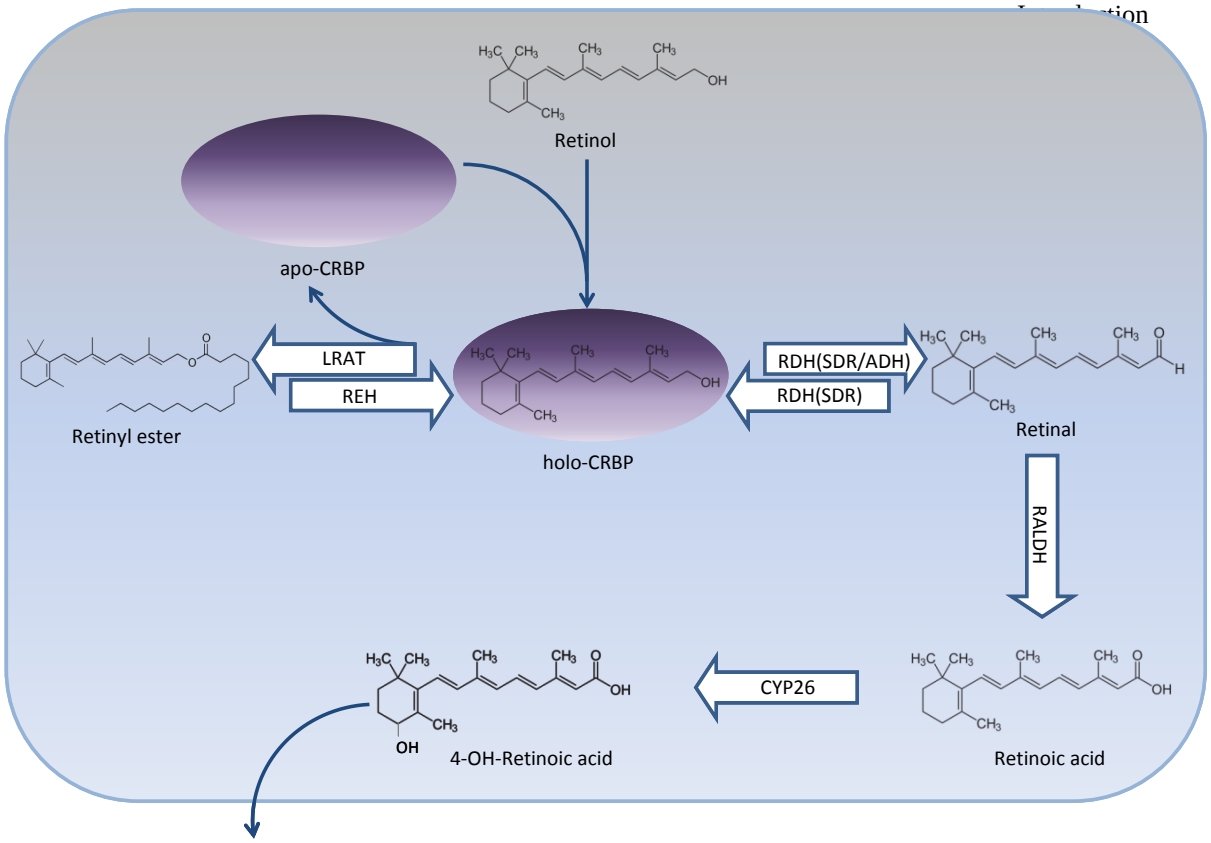

Figure 1.4 Intracellular retinol metabolism

Retinol is bound to cellular retinol binding protein (CRBP) intracellularly and this CRBP-ROH can then either be a substrate for either lecithin:retinol actyletransferase (LRAT) or retinol dehydrogenase (RDH). LRAT converts retinol to retinyl esters for storage and these retinyl esters can then be converted to retinol by retinyl ester hydrolase (REH) when required. CRBP-ROH can also act as a substrate for RDH enzymes and is converted to retinal. Retinal can then become retinoic acid by RALDH. Retinal can also be recycled back to retinol by short chain dehydroganse/reductase (SDR) RDH enzymes. Retinoic acid (RA) is a ligand for RARs. Retinoic acid is metabolised to 4-OH retinoic acid by CYP26 (Cytochrome P450-family 26) enzymes and is then removed from the cell. Enzymatic steps are indicated by open blue arrows.

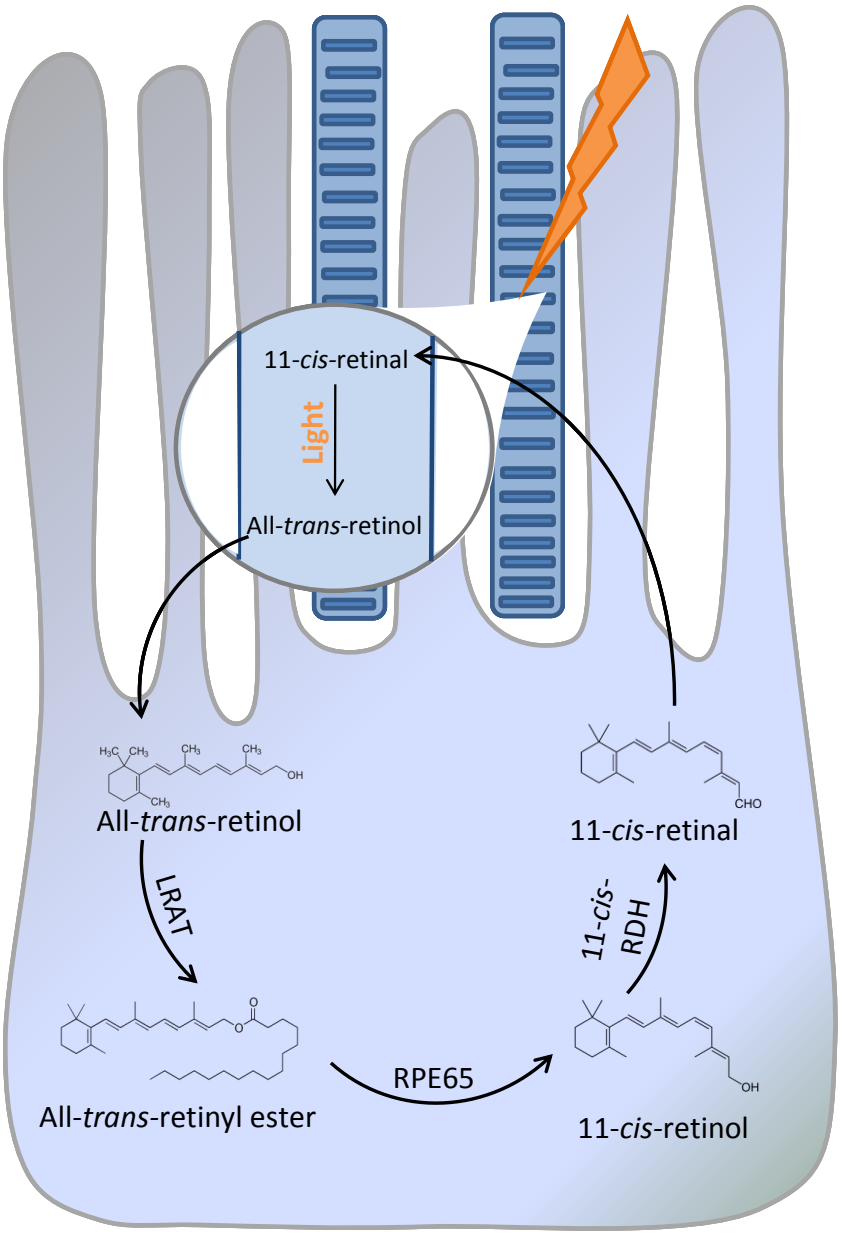
11-*cis*-retinal
Light
All-*trans*-retinol
All-*trans*-retinol
11-*cis*-retinal
LRAT
11-*cis*-
RDH
All-*trans*-retinyl ester
RPE65
11-*cis*-retinol

Figure 1.5 Retinoid visual cycle

Within the retinal pigmented epithelium (RPE) cell, all-trans retinyl esters are converted by RPE65 (Retinal pigment epithelium-specific 65 kDa protein) to 11-cis-retinol. 11-cis retinol is converted to 11-cis retinal by a specific 11-cis-retinol dehydroganse (RDH). 11-cis retinal is then transported to the photoreceptor and bound to opsins to form functional photoreceptor pigments. Upon exposure to light the 11-cis-retinal is converted to all-trans-retinal causing a conformational change in the opsin resulting in electrical impulses which are interpreted by the brain. The all-trans-retinal is recycled to the RPE where it is converted to all-trans-retinyl esters by lecithin: retinol acetyltransferase (LRAT) to form substrates for formation of new 11-cis-retinal.

Retinal is also an intermediate for the formation of retinoic acid (Figure 1.4). RALDH1, 2 & 3 are all known to function in the synthesis of retinoic acid from retinal in the embryo with developmental defects arising upon knockout of the corresponding genes. RALDH2 has the most widespread expression during development and is the main enzyme responsible for oxidation *in vivo*. RALDH1 and RALDH3 have more tissue specific functions inferred by the limited developmental perturbation upon gene knockout.

Retinoic acid has important functions in the control of gene expression and acts as a morphogen during development as will be discussed below. Catabolism of retinoic acid is of paramount importance to maintaining proper levels of retinoic acid (Figure 1.4). Retinoic acid can be catabolised by members of the cytochrome P450 family: CYP26A1, CYP26B1 and CYP26C1. Some evidence has been presented to suggest an independent role for the polar metabolites of retinoic acid; however it is unclear to what extent these are active *in vitro*.

The mechanism of action of retinoic acid was unknown until the identification of retinoic acid receptor alpha (RARα) in 1987 (Petkovich 1987). Retinoic acid receptor (RAR) α is a member of the steroid/thyroid hormone receptor family which activate transcription in a ligand dependent fashion through the binding of short DNA sequences (Giguere 1987). Identification of two additional RARs, β (Brand 1988) and γ (Krust 1989), and three retinoid-X receptors, RXRα, β and γ (Mangelsdorf 1992), were subsequently identified. These receptors function as heterodimers of an RAR and an RXR binding in *cis* to retinoic acid response elements (RAREs). RAREs are short DNA sequences consisting of direct repeats of consensus half sites, (a/g)g (g/t)tca, separated by two or five nucleotides and are commonly located upstream with no strand bias (Figure 1.6). RARs are regulated by RA through RAREs. RXRs in addition to binding to RARs are able to bind other nuclear receptors such as PPARγ (Iipenberg 1997) and TR (Yu 1991). The retinoid binding potential of RXRs is unclear and some evidence suggests that the RA isomer, 9-cis RA, acts as a ligand for the RXRs (Mangelsdorf 1992) although if this ligand binding is physiologically relevant *in vivo* is still unclear.

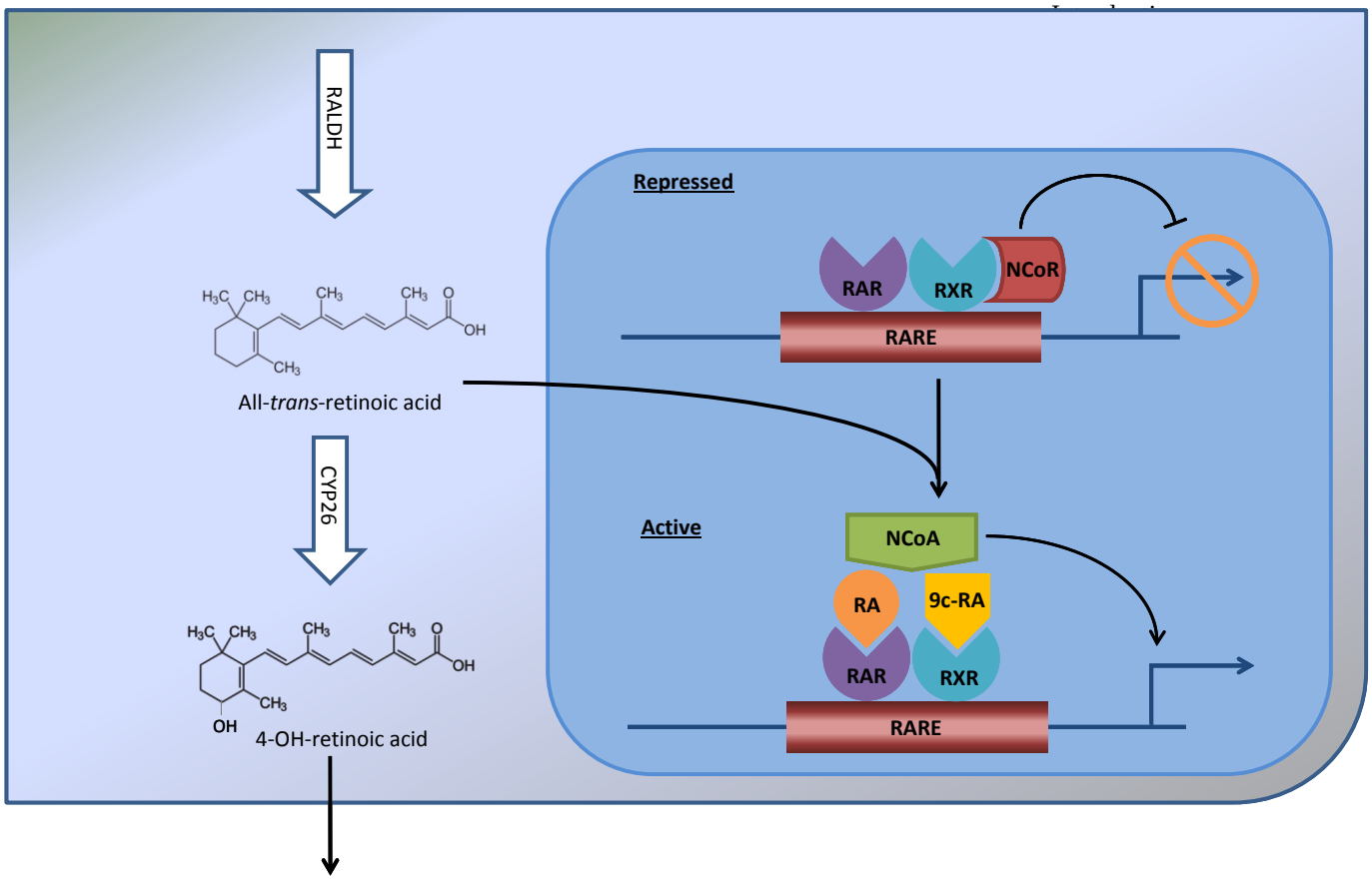

Figure 1.6 Transcriptional regulation by retinoic acid

Retinoic acid response elements (RARE) are found localised to promoters and enhancers of genes. These elements bind heterodimers of retinoic acid (RAR) and retinoid-X (RXR) receptors. In the absence of the retinoic acid (RA) ligand, these heterodimers allow the binding of nuclear receptor co-repressor protein (NCoR) which can act to recruit other repressive proteins in order to surpress gene expression in the absence of RA. In the presence of RA, RAR bind RA and this allows the binding of nuclear receptor co-activator protein (NCoA) resulting in gene activation and transcription. 9-cis-retinoic acid (9c-RA) is able to bind RXR but the significance of this for gene activation is unclear.

1.2 Vitamin A deficiency

1.2.1 In the adult

The symptoms of vitamin A deficiency have been described throughout history despite vitamin A only being discovered in 1914. Historical texts described common symptoms of vitamin A deficiency affecting the eye; night blindness and xerophthalmia. Night blindness was described by Hippocrates and is typified by normal bright-light vision but an inability to see in dim light. Hippocrates also prescribed an appropriate cure for this affliction in raw beef liver. Xerophthalmia is a drying of the cornea and conjunctiva which can result in corneal ulceration and was described by physicians of the nineteenth century. The corneal lesions that occur upon vitamin A deficiency in rats were described by Wason (Wason 1921), in which edema, infiltration of capillaries and immune cells into the cornea and thickening of the cornea were noted. Folk remedies for such conditions included liver, liver extracts and cod liver oil and these were shown to be effective in the work of C. E. Bloch on institutionalised children from Denmark. In which he cured, with cod liver oil, the symptoms of vitamin A deficiency due to a diet consisting only of fat-free milk, oatmeal and barley soup. His knowledge of the animal work of Mc Collum and others allowed him to identify and treat human disease. Vitamin A deficiency, although now rare in the developed world, is still a major public health concern in the developing world (Figure 1.7). Maternal mortality is increased (West 1999) and there is an increased risk of disease (Hussey 1990; Semba 1994) and death (Humphrey 1992) in those children who are vitamin A deficient or who are born to vitamin A deficient mothers.

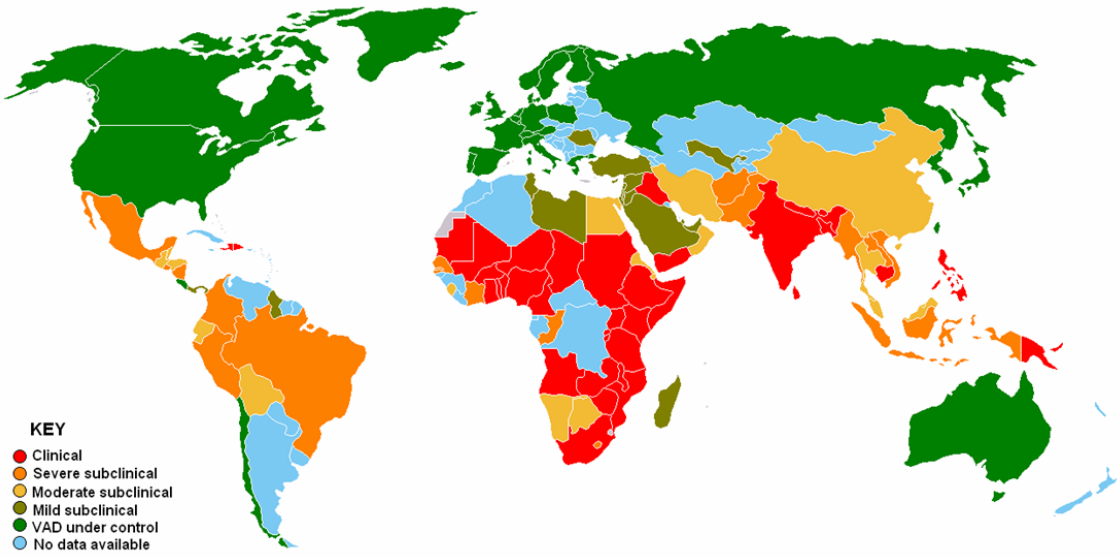

Figure 1.7 World map of vitamin-A deficiency

Vitamin A deficiency is uncommon in the developed world however VAD is observed in variable severity across many developing countries of the world.

1.2.2 During development

The effects of vitamin A deficiency on the foetus have been described in both rodents and farm animals since 1933. There is also some evidence to suggest that human development may also be effected by maternal vitamin A deficiency. A study by Hornby *et al* (Hornby 2000) highlighted the link between areas with high percentage of vitamin A deficiency and those with a great incidence of congenital eye malformation. The possible relationship between low serum retinol levels and developmental eye defects such as coloboma, anophthalmia and microphthalmia in South Indian populations was also investigated with 16% of mothers recalling night blindness, and were therefore likely vitamin A deficient, during pregnancy (Hornby 2002). Newborns with congenital diaphragmatic hernia (CDH) were also found to be more likely to have low serum retinol levels than control newborns, although no association was found to maternal serum retinol levels in this study (Beurskens 2010). Bilateral microphthalmia with ventricular asymmetry of the heart was observed in a child born to a mother who was deficient for vitamin A and also had a history of previous preterm births and a miscarriage since a gastric bypass operation (Smets 2006).

The vitamin A deficiency experiments were carried out first in pigs by Hale *et al*. Sows, who were fed a deficient diet during pregnancy, gave birth to offspring with micro- or anophthalmos, accessory ears, harelip, cleft palate, subcutaneous cysts and kidney misplacement (Hale 1935). Further work in vitamin A deficiency then moved into the more convenient model system of the rat and quail. Vitamin A deficiency during pregnancy in the rat resulted in 75% of the offspring exhibiting one or more defects of various organs. The eye was most sensitive to deficiency being most commonly affected organ and the only organ affected in some animals. Defects of the genito-urinary tract, diaphragm (diaphragmatic hernia), heart and lung were also observed. The defects observed could be rescued by dosing the females once with retinol, between day 10-13 for the eye and day 10 or 11 for other affected organs, except the heart which could not be fully rescued using this window of treatment (Wilson 1953).

Vitamin A deficiency (VAD) in the quail results in death of the embryo by day 4. The heart, although able to contract, is dilated and thin walled with no chambers. Treatment with RA at various stages has pinpointed a role for vitamin A in providing the proper environment for heart asymmetry specification by other genes. The early lethality seen in VAD quails is likely to be due to a lack of cardiac inflow tract to allow entrance of the vitelline veins to deliver blood to the embryonic heart possibly due to changes in the expression of GATA4. The central nervous system is also affected with vitamin A required for hindbrain specification and neural crest survival (Zile 2001).

1.3 Vitamin A (& retinoic acid) excess

1.3.1 In the adult

Hypervitaminosis A is caused by ingestion of either a single high dose, acute, or long term excessive intake, chronic, of vitamin A. Acute hypervitaminosis A occurs approximately 4 hours after ingestion of a toxic dose causing abdominal pain, nausea and vomiting with additional headache, dizziness, fatigue and irritability. Intracranial pressure is often raised and pain in the long bones is also experienced. Chronic hypervitaminosis A also resulted in the same symptoms as for acute toxity along with drying and thinning of the skin, anorexia, dry eyes, abnormal liver function and cirrhosis, disregulation of calcium balance and splenomegaly (Silverman 1987).

1.3.2 During development

Human pregnancies in which the mother has been undertaking isotretinoin treatment have a high risk of developmental abnormalities and spontaneous abortion. Isotretinoin is a synthetic retinoic acid analogue developed for pharmaceutical treatment for severe recalcitrant cystic acne. In a group of 154 pregnancies with exposure to isotretinoin resulted in 95 elective abortions and the remaining pregnancies resulted in 12 spontaneous abortions, 26 infants with no malformations and 21 infants with developmental malformations. These malformations generally affected the craniofacial region, cardiac system, thymus and CNS. Craniofacial abnormalities included small jaw, small or missing external ears and cleft palate. The retina and optic nerve were abnormal consistent with the eye's sensitivity to retinoid levels. The involvement of the cardiac, craniofacial and thymic structures possibly indicate a defect neural crest cells from the cephalic region which are known to be regulated by RA (Lammer 1985).

Maternal treatment of mice with a single vitamin A dose of 10,000 I.U. during pregnancy causes perturbations of the development of mouse embryos. Treatment early in pregnancy at ~E7 caused most embryos to be reabsorbed by the time of sacrifice at E17.5. Treatment between E8-12 caused the reabsorption of some embryos with almost all surviving offspring malformed and the ratio of surviving

offspring increasing the later in pregnancy the treatment was given. Treatment at any period during pregnancy caused defects in thymus position and in some cases an accessory thymus was noted. In embryos from E8 or E9 treatment group resulted in many cases in spina bifida, exencephaly, cardiac defects (transposition of the great vessels, ventricular septal defect and overriding aorta) and kidney defects-including horseshoe kidney. The eye was affected with exophthalmous frequently observed with no eyelids also associated with this defect which appears to be due to a reduction in orbit size. The external ear was often absent or reduced in size and becomes low set in relation to untreated animals. Treatment at E10-12 resulted in malformation of ~60% of the surviving offspring with cleft palate and small mandible common defects observed in this group. Limb defects were also observed in this group with micromelia and oligodactyly common. Skeletal analysis of these animals showed shortening or loss of a number of the limb long bones and malformations of the skull (Kalter 1961).

Defects observed in both mouse and human upon gestational exposure to excessive retinoid doses show a similar constellation of defects affecting the thymus, craniofacial region, eye, heart and the pinnea showing a conservation of the role of RA in the morphogenic processes of development across the mammals

1.4 Genes of the RA pathway

1.4.1 Retinol Binding Protein 4

Retinol binding protein 4 (RBP4) is the physiological carrier for retinol in the plasma with at least 90% of the plasma retinol associated with RBP4. RBP4 has a molecular weight of 21kDa and has a binding site for one retinol molecule (Figure 1.8 A). RBP4-retinol is associated with TTR which prevents the removal of RBP4-retinol by the kidney filtration system (Kanai 1968). *Rbp4*-/- mice are viable and fertile (Figure 1.8 B). The only phenotype in these animals is a non-developmental vision impairment of the retina in which a dark-adapted electroretinogram showed an increase in b-wave threshold level indicating a 100-fold decrease in light sensitivity. The visual impairment was resolved by 24 weeks on a retinoid sufficient diet (Quandro 1999). The eye has a requirement for retinol supplied by RBP but can accumulate retinol to support vision from the low circulating levels found in complex with LDL or albumin (Vogel 2002). The visual defect was accompanied by low levels of 11-cis retinal within the eye consistent with the visual impairment. The plasma retinol levels of *Rbp4*-/- mice was 12.5% that of wild type animals. *Rbp4*-/- animals are able to create hepatic stores of retinoids but they cannot mobilise these stores under conditions of low-retinoid dietary provision and in fact accumulate hepatic retinoids resulting in higher hepatic retinol concentrations in *Rbp4*-/- than wild type animals (Quandro 1999).

Rbp4-/- embryos do however have a developmental phenotype when dams are maintained on a retinoid-deficient diet from plug discovery (E0.5) till E14.5 when the embryos were analysed. *Rbp4*-/- embryos had small eyes compared to wildtype or *Rbp4*+/- embryos and showed signs of cardiac insufficiency in peripheral edema (Figure 1.8 C&D). Increasing the time on retinoid-deficient diet before pregnancy increased the severity of the phenotype from extreme reduction in eye size, abnormal midfacial region and limb defects from dams on retinoid-deficient diets for 5 weeks pre-plug to a complete lack of axial rotation in those embryos from those dams that had been maintained on a retinoid-deficient diet for three months (Figure 1.8 E-G)(Quandro 2005). Retinoid deficient diet also affects the testes of adult male *Rbp*-/- animals, although under normal dietary conditions the morphology of the testis is not

affected. When *Rbp*-/- males are maintained on a retinoid-deficient diet histological changes to the testis are observed after 5 weeks and increase in severity with further time under retinoid deficiency. Retinoid deficiency in a *Rbp*-/- males causes a spermatogonia differentiation arrest but does not affect the transition to meiotic spermatocytes and spermiogenesis. Spermatogonia differentiation is affected by VAD in *Rbp*-/- animals and spermatid adhesion to the sertoli cells resulting in the observed loss of germ cell layers in testis histological sections (Figure 1.8 H-I) (Ghyselinck 2006).

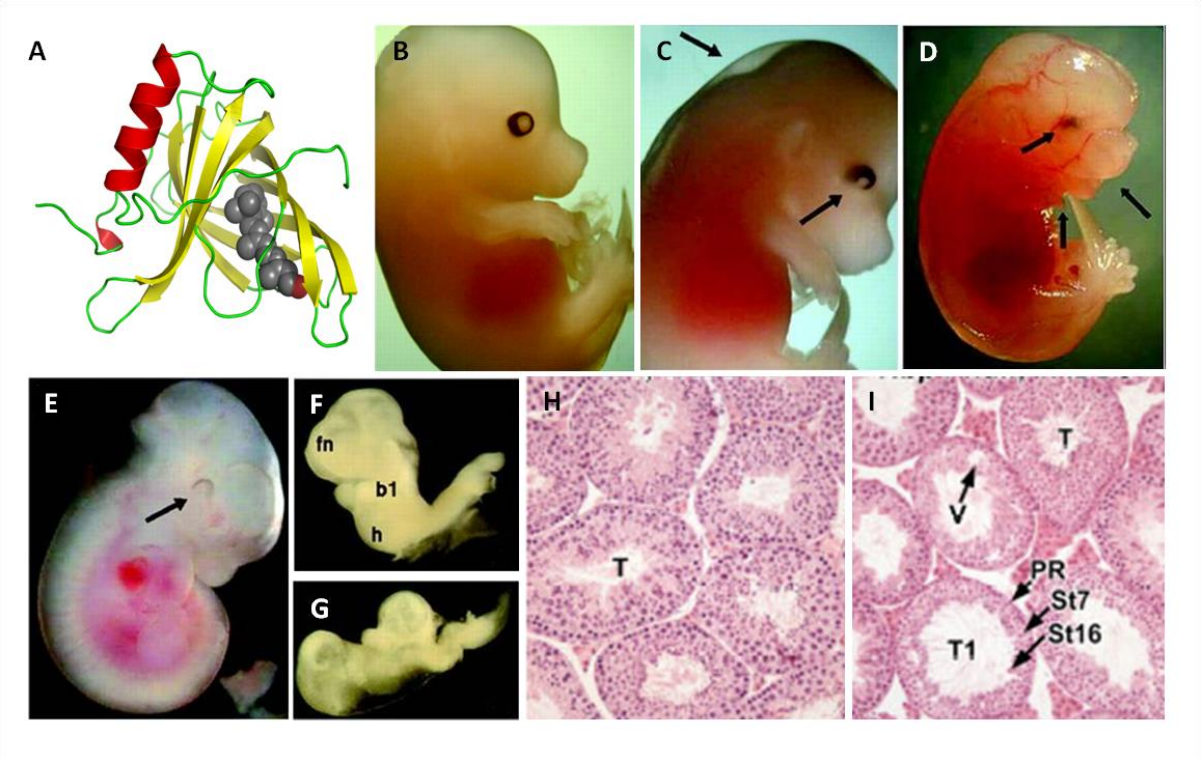

Figure 1.8 RBP4 is not essential for development or testis maintenance under normal dietary conditions.

The protein structure of RBP4 indicating the binding site for retinol within the protein (**A**). The hydrophobic pocket where retinol binds allows hydrophobic retinol to be transported within the blood. RBP4-/ animals are viable and fertile when dams are maintained on a retinoid-sufficient diet throughout pregnancy (**B**). RBP4-/- (**C**) embryos show reduction in eye size and peripheral edema (black arrows) when dams were maintained on a vitamin A deficient from plug till analysis at E14.5. RBP4+/- embryos are unaffected by this dietary regime (**D**). Increasing the time spent on vitamin A deficient diet before plug increases the severity of phenotype from extreme eye-size reduction, and midfacial and limb abnormalities (black arrows, **E**) to a complete lack of axial rotation (**F**&**G**). Embryos **B**-**E** at E14.5 and embryos **F**&**G** at E11.5. Testis of RBP4/- males maintained on a vitamin- A deficient diet degenerate (I) with a loss of germ cell layers as can be observed by the large empty spaces in the centre of the tubules ('T' in **H** compared to 'T1' in **I**) however wild type testes are unaffected (**H**). B-G adapted from Quandro, L.H. et al (2005) and H-I adapted from Ghyselinck, N.B. et al (2006).

1.4.2 Cellular Retinol Binding Protein

Many genes within the retinoid pathway form part of families with similar functions; this is true for the Cellular retinol binding proteins (CRBP) in which three members have been identified.

1.4.2.1 Cellular retinol binding protein 1

CRBP1 is expressed during development in both neural tissues; motor neurons and spinal cord, and organs; lung, liver and placenta. In the adult the expression is also found in the lung and liver additionally it is also observed in the RPE, kidney, brain and genital tract, all organs/tissues known to be sensitive to retinoids. *Crbp1*-/- animals are morphological normal and growth postnatal proceeded normally on a retinoid sufficient diet (Ghyselinck 1999). Developmental levels of retinol and retinyl esters were reduced significantly in *Crbp1*-/- but levels of RA were not significantly affected (Figure 1.9 A). Consistent with these observations pattern of RA responsive genes was unaffected (Matt 2005). *Crbp1*-/- animals maintained on a retinoid deficient diet became VAD within 5 months and upon this treatment retina morphology was disrupted with RPE and outer segment association looser than WT and the outer segments became distorted and myelinated (Figure 1.9 B&C) (Ghyselinck 1999). *Crbp1*-/- had a two-fold delay in dark adaptation of the retina (Figure 1.9 D) but rhodopsin regeneration during flash recovery, and therefore visual cycle function, were not significantly affected (Saari 2002).

1.4.2.2 Cellular retinol binding protein 2

Crbp2 is highly expressed in the adult small intestine, specifically higher in the absorptive cells compared to both the proliferating and goblet cells (Crow 1985), and transiently in the perinatal liver and lung. Developmental expression is detected in the decidua and trophoblastic cells and then later in the yolk sac indicating a possible role for maternal-fetal transfer of retinoids. Under normal maternal dietary conditions *Crbp2*-/- animals are viable and no defects were observed either perinatally or in the adult. Dams fed a marginal retinoid diet from E10 gave birth to *Crbp2*-/- pups that all

died within 24hrs of birth and this effect seemed partially due to maternal genotype as when *Crbp2*+/- pup mortality was compared between those with a +/+ dam (27%) and those with a -/- dam (79%) some of the mortality rate was diminished; WT pups from WT to WT matings on the same diet regime showed no mortality. Death of these heterozygous pups appeared to be due to heart defects, right-sided engorgement and enlargement, and lung defects, decreased airspaces and haemorrhage (Figure 1.9 E-H)(Xueping 2002).

1.4.2.3 Cellular retinol binding protein 3

Crbp3 was identified on the conditions of being expressed highly in heart and skeletal muscle; which take up retinol but have low expression levels of CRBP1 and 2. It is able to bind all retinol isomers: trans-, 9-cis- and 13-cis-, but not other retinoids or fatty acids (Vogel 2000). Despite the high expression levels of CRBP3 compared to CRBP1 and 2 in the heart and skeletal muscle, *Crbp3*-/- animals do not show any defects in the development or adult maintenance of these tissues. CRBP3 is, along with CRBP1, highly expressed within the mammary gland but the relative levels of these proteins differ during pregnancy and lacatation. CRBP1 is more highly expressed in the mammary tissue during pregnancy and CRBP3 during lactation; consistent with this observation *Crbp3*-/- animals produce milk with low levels of retinyl esters, specifically retinyl palmitate (Figure 1.9 I). CRBP3 appears to normally provide substrates to LRAT in the mammary gland allowing the formation of retinyl esters for incorporation into the milk. CRBP1 is also upregulated in CRBP3 mice in the tissues where the two proteins are co-expressed, such as the adipose, but not in tissues where they are not co-expressed, such as testis (Figure 1.9 J). The levels of CRBP1 also increase in the lactating *Crbp3*-/- animals but this is obviously not sufficient to rescue retinyl ester provision to the milk (Piantedosi 2005).

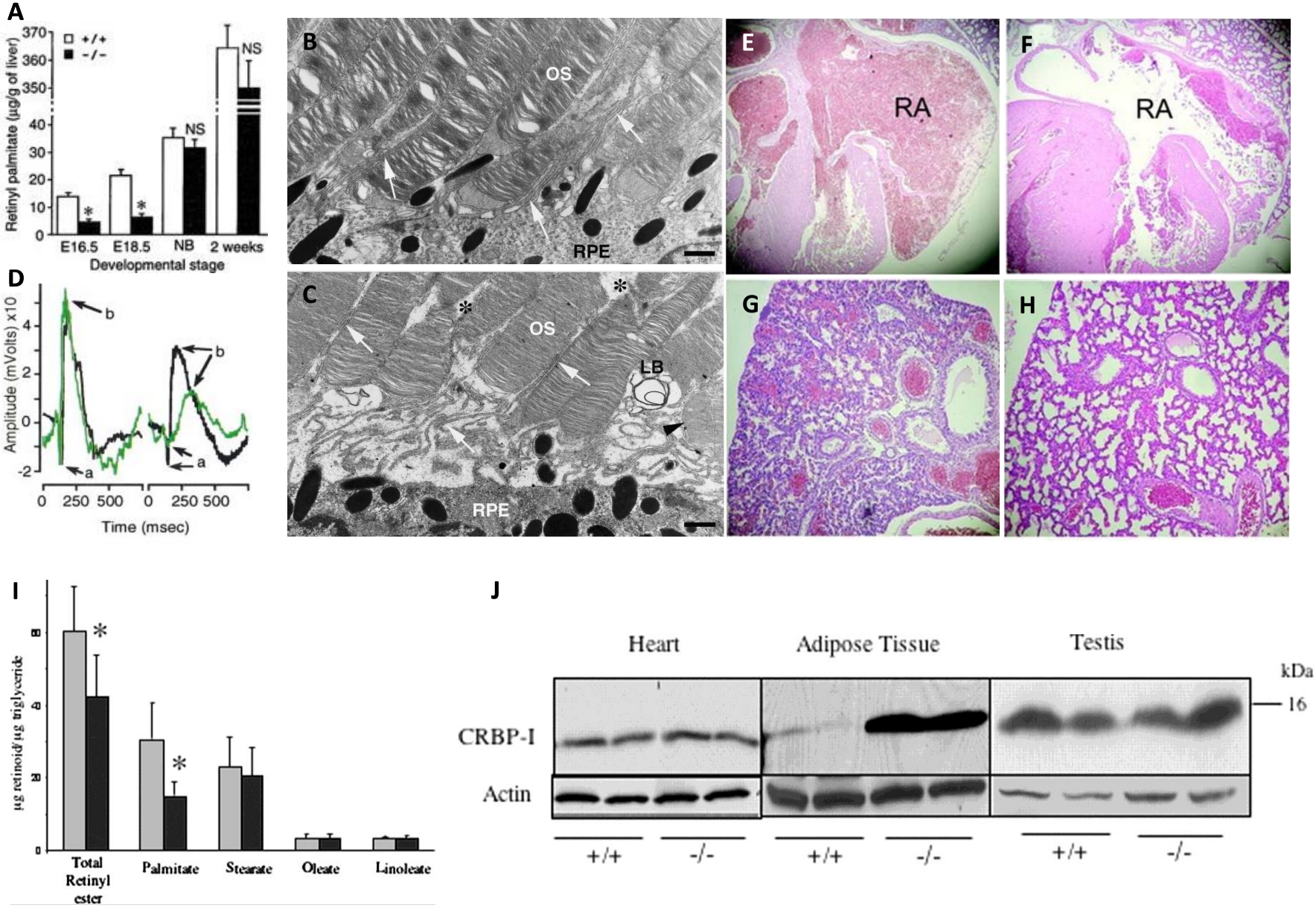
A
Retinyl palmitate (µg/g of liver)
+/+
-/-
NS
E16.5
E18.5
NB
2 weeks
Developmental stage
B
OS
RPE
C
OS
LB
RPE
D
Amplitude (mVolts) x10
Time (msec)
E
RA
F
RA
G
H
I
µg retinoid/µg triglyceride
Total Retinyl ester
Palmitate
Stearate
Oleate
Linoleate
J
Heart
Adipose Tissue
Testis
kDa
16
CRBP-I
Actin
+/+
-/-

Figure 1.9: Members of the CRBP family are required for normal vision and development under vitamin-A deificient conditions and to provide retinoids for lactation.

Crbp1-/- embryos have reduced levels of retinyl esters but during development (**A**). Crbp1-/- animals become VAD after 5 months and this affects retinal morphology however WT animals under a similar regime are unaffected (**B**). The outer segment (OS) and the retinal pigmented epithelium (RPE) in Crbp1-/- separate (bracket) and the RPE no longer intercalates amongst the OS (**C**). Microvilli are present within this space (arrows) and the OS is disrupted (arrowhead) and replaced by lamellar bodies (LB) in some areas. Dark adapted ERG function in Crbp1-/- animals (green line) is comparable to WT (black line) when fed vitamin-sufficient diet (**D**- left panel) but under vitamin-A deficiency Crbp1-/- animals show delayed dark adaption (**D**-right panel). Crbp2-/- animals die within 24 hours of birth when their dams are fed on a VAD diet from E10 till birth. Wildtype animals are unaffected by this dietary modification and have normal hearts (**E**) and lungs (**G**). Crbp2-/- animals appear to die due to heart defects (**F**) such as enlargement of the right atrium (RA) and a diminished number of air spaces within the lungs (**H**) compared to WT (**G**). Crbp3-/- lactating females have reduced retinyl ester levels in their milk with this reduction being made up mainly be a significant reduction in the level of retinyl palmitate (**I**). CRBP3 function is likely to be compensated by CRBP1 in Crbp3-/- animals as CRBP1 expression is increased in those tissues which they are co-expressed (adipose) but not in tissues where they are not (testis) (**J**). A-D adapted from Ghyselinck, N.B. et al (1999), E-H adapted from Xueping, E. et al (2002) and I-J adapted from Piantedosi, R. et al (2005).

1.4.3 Lecithin Retinol Acyltransferase (LRAT)

Lrat is widely expressed within the adult; with a high level of expression observed within the eye, adrenal gland, small intestine and testis. LRAT is located sub-cellularly in microsomes and appears to be a membrane protein with at least two hydrophobic domains. LRAT is able to catalyse the transfer of the *sn*-1 fatty acid of phosphatidylcholine to retinol bound to a cellular retinol binding protein thereby creating retinyl esters. Expression of LRAT is RA responsive being rapidly induced in response to RA treatment (Figure 1.10 A). In vitamin-A deficient animals, the levels of LRAT are undetectable (Figure 1.10 A). These observations therefore constitutes a regulatory loop in which, in excess RA conditions, further retinol supplies are channelled to storage and in retinol deficient conditions storage ceases with all available retinol allowed to enter the synthesis pathway (Zolfaghari 2000).

Lrat-/- mice develop normally, with females displaying normal fertility and all animals reaching a similar weight to wild type animals. However male animals are frequently infertile, consistent with both the known role of retinoids in reproduction (by vitamin A deficiency studies) and the known expression pattern of LRAT, in which expression is high in testis but undetected in ovary. Some changes to the retina are observed in *Lrat*-/- animals at 6-8 weeks-old, with the rod outer segment showing a ~35% reduction in length with this increasing to ~50% reduction by 4.5-months-old (Figure 1.10 B*).* A small reduction in photoreceptor nuclei was also seen and the synaptic terminal of the photoreceptors also showed less well-developed synaptic ribbons. Eye levels of retinoids were very low in *Lrat*-/- compared with WT and *Lrat*+/- animals, low levels of retinol were observed (possibly from the blood within the eye), trace amounts of retinyl esters and no other retinoids were detected, including 11-cis-retinal- a major retinoid within the eye required for visual function (Figure 1.10 C). Consistent with this lack of 11-cis-retinal, ERG data indicates that rod and cone function is greatly diminished (Figure 1.10 D). Human mutations in *LRAT* result in retinal dystrophy (Thompson 2001) and Leber congenital amaurosis (Senechal 2006), probably due to the lack of retinyl ester provision to RPE65 for the formation of 11-cis-retinal. Retinyl ester levels in the liver, blood and lung were also found at trace amounts with a slight reduction in blood retinol levels also noted

(Batten 2004). Abnormalities of the testes were further analysed in a second knockout line in which diffuse testicular hypoplasia and atrophy was noted (Figure 1.10 E-H). Mature sperm were found to be absent in *Lrat*-/- males but expression of a panel of testis-specific genes were un-changed between WT and *Lrat*-/- testis (Figure 1.10 I) (Liu 2005).

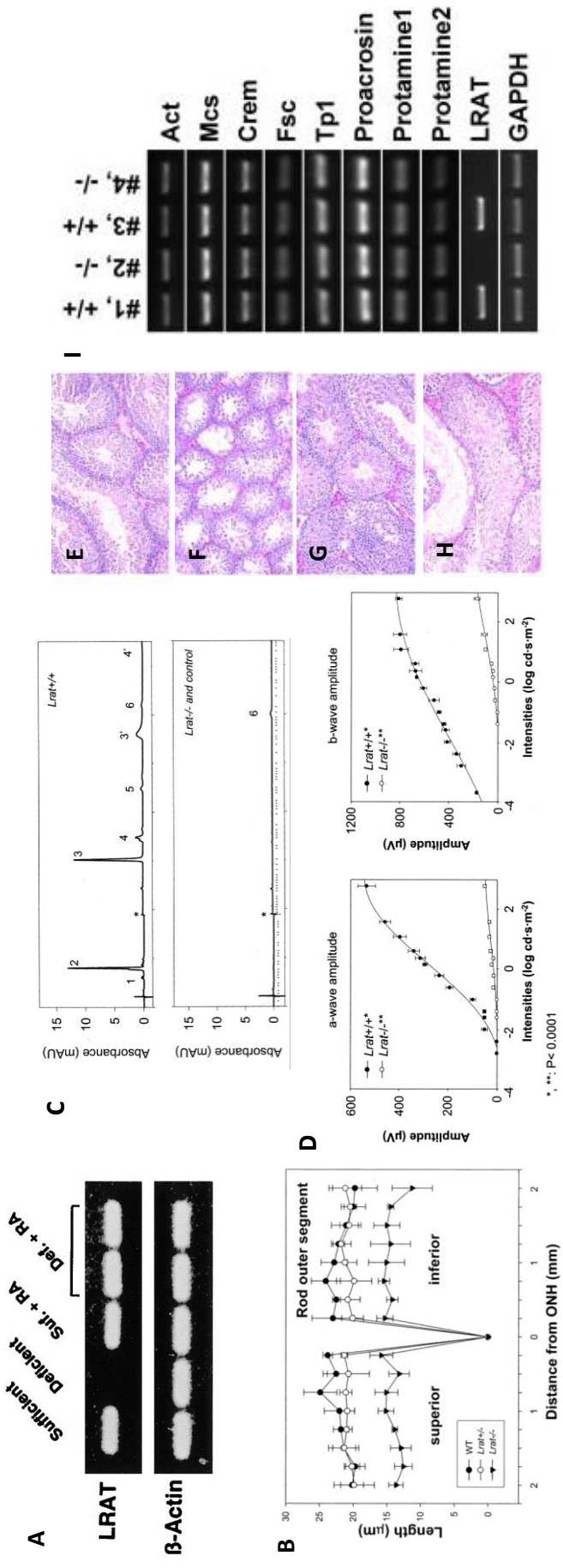
A
LRAT
β-Actin
Sufficient
Deficient
Suf. + RA
Def. + RA
B
Rod outer segment
inferior
superior
WT
Lrat+/-
Lrat-/-
Length (µm)
Distance from ONH (mm)
C
Lrat+/+
Lrat-/- and control
Absorbance (mAU)
D
a-wave amplitude
b-wave amplitude
Lrat+/+*
Lrat-/-**
Amplitude (µV)
Intensities (log cd·s·m-2)
*, **: P< 0.0001
E
F
G
H
I
Act
Mcs
Crem
Fsc
Tp1
Proacrosin
Protamine1
Protamine2
LRAT
GAPDH
#1, +/+
#2, -/-
#3, +/+
#4, -/-

Figure 1.10 LRAT is RA responsive and maintains testis and retinal function in adults.

Lrat expression is dependent of retinoid levels being lost upon VAD, to allow available retinol be metabolised, and induce by RA treatment, in order to maintain an equilibrium between storage and metabolism (**A**). Lrat-/- animals (triangles) have a reduction in the rod outer segment length compared to WT (filled circles) and Lrat+/- animal (open circles) (**B**). Lrat-/- eyes have very low levels of retinoids (**C**). Retinyl esters (2) are not detected in Lrat-/- eyes and a minimal level of retinol is observed (6). 13-/11-cis retinyl oximes (1), syn-/anti-11-cis-retinyl esters (3, 3'), syn-/anti-all-trans retinal oximes (4, 4') and 11-cis retinol (5) are also absent in Lrat-/- eyes. ERG analysis of Lrat-/- animals shows dysfunction of the photoreceptors with both a-wave (**D**-left panel) and b-wave (**D**-right panel) being significantly reduced in Lrat-/- (open circles) compared to WT (filled circles). The testes of 4-week WT (**E**) and Lrat-/- (**F**) show marked differences with hypoplasia evident in Lrat-/- animals. Testes morphology deteriorated with age and Lrat-/- (**H**) animals showed stark morphological differences compared to WT (**G**) males at 3 months. Despite morphological changes to the testes, gene expression of testes-specific genes was unchanged between WT (#1, #3) and Lrat-/- (#2, #4). A adapted from Zolfaghari, R. et al (2000), B-D adapted from Batten, M.L. et al (2004) and E-I adapted from Liu, L. et al (2005).

1.4.4 Retinol Dehydrogenase

Retinol dehydrogenase (RDH) enzymes function to catalyse the oxidation of retinol to retinal. Many RDH enzymes have been indentified and most show redundant functions in development. Knockout of many RDH enzymes results in retinal degeneration and human mutations in two RDH genes results in visual phenotypes: *RDH5* in mild night blindness (Yamamoto 1999) and *RDH12* in a childhood-onset retinal dystrophy (Thompson 2005).

1.4.4.1 Retinol dehydrogenase 5, 8, 11 & 12

RDH 5, 8, 11 and 12 all contribute to the visual cycle allowing reduction and oxidation of retinoids in order to maintain photoreceptor function. RDH8 acts to reduce all-trans retinal within the photoreceptor outer segments (Parker 2010) and knockouts show no retinal morphology defects but rod recovery was slow (Figure 1.11 A) and under bright light all-trans retinal accumulated within the eye (Maeda 2005). RDH12, like RDH8, also functions to reduce all-trans retinal. RDH8 is the major functional enzyme *in vivo* as little difference in RDH activity is observed between *Rdh8-/-* and *Rdh8-/-; Rdh12-/-* animals (Maeda 2007). Dark adaptation of *Rdh12-/-* animals is slower (Figure 1.11 A) and, as for *Rdh8-/-* animals, all-trans retinal accumulates after exposure to extended periods of bright light. Retina morphology is normal in young animals but the outer segment is reduced in animals of 10 months (Figure 1.11 B&C) and the central retina photoreceptors are lost in animals exposed to continuous bright light. RDH12 is important for maintaining the photoreceptor under excessive illumination but does not play a major role in normal retinal reduction *in vivo* (Maeda 2005). RDH5 and RDH11, in contrast to RDH8 and RDH12, function mainly to oxidise retinol. RDH5 is highly expressed in the RPE and recognises *cis*-isomer retinoids as substrates. RDH11 can catalyse both *cis*- and *trans*-retinoids and is also thought to be important for removing toxic aldehydes created as byproducts of the visual cycle. Both *Rdh5* and *Rdh11* mutants show no changes to retina morphology and both show delayed dark adaptation (Figure 1.11 D-F). Bleaching of the *Rdh5-/-* retina causes an accumulation of 11-cis-retinal

precursors, 11-cis-retinol and retinyl esters and a reduction in 11-cis-retinal production. In contrast the *Rdh11*-/- retina shows no such accumulation of these retinoids (Kasus-Jocobi 2005). Double knockouts suggest that RDH5 and RDH11 function cooperatively to produce 11-cis-retinal but RDH5 is likely to be the major enzymatic partner (Parker 2010).

1.4.4.2 Retinol dehydrogenase 1

Rdh1 knockout is not reported to effect eye morphology or function and does not give a developmental phenotype. *Rdh1* knockout results in no changes to retinoid levels under normal diet and increases RE and retinol under a retinol-minimal diet (Figure 1.11 G&H). The reduction in the provision of retinoic acid precursors is compensated by a reduction in CYP26A1 levels and thereby maintaining sufficient levels to facilitate normal development. *Rdh1*-/- animals maintained on a vitamin A copious diet were indistinguishable from WT animals in terms of growth and weight however when animals were born to dams on a vitamin-A minimal or deficient diets and weaned onto the same diets they weighed more than their WT counterparts despite food consumption not being significantly different between the two groups (Figure 1.11 I&J). The extra weight was derived only from the extra fat mass of *Rdh1*-/- animals which also showed a reduction in both water and body mass (Figure 1.11 K) (Zhang 2007).

1.4.4.3 Retinol dehydrogenase 10

In contrast to other RDHs, *Rdh10* loss from the embryo results in a developmental phenotype (Figure 1.11 L&M). RDH10 responsible for the majority of retinal synthesis in the embryo and this synthesis occurs on the intracellular membrane in a CRBP independent manner (Farjo 2011). *Rdh10*^{trex} mutants were created through an unbiased ENU approach and this mutation results in an unstable protein with no detectable RDH10 activity and therefore probably represents an *Rdh10* knockout (Sandell 2007; Cunningham 2011). The *Rdh10*^{trex} mutant was named after the limb phenotype in which the forelimbs show massive reduction in size however the hindlimbs appear unaffected analogous to a *Tyrannosaurus rex*, therefore *Rdh10*^{trex}

(Figure 1.11 N&O). *Rdh10*^{trex} mutants also show malformation of the optic and otic vesicles, lung bud agenesis and a neural crest patterning defect associated abnormalities of the cranial ganglia. *Rdh10*^{trex} mutants die at around E13.0 perhaps due to vascular defects as extensive haemorrhaging and blood pooling is observed (Figure 1.11 M). Organogenesis is generally affected with liver, lung, stomach, pancreas and gonads hypoplastic at E13.0 in *Rdh10*^{trex} mutants. Maternal RA supplementation between E7.5 and E10.5 resulted in *Rdh10*^{trex} embryos were morphologically indistinguishable from WT embryos at E13.0 (Figure 1.11 P-R). The *Rdh10*^{trex} phenotype can be attributed to a deficiency of RA which can be rescued by increased maternal RA contribution (Sandell 2007).

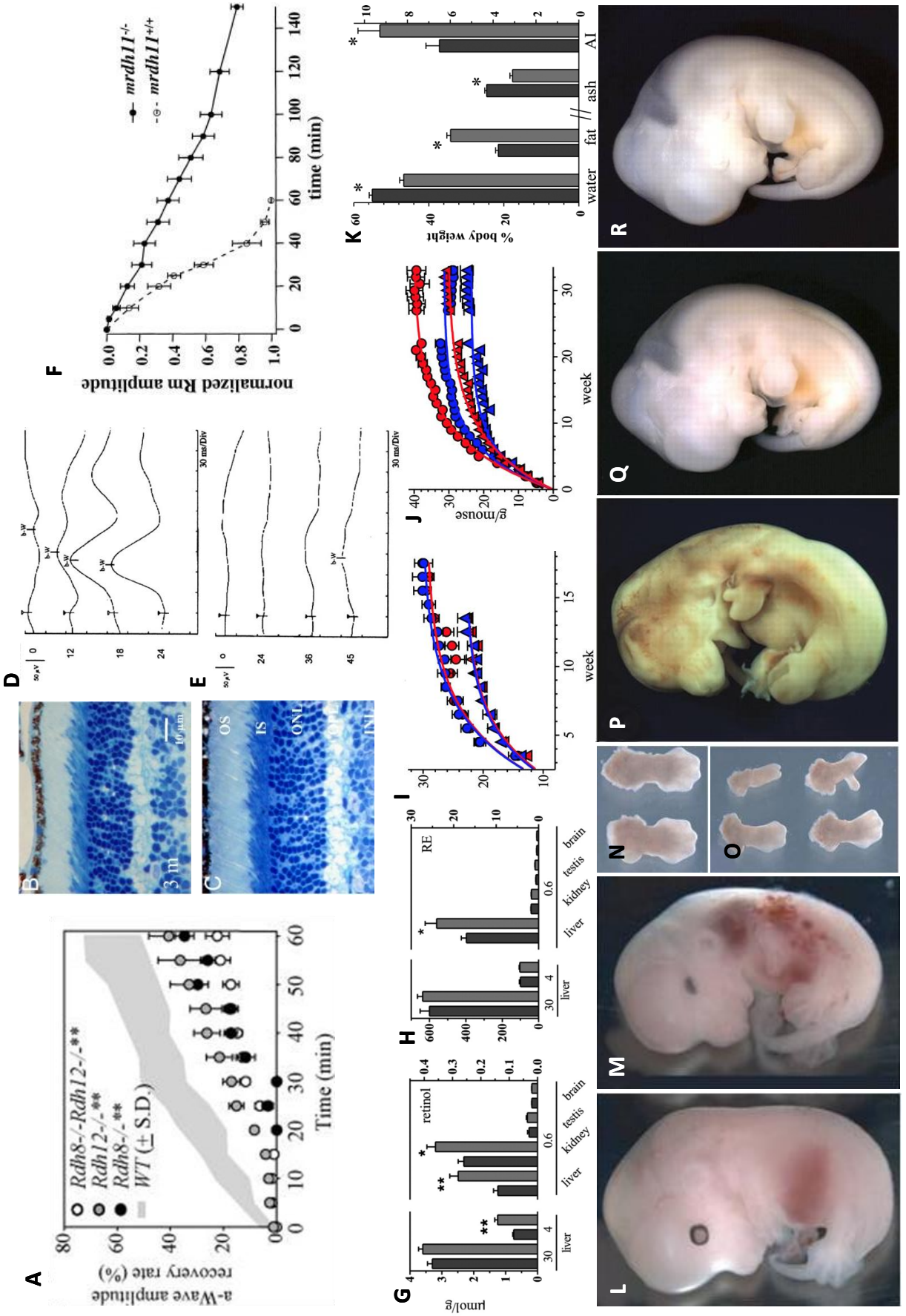
A
a-Wave amplitude recovery rate (%)
Time (min)
Rdh8-/-Rdh12-/-**
Rdh12-/-**
Rdh8-/-**
WT (± S.D.)
B
3 m
10 µm
C
OS
IS
ONL
INL
D
E
30 ms/Div
F
normalized Rm amplitude
time (min)
mrdh11-/-
mrdh11+/+
G
µmol/g
liver
kidney
testis
brain
retinol
H
RE
I
week
J
g/mouse
week
K
% body weight
water
fat
ash
AI
L
M
N
O
P
Q
R

Figure 1.11 Members of RDH family are required for normal vision, regulation of fat mass percentage and normal development.

Rdh8-/- (filled circles) and Rdh12-/- (grey filled circles) animals show reduced a-wave amplitude compared to WT range (gray) (**A**). Rdh8-/-; Rdh12-/- (open circles) are similar in a-wave profile to Rdh8-/- (**A**). Retinal outer segment (OS) length is reduced in older Rdh12-/- (**B**) compared to WT of the same age (**C**). Rdh5-/- animals (**E**) show delayed dark adaptation after bleaching as seen by the minimal b-wave (b-W) on ERG compared to WT (**D**). Rdh11-/- show slow recovery from photobleaching compared to WT animals (**F**). Retinol (**G**) and retinyl esters (**H**) levels are normal in Rdh1-/- animals (light grey bars) under vitamin-A excess diet (30) and retinol levels only are increased in Rdh1-/- fed a vitamin-A minimal diet (4) compared to WT (dark grey bars). Vitamin-A deficient diet (0.4) caused a significant increase in retinyl esters (RE) in the liver and a significant increase in retinol in the liver and kidney. WT (blue) males (circles) and females (triangles) and Rdh1-/- (red) when fed vitamin-A copious diets were indistinguishable in weight and growth (**I**). When fed on a vitamin-A deficient diet Rdh1-/- animals are significantly larger than WT animals (**J**). The extra weight in Rdh1-/- mice (light grey bars) is derived from an increase in fat mass with water and lean mass decreased compared to WT (dark grey bars) (**K**). Rdh10-/- are the only Rdh KO to display a developmental phenotype. $Rdh10^{trex}$ (**M**) die at around E13.0 with extensive haemorrhaging across the embryo surface and small eyes. $Rdh10^{trex}$ mutants (**O**) are so named due to reduction in forelimb size compared to WT (**N**) with normal hindlimb size. Maternal RA supplementation from E7 to E10.5 rescued the $Rdh10^{trex}$ mutants (**P**) and resulted in $Rdh10^{trex}$ embryos (**R**) indistinguishable from WT (**Q**). A-C adapted from Maeda, A. et al (2007), D-E adapted from Driessen, C.A. et al (2000), Kasus-Jacobi, A. et al (2005), G-K adapted from Zhang, M. et al (2007) and L-R adapted from Sandell, L.L. et al (2007).

1.4.5 Retinaldehyde Dehydrogenase

Three retinaldehyde dehydrogenases (RALDH) enzymes have been identified in mammals; RALDH1-3, and of these RALDH2 appears to be the most important for provision of developmental RA requirement. *Raldh2* was identified by cloning of cDNA from rat testis (Wang 1996) and shown to be RA-inducible in p19 carcinoma cells (Zhao 1996). RALDH acts on retinal to synthesise retinoic acid, both in its free state and also complexed with CRBP (Wang 1996), and its expression level is related to the RA synthesis potential of the tissue (Zhao 1996).

1.4.5.1 Retinaldehyde dehydrogenase 2

RALDH2 is essential for normal development with *Raldh2*-/- animals dying around E10.5. Morphologically E10.5 *Raldh2*-/- embryos more closely resemble WT E8.5, as *Raldh2*-/- do not undergo axial rotation (Figure 12A-H). In addition to a lack of axial rotation, the embryos were also smaller, had an open neural tube and dilated heart (Figure 1.12 D, F&H) (Niederreither 1999). Heart defects in *Raldh2*-/- embryos result not from defects in heart tube formation but a failure of rightward heart looping. The formation of the myocardium is impaired resulting in a loosely associated layer of prematurely differentiated cardiomyocytes and undifferentiated cells. Heart formation, other than the formation of the neural crest derived outflow tract, can be rescued by maternal RA supplementation (Figure 1.12 I&J) indicating that specific areas of RA synthesis are not essentially required for non-neural crest derived heart morphogenesis (Niederreither 2001). Gene expression of the looping associated genes *Nodal*/*Lefty*/*Pitx2* is not affected in *Raldh2* mutants but expression of secondary heart field associated genes *Tbx1*/*Fgf8*/*Islet1* are expanded posteriorly and this additional specified tissue cannot differentiate correctly (Figure 1.12 K&L) (Ryckebusch 2008). *Fgf3* expression was very weak in *Raldh2*-/- embryos (Figure 1.12 M&N) and consistent with its role in otocyst development *Raldh2*-/- embryos show a hypoplastic and abnormally position otocysts (Niederreither 1999). *Fgf8* and *Fgf10* expression is undetectable in *Raldh2*-/- embryo which is concomitant with limb bud development failure in *Raldh2*-/- embryos as *Fgf8/10* are required for limb

bud specification (Niederreither 1999). This interaction between FGF and RA is repeated throughout the embryo and during development with both genes sharing many developmental regulatory networks (Shiotsuga 2004). Maternal RA supplementation, in addition to rescuing some aspects of heart development, is also able to rescue embryo turning, somite and trunk development but only partially rescues forelimb development with small forelimbs observed in rescued *Raldh2*-/- and some embryos also show tail defects and shortening of the trunk region (Figure 1.12 I&J) (Niederreither 1999). Therefore many of the actions of RALDH2 can be maintained by ubiquitous flooding of the embryo with RA however some functions, i.e. limb development/cardiac outflow tract formation, require either the specific expression of *Raldh2* or perhaps a higher level of RA than is provided by maternal supplementation.

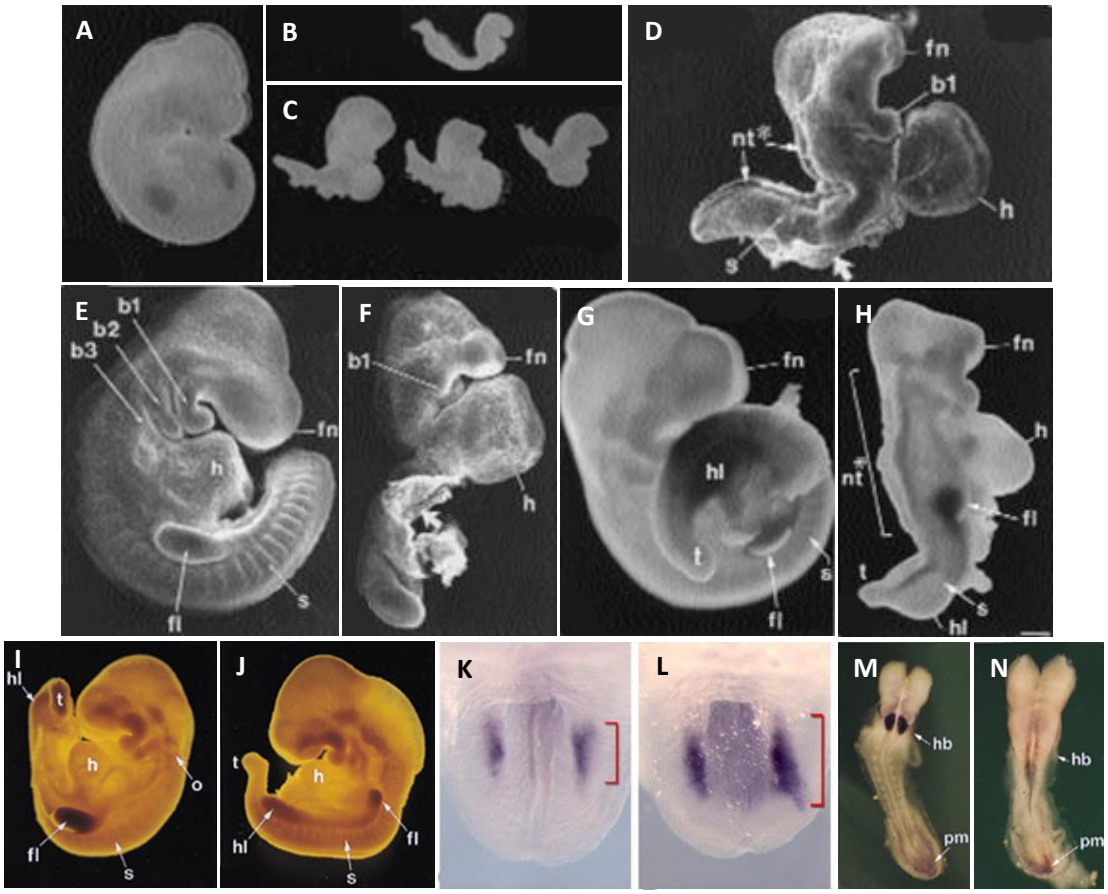
A
B
C
D
fn
b1
nt
h
s
E
b1
b2
b3
fn
h
fl
s
F
b1
fn
h
G
fn
hl
t
s
fl
H
fn
h
nt
fl
t
s
hl
I
hl
t
h
o
fl
s
J
t
h
hl
fl
s
K
L
M
hb
pm
N
hb
pm

Figure 1.12 RALDH2 is essential for normal heart and embryonic development.

Unlike WT embryos (**A**) Raldh2-/- embryos show a lack of axial rotation at E10.5 (**C**) and are equivalent to an E8.5 embryo (**B**). Raldh2-/- embryos (**D**&**F**) also exhibt an enlarged heart (h), reduction in the number of branchial arches (b1-3), hypoplastic frontonasal region (fn), somite defects (s) and in some embryos a failure of neural tube closure (nt*) compared to WT E9.5 embryo (**E**). Similarly at E10.5, compared to WT (**G**), the heart remains distended, the neural tube remains open and axial rotation is not complete and the forelimb (fl) buds are hypoplastic although hindlimb (hl) buds are still visable. Maternal RA treatment was able to almost completely rescue development to E10.5. WT embryos exposed to the same treatment were normal (**I**) and Raldh2-/- embryos had completed axial rotation (**J**). Secondary heart defects in Raldh2-/- embryos (**L**) are caused by an expansion of Fgf8 expression domain at the 3-4 somite stage compared to WT (**K**). Fgf3 expression at E8.5 is also lower compared to WT (**M**) in Raldh2-/- embryos (**N**) especially in the hindbrain (hb) but not affected in the posterior mesoderm (ps). A-J and M-N are adapted from Niederreither, K. et al (1999) and K-L are adapted from Ryckebusch, L. et al (2008).

1.4.5.2 Retinaldehyde dehydrogenase 1

RALDH1 is able to act on both *trans*- and 9-*cis* retinal at similar conversion efficiencies (Gagon 2003). RALDH1 is expressed in the lungs, liver and testis in addition to its expression within the eye. *Raldh1*-/- mice show no developmental defects or defects in postnatal viability or growth. Retina morphology is normal in knockout animals (Figure 1.13 A&B) and visual function is not affected with electroretinography (ERG) showing no signs of retinal degeneration or delayed dark adaptation (Figure 1.13 C). Retinol metabolism is affected in *Raldh1*-/- livers with an increase in retinol and retinyl esters, but no change to the level of RA (Figure 1.13 D). When *Raldh1*-/- animals are given a large oral dose of trans-retinol, however, they show a reduced accumulation of RA compared to WT animals (Figure 1.13 D) (Fan 2003). RALDH1 is therefore normally redundant to RALDH2 and 3 and not essential in the embryo or the adult.

1.4.5.3 Retinaldehyde dehydrogenase 3

Raldh3-/- animals die soon after birth due to respiratory distress from a persistence, rather than timely rupture, of the nasal fins resulting in choanal atresia (Figure 1.13 H-K). This lack of passage between the nasal and oral cavaties causes respiratory distress as newborn animals are unable to breathe through their mouths. *Raldh3*-/- embryos also show defects of other components of the nasal region, namely the absence of maxillary sinuses and nasolacrimal ducts and hypoplasia of the ethmoturbinates (Figure 1.13 L&M). These defects have also been described in various RAR compound knockouts highlighting a role for RALDH3 in directly providing RA ligand for RARs (Dupe 2003). The defects in nasal development coincide with the expression of *Raldh3* within the olfactory pit and maxillary process (Figure 1.13 E&F). Eye development is also affected in *Raldh3*-/- (Figure 1.13 N-Q) consistent with the expression of *Raldh3* widely in the optic vesicle during early development but later restricted to the ventral retina and future RPE (Figure 1.13 E-G) (Mic 2000; Suzuki 2000). *Raldh3*-/- animals, as for *Raldh2*-/-, can be rescued by maternal RA supplementation however supplementation of *Raldh3*-/- results in

healthy pups born which survive to adulthood and are indistinguishable from WT animals (Dupe 2003).

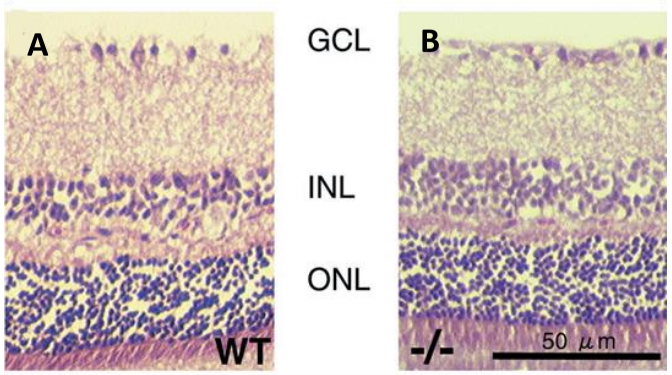

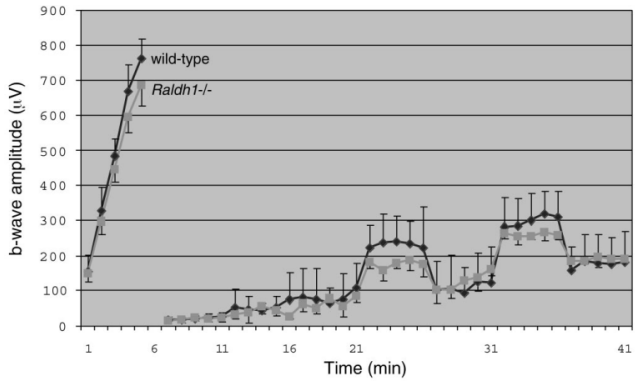

D

Group	Genotype	*all-trans*-RA (ng/g)	*all-trans*-Retinol (μg/g)	Retinyl esters (μg/g)
Untreated	Wild type	1.5 ± 0.2	8.5 ± 1.0	571 ± 59
	Raldh1$^{-/-}$	1.6 ± 0.3	14.4 ± 1.22^{b}	1,278 ± 68^{c}
Retinol treated	Wild type	3,100 ± 480	19.5 ± 0.2	570 ± 10
	Raldh1$^{-/-}$	990 ± 60^{b}	36.2 ± 3.2^{c}	1,244 ± 57^{c}

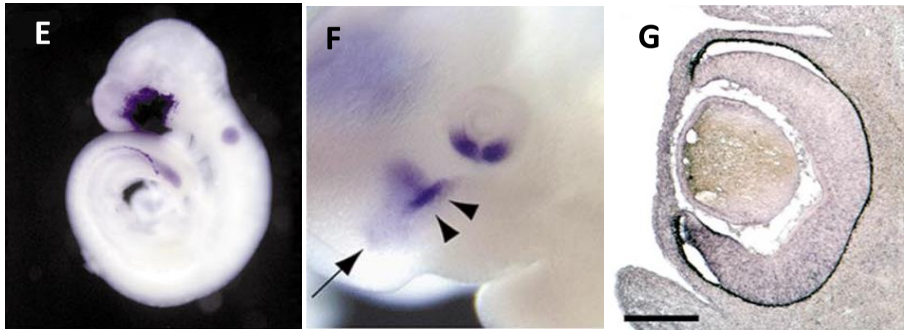

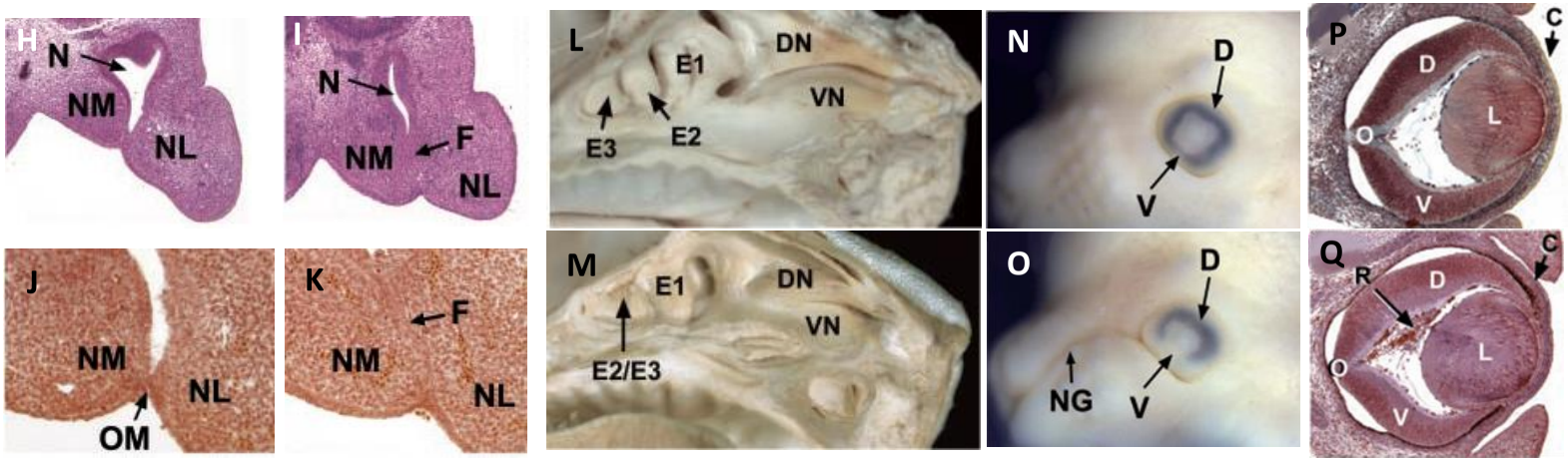

Figure 1.13 *Raldh1* is dispensable in the embryo and adult but loss of *Raldh3* results in neonatal mortality.

Retinal morphology is normal in *Raldh1-/-* animals with WT (**A**) and *Raldh-/-* (**B**) retinas being indistinguishable. ERG investigation of *Raldh1-/-* (grey) compared to WT (black) could not distinguish any differences in b-wave response (**C**). *Raldh1-/-* animals do show defective metabolism of retinoids (**D**) in the normal state, with a significant increase in retinol ([b] $P<0.05$) and retinyl ester ([c] $P<0.01$) amounts in the liver. Upon oral dosing with retinol, significantly less RA is produced by *Raldh1-/-* along with a significant increase in retinol and retinyl ester level. *Raldh3* is expressed highly within the surface ectoderm in the head region, specifically the lens and nasal placodes at E9.5 (**E**). Expression is further restricted to the ventral retina, nasal pit (arrow) and the mandibular arch (arrowheads) at E11.5 (**F**). Expression within the ventral retina was maintained at E14.5 (**G**). *Raldh3-/-* neonates die due to respitatory distress due defects in nasal development. Morphological defects in nasal development can be noted from E11.5 between the nasomedial process (NM) and nasolateral process (NL). The nasal cavity (N) is large in WT embryos (**H**) compared to *Raldh3-/-* embryos (**I**) and the nasal fins (F) have regressed. Nasal fins in WT embryos (**J**) have formed the oropharyngeal membrane (OM) while in *Raldh3-/-* the nasal fins remain fused (**K**). Multiple defects of the nasal region are noted including hypoplastic ethmoturbinates (E1-3) and fusion of the second and third (E2/E3) in *Raldh3-/-* (**N**) compared to WT (**M**). The nasalacrimal groove (NG) persists in *Raldh3-/-* at E12.5 (**O**) compared to WT (N) and the ventral (V) retina is also un-pigmented in *Raldh3-/-* compared to WT although the dorsal (D) is unaffected. Eye development is also affected in *Raldh3-/-* embryos with the retrolenticular membrane persisting at E14.5 in Raldh3-/- animals (**Q**) compared to WT (**P**). A-D adapted from Fan, X. et al (2003), E-G adapted from Suzuki, R. et al (2000) and H-Q adapted from Dupe, V. et al (2003).

1.4.6 Retinoic Acid receptors

Retinoic acid receptors (RAR) are part of the superfamily of ligand activated transcriptional regulators and function in heterodimers with RXRs (discussed below) to bind and effect gene expression of those genes with cis acting response elements known as RAREs. Commonly RAREs are direct repeats with a 5bp spacer although considerable heterogeneity has been observed in seemingly functional RAREs. In the absence of ligand, i.e all-trans- or 9-cis-RA for RARs and 9-cis-RA for RXRs, these heterodimers function as co-repressors until the availability of ligand allows them to function as co-activators (Chambon 1996). Three RAR genes are found in mammals with alternative transcripts derived from many of the genes due to the use of alternative promoters and alternative splicing.

1.4.6.1 Retinoic acid receptor alpha

RARα is found in two isoforms; α1 which is widely expressed under the control of a 'housekeeping-like' promoter and α2 which is under the influence of a RARE. *RARα1*-/- mice, a specific knockout of the α1 isoform, are viable and fertile with no skeletal or histological abnormalities identified. *RARα*-/-, a knockout for all *RARα* isoforms, represented the expected 25% proportion of the litter when analysed during gestation. After 12-24hours over half of the *RARα*-/- pups were lost and were found to be preferentially cannibalised by their dams. *RARα*-/- animals had a higher mortality rate representing only 3%, rather than the expected 25%, of the population at 2 months (Figure 1.14 A). These animals showed a slower growth rate 1-2 weeks after birth and, despite no obvious malformations other than interdigital webbing in 60% of the animals, died shortly after showing signs of emaciation and lethargy. Male *RARα*-/- animals that survived sired no pups with WT females and at 4-5 months showed degeneration of the germinal epithelium. Most of the tubules were atrophied and showed loss of the spermatogenic cells resulting in the low number of sperm observed in the epididymal duct therefore resulting in the observed infertility of *RARα*-/- males (Figure 1.14 B-D) (Lufkin 1993).

1.4.6.2 Retinoic acid receptor beta

RARβ-/- (loss of all isoforms *β1-4*) are found in the expected frequency and have normal life expectancy as WT littermates. They do however show a postnatal growth deficiency despite weighing the same as WT littermates at birth. Males show a 25% and females a 20% reduction in body weight at P20 (Figure 1.14 E) and this was also accompanied by a 10% decrease in the length of various bones indicating a systemic growth defect. *RARβ*-/- also show congenital defects of the eye with bilateral persistent hypoplastic primary vitreous (PHPV) bilaterally observed in 83% of knockouts and cataracts in 8% of animals compared to 0% in WT or +/- littermates (Figure 1.14 F&G). Folds of the neural retina due to the mechanical stress of the PHPV were also observed at E18.5 in 40% of the embryos analysed. A homeotic posteriorising transformation of the C7 cervical vertebra observed, in general unilaterally, in 11% of the knockouts resulting in an extra rib on the C7 vertebrate converting it to a more thoracic T1-like identity (Ghyselinck 1997).

1.4.6.3 RARE-LacZ

RARβ is also RA-responsive with a RARE within its promoter sequence and this RARE has been used in order to produce a transgenic reporter of RA signalling under normal conditions and perturbations of RA signalling including maternal RA treatment and gene knockout. Three copies of the 34bp RARE from *RARβ* have been placed in front of the *Hsp68* promoter linked to the *lacZ* gene (Figure 1.14 H&I) which results in *lacZ* staining in regions of active RA signalling. Using this transgene expression was seen early in E3.5 blastocysts in both cells of the ICM and the trophoblast but this expression was variable indicating RA signalling may be activated stochastically in individual cells of the blastocyst. Expression was not seen again until after E7.5, when expression was observed throughout the primitive streak, and the posterior of the embryo in all three germ layers (Figure 1.14 J). Expression was restricted to the optic eminence and in a region in the middle of the embryo from the first somite to behind the last formed somite at E8.5 (Figure 1.14 K). By E10.5 expression although superficially restricted to the region from the start of the spinal

cord to the base of the tail, internally expression was higher in the spinal cord and the endoderm of the developing gut. The eye was stained both in the future lens and retina consistent with the known role for RA in eye development (Figure 1.14 L). After maternal treatment with RA, the transgene became activated across the whole embryo and was activated earlier than untreated embryos at E6.5-7.5 (Figure 1.14 M) (Rossant 1991).

1.4.6.4 Retinoic acid receptor gamma

RARγ has two isoforms (γ1 and 2) and knockouts of γ2 alone result in no developmental or adult defects, however knockouts of both isoforms results in growth deficiency (as for *RARβ*-/-), early lethality and male sterility (as for *RARα*-/-). Loss of RARγ did not affect the expression of the RAR genes or the staining pattern of the RARE-*lacZ* reporter of RA signalling at E9.5 or 13.5. The expected number of *RARγ*-/- embryos (25%) was observed at E18.5 but half of the expected *RARγ*-/- animals were found at 1-3 weeks of age and this reduced to 20% of the number expected by 3 months (Figure 1.14 N). The growth deficiency in *RARγ*-/- animals occurred by P4 with null animals weighing 40-80% of WT littermates although these smaller animals experienced a higher degree of mortality such that there was little difference in body weight compared to WT littermates by 3 months. RARγ loss results in anteriorizing homeotic transformation of the cervical vertebra (Figure 1.14 O&P). Harderian gland epithelium was absence in some null animals and caused the eyelids to be closed and crusted in these animals. Male *RARγ*-/- animals were, as for *RARα*-/- males, found to be sterile but female fertility was normal consistent with the high expression of RARγ in the male but not female reproductive system. The seminal vesicles and prostate are hypertrophic and the normal glandular epithelia have undergone a transition to squamous epithelia with some keratinised cells (Figure 1.14 Q&R) (Lohnes 1993).

A

Age	No. alive (ratio to wild type) −/−	+/−	+/+
	RARα$^{+/-}$ × RARα$^{+/-}$ offspring		
8.5–18.5 dpc	34 (0.9)	64 (1.6)	39 (1.0)
1 day postpartum	13 (0.4)	56 (1.6)	36 (1.0)
2 weeks	15 (0.2)	123 (1.9)	64 (1.0)
1–2 months	4 (0.1)	90 (2.0)	45 (1.0)

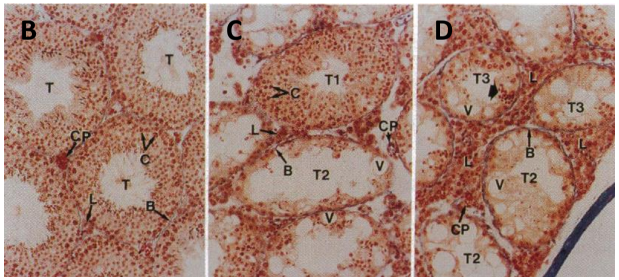

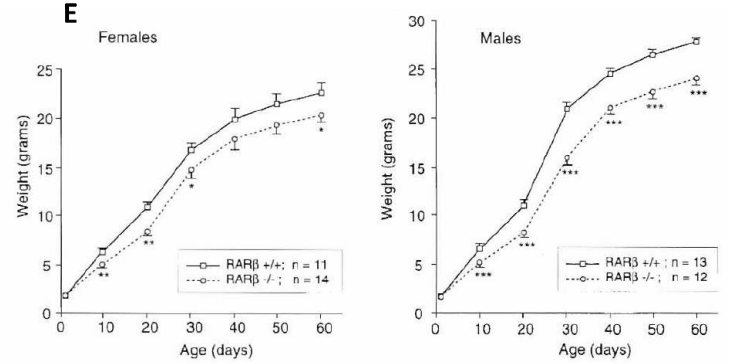

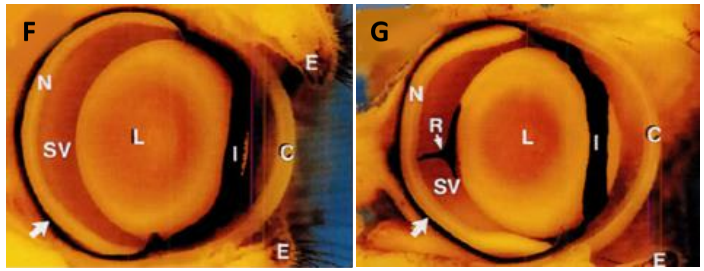

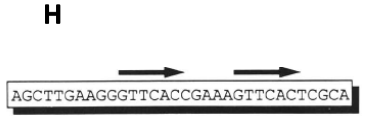

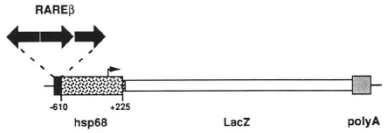

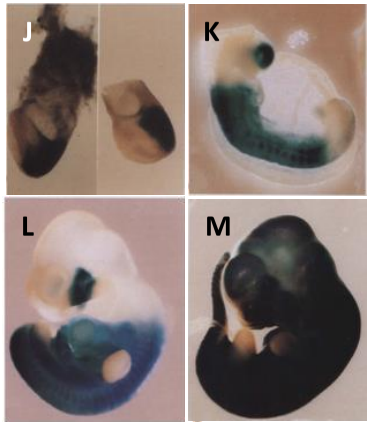

N

Age	Genotype of RARγ$^{+/-}$ Crosses +/+	+/−	−/−
18.5 dpc	69 (1.0)	146 (2.1)	65 (0.9)
1–3 weeks old	142 (1.0)	297 (2.1)	73 (0.5)
1 month old	140 (1.0)	295 (2.1)	53 (0.4)
3 months old	138 (1.0)	292 (2.1)	28 (0.2)

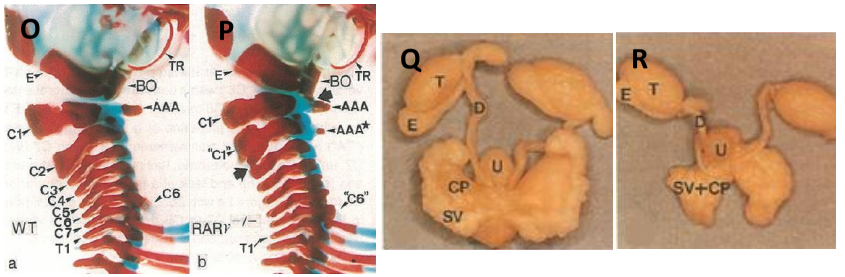

Figure 1.14 Individual members of RAR family are not essential for normal development but do play a role in postnatal survival, fertility and eye morphology.

RARα-/- are found in the expected ratio in embryonic stages but over half are lost within the first 24 hours after birth and this increased mortality is constant through the first months of life (**A**). Surviving *RARα-/-* males were infertile and exhibited testicular degeneration with normal tubules (**B**) containing spermatozoa (T) rarely observed in *RARα-/-* (T1, **C**). Most tubules in *RARα-/-* animals were atrophic (T3, **D**) and devoid of spermatogenic cells (T2, **C-D**) and contained vacuoles (V). *RARβ-/-* females (**E**, left panel) and males (**E**, right panel) are postnatal growth deficient despite weighing the same as WT pups at birth. *RARβ-/-* also show congenital eye defects with a persistence of the rentrolenticular membrane (R, **G**) which is lost in WT animals (**F**). RARβ contains a characterised RARE within its promoter (**H**) and three copies of this RARE have been linked to a hsp68 promoter and the LacZ reporter gene (**I**) in order to create a reporter of active RA signalling. Expression, and therefore RA signalling, is observed at E7.5 throughout all the germ layers within the posterior of the embryo and primitive streak (**J**). RA signalling is active in the optic eminence and in the middle portion of the embryo between the first and last somite at E8.5 (**K**). Expression at E10.5 was superficially observed across the embryo from the start of spinal cord through the tail excepting the limb buds and within the eye (**L**). Maternal RA supplementation highly activated the transgene across the entire embryo indicating that the transgene provides and accurate readout of RA signalling (**M**). The expected number of *RARγ-/-* embryos was observed at E18.5 but these were progressively lost during the postnatal period leaving only 20% of the expected number by 3 months (**N**). Loss of *RARγ* results in anteriosing homeotic transformation of the cervical vertebrae. WT animals (**O**) have 7 cervical vertebrae (C1-7) however in *RARγ-/-* (**P**) animals two C1-like vertebrae are observed. *RARγ-/-* males are also sterile and, compared to WT (**Q**), the seminal vesicles (SV) and prostate (CV) show marked atrophy. A-D adapted from Luftkin, T. et al (1997), E-G adapted from Ghyselinck, N.B. et al (1997), H-N adapted from Rossant, J. et al (1991) and N-R adapted from Lohnes, E. et al (1993).

1.4.6.5 Retinoic acid receptor compound knockouts

The RARs show considerable redundancy of expression and function with individual mutants showing minimal phenotypes mainly restricted to defects in adult tissue maintenance and postnatal growth. Double mutants have been studied in order to determine the roles of each gene in the absence of the compensatory effects of the other genes of the pathway. The table shows the combination of defects observed in various compound mutants and shows the necessity of RARs for the development of the eye, heart, thymus, thyroid, kidney, male and female genitals and respiratory tract (Table 1.1). RARs are also important for the transduction of the RA gradient to signalling cues for Hox code activation within the developing spinal column as seen by the homeotic transformations of the vertebrae. RARα and RARγ are required to specify correct digit number and are compensatory for each other in single knockout animals. RARα has a role in normal respiratory tract formation as seen on compound αβ2 mutants but this function is compensated in single knockout animals. RARγ is required for Hardarian gland formation with agenesis of this structure observed in all compound mutants including RARγ loss (Lohnes 1994; Mendelsohn 1994).

RARs are required to control gene expression in a RA dependent fashion and show significant functional redundancy as expected for an important class of developmental regulators.

	RAR mutant genotype (E18.5)					
	α1β2	αβ2	α1γ	α1γα2+/-	αγ	β2γ
Mutant frequency (expected)	29 (25)	9 (12.5)	12 (12.5)	13 (12.5)	3 (6.25)	13 (12.5)
Viability	V <12hrs	V <1hr	V <12hrs	V <1hr	EL	V <12hrs
Respiratory Tract Abnormalities	-	+++	-	-	-	-
Heart						
Persitent truncus ateriosus	+	+++	-	-	+++	-
Ventricular septal defect	++	+++	-	++	+++	-
Outflow tract defect	+++	+++	-	++	++	-
Diaphragmantic hernia	-	+	-	-	-	-
Thymus abnormalities	+	++	-	+	+++	+
Thyroid abnormalities	+	+	-	+	++	-
Kidney abnormalties	++	+++	-	+	++	+
Female genital tract	+++	+++	-	-	+++	-
Male genital tract	-	-	-	+	+++	-
Eye						
PHPV	++	+++	-	-	+++	+++
Agenesis of the lens	-	-	-	-	+	-
Agenesis of the cornea	-	-	-	-	+	-
Agenesis of Hardarian gland	-	-	+++	+++	+++	+++
Homeotic transformation of vertebrae	NS	++	+	++	++	+
Malformation of skeleton	NS	++	++	+++	+++	++
Digit number reduction	-	-	-	-	+++	-

Table 1.1 Loss of multiple RAR genes results in a range of developmental defects.

Loss of multiple RAR family genes results in developmental defects in a percentage of embryos. +: 25-50%, ++: 51-75%, +++: 76-100%, -: 0%/ same frequency as WT, NS: not studied. Viability (V) of multiple RAR mutants is reduced and in some mutants developmental defects resulted in embryonic lethality (EL). Table complied from Lohnes, D. et al (1994) and Mendelsohn, C. et al (1994).

1.4.7 Retinoid X Receptor (RXR)

RXRs also form a family of three isotypes; α, β and γ and are a distinct family of genes with divergent structure and ligand binding compared to the RARs. RXRs binds *all-trans*-RA but *9-cis*-RA elicits a 40-fold greater activation when bound (Mangelsdorf 1992). Despite the ability of *9-cis*-RA to trigger RXR activation, this RA isoform is not abundantly detected *in vivo*. RXRs are also able to a range of unsaturated fatty acids however, which may also act as ligands *in vivo* (Wolf 2006). RXR is also able to heterodimerise with thyroid hormone and vitamin D receptors in order increase DNA binding and transcriptional activity at their response elements, although RAR/RXR heterodimers are not able to interact with either thyroid or vitamin D response elements (Yu 1991).

1.4.7.1 Retinoid X receptor alpha

RXRα-/- animals die in the second half of gestation between E13.5 to E16.5 and the first defect observed is at E12.5 when liver volume was reduced to ~30% that of WT but this is increased to 60% by E14.5 (Figure 1.15 A-D). At E14.5 the embryos appear normal, apart from the smaller liver and a widespread edema under the dermal skin layer (Figure 1.15 C&D). Edema is a common sign of heart defects resulting in heart failure and *RXRα*-/- show defects of the ventricle with ventricular septal defects and thinning of the ventricle walls (Figure 1.15 E&F) (Sucov 1994). The cardiac defects in *RXRα*-/- animals are similar to those in VAD animals and therefore the main function of RXRα in development is likely to be in the RA signalling pathway. *RXRα*-/- have bilateral eye defects from E13.5 which could be observed externally as a reduction in paperpal fissure size and a lack of pigment in the ventral portion of the eye (Figure 1.15 G&H). Lens position was rotated (Figure 1.15 I&J) and the cornea thickened with a persistence of the primary vitreous at E14.5 (Figure 1.15 K&L) (Kastner 1994). The eye is known to be specifically sensitive to changes in RA signalling further highlighting RXRα's role in the RA pathway.

1.4.7.2 Retinoid X receptor beta

RXRβ is dispensable for development in around 50% of animals suggesting a stochastic effect of this mutation which results in loss of some *RXRβ*-/- animals *in utero* or perinatally and the survival of others to adulthood (Figure 1.15 M). Surviving adult males are sterile with an epididymis sparsely populated by differentiated spermatozoa which upon extraction were mostly immobile with tail coiling (Figure 1.15 N-P). Acrosomes and mitochondrial sheaths were abnormal through the period of spermatogenesis and probably contributed to the lack of sperm motility observed. RXRβ is expressed within the Sertoli cells and, consistent with this, Sertoli cells of *RXRβ*-/- males degenerate (Figure 1.15 Q-S) and accumulate unsaturated triglycerides (Figure 1.15 T&U) which progress in older males to form lipid-filled tubules (Kastner 1996). RXRβ is therefore not essential for development of all embryos but influences developmental success of the embryo and is required for spermatogenesis and Sertoli cell maintenance.

1.4.7.3 Retinoid X receptor gamma

RXRγ is entirely dispensable for normal development, postnatal growth, longevity and fertility and its knockout does not result in a compensatory up-regulation of the other RXRs (Krezel 1996). RXRγ does; however, seem to have a function within the brain and null animals have working memory defects. RXRγ is expressed within the frontal and perirhinal cortex both regions known to be important for the working memory process (Wietyrch 2005). RXRγ also controls affective behaviours and null animals show an increase in despair (Figure 1.15 V) and loss of pleasure responses indicating a depression-like state. RXRγ appears to function through the dopamine D2 receptor and in its absence expression of the dopamine D2 receptor (Figure 1.15 W) and serotonin are reduced causing depressive-like behaviourally responses (Krzyzosiak 2010). RXRγ may also play a role in brain regeneration after injury specifically in the remyelination by oligodendrocytes. RXRγ is highly expressed in spontaneous remyelination of the CNS (Figure 1.15 X&Y) and in *RXRγ*-/- animals oligodendrocyte differentiation was delayed despite normal repopulation of the

lesion by oligodendrocyte precursors. Addition of the RXR ligand 9-cis-RA increased the number of remyelinated neurons (Figure 1.15 Z) (Huang 2011) indicating the action of RXRγ in this process is through a ligand dependent action perhaps upon gene regulation of oligodendrocyte differentiation or myelin production.

1.4.7.4 Retinoid X receptor compound knockout

RXRs show significant functional redundancy in development and such it was found that *RXRα*+/-;*RXRβ*-/-; *RXR*γ-/- animals were found to be viable. *RXRα*+/-;*RXRβ*-/-; *RXR*γ-/- animals showed only a defect in spermatogenesis as for *RXRβ*-/- and a growth deficiency of around 20% (Krezel 1996). A single copy of *RXRα* seems to be sufficient to support both development and most postnatal RXR functions consistent with its severe single knockout phenotype when compared to single knockouts of the other RXR genes.

A
B
C
D
E
F
G
WT
P
H
RXRα-/-
DE
DR
VE
I
J
K
DR
C
AC
VE
L
V
ON
VR
VJ
RE
L
DR
V
L
F
CON
FE
C
VJ
VR
RE
M
RXRβ mutant intercrosses
♀ +/− × ♂ +/−
♀ −/− × ♂ +/−
+/+
+/−
−/−
+/−
−/−
~3-week-old
132
288
73
128
38
(1)
(2.2)
(0.55)
(1)
(0.3)
1-day-old
15
33
5
70
29
(1)
(2.2)
(0.3)
(1)
(0.4)
18.5 dpc fetuses
76
129
56
66
39
(1)
(1.7)
(0.7)
(1)
(0.6)
Expected Mendelian ratio
1
2
1
1
1
N
WT
H
O
RXRβ-/-
H
P
H
Q
T
Y
R
T
Y
S
Y
T
T
T
WT
T
U
RXRβ-/-
T
V
Immobility time (s)
200
150
100
50
0
WT
Rarβ-/-
RXRγ-/-
***
W
mRNA level relative to 36B4
80
75
70
65
15
10
5
0
CPu
NAc
**
X
Y
Z
Relative rank
15
10
5
0
Saline
9cRA

Figure 1.15 Members of the RXR family are required for normal development, testis maintenance and for memory and oligodendrocyte regeneration.

RXRα-/- embryos (**B**) show a reduction in liver (white arrow) volume compared to WT (**A**) at E12.5 although this reduction is not as marked between WT (**C**) and *RXRα-/-* (**D**) by E14.5. Edema is also noted at E14.5 in *RXRα-/-* embryos (arrowhead, **D**) and this is consistent with heart failure caused by a ventricular septal defect (arrow, **F**) and thinning of the ventricular wall compared to WT (**E**). WT embryos at E13.5 (**G**) have pigment in both dorsal and ventral regions of the eye however *RXRα-/-* embryos (**H**) show a lack of ventral pigment. The cornea (C) is also thickened in *RXRα-/-* (**J**) compared to WT (**I**) and the lens (L) is rotated in respect to the retina. The primary vitreous of the *RXRα-/-* eye (arrow, F) has also not receded as extensively as in WT (V). The primary vitreous of the WT eye (**K**) at E14.5 has further receded (V) but in *RXRα-/-* embryos (**L**) have persistent hyperplastic primary vitreous (arrow, F) and fused eyelids (FE). *RXRβ-/-* is variably required for embryonic development with loss of some *RXRβ-/-* embryos before E18.5 and an increase in perinatal lethality compared to WT and *RXRβ+/-* (**M**). Surviving male *RXRβ-/-* animals were infertile and have a reduction in sperm count (**O**) compared to WT (**N**) as counted by spermheads (H) and those mature sperm observed have tail coiling (arrowhead, **P**). *RXRβ-/-* testes degenerate with age and demonstrate focal hyperplasia of the Leydig cells (**R**, Y) compared to WT (**Q**) at 8 months. By 12 months, the testes are filled with lipid-filled vacuoles (**S**). Oil-red staining of 6-month WT (**T**) and *RXRβ-/-* (**U**) testes highlighted the accumulated triglycerides (red staining on the periphery of the testes, T) exclusively in *RXRβ-/-* testes. *RXRγ-/-* animals show an increase in despair behaviours including an increase in immobility time (**V**) during the forced swim test. Expression of the dopamine Dr2 receptor is significantly reduced in the *RXRγ-/-* nucleus accumbens (NAc) compared to WT, but not in the caudate putamen (CPu) (**W**). *RXRγ* is upregulated upon re-myelination (**Y**) of a lesion within the caudal cerebellar penduncle compared to unlesioned tissue (**X**). Treatment with the proposed RXR ligand 9-cis-RA increased remyelination of lesioned axons compared to saline treated mice (**Y**). A-F adapted from Sucov, H.M. et al (1994), G-L adapted from Kastner, P. et al (1994), M-U adapted from Kastner,

P. et al (1996), V-W adapted from Kyzkzosiak, A. et al (2010) and X-Z adapted from Huang, J.K. et al (2011).

1.4.8 Cytochrome P450 family 26

CYP26A1 was identified as the first member of a new cytochrome P450 family due to its up-regulation in ES cells directed towards neuronal differentiation by RA-induction (Ray 1997). By homology it was found to be the mammalian homologue of the zebrafish P450RAI, known to be capable of oxidising RA predominately to 4-oxo-RA and 4-OH-RA(White 1996). CYP26A1 expression was induced by RA in both ES cells, including those that are not being induced to neuronal fates, and in the adult mouse liver upon RA injection. CYP26A1 appears to be expressed within the adult mouse liver, brain and at low levels within the spinal cord. The expression in human is similar with expression observed in the liver, the brain and the placenta (Ray 1997). *Cyp26a1* is observed early in mouse development from E6 in both the embryonic endoderm and extra-embryonic tissue and these same regions express at E7 with the mesoderm beginning to express. The mesoderm expression increases and the primitive streak becomes positive at E7.25, with the anterior region of all the germ layers becoming positive at E7.5. This pattern is erased at E8 and by E8.5 the posterior region of the embryo becomes positive including the neural plate, tailbud and hindgut. Some expression is observed within the anterior region in the cranial neural crest cells. These regions of expression are maintained until E10.5 by which time the posterior expression region has become restricted to the tail end. Expression across the whole limb bud is weakly detected from E9.5 and then becomes restricted to the interdigital space at E11.5. The developing eye also shows expression in the dorsoventral boundary of the neural retina. In the later stages of development (E12-16), expression of Cyp26a1 decreased (Fujii 1997).

The phenotype of *Cyp26a1*-/- embryos is consistent with the expression pattern of the gene during development with sirenomelia (Figure 1.16 A&B), caudal truncations (Figure 1.16 C), spina bifida (Figure 1.16 D) and hindgut blind termination but the anterior of the embryo was generally spared but some embryos

did develop exencephaly (Figure 1.16 E). Defects could be first seen from E9.5 with posterior truncations noted with some embryos failing to close the neural tube. Severely affected embryos showed heart defects, incomplete axial rotation, irregular somites and neural tube (Figure 1.16 F). The defects of the posterior region also included horseshoe kidney and incomplete development of the urogenital system (Abu-Abed 2001; Sakai 2001).

CYP26A1 is required to maintain specific regions of RA signalling. Regions of active RA signalling, as defined by lacZ expression from the RARE-LacZ reporter, are expanded in the absence of CYP26A1 (Rossant 1991). Regions which would express normally express *Cyp26a1* and therefore would not have active RA signalling become positive for Lacz indicating inappropriate RA signalling in *Cyp26a1*-/- embryos (Figure 1.16 G&H) (Sakai 2001). Hox genes are known to be highly regulated by RA through a RARE at the 3' of the cluster (Marshall 1996) and therefore, unsurprisingly, homeotic transformations of both the hindbrain and the skeletal system are observed in *Cyp26a1*-/- animals. *Cyp26a1*-/- show an increase in the number of thoracic vertebrae associated with a rib, fusions of many of the cervical vertebrae and an anterior transformation of the first lumbar vertebrate to a thoracic fate (Figure 1.16 I). This posterior transformation of the caudal vertebrae is consistent with anterior expansion of the expression domain of *Hoxb1*, a marker of rhombmere 4 (Sakai 2001). *Cyp26a1*-/- embryos showed an increase in the size rhombomere 4 and, in addition, ectopic stripes and patches of *Hoxb1* positive cells were noted rostrally of their normal position within rhombomere 3 (Figure 1.16 J-L). CYP26A1 is not required to segment the hindbrain as rhombomere number and location were not disrupted in *Cyp26a1*-/- embryos. CYP26A1 is, however, required to determine rhobomere identity, as r2-3 are partially posteriorly transformed in *Cyp26a1*-/- (Abu-Abed 2001).

In addition to regulating RA synthesised by RALDH in the embryo, CYP26 enzymes are required before embryonic retinoic acid synthesis in order to restrict the effects of the maternal RA supply. In the absence of all the *Cyp26* genes, body axis duplication (Figure 1.16 M-S) is observed due to the activation of nodal, a RA responsive gene with a RARE within intron 1, across the entire epiblast before gastrulation (Figure

1.16 T&U) (Uehara 2009). RA must therefore be controlled spatially by catabolism from the very earliest stages of development due to its potent gene activation potential.

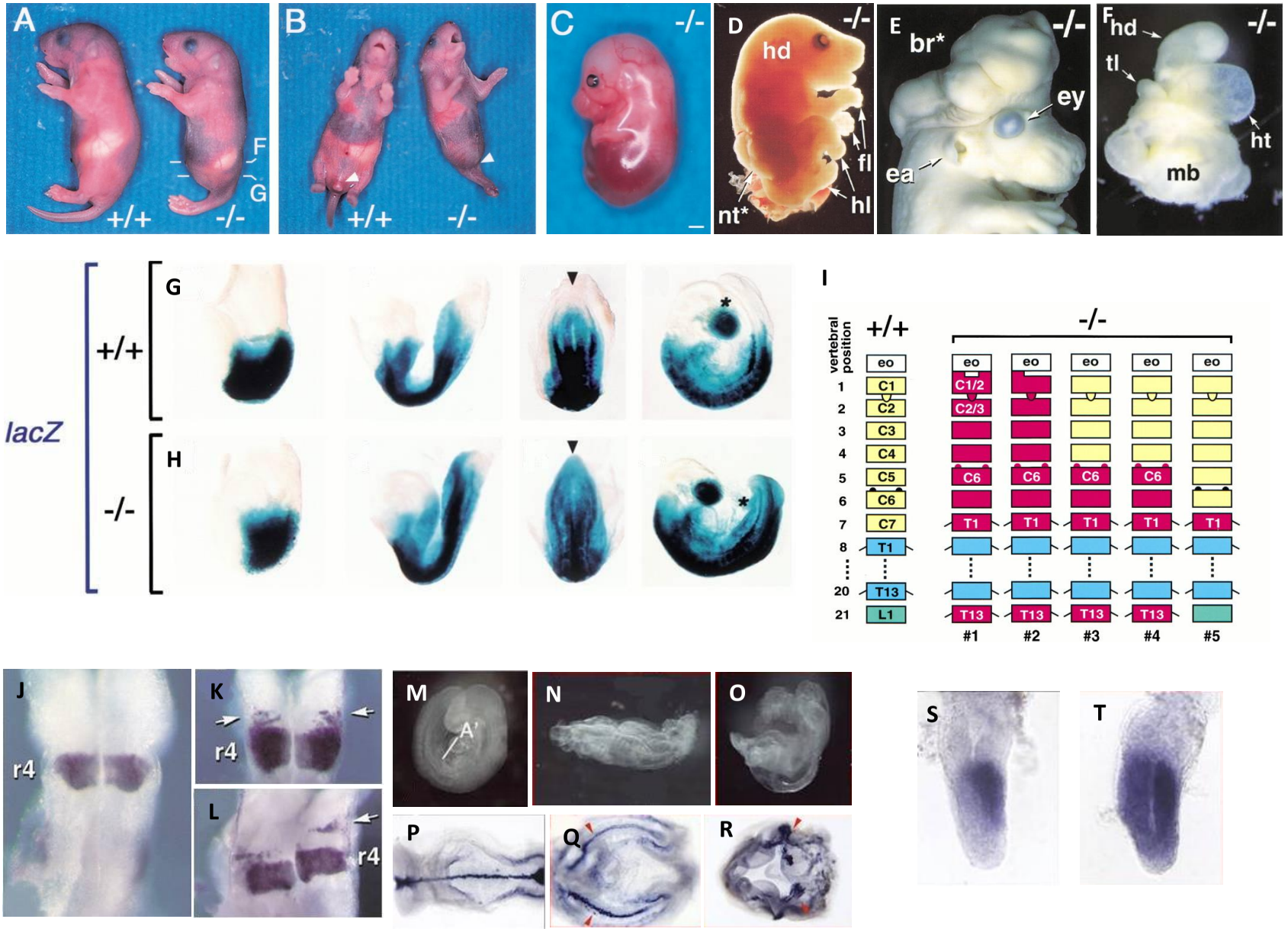
A
+/+
-/-
F
G
B
+/+
-/-
C
-/-
D
-/-
hd
fl
hl
nt*
E
br*
-/-
ey
ea
F
hd
-/-
tl
ht
mb
lacZ
+/+
-/-
G
H
I
vertebral position
+/+
-/-
eo
C1
C2
C3
C4
C5
C6
C7
T1
T13
L1
C1/2
C2/3
#1
#2
#3
#4
#5
J
r4
K
r4
L
r4
M
A'
N
O
P
Q
R
S
T

Figure 1.16 *Cyp26a1* is required for caudal development and all *Cyp26* genes are required to restrict the effects of maternal RA supply in early development.

Cyp26a1-/- embryos show sirenomelia and loss of the urogential opening (arrowheads) (**A**&**B**), complete caudal truncations (**C**) and spina bifida (*nt, **D**). Exencephaly was observed in some *Cyp26a1-/-* embryos (br*, **E**). Some *Cyp26a1-/-* embryos are severly affected at E9.5 with no axial rotation and heart defects (**F**). LacZ RA reporter expression is increased in the posterior of the embryo (arrowhead) of *Cyp26a1-/-* (**H**) compared to WT (**G**). Homeotic transformation of the vertebrae is observed in *Cyp26a1-/-* mutants compared to WT vertebrae arrangement (**I**). Loss of *Cyp26a1* causes an anterior expansion of the Hoxb1 expression domain. Hoxb1 expression is found exclusively in rhombomere 4 (r4) in WT embryos (**J**) but *Cyp26a1-/-* embryos show expansion of the expression domain (arrows, **K**) and expression within a stripe rostral to r4 (arrows, **M**). Loss of all *Cyp26* genes results in axial duplication (**N**&**O**) compared to WT (**M**) at E9.5 and staining for *Shh* highlighted the duplication of the embryo by staining the duplicate neural tube in *Cyp26-/-* embryos (**Q**&**R**) compared to WT (**P**). Nodal expression is restricted to the anterior portion of the WT embryo (**S**) but is expressed throughout the *Cyp26-/-* embryo (**T**). A-C adapted from Sakai, Y. et al (2001), D-F adapted from Abu-Abed, S. et al (2001), G-H adapted from Sakai, Y. et al (2001) and M-T adapted from Uehara, M. et al (2009).

1.5 Stimulated by Retinoic Acid 6 (Stra6)

1.5.1 Identification

Stra6 was first identified in a screen to find genes whose expression was up-regulated by RA. P19 embryonic carcinoma cells were treated with retinoic acid and up-regulated cDNAs identified by subtractive hybridisation. This method characterised 12 genes named *Stra1-12* respectively which could be divided into four classes according to their kinetics of RNA accumulation. *Stra6* fits into class III with *Stra6* RNA accumulating after 2 hours of RA treatment and not reaching plateau after 12 hours (Figure 1.17 A) (Bouillet 1995). Upon its identification as a retinoic acid inducible gene, a role for *Stra6* was unknown with the protein sequence giving limited clues to function as no conserved domains or motifs were found using multiple databases. STRA6 was found to have more than 50% hydrophobic residues (Figure 1.17 B) and predicted to contain nine trans-membrane domains (Bouillet 1997).

1.5.2 Expression – Adult

Expression analysis by RT-PCR in the adult mouse detected expression in the testis, spleen, kidney, brain and female genital tract, whereas little or no expression could be detected in the heart, lungs and liver (Figure 1.17 C). The areas of *Stra6* expression were enriched for those organs which have blood-organ barriers, such as brain, eye and testis (Bouillet 1997). Expression in the testis was restricted to the basal layer of the seminiferous epithelium in a tubule-stage dependent manner. *Stra6* positive tubules were also found to be *Stra8* positive, linking *Stra6* expression to premeiotic tubule stages VI and VII for which *Stra8* is a marker. In RARα-/- testis, *Stra6* and *Stra8* were expressed in all tubules (Bouillet 1997) suggesting that normally they are transcriptionally repressed by the binding of RARα in the absence of RA and activated in the presence of RA. *Stra6* expression in the adult eye is detected only within the RPE and the meninges surrounding the optic nerve (Bouillet 1997). *Stra6* expression within the RPE is concurrent with its role in the uptake of retinol ‘waste’ from photoreceptor-retinal isomerisation (Marmorstein 2001). *Stra6* was also expressed within the meninges of the brain, in addition to expression within

the choroid plexus and brain microvessels. The distribution of *Stra6* expression was not uniform amongst all capillaries but was not found in any other microvasculature of other adult organs. The endometrium and granulosa cells of the ovarian follicles are areas of strong *Stra6* expression within the female genital tract (Bouillet 1997). Retinoids are known to be important for the function of both of the endometrium (Kamelle 2002) and granulosa cells (Bagavandoss 1987) *in vitro*.

1.5.3 Expression – Embryo

1.5.3.1 Mouse

Developmental expression of *Stra6* is detected from E7.5 in the posterior mesoderm but excluded from the headfold mesoderm and the primitive streak (Figure 1.17 D). Mesoderm and its derivatives continue to express *Stra6* at E8.5 with expression observed in the neural plate, presomitic mesoderm and intermediate mesoderm at the level of the pronephric duct (which will later become kidney and genital tissue - sites of adult *Stra6* expression) (Figure 1.17 E). At E9.5, *Stra6* is expressed in the somites, gut, otocyst, pharyngeal pouch epithelium and parts of the developing brain – specifically the mid-hindbrain boundary and the forebrain (Figure 1.17 F). Expression within the developing brain and eye is consistent with later adult expression in derivatives of these tissues.

Sensory organ expression of *Stra6* increased from E11.25-12.5 in the nasal cavities, from E11.5 in the inner ear mesenchyme and by E15.5-16.5 the expression becomes restricted to the olfactory and respiratory mesenchymes and the respiratory epithelium. Expression in the eye was restricted to the retinal pigmented epithelium, inner nuclear layer, lens and the periocular mesenchyme from E9.5 to adulthood (Figure 1.17 F-I*)*.

Embryonic gut from E11.5 onwards expressed *Stra6* and expression was also seen in the submandibular salivary glands and tooth bud mesenchyme. Embryonic foregut derivatives, the lungs, have *Stra6* expression within the mesenchyme surrounding the bronchi.

Stra6 was found to be expressed in myogenic cells from around E11.5 and later within the skeletal muscle. *Stra6* is also expressed in the mesenchyme surrounding various chondrogenic condensations, being later restricted to the perichondrium and further restricted within this region to ossification centres by E16.5 (Figure 1.17 I).

Expression of *Stra6* in the genital tract of both the female and male embryo was observed from E16.5, specifically the epithelia and mesenchyme of the oviduct and uterus and the vas deferens and seminiferous tubules of the fetal testes. Expression was observed from the mesonephric mesenchyme to the definitive kidney stages, within renal cortex and metanephric collecting tubules, of kidney development (Figure 1.17 H&I) (Bouillet 1997).

1.5.3.2 Chick

Expression of *STRA6* was detected in Hensen's node at stage 4 (Figure 1.17 J) in the chick and was maintained in the mesoderm of the node at stage 5 (Figure 1.17 K), but was absent from the primitive streak. Mesodermal cells migrating away from the node lost expression as they moved further away (Figure 1.17 L-N) and a cup shaped domain of expression is formed around the node at stage 7 and 8 (Figure 1.17 O&P). The newly formed somites at stage 8 (Figure 1.17 P) also express *STRA6*, with this expression in the somites a constant feature throughout development (Figure 1.17 P-U). The newly formed somites are stained throughout with older somites adopting a higher level of expression along their medial edge at stage 10 onwards (Figure 1.17 R-U). At later stages, stage 16 for rostral somites (Figure 1.17 T) and stage 20 for more posterior somites (Figure 1.17 U), the expression becomes further restricted to only the posterior medial region. Expression within the node is re-activated from stage 9 (Figure 1.17 Q) onwards and from stage 11 this expression is specifically in the anterior part of the node. At stage 16, expression within the mesenchyme surrounding the hindbrain at the level of rhombomere 3-7 is detected (Figure 1.17 T). As in mouse expression was detected within the developing eye, specifically the retinal pigmented epithelium from stage 16 (Figure 1.17 T&U), and within the mesonephros, a precursor to the kidney (Reijinjes 2010).

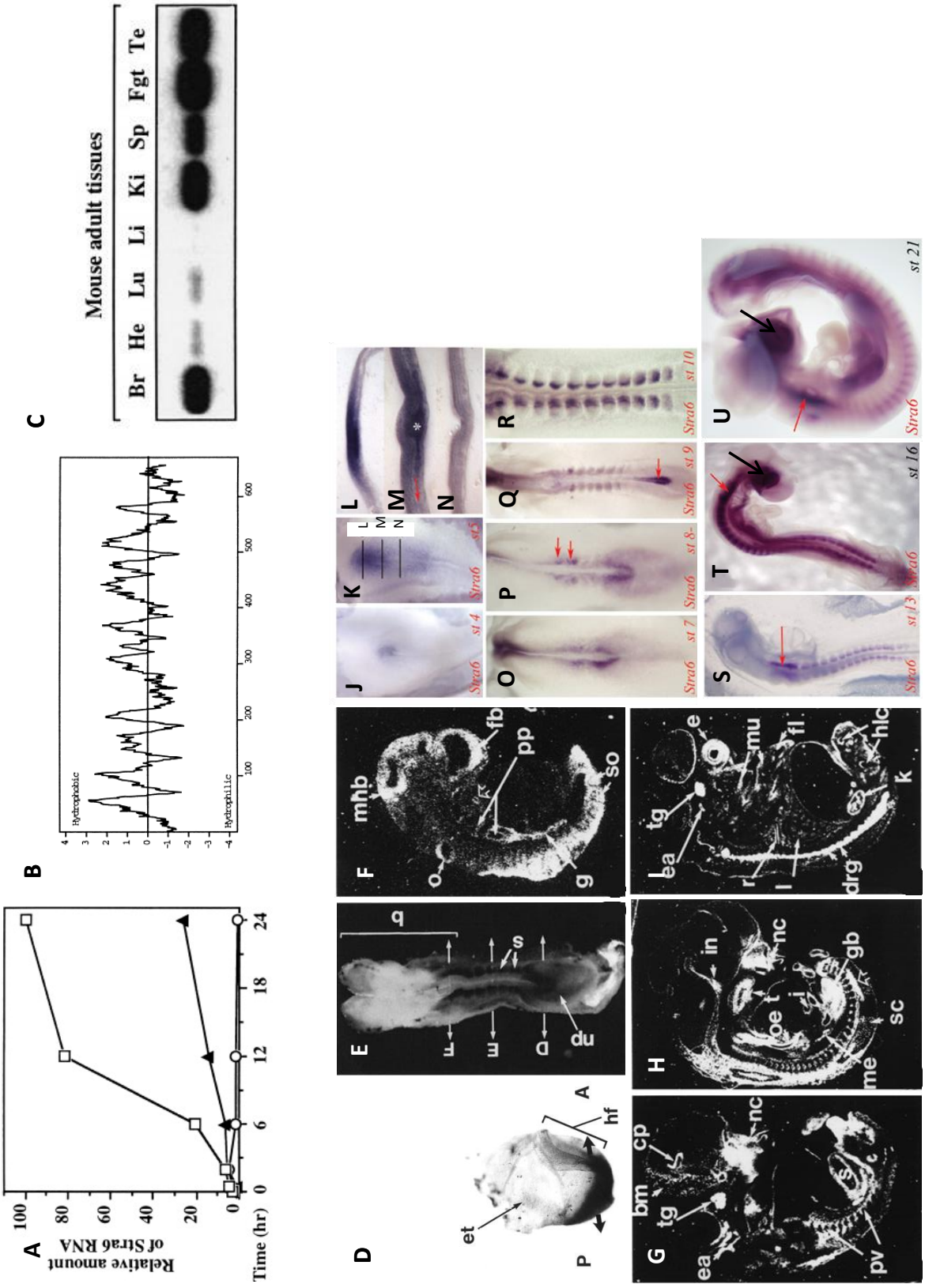
A
Relative amount of Stra6 RNA
Time (hr)
B
Hydrophobic
Hydrophilic
C
Mouse adult tissues
Br He Lu Li Ki Sp Fgt Te
D
E
F
G
H
J
K
L
M
N
O
P
Q
R
S
T
U
st 4
st5
st 7
st 8-
st 9
st 10
st 13
st 16
st 21
Stra6

Figure 1.17 *Stra6* is retinoic acid-inducible and expressed in both the adult and embryo.

Stra6 expression is up-regulated by RA (**A**) in a concentration dependent manner (filled triangle: 10nM RA, open square: 1µM) in P19 cells compared to control treated cells (open circles: ethanol) over 24 hours. Hydrophobicity plotted across the protein (**B**) highlights over 50% of the protein is hydrophobic. *Stra6* expression was detected in adult mouse tissues using RT-PCR (**C**). Stra6 expression was detected by in situ hybridisation in the E7.5 embryo (**D**) in the posterior (P) mesoderm, but excluded from the headfold mesoderm (hf), and in the E8.5 embryo (**E**) in the neural plate (np) and the somites (s). *Stra6* is expressed in various tissues at E9.5 (**F**), including mid-hindbrain barrier (mhb), forebrain (fb), pharyngeal pouches (pp), somites (so) and gut (g). Expression is further observed at E11.5 (**G**), E12.5 (**H**) and E13.5 (**I**) in various tissues. Brain microvasculature, bm; Ear, ear; Eye, e; genital bud, gb; hindlimb cartilages, hlc; kidney, k; lung, l; meninges, m; muscles, mu; nasal cavaties, nc; otocyst, o; prevertebrae, pv; somite, so; stomach, s. *Stra6* expression in the chick is observed from stage 4 (**J**) and at stage 5 (**K**) is maintained in the mesoderm of the node. Position of the figures **L**, **M** and **N** is indicated on **K**. **L-N** show loss of *Stra6* expression by migratory cells away from the node. Expression around the regressing node is seen at stage 7 (**O**) and the first formed somites (red arrows) are *Stra6* positive at stage8 (**P**). The node re-expresses at stage 9 (**Q**) and expression within the somites is restricted to the medial end by stage 10 (**R**). The hindbrain mesenchyme is positive at stage 13 (red arrow, **S**), stage 16 (red arrow, **T**) and stage 21 (**U**) and the developing eye at stage16 (black arrow, **T**) and stage 21 (black arrow, **U**). A-I adapted from Bouillet, P. et al (1997) and J-U adapted from Reijntjes, S. et al (2010).

1.5.4 Function

The function of STRA6 has been known for some time, although not attributed to the *Stra6* gene itself. The existence of a membrane protein capable of binding RBP4 and transporting retinol intracellularly to be met by CRBP had been known since 1975. The transient nature of RBP-STRA6 binding made identification of the RBP4 receptor technically challenging; however in depth information about the kinetics of the binding interaction and the location of the receptor were known. Retinol-RBP (holo-RBP) was found to bind in a linear function with the number of binding sites, in this case number of retinal pigmented epithelium cells, being directly proportional to the amount of labelled-RBP specifically bound (Figure 1.18 A). Bound RBP-retinol could be displaced easily by other retinol-RBP complexes; however, apo-RBP (RBP without retinol) was less effective at displacing holo-RBP from the receptor (Figure 1.18 B). Even this early work defined some important features of the RBP-receptor, such that one RBP-retinol binds to a single binding site within the STRA6 protein and the internalisation of retinol-RBP is not dependent on endocytosis (Heller 1975). The membrane localised retinol-RBP receptor (Figure 1.18 C, upper panel) was also known to transfer retinol to CRBP in a specific manner, with other proteins capable of binding retinol not interacting with the receptor (Figure 1.18 C, lower panel) (Sundaram 1998).

Identification of *Stra6* as the retinol-RBP receptor used a bi-functional crosslinker to link His-tagged RBP to its receptor. The crosslinker, sulfosuccinimidyl-6-[4´-azido-2´-nitrophenylamino]hexanoate, was first linked to his-RBP by reaction with a primary amine group and then combined with RPE membranes to allow binding. Interactions were stabilised by UV crosslinking, which activated the nitrophenyl azide group, covalently linking RBP with its receptor allowing purification through the His tag on RBP (Figure 1.18 D). This method isolated an 80kDa complex, which was identified by mass spec as containing STRA6 (Figure 1.18 E) (Kawaguchi 2007).

Mutational analysis of a region of the protein from the intracellular loop between transmembrane domains V and VI to the end of the extracellular loop before transmembrane domain VII revealed three amino acids which appear required for

RBP binding; namely Y336A, G340L, and G342L (Figure 1.18 F). Interestingly the human polymorphism G399S (equivalent to G340) significantly reduces RBP4 binding to around 10% of WT (Kawaguchi 2008).

STRA6 also functions to catalyze the release of retinol from RBP and this action is inhibited by free intracellular retinol thereby regulating free retinol levels intracellularly. STRA6 is also able to catalyze retinol loading to apo-RBP when intracellular free retinol concentrations are high and the actions of LRAT to convert retinol to retinyl esters prevents this loading action (Figure 1.18 G) (Kawaguchi 2011). This mechanism therefore ensures retinol transported by STRA6 is effectively stored as RE by LRAT and prevents high concentrations of intracellular free retinol which could be metabolised to RA causing non-specific gene activation.

STRA6, in addition to its role in retinol transport, has a role in signalling through the JAK-STAT pathway in an RBP4-retinol dependent manner. STRA6 contains, within the long intracellular C-terminal tail, a Src Homology 2 (SH2) domain in the sequence YTLL (Figure 1.19 A). SH2 domains recognise phosphorylated tyrosine residues on other proteins allowing recognition and specific interaction between proteins (Russell 1992). Exposure of cells over-expressing *Stra6* to RBP-ROH increases the level of tyrosine phosphorylation within the protein (Figure 1.19 B) and this effect was abrogated when cells over-expressed mutant *Stra6* in which either the tyrosine or theonine residue of the YTLL binding motif were substituted for alternative amino acids (Figure 1.19 C). In the presence of RBP-ROH, the association between STRA6 and STAT5 increased (Figure 1.19 D). JAK2 was also found to associate and become phosphorylated in response to RBP-ROH (Figure 1.19 E&F). RBP-ROH therefore activates a STRA6 dependent STAT5/JAK2 signalling cascade. This signalling cascade has functional consequences with the transcriptional activity of STAT5 being increased in response to RBP-ROH (Berry 2011). STAT5 forms dimers which act as transcription factors. STAT5 must be activated by tyrosine phosphorylation before it is able to translocate to the nucleus and bind to STAT5 response elements. RBP-ROH increases the transcriptional output of a luciferase reporter driven by STAT5 response elements (Figure 1.19 G)

and also increased transcription of known STAT5 target genes *SOCS3* and *PPARγ* (Figure 1.19 H). The effects of RBP-ROH on the phosphorylation and association of STAT5, JAK2 or STRA6 and the increase in STAT5 dependent transcription was specific. Treatment with RA, RAL or ROH and apo-RBP was unable to elicit the same response (Figure 1.19 I&J) and shows a specific role of RBP bound ROH separate from its action as a precursor for RA (Berry 2011). The ability of Stra6 to act as mediator for RBP-ROH on STAT5 dependent transcription of *SOCS3* and *PPARγ* may explain the suggested link between Stra6 and diabetes, which will be discussed further below.

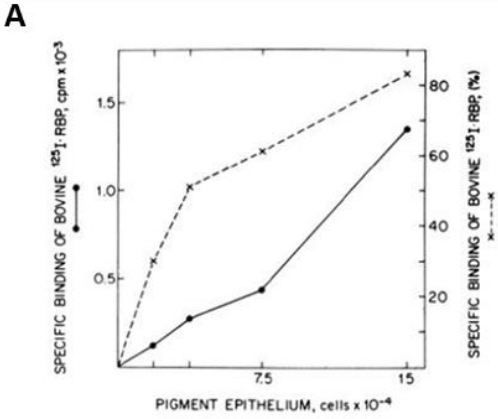

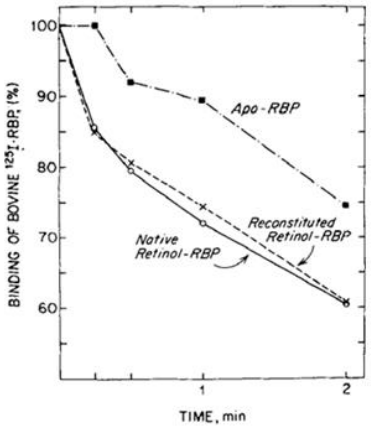

C

Experimental condition	[^{3}H]Retinol transferred to CRBP
	dpm
No membranes	2826 ± 300
PBS-treated membranes	9876 ± 806
Heat-denatured membranes	2368 ± 345
pCMBS-treated membranes	3227 ± 239
Erythrocyte membranes	1841 ± 165

Acceptor protein	[^{3}H]Retinol transferred from RBP
	dpm
None	752 ± 144
Apo-CRBP	15,660 ± 576
Holo-CRBP	1,440 ± 20
Human serum albumin	4,492 ± 300
β-Lactoglobulin	4,888 ± 45

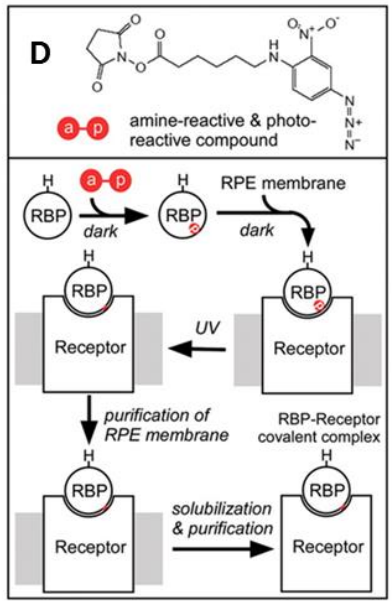

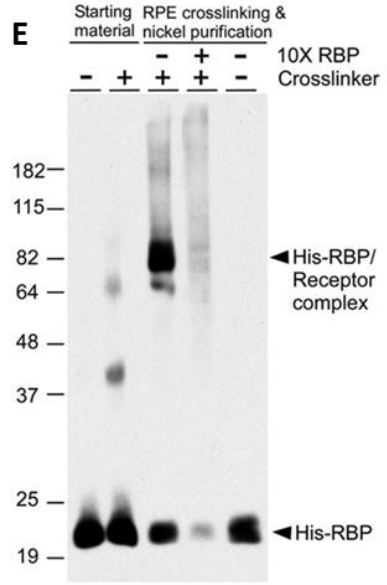

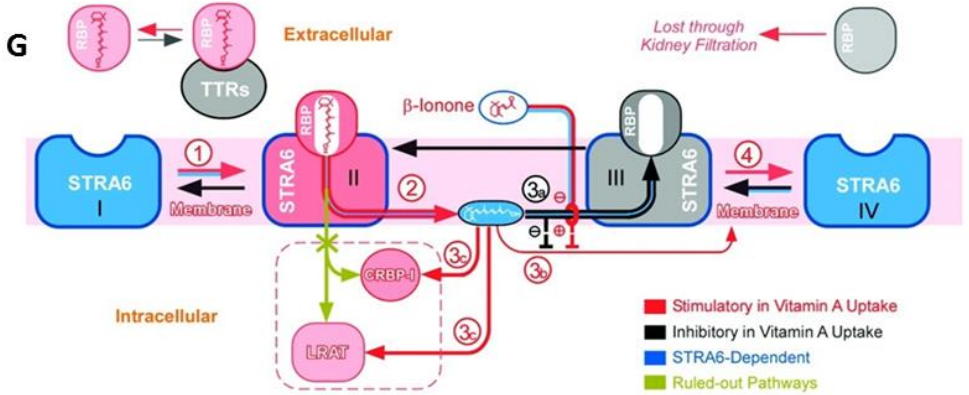

Figure 1.18 *Stra6* acts as an RBP4 receptor and transporter for retinol bound to RBP4.

Specific RBP4 binding is a linear function of RPE cell number (**A**) and bound-RBP4 could be removed by other RBP-retinol (circles, crosses) complexes but not as effectively by apo-RBP (squares, **B**). STRA6 is a membrane protein (**C**, upper panel) and transfers retinol specifically to CRBP (**C**, lower panel) and not to other proteins able to bind retinol. STRA6 was identified as the RBP4 receptor/retinol transporter via a novel UV activated crosslinker method (**D**) which allowed STRA6 to be identified via mass spectrometry (**E**). Mutational analysis of STRA6 identified the three amino acids essential for RBP4 binding and consistent with this these residues were evolutionarily conserved (**F**). Further investigation of STRA6 highlights a complex regulatory loop to prevent intracellular build-up of free retinol (**G**). A-B adapted from Heller, J. (1975), C adapted from Sundaram, M. et al (1998), D-E adapted from Kawaguchi, R. et al (2007), F adapted from Kawaguchi, R. et al (2008) and G adapted from Kawaguchi, R. et al (2011).

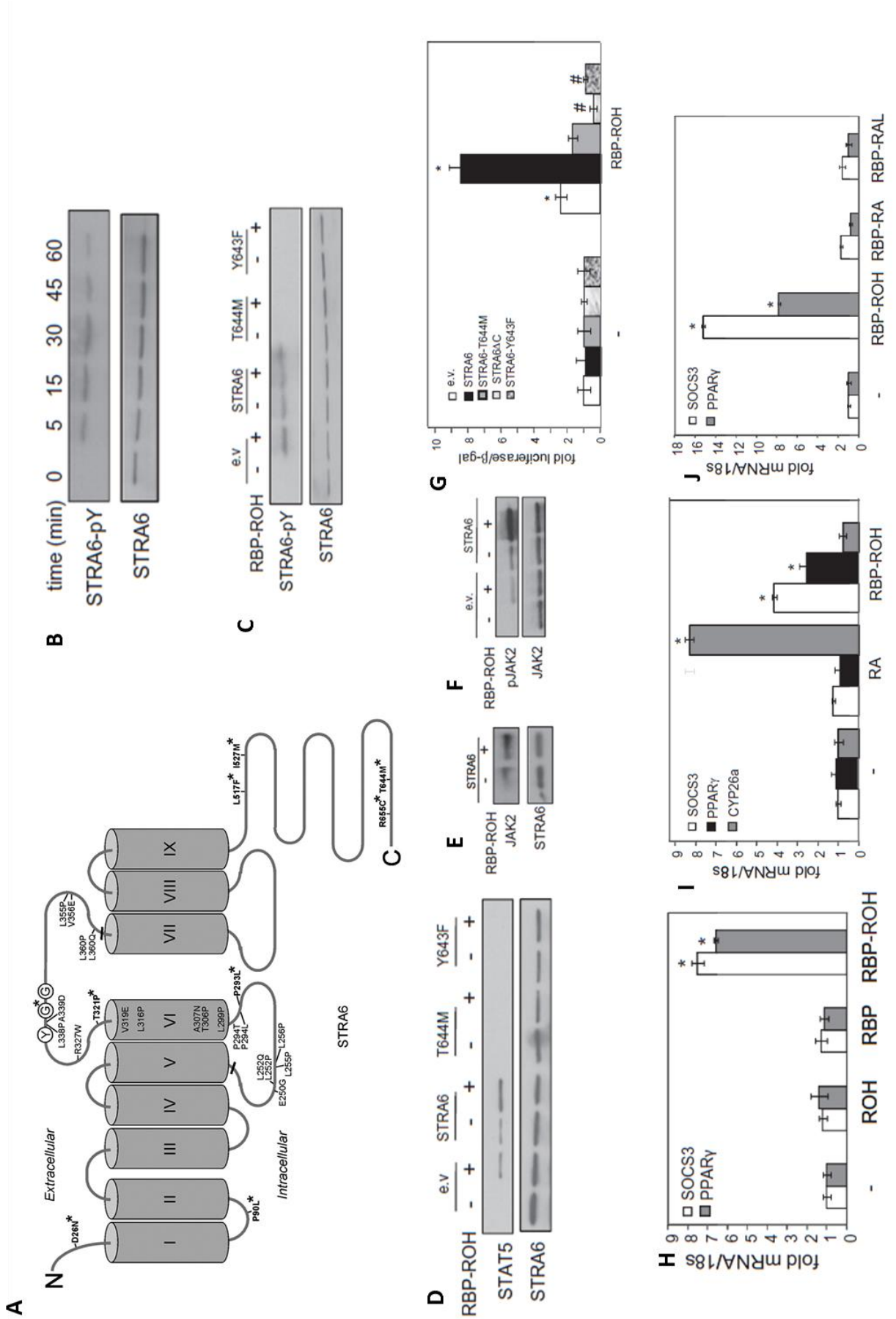
A
N
Extracellular
Intracellular
STRA6
D26N*
P90L*
R327W
L338P A339D
T321P*
V319E
L316P
A307N
T306P
L299P
P294T
P294L
P293L*
L252Q
L252P
E250G
L255P
L256P
L355P
V356E
L360P
L360Q
L517F* I527M*
R655C* T644M*
B
time (min) 0 5 15 30 45 60
STRA6-pY
STRA6
C
e.v STRA6 T644M Y643F
RBP-ROH
STRA6-pY
STRA6
D
e.v STRA6 T644M Y643F
RBP-ROH
STAT5
STRA6
E
STRA6
RBP-ROH
JAK2
STRA6
F
e.v. STRA6
RBP-ROH
pJAK2
JAK2
G
e.v.
STRA6
STRA6-T644M
STRA6ΔC
STRA6-Y643F
fold luciferase/β-gal
RBP-ROH
H
SOCS3
PPARγ
fold mRNA/18s
- ROH RBP RBP-ROH
I
SOCS3
PPARγ
CYP26a
fold mRNA/18s
- RA RBP-ROH
J
SOCS3
PPARγ
fold mRNA/18s
- RBP-ROH RBP-RA RBP-RAL

Figure 1.19 STRA6 facilitates RBP-retinol dependent signalling through the JAK-STAT pathway.

The predicted structure of STRA6 features a C-terminal intracellular tail which contains a SH2 domain (**A**). The tyrosine within this domain becomes phosphorylated upon exposure to RBP-retinol (**B**) and this is dependent upon the SH2 domain with STRA6 proteins mutated in this motif (T644M, Y643F) not being phosphorylated in response to RBP- retinol (**C**). RBP-retinol also causes an increase in STAT5 association with STRA6 and this association is also dependent on the SH2 domain (**D**). JAK2 also associates with STRA6 (**E**) and becomes phosphorylated in response to RBP-retinol (**F**). RBP-retinol activates a luciferase reporter driven by STAT response elements and this activation requires the functional SH2 domain (**G**). STAT target genes *SOCS3* and *PPARγ* are also activated by RBP-retinol but not RBP or retinol alone (**H**). The transcriptional response to RBP-retinol is not due an increase in RA- responsive gene expression (**I**) and only RBP-retinol, and not any other RBP-bound retinoid, is able to elicit this transcriptional response (**J**). A adapted from Kawaguchi, R. et al (2008) and B-J adapted from Berry, D.C. et al (2011).

1.5.5 Matthew-Wood syndrome

Anophthalmia is seen in around 30 people per 100,000 population (Verma 2007) and pulmonary hypoplasia at an incidence of 14 per 10,000 births (Laudy 2000); however the combination of these developmental disorders is rare and is generally described as Matthew-Wood syndrome. The first case reported was in 1978, in which a premature stillborn infant was described with bilateral anophthalmia and pulmonary agenesis (Ostor 1978). The syndrome was named in 1996, at the request of the parents of a sib pair with pulmonary hypoplasia and bilateral anophthalmia. The first child was born at 38 weeks upon induction and survived only one hour presumably due to the malformations of the lungs observed upon autopsy (bilateral unipolar lung). The orbits were recessed, the palpebral fissures were barely opened and upon autopsy the orbits were found to contain mostly fat tissue although the optic nerve was intact (Figure 1.20 A). After a second normal birth, a second affected foetus was terminated due to the discovery of bilateral anophthalmia and hypoplastic lungs upon a scan. In addition to the eye and lung defects; micrognathia, a midline cleft of the secondary palate, low-set ears, hypoplastic spleen and the heart had a single ventricle with a hypoplastic left atrium were noted (Seller 1996). Further cases were reported in 2006 (Li 2006) and two separate reports in 2007 of two terminated foetuses (Martinovic-Bourial 2007) and eight cases, including three sibs and a surviving patient of 9.5 years (Chitayat 2007). The report of eight cases also suggested a new name for the condition to be PDAC syndrome (Pulmonary hypoplasia, Diaphragmatic hernia, Anophthalmia, Cardiac defects) which highlights the main features of the condition (Figure 1.20 B-E).

Homozygosity mapping of probands and parents highlighted a single locus on chromosome 15 with a LOD score of 4.8 (Figure 1.20 F). Sequencing of candidate genes within this region discovered homozygous mutations within *STRA6* (Figure 1.20 G&H). Thirteen further patients with clinical similarities to the mapped probands were assessed for mutations within *STRA6*; four new mutations were identified in three of these patients (Pasutto 2007). Sequence analysis of *STRA6* in another two probands highlighted an insertion and a deletion respectively resulting in

a premature stop codon in both cases (Golzio 2007). Further mutations were identified in a third sequencing study, which included two living patients. The living patients may represent a milder presentation of the syndrome perhaps due to their compound heterozygous mutation status. However a sister died within the first few days of life with cardiac defects and anophthalmia (Chassainq 2009), it is therefore also possible that variation in the condition can exist even between patients with the same mutation profile within *STRA6*.

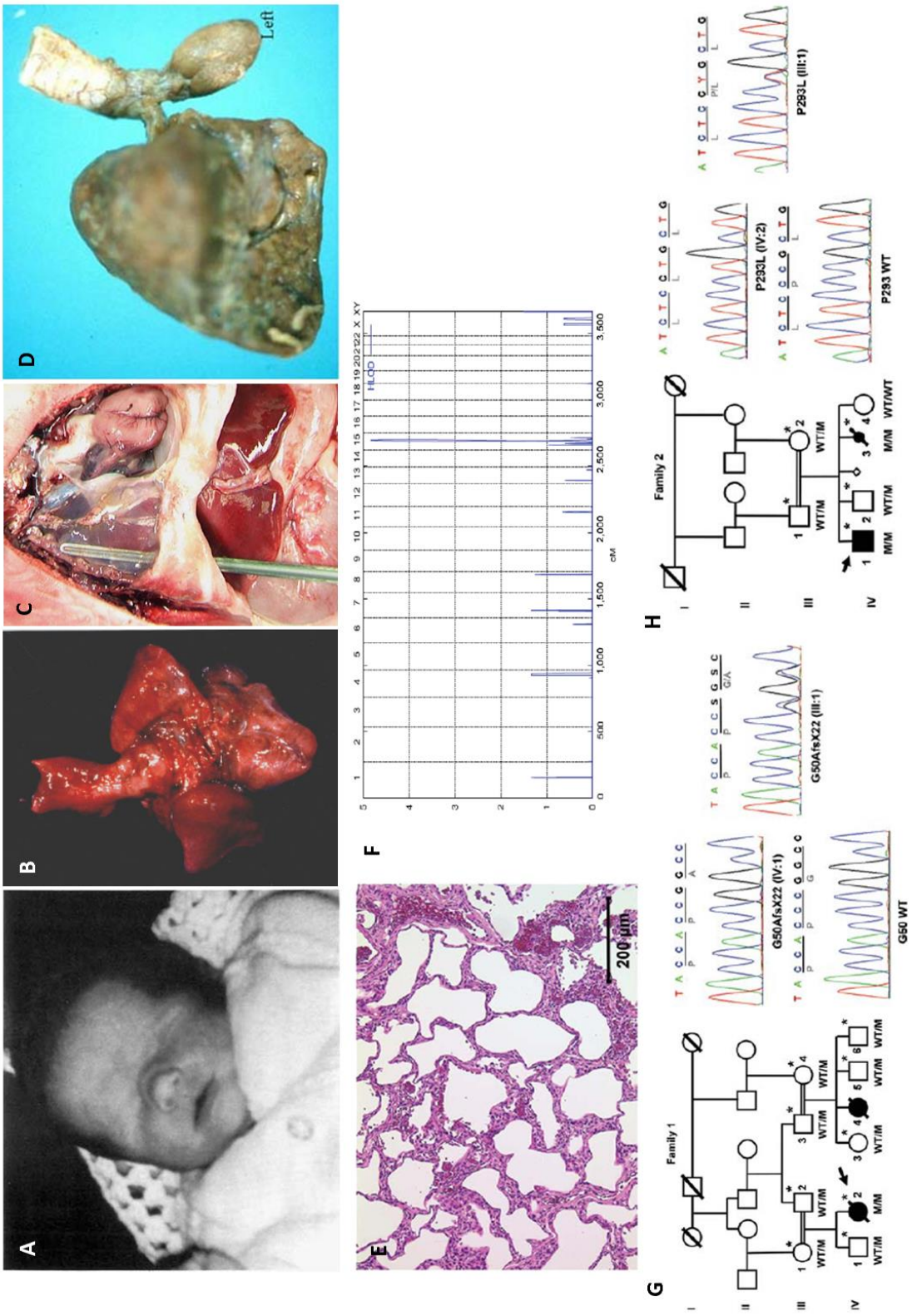
A
B
C
D
Left
E
200 µm
F
cM
G
Family 1
G50AfsX22 (IV:1)
G50 WT
G50AfsX22 (III:1)
H
Family 2
P293L (IV:2)
P293 WT
P293L (III:1)

Figure 1.20 Matthew-Wood syndrome is caused by homozygous mutations in *STRA6*.

Matthew-Wood patients present with anophthalmia, deeply recessed orbits and very short palpebral fissures (**A**). Dissection of the cardiopulmonary block indicated the presence of only the upper lung lobes on both the right and left side with dilation of the right ventricle, atrium and superior vena cava of the heart (**B**). Diaphragmatic hernia is observed in Matthew-Wood patients, probe indicates location of diaphragmatic eventration (**C**). Lung size is greatly reduced in some Matthew-Wood patients with small right lung and rudimentary left lung observed in this patient (**D**) and pulmonary hypoplasia can be noted on sectioning of lung tissue (**E**). Homozygosity mapping of two affected families resulted in a significant peak in chromosome 15 (**F**). Sequencing of candidate genes, within this region of homozygosity, in two families revealed mutations in *STRA6* (**G**&**H**). A adapted from Seller, M.J. et al (1996), B adapted from Li, L., & Wei, J. (2006), C adapted from Martinovic-Bouriel, J. et al (2007), D adapted from Chitayat, D. et al (2007) and E-H adapted from Pasutto, F. et al (2007).

1.5.6 Diabetes

A case-control study of type 2 diabetes identified a significant association of SNPs within Stra6 with type 2 diabetes in a Dravidian ethnicity group from Kerala, South India. Three SNPs, namely rs974456, rs736118 and rs4886578, were all found to be significantly associated with type-2 diabetes (Figure 1.21 A). The minor alleles of all the SNPs were associated with a decreased risk of type 2 diabetes. Haplotype analysis revealed that haplotype 1 (GGC), consisting of the major alleles, was more often observed in cases (61.8% vs. 56.9%) whereas haplotype 2 (AAT), consisting of the minor alleles, was more often observed in controls (12.5% vs. 9.4%) (Nair 2010).

Identification of a possible role for *STRA6* in susceptibility to type-2 diabetes provides a biological link between observations of changes to RBP4 level in diabetic patients. In both human diabetics and a mouse model of type 2 diabetes, serum RBP4 level was found to be elevated (Figure 1.21 B). Over-expression of *RBP4* in normal mice also resulted in insulin resistance (Figure 1.21 C) and deletion of *RBP4* enhanced insulin sensitivity (Figure 1.21 D) (Yang 2005).

The role of *Stra6* in JAK-STAT signalling provides explanation to the link between STRA6, RBP4 and diabetes. In an adipocyte cell model, RBP-ROH was also able to trigger phosphorylation of STAT5 and up-regulate SOCS3 and PPARγ expression in a STRA6 dependent manner. PPARγ is known to regulate lipid storage and as such RBP-ROH, in the presence of STRA6, increases triglyceride accumulation (Figure 1.21 E). RBP-ROH also influences insulin receptor function through SOCS3. Both direct, insulin receptor autophosphorylation (Figure 1.21 F), and downstream, phosphorylation of insulin receptor effector AKT1 (Figure 1.21 G), actions of the insulin receptor were inhibited by RBP-ROH. GLUT4 translocation to plasma membranes in response to insulin activity was also decreased in adipocytes pre-treated with RBP-ROH (Figure 1.21 H). Phosphorylation of STRA6, STAT5 and JAK2 and increased expression of SOCS3 and PPARγ were also seen in an *in vivo* mouse model injected with RBP (Figure 1.21 I) (Berry 2011). These observations of ability of STRA6 to act a facilitator for the effect of RBP-ROH on transcription provide a mechanism for the long reported link between RBP expression levels and diabetes.

A

SNP ID	Gene	Allele major/minor	MAF		OR (95%CI)	*P/P**	*P*(add)
			Cases	Control			
rs974456	*STRA6*	*C/T*	0.25	0.30	0.79(0.69–0.91)	**0.001/0.012**	**0.003**
rs736118	*STRA6*	*G/A*	0.30	0.35	0.81(0.71–0.93)	**0.003/0.036**	**0.01**
rs4886578	*STRA6*	*G/A*	0.12	0.16	0.74(0.62–0.89)	**0.001/0.012**	**0.0009**
rs3758538	*RBP4*	*A/C*	0.19	0.18	1.06(0.9–1.2)	0.43/NS	0.63
rs3758539	*RBP4*	*G/A*	0.33	0.35	0.91(0.79–1.04)	0.18/NS	0.48
rs36014035	*RBP4*	*T/G*	0.43	0.42	1.02(0.9–1.16)	0.71/NS	0.18
rs34571439	*RBP4*	*T/G*	0.35	0.36	0.93(0.82–1.07)	0.35/NS	0.63
rs2654185	*GLUT4*	*C/A*	0.37	0.36	1.01(0.89–1.15)	0.83/NS	0.5
rs5412	*GLUT4*	*G/A*	0.29	0.31	0.88(0.76–1.01)	0.07/NS	0.05
rs5418	*GLUT4*	*A/G*	0.37	0.40	0.89(0.77–1.02)	0.09/NS	0.25
rs5435	*GLUT4*	*G/A*	0.29	0.32	0.87(0.76–1.00)	0.05/NS	0.1

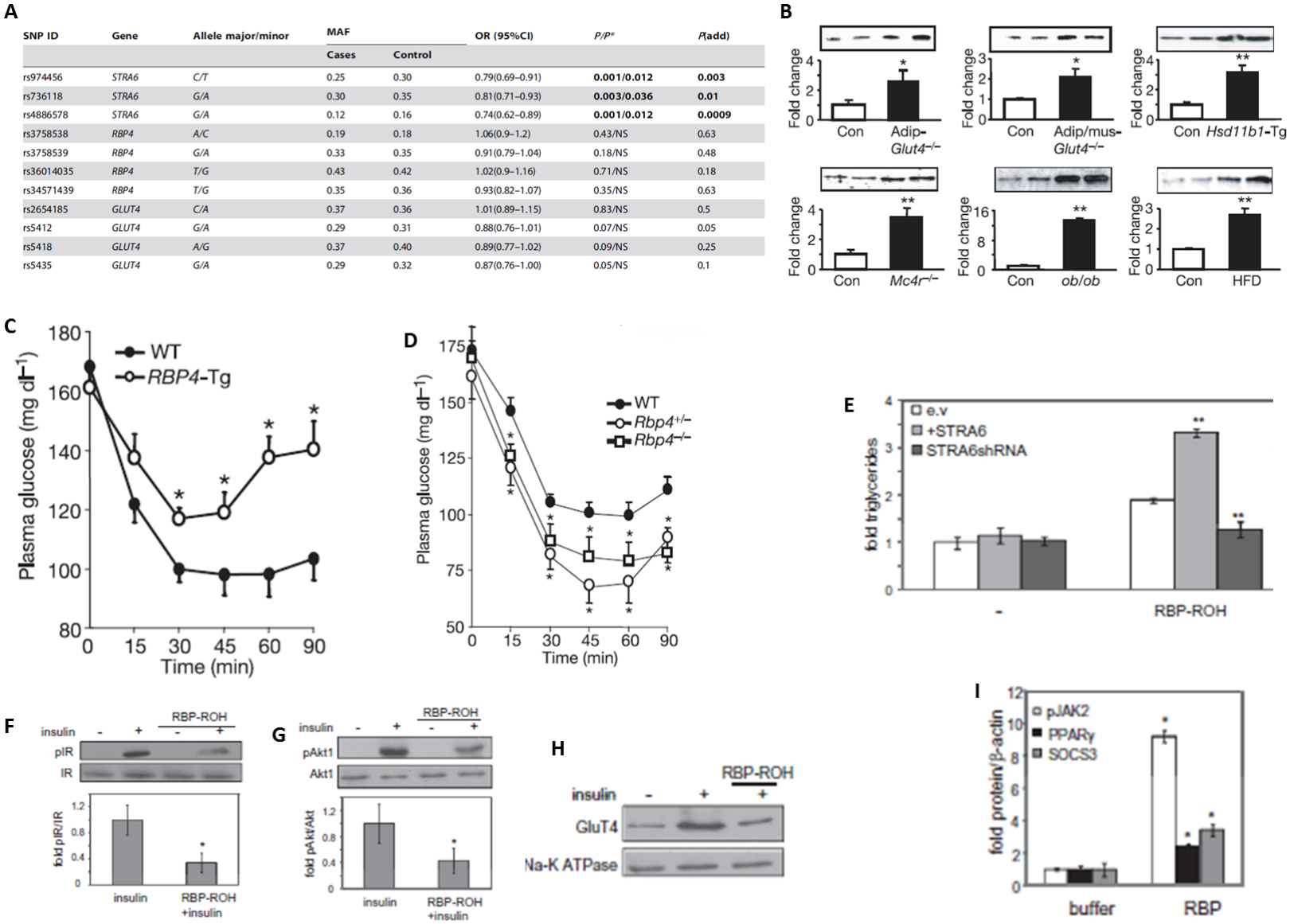

Figure 1.21 A link between STRA6 and diabetes?

SNPs within *STRA6* are significantly associated (bold type) with diabetes in a South Indian population (**A**). RBP4 is known to overexpressed in various mouse models of insulin-resistant diabetes (**B**): Adip/mus-*Glut4*$^{-/-}$, *Glut4* knockout in either adipose or muscle respectively; *Hsd11b1*-Tg, overexpression of hydroxysteroid 11-β dehydrogenase-1; *Mcr4r*$^{-/-}$, melanocortin 4 receptor knockout. Increased RBP4 expression in RBP4 transgenic mice (*RBP4*-Tg) resulted in insulin-resistance(**C**) and reduction in RBP4 through gene knockout (*Rbp4+/-*, *Rbp4-/-*) caused an increase in insulin sensitivity (**D**). STRA6 regulates RBP-retinol dependent triglyceride accumulation (**E**). RBP-retinol inhibits insulin signalling in both the direct phosphorylation of the insulin receptor (**F**) and downstream activation of the effector Akt1 (**G**). GLUT4 translocation to the plasma membrane was also inhibited upon treatment with RBP-retinol (**H**). RBP injection into the mouse also results in an increase in JAK2 phosphorylation and an up-regulation in PPARγ and SOCS3 expression (**I**). A adapted from Nair, A.K. et al (2010), B-D adapted from Yang, Q. et al (2005) and E-I adapted from Berry, D.C. et al (2011).

1.6 Development of the eye

The importance of retinoids to development of the eye is unmistakable in the phenotypes observed in various retinoid pathways mutants. One of the defining characteristics of Matthew-Wood syndrome is clinical anophthalmia and therefore an understanding of eye development and the mechanism of actions of retinoids in this process is pertinent to the understanding of this developmental disorder.

Vertebrate eye development begins with the specification of part of the anterior neuroectoderm as the retinal anlage at the end of gastrulation. *Otx2* is required to specify the anterior neuroectoderm, from which the retinal anlage will be form, but down-regulation of *Otx2* is required at the end of gastrulation in the medial region of its expression domain in order to allow eye field specification. *Rx1* is then expressed solely within the eye field and in complete isolation from the surrounding *Otx2* positive tissue. *ET*, *Pax6*, *Six3* and *Lhx2* are also expressed in the eye field at this inductive phase (Chow 2001). The eye field divides into two symmetrical retinal primordial and, although, the eye field is specified physiologically at the cellular level during gastrulation it remains morphologically indistinguishable until the early neurula (Graw 1996).

In the early neurula stage, the bilateral evagination of the diencephalon forms the optic pit in mammals and can be divided into the presumptive neural retina and RPE in the dorso-distal region and the presumptive ventral optic stalk in the proximo-ventral region. The fate of these opposing domains is specified by mutually exclusive expression of *Pax2* and *Pax6* by reciprocal repression. This results in *Pax2* expression within the ventral future optic stalk region and *Pax6* expression within the dorsal future neural retina (Chow 2001). The optic pit, through further evagination of the optic primordia, forms the optic vesicle and the morphological changes required for the formation of this structure bring it into contact with the non-neural surface ectoderm. The mesenchyme between these structures becomes displaced and the inductive signals passed between the optic vesicle and the surface ectoderm are facilitated by a network of cytoplasmic processes and collagenous fibrils. The interaction of the optic vesicle with the surface ectoderm initiates the thickening of the surface ectoderm to form the lens placode, the first morphological sign of lens

formation. Crystallin expression is also initiated concordantly with these morphological changes and specifies the future lens molecularly, as well as morphologically (Chow 2001).

The lens vesicle and the optic cup form upon co-invagination of both the lens placode and the optic vesicle (Jean 1998). The optic cup at this stage can be divided into the neural retina, positioned interiorly closest to the lens vesicle, and the RPE, forming the outer region. In the ventral region of the optic vesicle, a groove forms which passes through the neural retina and optic stalk to its junction with the neural tube. This groove is known as the choroidal fissure at the point in which it fuses within the optic cup and provides a channel for the growing blood vessels and projecting axons from the eye (Chow 2001).

The empty cavity within the newly formed lens vesicle is filled with the primary lens fibres formed from an elongation of the epithelia cells in the posterior of the lens vesicle. These cells lose their nuclei as they elongate and begin to synthesise crystallin. The anterior region of the lens remains epithelial in nature and becomes quiescent, whereas those cells in the equatorial region continue to proliferate (Graw 1996). These cells arising in the equatorial region become secondary lens fibres through elongation, crystallin expression and loss of cellular organelles (Chow 2001). This process occurs throughout life, albeit at a slower rate, with new secondary lens fibres produced on the outer regions to replace those lost in the central region of the lens (Graw 1996).

The cornea is induced via interaction between the surface ectoderm and the lens vesicle which specifies the corneal epithelium. The expression of collagen-rich extracellular matrix by the corneal epithelium creates a primary stroma, which attracts neural crest-derived mesenchymal cells, in turn leading to the hydration of the region resulting in the attraction of a second wave of neural crest-derived mesenchymal migration into the region. The hard, transparent cornea of the adult is formed upon the increase in thyroxine levels, which results in dehydration and compaction of the immature corneal structure (Graw 1996; Chow 2001).

The neural retina requires both the RPE and the developing lens for correct development. The developing lens secretes FGF1 and BMP7 and these are required for, and can support, neural retina development. The RPE secretes various neurotrophic factors, such as BDNF, PEDF and NT-3, which support neural retina development and in the absence of the RPE development of the neural retina arrests (Jean 1998). The mature neural retina cell contains many cell types and these can be divided into neuronal or Müller glial cells, with neuronal cells divided into the light-sensitive photoreceptor neurons, interneurons and the retinal ganglion cells. Retinal ganglion cells are the first to differentiate from the *Otx2*-positive postmitotic neuroblasts in the germinative zone and the photoreceptors the last to be formed (Bovolenta 1997; Jean 1998). The differentiation into each cell type is controlled by a range of factors which narrow the differentiation potential of the emerging postmitotic neuroblasts with time in order to produce the characteristic differentiated, layered structure of the mature retina. Secreted ligands are responsible for promoting this differentiation, with *BRN3* promoting RGCs, *Chx-10* promoting bipolar cells and *Crx* stimulating photoreceptor production, for example. The only cell type not to be produced from this differentiation process is the astrocytes, which migrate into the retina guided by the chemoattractant *PDGF* secreted by the retinal ganglion cells and retinal capillaries (Jean 1998).

Vascularisation of the eye begins with the entry of the hyoid artery through the choroidal fissure and migration of the vessel continues until it reaches the posterior of the developing lens. Branching of this vessel over the lens surface forms the tunica vasculosa lentis and this expands to reach the anterior region of the lens forming the pupillary membrane (Saint-Geniez 2004). VEGF is important in the formation of these vessels, particularly in the branching process (Shastry 2009). The hyoid vessel system nourishes the developing eye until the formation of the retinal vasculature which will support the mature eye, at which point the embryonic support network of hyoid vessels regress (Saint-Geniez 2004). Regression of the hyoid vasculature is dependent upon the p53 apoptosis pathway (Shastry 2009).

1.7 Aims and hypotheses

Matthew-Wood syndrome is a rare human birth defect condition caused, in some, cases by mutations in the retinol transporter gene *STRA6*. STRA6 is therefore known to have a developmental function and in order to understand the etiology of the developmental abnormalities observed in Matthew-Wood patients an animal model was desired.

1.7.1 *Stra6-/-* mouse

Stra6-/- mice were hypothesised to be an appropriate animal model of Matthew-Wood syndrome and may also provide an important insight into the role of retinol in development as STRA6 provides the only known import route for RBP4-bound retinol. The original aim of the work was therefore to investigate the phenotype of *Stra6-/-* mice in the expectation that they would demonstrate a phenotypic constellation similar to that seen in human Matthew-Wood patients, namely ano- or micro-phthalmia, cardiac defects, diaphragmatic hernia and pulmonary hypoplasia. This constellation of phenotypes would be predicted to be perinatal lethal in most cases and therefore minimal or no *Stra6-/-* animals would be hypothesised to be observed from *Stra6+/-* matings, resulting in changes to be expected versus the observed genetic ratios.

1.7.2 *Stra6.2* and zebrafish

Previous work within the laboratory had preliminarily identified a possible paralogue of *Stra6, Stra6.2,* and I hypothesised that this paralogue may function similarly to *Stra6* in development and within the retinoid pathway. Investigation of the evolutionary conservation of *Stra6.2* would be hypothesised to provide hints as to its functionality; with its presence or absence against the background of retinoid pathway genes in the genome through evolution highlighting possible functional modules of protein or retinoid-substrate interaction.

A zebrafish morpholino knockdown approach was selected in order to investigate the function of *stra6.2* as this approach had previously been used to investigate *stra6* function in the fish in work previously published by Isken *et al* (2008). The

availability of chemical inhibitors of the retinoid pathway and the rapid developmental progression in the fish also made this an attractive methodology to understand the function of this gene. The use of morpholino knockdown also allows investigation of the hypothesised cooperative roles between *stra6* and *stra6.2* through co-knockdown of both genes with the developing fish.

The developmental phenotypes observed in *stra6.2* knockdown fish led to the development of a *Stra6.2-/-* mouse in order to investigate the requirement for *Stra6.2* in the mammalian system. The function of *Stra6.2* within the mouse was unknown and knockout of *Stra6.2* was hypothesised to result in either no or minimal phenotypic consequences due to functional redundancy or, extrapolating from the zebrafish results, result in greater phenotypic consequences to those observed in *Stra6-/-* animals.

1.7.3 Further hypotheses

Further hypotheses were formed during the course of the project; when it became clear that *Stra6-/-* mice did not represent a model for Matthew-Wood syndrome perhaps due to the presence of *Stra6.2* within the mouse compared to human. *Stra6* and *Stra6.2* were therefore hypothesised to function redundantly in the mouse and therefore, it was hypothesised that, both genes may need to be lost in order to recapitulate Matthew-Wood syndrome in the mouse.

Chapter Two

Materials and Methods

2.1 General methods

2.1.1 Sectioning for histology

Histological sections were taken from paraffin-embedded tissue using a microtome to cut 5µM slices. These sections were then orientated and floated in a 40°C water bath onto Superfrost slides. Slides were then dried on a heated slide drier to remove excess water before transferral in metal racks to a 50°C oven overnight.

2.1.2 Haematoxylin and eosin

Haematoxylin and eosin staining was performed on histological sections in order to investigate tissue and cellular morphology. Sections on glass slides were de-waxed by 3x 5-minute changes in xylene and then 3 x 5-minutes in 100% ethanol. Slides were then re-hydrated through an ethanol series (90%, 70%, 50% and 30%) over 10 minutes and into water for 5-minutes. Slides were stained in haematoxylin for up to 5-minutes (depending on the freshness of the stain) and rinsed in water to remove excess stain. Slides were differentiated in acid:alcohol for a few seconds, rinsed in water and transferred to saturated lithium choride (LiCl) for a few seconds. After rinsing in water, slides were stained with eosin for up to 2-minutes and washed in water and 100% ethanol. Slides were then dehydrated through 3 x 5-minutes in 100% ethanol and 2x 5-minutes in xylene before being mounted in DePeX (VWR, Leicestershire) under coverslips.

2.1.3 Bioinformatic analysis

The sequences were usually compared using Blast web servers (http://www.ncbi.nlm.nih.gov/blast/; (Tatusova 1999)) and databases were searched using the blast software (version 2.1.1 with default settings; (Altschul 1997)), as well as the “in house” Ensembl blast and blat servers. Sequences were manipulated using programs from the EMBOSS package (Rice 2000).Gene predictions were done using genewise (Birney 2004), using various published protein as model. In an attempt to look harder for the exons 16-19, we used genewise with a Hidden Markov Model (HMM) as model. The model was constructed using the HMMER package. The multiple protein alignment was performed using Clustalw (Higgins 1996) and visualised using Genedoc (Nicholas 1997). Positions in alignments containing gaps

were omitted from subsequent analyses. The phylogenetic tree was constructed by the neighbour-joining method (Saitou 1987) based on the proportion of amino acid sites at which sequences compared were different. The reliability of each interior branch of a given topology was assessed using the bootstrap interior branch test with 1000 bootstrap. Phylogenetic trees were constructed using MEGA (version 3.1; http://www.megasoftware.net/; (Kumar 1994)). Tree structure was verified by Bayesian phylogeny using BEAST v1.6.1 (Drummond 2007).

2.1.4 KOD Hot Start PCR

Each reaction contains 1x KOD Hot Start buffer, 1.5mM $MgSO_4$, 0.3µM forward and 0.3µM reverse primer, 0.2mM dNTPs (each), 1 unit KOD Hot Start DNA polymerase (Novagen, Merck, Germany) and 5 µl cDNA per 50µl reaction. PCR cycling conditions were 95°C for 2-minutes, followed by 30 cycles of 95°C for 20-seconds, lowest primer Tm (generally ~60°C) for 10-seconds and 70°C for 20-seconds. Blank controls were identical with the exception of cDNA which was substituted with water.

2.1.5 Culture of KOMP *Stra6.2* ES-Cells

1300002K09Rik$^{tm1a(KOMP)Wtsi}$ ES-cells were obtained from KOMP on dry-ice and cultured prior to micro-injection in DMEM media (1X KO DMEM (Gibco, Invitrogen), 15% FBS, 2mM GlutaMax (Gibco, Invitrogen), 1mM NE amino acids (Gibco, Invitrigen), 1000U/ml LIF (Gibco, Invitrogen), 1µM β-mecaptoethanol (Sigma-Aldrich, Dorset)).

2.2 Mouse methods

2.2.1 *Stra6* knockout

Stra6-/- mice were created via homologous recombination between homologous arms identical to the *Stra6* gene surrounding a selection cassette containing a neomycin-resistance gene. A vector containing a 2.7kb 5' homology arm containing exons 3 and 4 with surrounding intronic sequence and a 1.3kb 3' homology arm containing exon 7 with surrounding intronic sequence flanking a PGK-neo cassette for positive selection was created (Fig 3.1). This vector was linearized and

electroporated into E14 ES cells. Targeted ES cells were then grown in the presence of G418 in order to select for those clones which contained the targeting construct conferring resistance to G418 through the *Neo* gene. Surviving cell clones were picked and cultured in duplicate; one culture for freezing-down for further use and another for DNA extraction. DNA was extracted from surviving cell clones and analysed via southern blotting in order to identify recombinant clones with the targeting construct present at the targeted location within the *Stra6* gene. The cassette was targeted to remove exon-5 and 6 of the *Stra6* gene and this is predicted to cause a frame-shift in the resulting transcript and loss of STRA6 protein.

A correctly targeted recombinant clone was expanded and *Stra6*+/- ES cells injected into C57Bl/6J blastocysts. Male coat colour chimeras were selected and mated to C57Bl/6J females in order to create *Stra6*+/- animals which were then further bred to C57Bl/6J animals for colony maintenance, expansion and backcrossing or inter-crossed to create *Stra6*-/- offspring. *Stra6* knockout mice were genotyped via PCR targeted to the neomycin-cassette and against exon 5 which has been removed during the insertion of the selection cassette using the following primers;

Exon-5 forward 5'-TGAAGGCTCAGGGACTGACT,

Exon-5 reverse 5'-TTGATGCTGCAGTGAGGTTC,

Neo forward 5'-TGAATGAACTGCAGGACGAG,

Neo reverse 5'-ATACTTTCTCGGCAGGAGCA.

The *Stra6* knockout vector was created by Carlo DeAngelis, ES cell electroporation and culture was performed by Fiona Kilanowski and blastocyst injections and embryo transfer were undertaken by Paul Devenney.

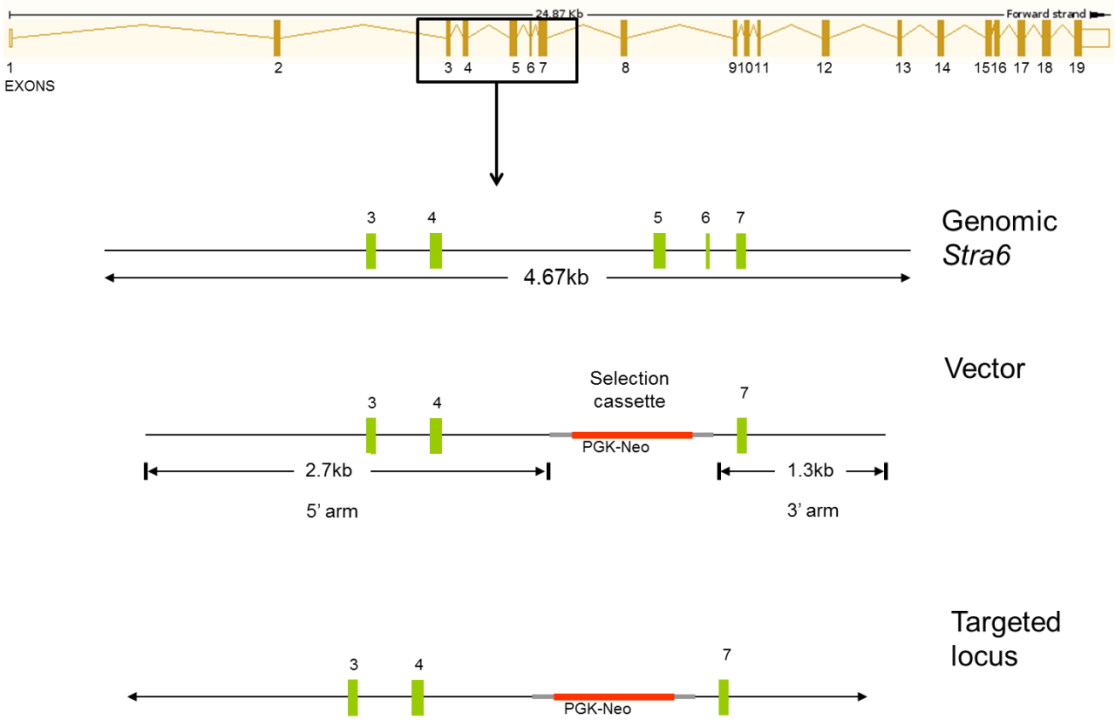

Figure 2.1: *Stra6* targeted knockout via homologous recombination.

Stra6 knockout mice were created through the removal of the exon-5 and 6 by homologous recombination with a vector comprising of a selection cassette containing the neomycin resistance gene (PGK-Neo, red box) with a pair of homology arms encompassing exons 3 and 4 (5' arm) and exon 7 (3' arm) respectively.

2.2.2 Mouse Strains

Stra6 knockout mice were a mixture of 129Sv and C57Bl/6J created from the injection of E14 ES cells derived from the 129Sv strain injected into C57Bl/6J blastocysts. Chimeras produced were crossed onto C57Bl/6J and further generations were backcrossed to C57Bl/6J in order to increase the genetic homogeneity for clearer analysis of any resulting phenotypes.

Stra6.2 knockout mice are C57Bl/6J being derived from C57Bl/6J ES cells injected into C57Bl/6J blastocysts. All further breeding for colony expansion was to C57Bl/6J animals. *Stra6.2* animals analysed for β-galactosidase activity from expression of the integrated lacZ sequence were the offspring of C57Bl/6J *Stra6.2+/-* males to CD1 females, in order to achieve large litter sizes for analysis.

2.2.3 Dietary provision for *Stra6* and *Stra6.2* mice.

Mice were normally provided with Rat and Mouse No.3 breeding chow (801700, Special Diets Services, UK) and water *ad libitum* within the cage. During the retinoid-free diet study, normal chow was removed and dams were fed a retinoid-free modified AIN-93G diet (#119135, Dyets Inc, PA, USA) *ad libitum*.

2.2.4 DNA preparation for mouse genotyping

Mice were identified by ear-notching and this tissue was used to extract DNA for genotyping. Ear notches were collected in 0.5ml tubes and 75µl of alkaline lysis solution (25mM NaOH, 0.2mM EDTA) was added. These tubes were transferred to a PCR machine and heated to 95°C for 1-hour. The solution was then neutralised with 75µl of neutralisation solution (40mM Tris-HCl) and 5µl of the DNA sample used per PCR reaction. DNA solutions were stored at 4°C.

2.2.5 Genotyping PCR

Each reaction contains 1x PCR buffer, 2.5mM $MgCl_2$, 25µmol forward, 25µmol reverse primer, 4.2µM dNTPs, 1 unit of Platinium Taq (Invitrogen/Life Technologies, Paisley) and 5 µl earclip DNA per 25µl reaction. PCR cycling conditions were 96°C for 10-minutes, followed by 30 cycles of 96°C for 30-seconds, 60°C for 30-seconds and 72°C for 1-minute and a final extension of 72°C for 5-

minutes. 5µl of loading buffer were added per 25µl sample and 12µl run out on a 2% agarose gel containing ethidium bromide. Positive and negative control samples were run with all genotyping reactions to ensure PCR functionality. Blank controls were identical with the exception of DNA which was substituted with water.

2.2.6 Dissection and pathology of adult mice

Mice older than 6-weeks old were sacrificed via cervical dislocation. Mice were weighed and measured from nose-to-tail base and nose-to-tail end. Thoracic and abdominal organs and the brain were then dissected, their general external appearance noted, and weighed. Control and experimental animals were examined concomitantly and where possible littermates were used, in situations where this was not possible, animals of a similar age were examined.

2.2.7 Fixation and embedding of mouse organs

Organs were dissected from the mouse and fixed rocking, overnight in 4% PFA in 50ml falcon tubes at 4°C. Organs were then washed in PBS and taken through 30% and 50% ethanol for 1-hour in each and then stored at 4°C in 70% ethanol. Organs were then transferred to a processing machine in plastic cassettes. The samples were then processed through 70% ethanol, 1 x 80% ethanol, 1 x 90% ethanol and 100% ethanol at 30 minutes per cycle. The samples were then incubated through two changes of 100% xylene again for 30 minutes per cycle and through 4 changes of molten wax at 60°C again at 30-minutes per cycle. The samples were then embedded in the appropriate orientation and allowed to set before sectioning.

2.2.8 Fixation and embedding of mouse eyes

Mouse eyes were removed from the sockets by pulling the eyelids open and extracting the eye from the orbit with forceps. The eyes were then fixed individually in epindorfs in 4% PFA overnight at 4°C rocking. The eyes were then washed 2 X 15 minutes in PBS followed by 15 minutes in 0.9% saline. The eyes were then dehydrated through 15 minutes in 50% ethanol in saline, 2 X 15 minutes in 70% ethanol and 1 hour in 70% ethanol. This was followed by 15 minutes each in 85% and 95% ethanol and finally 2 x 30 minutes then 1 hour in 100% ethanol. The eyes

were then transferred to glass vials and washed in xylene for 2 X 5 minutes before overnight incubation in xylene at room temperature. Xylene was removed, molten wax added for 1 hour at 60°C and transferred to fresh wax for 2-3 hours at 60°C. The eye were then embedded in wax and orientated horizontal to the block surface with the optic nerve visible. Histological sections were taken from paraffin-embedded eyes using a microtome to cut 7µM slices. In order to preserve the morphology of the lens, a small drop of water was applied to the embedded lens before each section was taken. The slides were dried overnight at room temperature in a metal slide-rack.

2.2.9 Immunohistochemistry

Sections from the centre of the eye at the level of the pupil opening were selected for immunohistochemistry and were dried overnight in metal racks at 50°C to ensure the sections are fully bonded to the slide prior to antigen retrieval. Sections were deparaffinised in xylene for 2 X 5-minutes and 2 X 5-minutes in 100% ethanol. Sections were hydrated through 90%, 70%, 50% and 30% ethanol series at 3-minutes in each solution. The slides were then rinsed 3 x 3-minutes in distilled water. The slides were then put into a plastic slide rack and then into a beaker containing 10mM citrate buffer, 0.1% tween, 1mM EDTA. The solution was then heated in a microwave for 15-minutes boiling. The slides were then equilibrated to room temperature and the slides are rinsed 3 X 5-minutes in PBS. The slides were then blocked in 1% BSA, 0.5% triton-X100 in PBS for 1-hour at room temperature. The slides were then incubated with primary antibody diluted in blocking solution (BRN3 – 1/100, GFAP, Col IV & Rhopdopsin - 1/500) under cover-slips for 1-hour at room temperature or at 4°C overnight. The slides were then washed 3 X 5-minutes in PBS. The slides were then incubated with florescent secondary antibody diluted 1:1000 in blocking buffer for 1-hour and washed 2 X 5-minutes in PBS. The slides were then mounted with Vectashield (Vector Laboratories, Peterborough) containing DAPI under cover-slips sealed with nail varnish. Control slides were subjected to the same process without the addition of primary antibody.

2.2.10 Embryo collection

Embryos were collected from timed matings with E0.5 defined as the morning of plug discovery. Dams were sacrificed via cervical dislocation and the uterus removed into ice cold PBS. Deciduae were removed from the uterus in ice cold PBS with size 5 forceps and embryos were dissected from their decidua with any extraembryonic membranes and the placenta removed. Yolk sacs were removed for genotyping and prepared as described in 2.1.1 and 2.1.2.

2.2.11 FACS

FACs analysis was performed on both spleen and bone marrow from *Stra6+/-* and *Stra6+/-* diet study mice. The spleen was dissected from the mouse and separated into two pieces to allow histological and FACS analysis of the same tissue. The spleen sample was homogenized using a hand held homogenizer. Bone marrow was collected from the all the long bones of the legs by dissecting out the bones and removing all associated muscle tissue. The joints at either end were then removed using small scissors and the bone marrow forced from the cavity by irrigation with FACS PBS through a 25-gauge needle. Cells were homogenised into FACS PBS using a 21-gauge needle. Final concentration of bone marrow and spleen cells was approximately 1 x 10^7/ml in 5mls FACS PBS. The cell samples were then sieved through a 70µm cell sieve (VWR, England) to remove and lumps or extraneous tissue. The 3µl each of the appropriate antibodies were aliquoted into 5ml FACS tubes (BD Biosciences, Oxford) along with 100µl of cell suspension. The tubes were covered in tin-foil and incubated at room temperature for 30-minutes shaking. The cells were then washed in 3mls of FACS-PBS and centrifuged for 5-minutes at 1600rpm to pellet the cells. The supernatant was discarded and the pellet re-suspended in the residual supernatant. Samples were run using a FACSAriaII sorter (BD Biosciences, Oxford) and analysed using FloJo (Celeza, Switzerland). Analysis was performed only on live cells selected based on side vs. forward scatter profiles. The boundary between cells that stained positive and negative was determined according to the fluorescence distribution of positively stained relative to unstained samples. CD45 FITC, Thy-1 PE, CD8 PE, CD4 APC, TER119 PE, B220 APC and

CD71 FITC (Abcam, Cambridge, UK) were used in combination to identify cell populations and singularly to allow signal compensation.

2.2.12 Visual testing of mice

Visual competency was tested using drum mounted on a motorized base lined with panels consisting of black and white vertical stripes inside at either 0.25 cycles per degree (2°), 0.125 cycles per degree (4°) or 0.0625 cycles per degree (8°) (Thaung 2002). Mice were placed on a stationary circular platform in the centre of the drum and allowed to habituate for 30-seconds (Figure 2.1). The drum was rotated clockwise for 1-minute and then rotated clockwise for 1-minute at a speed of 2 revolutions per minute. Animals were initially tested at 4° and if head-tracking was noted animals were further tested at 2°. Mice which lacked a head-tracking response at 4° were then tested at 8°.

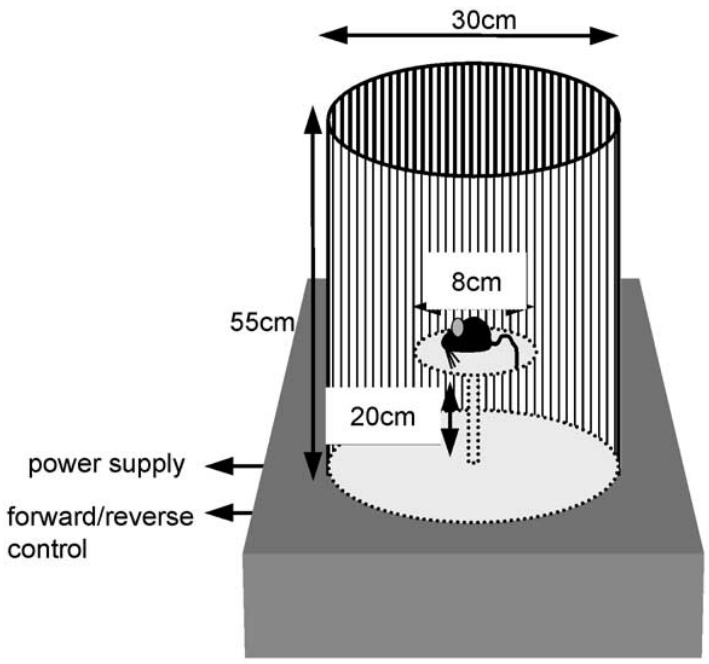

Figure 2.1: Mouse visual testing equipment

Schematic drawing (not to scale) of the visual testing drum used for visual assessment in mice. Figure from Thaung *et al* (2002).

2.2.13 Mouse wholemount *in situ* hybridisation

Probes for *in situ* were designed to hybridise to ~500bp of the 3'-UTR of the gene of interest with T3 and T7 promoter sequences added to the 5'-end of the forward and reverse primer respectively. DNA templates for *in vitro* transcription were created using KOD polymerase (Novagen, Merck, Germany), as described in 2.1.4, to reduce PCR-introduced errors in the template obtained. The following primers were used to create PCR templates for *Stra6.2* probe production; Forward 5'-AATTAACCCTCATAAAGGCCCTTGGCACAAAAGAAAAA, Reverse 5'-TAATACGACTCACTATAGGTCTGCTTGGCTTTGCTAGGT; T3/T7 promoter sequences underlined. These primers contain a region complementary to *Stra6.2* and an additional region encoding either T3 or T7 promoter creating fusion PCR products. PCR products were cleaned using a PCR purification kit (Qiagen, West Sussex) following the standard protocol. The purified PCR product (10µl) was transcribed in 1X transcription buffer, 20 units RNasin (Promega, Southampton), 1 X DIG labelled NTPs (Roche, UK) and 10 units T7 RNA polymerase (Promega, Southampton). The transcription reaction was incubated at 37°C for 2-hours and the template DNA removed by the addition of 2 units of DNase (NEB, Hitchin, UK) for 15-minutes at 37°C. Probes were precipitated by adding 80µl distilled water, 25µl NH_4OAc and 312.5µl 100% ethanol and incubating on dry ice for 1-hour. Probe was pelleted by centrifugation at 13,000rpm for 15-minutes, the pellet washed in 70% ethanol and re-pelleted at 7000rpm for 5-minutes. The supernatant was discarded and the pellet air-dried before resuspension in 50µl 0.1% DEPC (Sigma-Aldrich, Dorset) water. Products of *in vitro* transcription were run on a 2% agarose gel to confirm successful transcription. Embryos were collected from CD1 females from timed matings at E9.5, E10.5 and E11.5 then fixed overnight in 4% PFA, 0.1% DEPC at 4°C. Embryos were then dehydrated and stored in 100% methanol at -20°C until required. Embryos were rehydrated through a methanol: PBS-0.1% triton-X100 (PBST) series of 75%, 50% and 25% with the embryos allowed to sink in each solution before transferral to the next. Embryos were then washed 3 X 5-minutes in PBS-triton, 0.1% DEPC (dPBST) before proteinase-K treatment (10µg/ml) in dPBST for a time dependent on stage (E9.5 – 15-minutes, E10.5 – 20-minutes, E11.5 – 25-minutes). Embryos were then re-fixed for 45-minutes in 4% PFA on ice. Embryos

were then washed twice in pre-hybridisation solution (50% formamide, 5X SSC, 2% (w/v) blocking powder, 0.1% triton-X100, 0.5% CHAPS, 50mg yeast RNA, 2.5mg heparin) and then incubated for 1-hour at 65°C and an additional 2-hours at 65°C in fresh pre-hybridisation solution. Probe was then diluted 250ng/ml in hybridisation buffer and embryos incubated overnight at 65°C in the hybridisation buffer. Embryos were subsequently washed for 10-minutes in 100% hybridisation buffer and then 10-minutes each in 75:25%, 50:50% and 25:75% hybridisation buffer:2X SSC. Embryos were then transferred to 2X SSC, 0.1% CHAPS for 2 X 30-minutes at 65°C followed by 2 X 30-minutes in 0.2X SSC, 0.1% CHAPS at 65°C. Embryos were then transferred to room temperature and washed for 10-minutes in PBST before staining in BM purple (Roche, UK) until stain developed. The embryos were then post-fixed in 4% PFA overnight at 4°C. Sense probes were used as controls and subjected to the same methodology and timings as their anti-sense counterparts.

2.2.14 Detection of β-galactosidase activity in mouse embryos.

Embryos were dissected as described in chapter 2.3 and fixed in 4% PFA at 4°C dependent on their stage; E7.5 – 20 minutes, E8.5 – 30 minutes, E9.5 – 1 hour, E11.5 & 12.5 – 2 hours. The embryos were then washed 3 X 20-minutes in detergent wash (100mM sodium phosphate, 2mM magnesium chloride, 0.01% sodium deoxycholate, 0.02% Nonidet P-40) at room temperature on a shaker. 300µg/ml X-gal was added to stain solution (35 mM potassium ferrocyanide, 35 mM potassium ferricyanide, 2 mM MgCl2, 0.02% Nonidet P-40 (NP-40), 0.01% Na deoxycholate in detergent wash) and the embryos were stained overnight at 37°C in the dark. Embryos were then washed in PBS and post-fixed in 4% PFA overnight at 4°C. Matings to obtain embryos for detection of β-galactosidase activity were set-up to ensure that a proportion of the embryos would be negative for β-galactosidase activity providing controls for any non-specific β-galactosidase activity. Embryos were also additionally genotyped to ensure correlation between genotype and β-galactosidase activity.

2.3 Zebrafish methods

2.3.1 Zebrafish husbandry

Wild type adults of AB and TL strains, mutant line *p53-/-* and transgenic reporter line *shha*-GFP were maintained in aquaria at 28°C under a 13:12 hour light:dark cycle according to standard husbandry techniques. Embryos were collected from natural matings with three hours of the commencement of the light period. Embryos were cultured in the dark in 28°C incubators in 1x E3 media (5mM NaCl, 0.17mM KCl, 0.33mM $CaCl_2$, 0.33mM $MgSO_4$, 0.00001% methylene blue). Dead embryos were removed and E3 media replenished daily. Embryos were sacrificed at the end of the experimental period, before 5 dpf, by emersion in tricaine.

2.3.2 Morpholino injection

Zebrafish embryos collected from natural matings were injected with morpholino into the yolk generally at the 1-cell stage, but no later than the 4-cell stage, to allow sufficient distribution of the morpholino to all embryo cells during the period of cytoplasmic streaming from the yolk. Sequences of the morpholinos are as follows: *stra6*, 5'-GTTATTCACAGTTTCAGCACTCATG ; *stra6.2* translation blocking morpholino 1, 5'- GCTGCACTAATGAGAGCAGAAACAT; *stra6.2* translation blocking morpholino 2, 5'- ACATAATGAAGACCTGAAACACAGA; *stra6.*2 splice morpholino, 5'-CAATGGCTGAAAGAGACAAATTCAG and *rbp4* translation blocking morpholino, 5'-ACACTGCTATACAGAGCCTTAACAT. Morpholinos were dissolved in sterile water to a stock concentration of 1mM. *stra6* MO was injected at 0.5mM, *stra6.2* MO1 injected at 0.25mM, *stra6.2* MO2 injected at 0.5mM, *stra6.2* spliceMO injected at 0.5mM and rbp4 MO injected at 0.0125mM unless otherwise stated. A standard control morpholino, 5'-CCTCTTACCTCAGTTACAATTTATA was also used as a control for the non-specific effects of morpholino injection, such as developmental delay.

2.3.3 Phenotypic scoring system

The morphology of live morphant embryos was assessed via light microscopy at 48hpf. *stra6.2* morphants were assigned to the phenotypic class if they showed two

or more of the following features; microphthalmia, ventral curving of the body axis, flattened somites, reduced startle response and stationary movement about the yolk, edema surrounding the heart region and abnormal yolk extension morphology.

2.3.4 Alcian blue staining for jaw cartilage

Zebrafish embryos were collected at 5dpf, over-anethesised in tricaine and fixed overnight in 4% PFA at 4°C. Embryos were washed in 1x PBS-tween for 3 x 5 minutes. Embryos were then stained in filter-sterilised 0.1% alcian blue stain for ~6 hours until cartilage was apparent. The embryos were washed 2 x 5minutes in 100% ethanol and rehydrated through an ethanol:PBS-Tween series of 70%:30%, 50%:50% and 30%:70% for 5 minutes each before overnight storage in PBS-Tween at 4°C. The tissue was cleared with 0.05% trypsin in PBS for 3 hours and then bleached with 3% hydrogen peroxide: 1% potassium hydroxide in PBS for ~15 minutes until the pigment was removed and the cartilages could be clearly visualised. Embryos were washed 3 x 5 minutes in PBS-Tween and then taken through a glycerol series of 30% and 50% for 5 minutes each and then stored at 4°C in 70% glycerol prior to imaging.

2.3.5 Zebrafish whole-mount *in situ* hybridisation

Probes were produced as described for mouse wholemount *in situ* (2.2.11) using the primers listed in Table 2.1. T7- transcribed anti-sense experimental probes were compared to T3 transcribed sense control probes in order to asses for any non-specific staining patterns associated with the probe sequence.

Zebrafish embryos were collected at the appropriate stage and over-anesthetised in tricaine (Sigma-Aldrich, Dorset) before fixing overnight in 4% PFA, 0.1% DEPC (Sigma-Aldrich, Dorset) at 4°C. Embryos were then dehydrated and stored in 100% methanol at -20°C. Embryos were re-hydrated through a methanol:PBS-0.1% tween series of 75%, 50% and 25% and then washed 5 X 5-minutes in PBS-tween. Embryos were then incubated with Proteinase-K at 10µg/ml in PBS-tween for 3-minutes for 24hpf and 5-minutes for 48hpf for 48hpf embryos. The embryos were then re-fixed in 4% PFA, 0.1% DEPC for 1-hour at room temperature and washed 5 X 5-minutes in PBS-0.1% tween. Embryos were incubated in pre-hybridisation

buffer (50% formamide, 5 X SSC, 50µg/ml heparin, 500µg/ml tRNA, 0.1% tween, 0.0092M citric acid, pH 6.0) for 1 hour at 65°C rotating before an overnight incubation at 65°C in hybridisation buffer containing 1:200 dilution of the probe. Hybridisation buffer was removed and the embryos transferred into SSC through a 66% hybridisation buffer then 33% hybridisation buffer in 2% SSC for 5-minutes per solution at 65°C and then for 5-minutes in 2 X SCC at 65°C. Embryos were then incubated at 65°C 1 X 20-minutes in 0.2% SSC, 0.1% tween and 2 X 0.1% SSC, 0.1% tween before transfer to room temperature for 5-minutes each in 66% 0.2% SSC: 33% PBS-tween, 33% 0.2% SSC: 66% PBS-tween and PBS-tween. Embryos were then blocked in 2% sheep serum, 2mg/ml BSA in PBS-tween for 1 hour at room temperature. Embryos were incubated overnight with anti-digoxigenin-AP, fab fragments from sheep (Roche, UK) diluted 1:1000 in blocking buffer rocking at 4°C. Embryos were washed 5 X 15-minutes in PBS-tween and incubated in BM purple reagent (Roche, UK) until specific staining was observed. BM purple was removed once the desired staining intensity was achieved and the embryos washed twice in 0.1% DEPC water. The embryos were then transferred through a glycerol series of 30% and 50% in PBS up to 70% glycerol. Embryos were stored in the dark at 4°C prior to imaging.

Gene		Primer Sequence
cdh17	F	AATTAACCCTCACTAAAGGCCCATCACCATAAACACTCACA
	R	TAATACGACTCACTATAGGTGTGCTTTTAACGCCTTTTG
slc12a3	F	AATTAACCCTCACTAAAGGGGGTGCTTGTCTGAATTGGT
	R	TAATACGACTCACTATAGGTGCATCGTCTCCCCTAAATC
gata3	F	AATTAACCCTCACTAAAGGTTCTTCATTGCCCCTTCAAC
	R	TAATACGACTCACTATAGGACAACCAATTGCCCAAGAC
ntla	F	AATTAACCCTCACTAAAGGTGGACTTGATCTTGGCTTCA
	R	TAATACGACTCACTATAGGCAATGAAACCGGACGTTAATTT
eve1	F	AATTAACCCTCACTAAAGGTGGGCAATAGGCTACGAGAAATG
	R	TAATACGACTCACTATAGGTGTTCAGGTGCAAAACAGTCA
islet1	F	AATTAACCCTCACTAAAGGTGGCGGCGCACATATTCACTAC
	R	TAATACGACTCACTATAGGGGAACGAAACAAACCTCCA
cyp26a1	F	AATTAACCCTCACTAAAGGTGGGAAAAGGCTTGAGCATGGAG
	R	TAATACGACTCACTATAGGGTTTTTCGCTTCCTCGCATAG
raldh2	F	AATTAACCCTCACTAAAGGTGCAGCTGGAAGTCTTGATG
	R	TAATACGACTCACTATAGGCATTGGTCAAGACATCGACAA

Table 2.1: Primer sequences for zebrafish WISH probe synthesis.

Primer sequences used to produce *in situ* probes for wholemount *in situ* hybridisation in the zebrafish.

2.3.6 Zebrafish fixation and embedding

Zebrafish embryos were collected at the appropriate stage and over-anesthetised in tricaine (Sigma-Aldrich, Dorset) before fixing overnight in 4% PFA at 4°C. Embryos were then washed in PBS and stored in 100% methanol at -20°C. Methanol was removed and 100% ethanol added for 3 X 20-minutes. Embryos were then transferred to xylene for 2 X 20-minutes with the first incubation at room temperature and the second at 60°C. The embryos were then incubated in molten wax at 60°C for 3 X 20-minutes with the wax aspirated and replaced with fresh wax in-between. Embryos were then appropriately orientated and embedded. Histological sections were taken as described in section 2.2.2.

2.3.7 qRT-PCR

RNA was extracted via standard TRIzol (Invitrogen) protocol. First strand cDNA was reverse transcribed using oligo-dT primers and AMV reverse transcriptase (Roche, West Sussex). For amplification the following PCR primers were used: *β-actin*, 5'-TCACTCCCCTTGTTCACAATAA and 5'-GGCAGCGATTTCCTCATC; *shha*, 5'-AAAGCCCACATTCATTGCTC and 5'-CCTTCTGTCCTCCGTCCTG; *raraa*, 5'-GCCTGCCTCGACATACTGAT and 5'-GTGCATCTGTGTTCGGTTGA. These primers were tested using standard PCR and shown to amplify a single band of the correct size with no primer dimer. cDNA reaction was diluted 1:20 and 8µl added to each 20µl QPCR reaction. Reaction also contained 1x SYBR green master mix (Brilliant II SYBR Green QPCR Master Mix; Agilent Technologies) and primers at a final concentration of 200nmol. Reactions were initially heated to 94 ºC for 15 minutes followed by 40 cycles of 95ºC for 15 seconds, 60ºC for 30 seconds and 72ºC for 30 seconds. Cycling and fluorescence quantification was performed on 7900HT Fast Real-Time PCR System (Applied Biosystems). The PCR products created were checked on a 2% agarose gel to confirm single-band amplification of the expected size. Gene expression was normalised to *β-actin* expression and relative values to expression in standard control MO injected embryos was calculated using the $2^{(-\Delta\Delta C(T))}$ method (Livak & Schmittgen, 2001).

2.3.8 Chemical rescue of zebrafish morphants.

Embryos treated with 1-phenyl-2-thiourea (PTU) were transferred to 200μM PTU in E3 medium at the end of gastrulation. Embryos treated with 4-Diethylaminobenzaldehyde (DEAB; Sigma-Aldrich) were transferred to fresh E3 medium at 5 hpf. DEAB dissolved in DMSO was added to the E3 medium to a final concentration of 10^{-7}M. Control embryos were treated with the same volume of DMSO.

Chapter Three

Stra6 knockout mice as a model for Matthew-Wood syndrome

3.0 Introduction

Homozygous and compound heterozygous mutations in *STRA6* are causative for some cases of Matthew-Wood syndrome in humans. Matthew-Wood syndrome is typified by clinical anophthalmia, pulmonary hypoplasia, diaphragmatic hernia and various cardiac defects. STRA6 is known to be a transporter for retinol when bound to RBP4 and also acts as an affecter for the role of RBP-retinol in insulin receptor phosphorylation. A mammalian model for Matthew-Wood syndrome was not in existence, although a zebrafish morpholino knockdown model has been previously described (Isken 2008). A mammalian model of Matthew-Wood syndrome was desired in order to understand the role of STRA6 in development and how in its absence the various developmental defects observed in human patients occur. Due to the role of STRA6 in retinol transport (Kawaguchi 2007), a mouse knockout model may also provide a useful tool in understanding the role of retinol in development as much previous work in the retinoid field has been concentrated on retinoic acid, the terminal metabolite of the retinoid pathway.

3.1 *Stra6* knockout mice

Stra6-/- mice were created via homologous recombination between homologous arms identical to the *Stra6* gene surrounding a selection cassette containing a neomycin-resistance gene. The cassette was targeted to remove exon-5 and 6 of the *Stra6* gene and this is predicted to cause a frame-shift in the resulting transcript leading to changes to the protein produced.

Stra6 knockout mice were genotyped via PCR targeted to the neomycin-cassette and against exon 5 which has been removed during the insertion of the selection cassette (Figure 3.1).

3.1.1 *Stra6-/-* mice have no defects in eye, heart or lung development.

Stra6 knockout mice have no gross developmental phenotypes. Genetic mutations of *STRA6* in human result in the multisystem developmental disorder Matthew-Wood syndrome. *Stra6* knockout animals did not represent an animal model of the human condition with no developmental defects of the eyes, heart, lung or diaphragm.

Stra6-/-, *Stra6+/-* and wild-type littermates had comparable eye size and shape when viewed in the cage and were indistinguishable before genotyping. The human condition is typified by clinical anophthalmia, a loss of most eye tissue anterior to the optic nerve, a feature not seen in *Stra6-/-* animals. Histological sections were taken through the eye of both *Stra6-/-* and *Stra6+/-* littermates. Eye morphology was normal with no defects of the retina, lens or cornea (Figure 3.2 A-B).

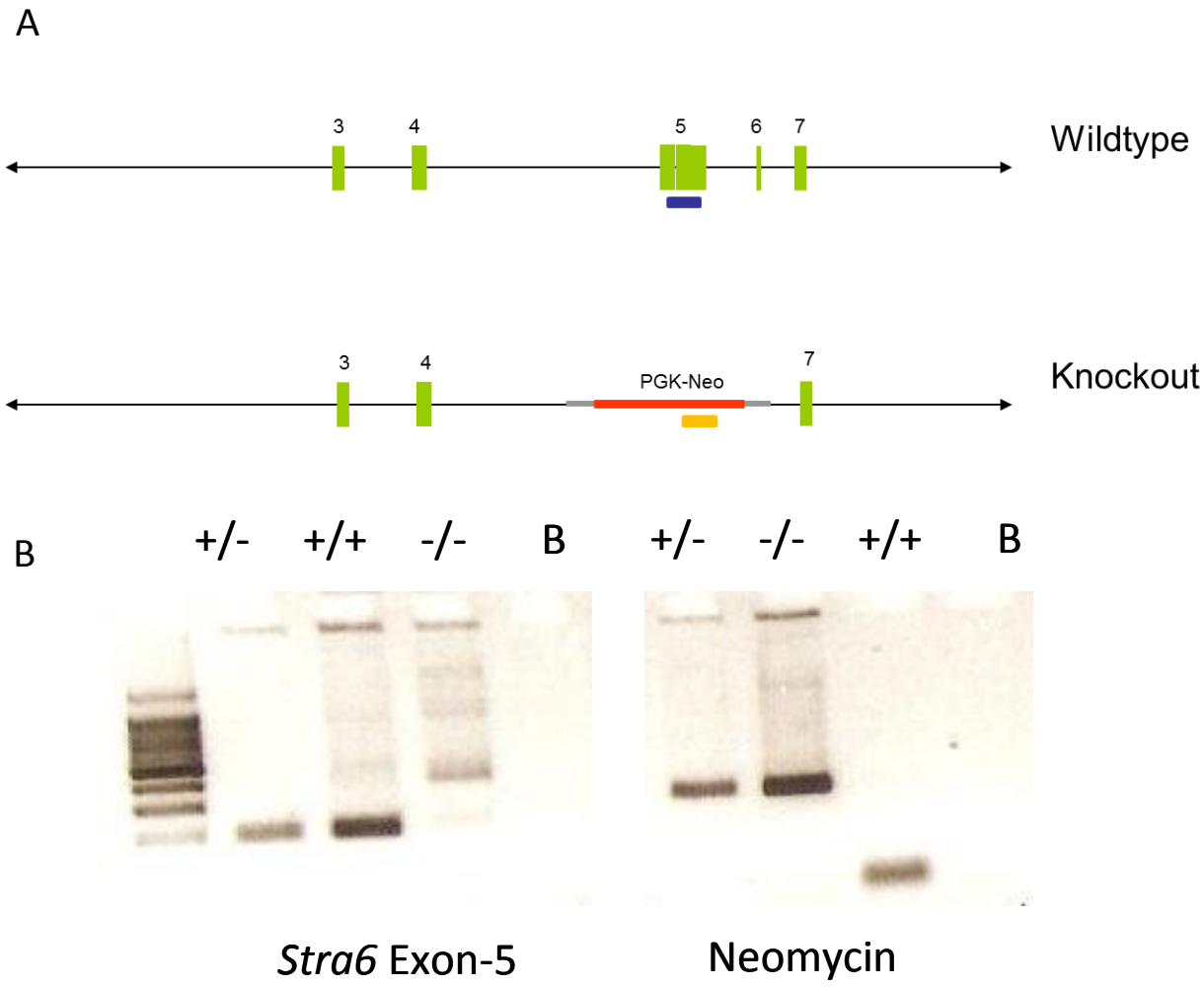

Figure 3.1: *Stra6* knockout mice were created through the removal of exon-5.

Stra6 knockout mice were created through the removal of the exon-5 and 6 by homologous recombination with a selection cassette containing the neomycin resistance gene. *Stra6* animals could then be genotyped using primers targeted to exon-5 to identify the wildtype allele (A, blue rectangle) and neomycin to identify the knockout allele (A, orange rectangle). PCR generated reliable bands which could be identified via gel electrophoresis (B). *Stra6* genotype is designated above the appropriate lane. Blank lanes containing all reaction components except DNA are designated B.

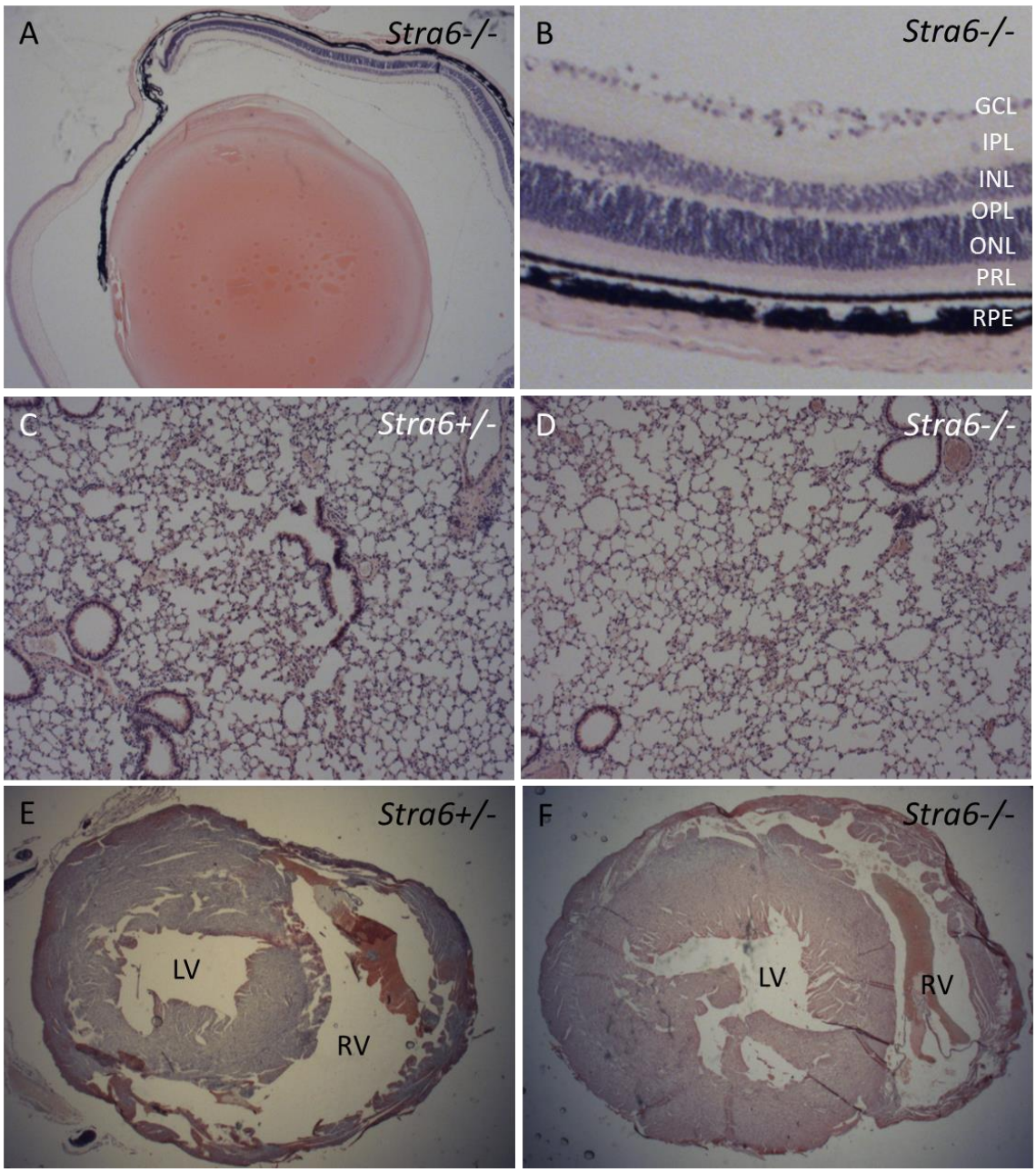
A
Stra6-/-
B
Stra6-/-
GCL
IPL
INL
OPL
ONL
PRL
RPE
C
Stra6+/-
D
Stra6-/-
E
Stra6+/-
LV
RV
F
Stra6-/-
LV
RV

Figure 3.2: *Stra6+/-* and *Stra6-/-* animals show none of the defects associated with Matthew-Wood syndrome.

Eye morphology is normal in *Stra6-/-* animals (A) with lens, cornea and retina intact and correctly arranged. The retina is made up of the expected layers (B); namely the ganglion cell layer (GCL), inner plexiform layer (IPL), Inner nuclear layer (INL), outer plexiform layer (OPL), outer nuclear layer (ONL), photoreceptor layer (PRL) and retinal pigmented epithelium (RPE). Histological sections of the lung show no major morphological differences in alveoli size or shape between a *Stra6+/-* (C) and a *Stra6-/-* (D) animal. Histological sections through the ventricular region of the heart show no major defects in the right- (RV) or left ventricle (LV) between a *Stra6+/-* (E) or a *Stra6-/-* (F) animal.

Human Matthew-Woods patients commonly have severe developmental lung defects which often result in death due to respiratory insufficiency. However, survival of *Stra6-/-* animals and the lack of respiratory distress in these animals at birth indicate that severe lung defects were not a feature of *Stra6-/-* animals. Pathological investigations of adult mice showed normal lung morphology with the expected number of lobes noted appropriate for laterality. Histological sectioning of adult lungs from a *Stra6-/-* and a *Stra6+/-* animal showed normal alveoli size and shape (Figure 3.2 C-D).

Heart defects in Matthew-Wood patients are variable but some malformations are more commonly seen. Patent ductus arteriosus and ventricular septal defects were seen in a number of patients. *Stra6-/-* animals showed no signs of congenital heart defects; they fed and grew normally and showed normal activity levels in the cage. Histology sections from a *Stra6-/-* and a *Stra6+/-* animal showed no gross defects in heart morphology with normal ventricular walls and intact ventricular septum (Figure 3.2 E-F).

Congenital diaphragmatic hernia is commonly noted in Matthew-Wood patients; being, along with clinical anophthalmia, a defining diagnostic characteristic. *Stra6-/-* animals had intact diaphragms and showed no eventration of the liver into the thoracic cavity.

3.1.2 *Stra6-/-* animals are observed in the expected genetic ratio.

Stra6-/- animals were observed in the expected ratio when routinely genotyped at 2-3 weeks of age indicating that *Stra6* is not required for survival through the embryonic or neonatal period (Table 3.1). Depression of the number of homozygotes would be expected if loss of *Stra6* affected the survival threshold.

3.1.3 *Stra6-/-* animals have normal visual function.

The expression of *Stra6* within the RPE of the adult mouse eye and the gross eye defects in Matthew-Woods patients highlighted a role for *Stra6* in visual function. Adult animals older than 6 weeks were tested for visual function by monitoring head tracking in response to moving grating in a visual tracking drum. Consistent with the

normal eye size and histological appearance, *Stra6-/-* animals were able to see a well as wild-type animals of a similar genetic background (Table 3.2). *Stra6-/-* animals tracked the moving grating when set at both 4° and at 2° for approximately 3-5 seconds at a time consistent with the normal visual response of a C57BL6. This response was consistent with all *Stra6-/-* animals tested tracking for a similar length of time and in response to the same grating range.

	Stra6		
	+/+	+/-	-/-
Observed	12	29	15
Expected	14	28	14

Table 3.1: *Stra6-/-* are observed at the expected genetic ratio.

No significant difference in the number of *Stra6+/+*, *Stra6+/-* and *Stra6-/-* animals between the expected and observed values (P= 0.8217, Chi-square test, n=56).

		Stra6	
		+/-	-/-
Sight at 2°	response	2	4
	no response	0	0
Sight at 4°	response	2	4
	no response	0	0

Table 3.2: *Stra6+/-* and *Stra6-/-* animals demonstrate a normal visual response.

Stra6+/- (n=2) and *Stra6-/-* (n=4) animals showing normal head tracking (response) to both 4° and 2° grating. No animals failed to head track (no response).

3.2 *Stra6* diet study mice

3.2.1 *Stra6-/-* dams were transferred to a retinoid-free diet during pregnancy.

Stra6-/- animals do not display the expected developmental phenotypes for a model of Matthew-Wood syndrome. Certain mutants in some retinoid pathway genes also do not have any developmental phenotypes which would be expected due to the known importance of the retinoid pathway for normal development. *Rbp4*, *Crbp* and *Lrat* knockouts all show no developmental phenotypes until the maternal retinoid supply is challenged during embryonic development.

Matings were designed with *Stra6-/-* females to *Stra6+/-* males in order to produce *Stra6-/-* experimental animals and *Stra6+/-* littermates as controls for any non-specific retinoid deficiency effects. Maternal retinoid supply was altered through provision of retinoid-free chow for various periods during pregnancy. Initially maternal diet was modified to a retinoid-free diet from the discovery of vaginal plug to the birth of pups. Further experiments were undertaken subsequent to this in order to define a window of action by transferring the females to the retinoid-deficient diet for 10-day windows during pregnancy: 0-10dpc, 5-15dpc and 10dpc-birth (Figure 3.4).

3.2.2 A retinoid-free diet during pregnancy does not alter the expected ratio of *Stra6-/-* to *Stra6+/-* offspring.

Transfer of *Stra6-/-* dams from normal mouse chow to a retinoid-free diet during pregnancy neither caused embryonic lethality nor increased mortality in the neonatal period. The ratio between *Stra6+/-* and *Stra6-/-* animals was as expected at 1:1 indicating that even under low-retinoid stress these animals were viable (Table 3.3). The diet study did not reveal an increased risk of mortality in the *Stra6-/-* animals in the neonatal period. The expected number of animals was observed at ~2weeks and the *Stra6-/-* diet study animals were not lost preferentially at weaning or in adulthood.

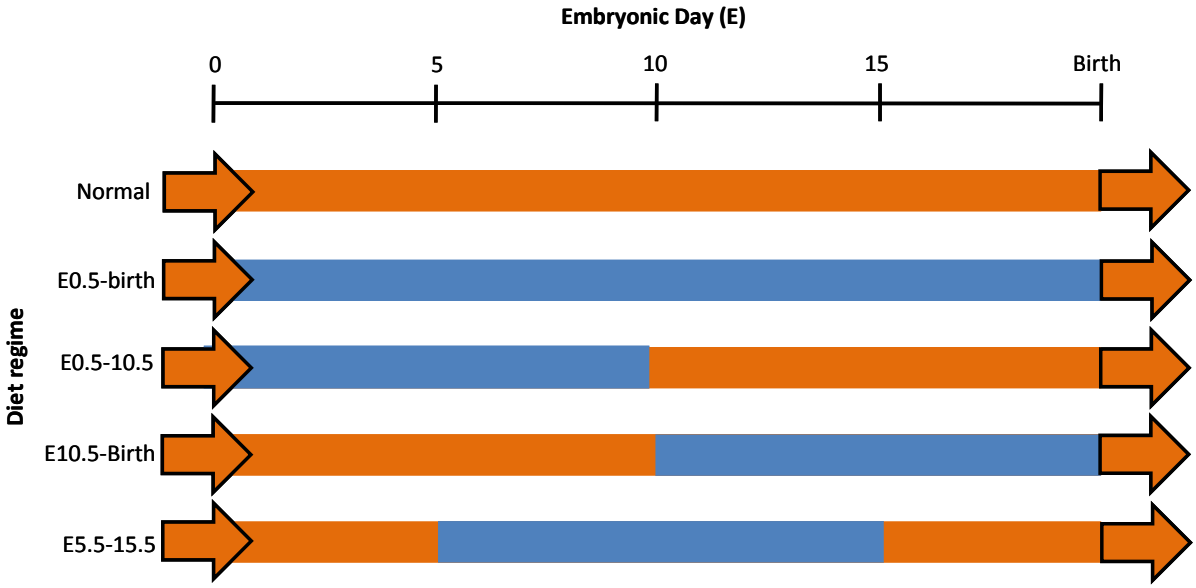

Figure 3.4: *Stra6-/-* dams were fed a retinoid-free diet for various portions of their pregnancy.

Stra6-/- dams were fed a retinoid-free diet (blue) instead of the normal mouse chow (orange) for various time periods between plug discovery (E0.5) and birth. Timing of dietary changes was calculated according to embryonic days counted from plug discovery.

	Stra6	
	+/-	-/-
Observed	19	22
Expected	20.5	20.5

Table 3.3: *Stra6-/-* animals born to dams under dietary retinoid stress are observed at the expected genetic ratio.

No significant difference in the expected and observed number of *Stra6+/-* and *Stra6-/-* animals born to dams fed a retinoid-free diet between E0.5-birth was seen (P= 0.6394, Chi-square test, n=41).

3.2.3 *Stra6-/-* animals from dams fed a retinoid-free diet during pregnancy affects some aspects of development.

3.2.3.1 *Stra6-/-* $^{E0.5\text{-}Birth}$ diet study offspring have defects in eye development.

The reduction in eye-size in *Stra6-/-* animals versus *Stra6+/-* control littermates was evident in the live animal and *Stra6-/-* animals could easily be distinguished in the cage. The eye does not have the normal convex appearance and rather than protruding from the socket sits deeper in the orbits (Figure 3.5).

Eyes from *Stra6-/-* animals weighed significantly less than those from *Stra6+/-* control animals in both grams and as a percentage of body weight (Table 3.4, Figure 3.6 A-B). The difference in eye weight between *Stra6-/-* and *Stra6+/-* male (Table 3.5, Figure 3.6 C-D) and female (Table 3.6, Figure 3.6 E-F) animals was roughly similar; however the weight of the eye represented a greater percentage of body weight in female mice, probably due to the greater body mass of male animals.

In addition to reduction in eye size, lens size was also reduced in *Stra6-/-* compared to *Stra6+/-* controls. Clouding of the eye was seen in some *Stra6-/-* animals (6/22 eyes, 27%) but was not seen in any *Stra6+/-* animals (0/14, 0%). Histological investigation of those clouded eyes revealed cataracts of the lens containing large vacuoles within the lens tissue. Cataractous lens were also found to be incorrectly shaped being ovoid compared within the spherical appearance of the *Stra6+/-* lens (Figure 3.7 A-B). The ovoid appearance and the cataractous nature of some *Stra6-/-* lens may be associated with other aspects of the eye phenotype in *Stra6-/-* diet study mice, such as PHPV, discussed below.

Microphthalmia is often associated with other morphological eye defects therefore histological sections were taken of *Stra6-/-* and *Stra6+/-* eyes. Bilateral persistent hyperplastic primary vitreous or PHPV was observed in all *Stra6-/-* eyes (22/22) and was pigmented in all cases (Figure 3.7 B-C). PHPV was not observed in any *Stra6+/-* control animals (0/14). In *Stra6-/-* animals with abnormal lens structure and shape, the PHPV was often intimately associated with the extruded lens tissue (black arrow, Figure 3.7 B). Pigmentation of the persistent vessels is a common feature

observed in cases of PHPV as mobilized retinal pigmented epithelial cells migrate along the vessel (Ikeda 1999). The pigmented mass at the rear of the eye is positive for a marker of blood vessels, collagen IV, definitively identifying it as blood vessel in origin (Figure 3.7 D). The persistence of the hyloid vascultature and its continued association with the posterior lens capsule may result in the cataract formation observed. PHPV and cataract formation are linked in humans (Khaliq 2001) and animal models of PHPV (Boeve 1988) and is thought to be due to the formation of a fibrolenticular plaque at the site in which the association between the vasculature and the lens capsule persists (Reichel 1998).

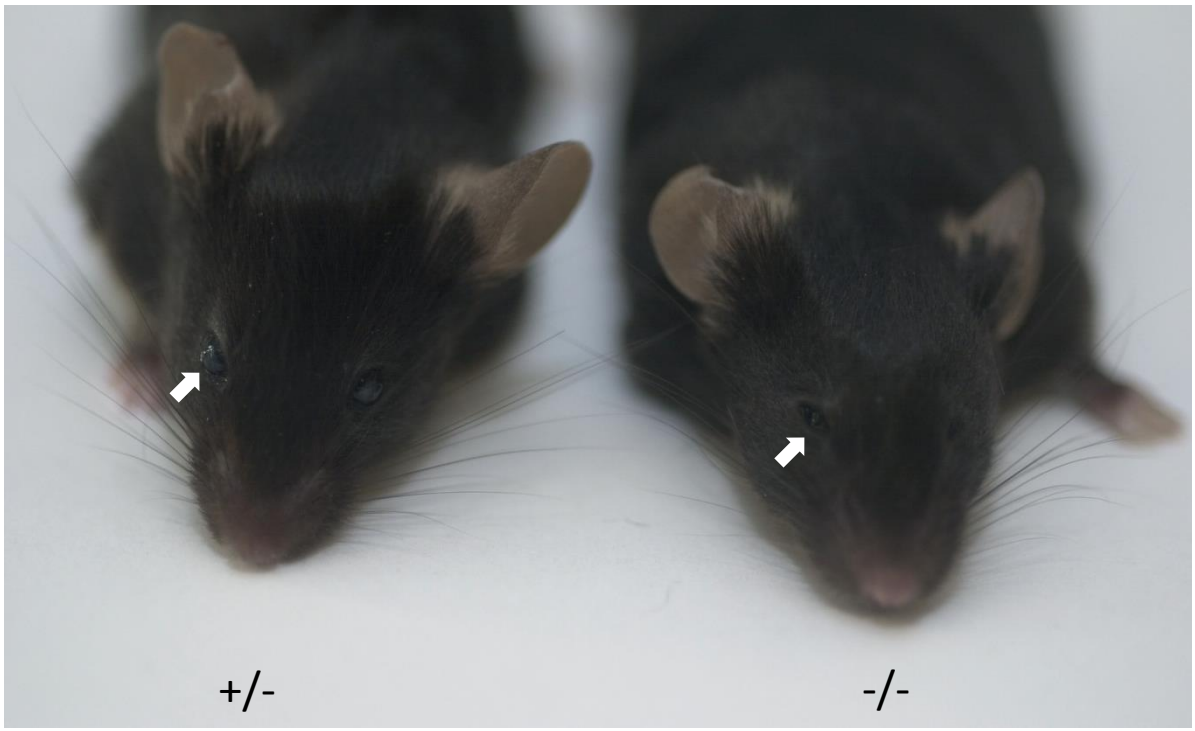

Figure 3.5: *Stra6-/-* from dams fed a retinoid-deficient diet during pregnancy have small eyes compared to *Stra6+/-* littermates.

Frontal view of *Stra6-/-* (-/-) and there *Stra6+/-* (+/-) littermates could be identified in the cage based on their eye size and shape. Eyes (white arrow) of *Stra6-/-* animals were smaller and sat deeply within the orbits with short palpebral fissures compared to *Stra6+/-* littermates.

		Eye Weight	
		%	g
Stra6	+/-	0.083%	0.0258
	-/-	0.067%	0.0190

Table 3.4: *Stra6-/-* eyes weigh significantly less than the eyes of their *Stra6+/-* littermates.

g: eye weight in grams, %: eye weight as a percentage of body weight. Values shown are averages. P< 0.0001, Student t-test. *Stra6+/-* n=7, *Stra6-/-*n=11

Male		Eye Weight	
		%	g
Stra6	+/-	0.082%	0.0256
	-/-	0.065%	0.0188

Table 3.5: *Stra6-/-* eyes weigh significantly less in males.

g: eye weight in grams, %: eye weight as a percentage of body weight. Values shown are averages. P< 0.0001, Student t-test. *Stra6+/-* n=6, *Stra6-/-*n=6

Female		Eye Weight	
		%	g
Stra6	+/-	0.090%	0.0267
	-/-	0.070%	0.0194

Table 3.6: *Stra6-/-* eyes weigh significantly less in females.

g: eye weight in grams, %: eye weight as a percentage of body weight. Values shown are average. P=0.0316, Student t-test. *Stra6+/-* n=2, *Stra6-/-*n=5

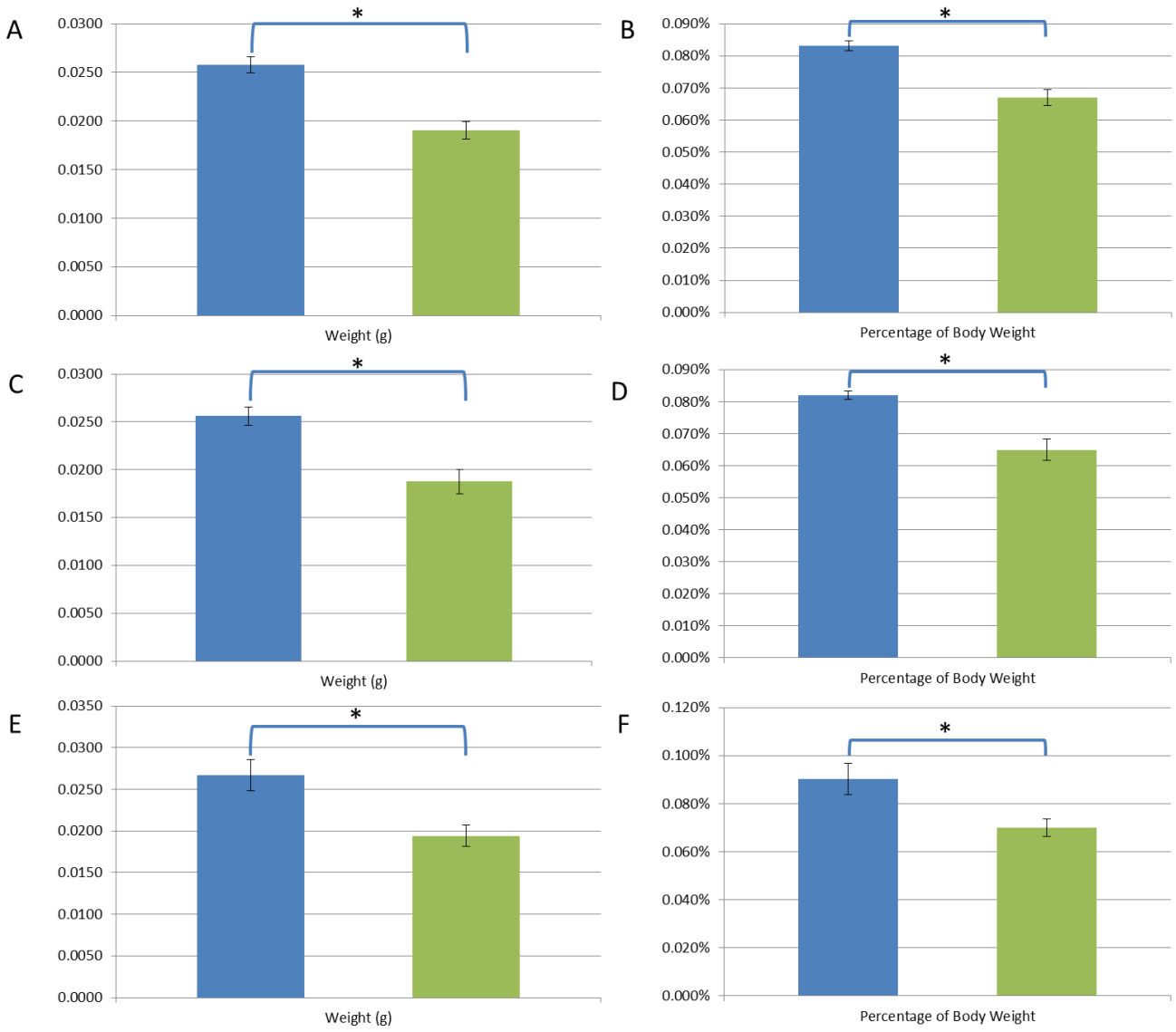

Figure 3.6: *Stra6-/-* eyes weigh significantly less than their *Stra6+/-* littermates.

Eye weight was significantly reduced in *Stra6-/-* (green) animals compared to *Stra6-/-* littermates (blue) both in grams (A) and as percentage of body weight (B). The reduction in eye size is observed in both in male (C & D) and female animals (E & F).

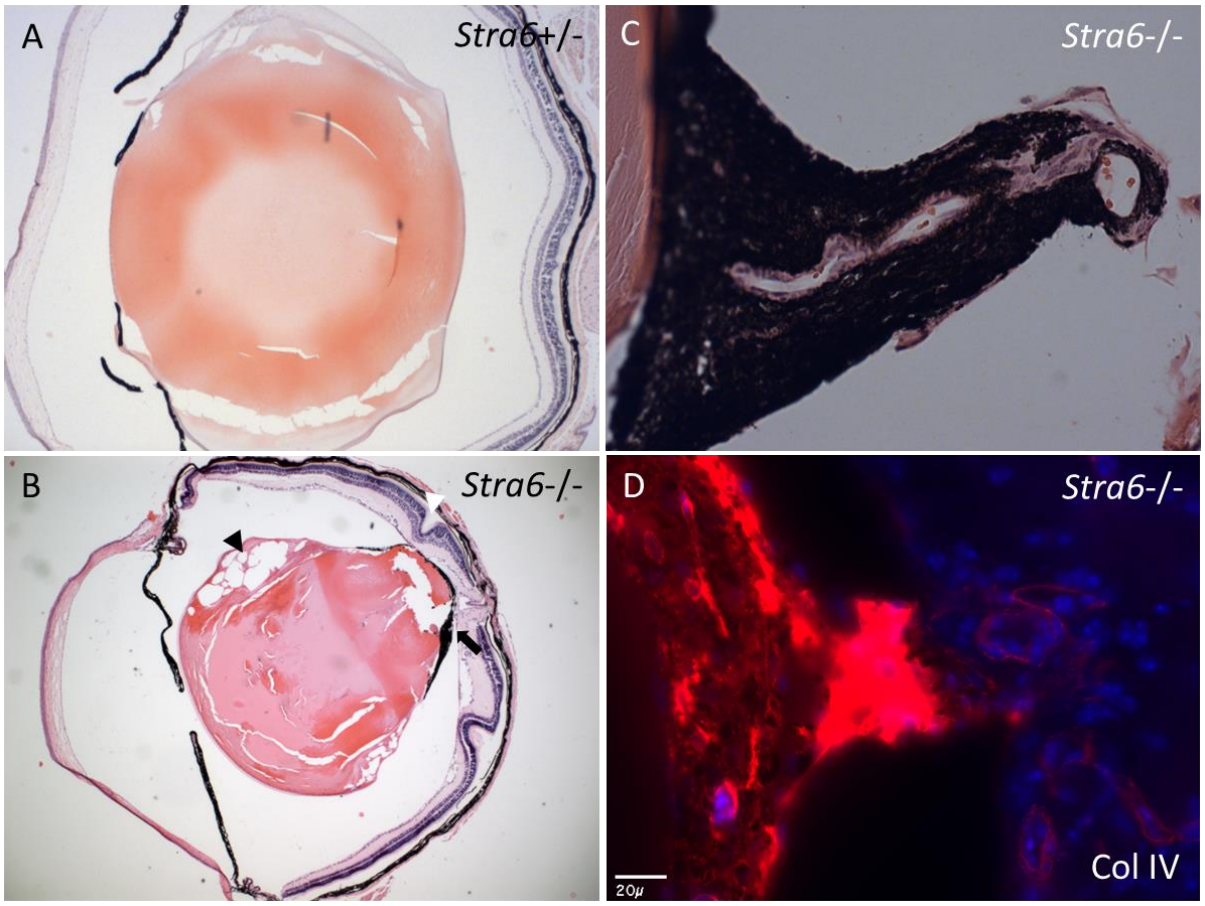

Figure 3.7: Eye morphology is disrupted in *Stra6-/-* animals from dams fed a retinoid-free diet.

Eye morphology of *Stra6+/-* animals from dams fed a retinoid-free diet is normal (A), however the morphology of *Stra6-/-* animals is disrupted in several regions (B). Lens morphology is affected with large vacuoles observed (black arrowhead) and the retina is folded (white arrowhead). A pigmented PHPV (black arrow) was also observed associated with the posterior of the lens. A high magnification view of the pigmented mass at the rear of the eye highlighted the vessel structure of the PHPV (C) with the blood cells visible. The pigmented PHPV also expresses a marker of blood vessels, collagen IV (red).

The structure of the retina is well defined with cells arranged into layers easily identified on histological sections (Figure 3.8 A). Formation of the typical layered structure of the retina appears unaffected in homozygous animals with the expected layers observed as for heterozygous littermates. The photoreceptor layer is often dissociated from the RPE in histological sections of the homozygous eye but it is unclear if this is representative of the intact eye or an artefact of the histological process (Figure 3.8 B). The interaction between the RPE and the photoreceptor layer may be more fragile in *Stra6-/-* animals compared to their littermates and therefore more easily dissociated during processing. *Stra6-/-* animals do however show folds of the retinal layers visible on sections indicating folding of the entire retinal sheet in the eye (Figure 3.8 C).

In contrast to heterozygous littermates, in which the ganglion cell layer is smooth and generally around one cell thick (Figure 3.8 A), *Stra6-/-* animals show an increase in the number of cells within, and therefore an increase in the thickness of, the ganglion cell layer with an uneven thickness of cells in this layer across the retina (Figure 3.8 C & D). The ganglion cell layer was found on average to be 4-times thicker in *Stra6-/-* animals (n=4) compared to *Stra6+/-* (n=3) controls (P= 0.0206, Student t-test). Expression of BRN3 is a useful marker for retinal ganglion cells. An anti-BRN3 antibody appears to stain positively in the ganglion cell layer in *Stra6+/-* and *Stra6-/-* animals (Figure 3.9 A-B), although further control experiments are required to confirm this. Despite the increase in the number of cells within the ganglion cell layer of *Stra6-/-* animals, the cells present were have the correct identity for their position as they were positive for BRN3 (Figure 3.9 C-D) and therefore ganglion cell proliferation is likely to be increased or apoptosis reduced in these animals.

Astrocyte cell bodies are also present within the ganglion cell layer and using an antibody for GFAP marks astrocytes and their projections. *Stra6+/-* animals seem to show a low level of staining only within the ganglion cell layer and the vertical projections from the astrocytes into the inner nuclear layer (Figure 3.10 A & C) although further control experiments are required to confirm this. *Stra6-/-* animals show a higher density of GFAP positive cells and this therefore indicates that

multiple cell types of the GCL are increased in number in homozygous animals (Figure 3.10 B). The projections from GFAP positive cells in *Stra6-/-* animals are not single stained lengths but have a rather more branched and 'feathered' appearance (white arrow, Figure 3.10 D). The Müller cell layer is also positive for GFAP in *Stra6-/-* animals (white arrow head, Figure 3.9 B). Expression of GFAP in the Müller cell layer is a marker of retinal stress (Wu 2003) therefore indicating the *Stra6-/-* retina appears to be experiencing stress possibly induced by the presence of PHPV and folds within the retina.

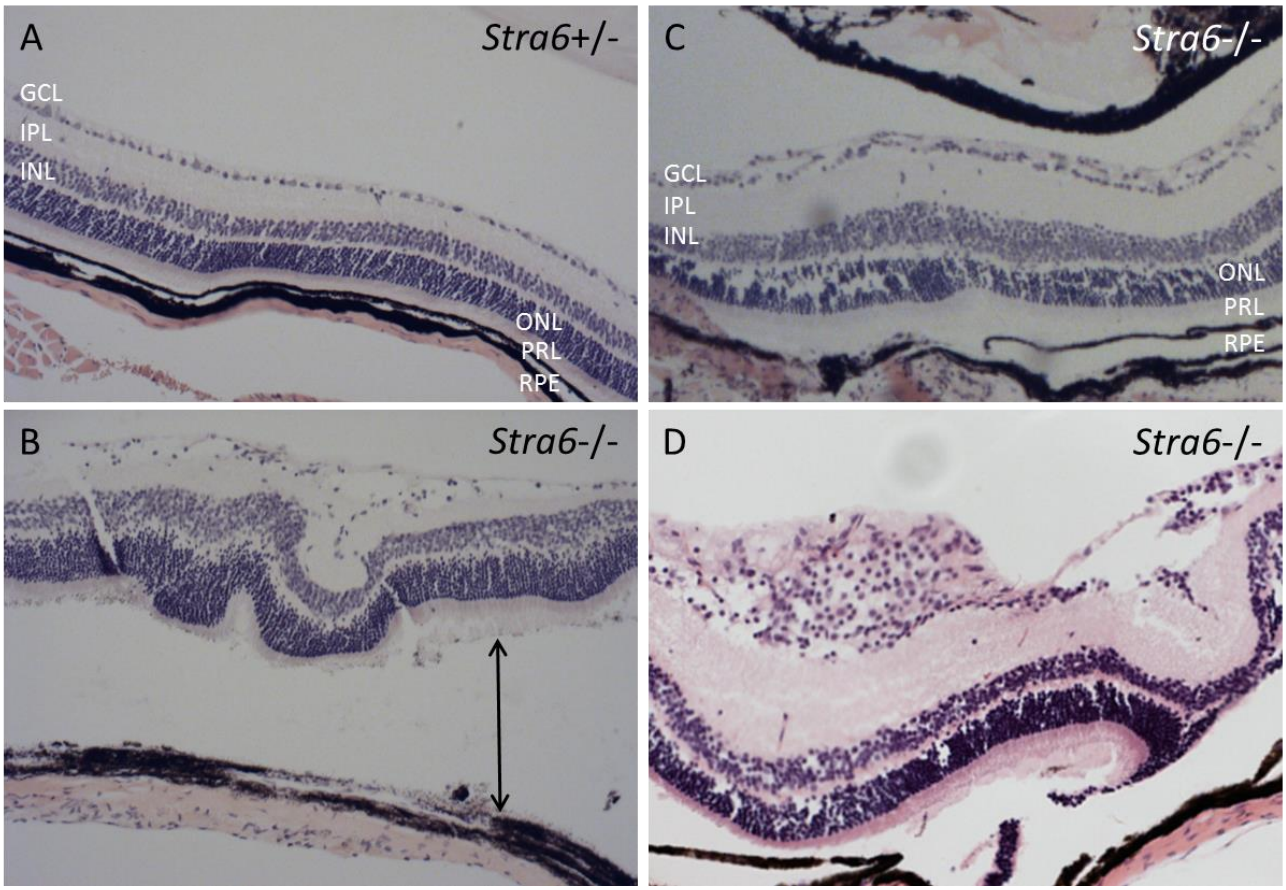

Figure 3.8: *Stra6-/-* retina morphology is disrupted.

The *Stra6+/-* retina (A) is made up of the expected layers (B); namely the ganglion cell layer (GCL), inner plexiform layer (IPL), Inner nuclear layer (INL), outer plexiform layer (OPL), outer nuclear layer (ONL), photoreceptor layer (PRL) and retinal pigmented epithelium (RPE). The *Stra6-/-* photoreceptor layer is dissociated from the RPE (double-headed arrow, B) and the entire retinal layer is folded, however all of the retinal layers can be identified in histological sections (C). The ganglion cell layer in *Stra6-/-* animals, compared to the even generally single cell thick layer in *Stra6+/-*, is un-even across its length with many regions with a ganglion cell layer many cells thick (D).

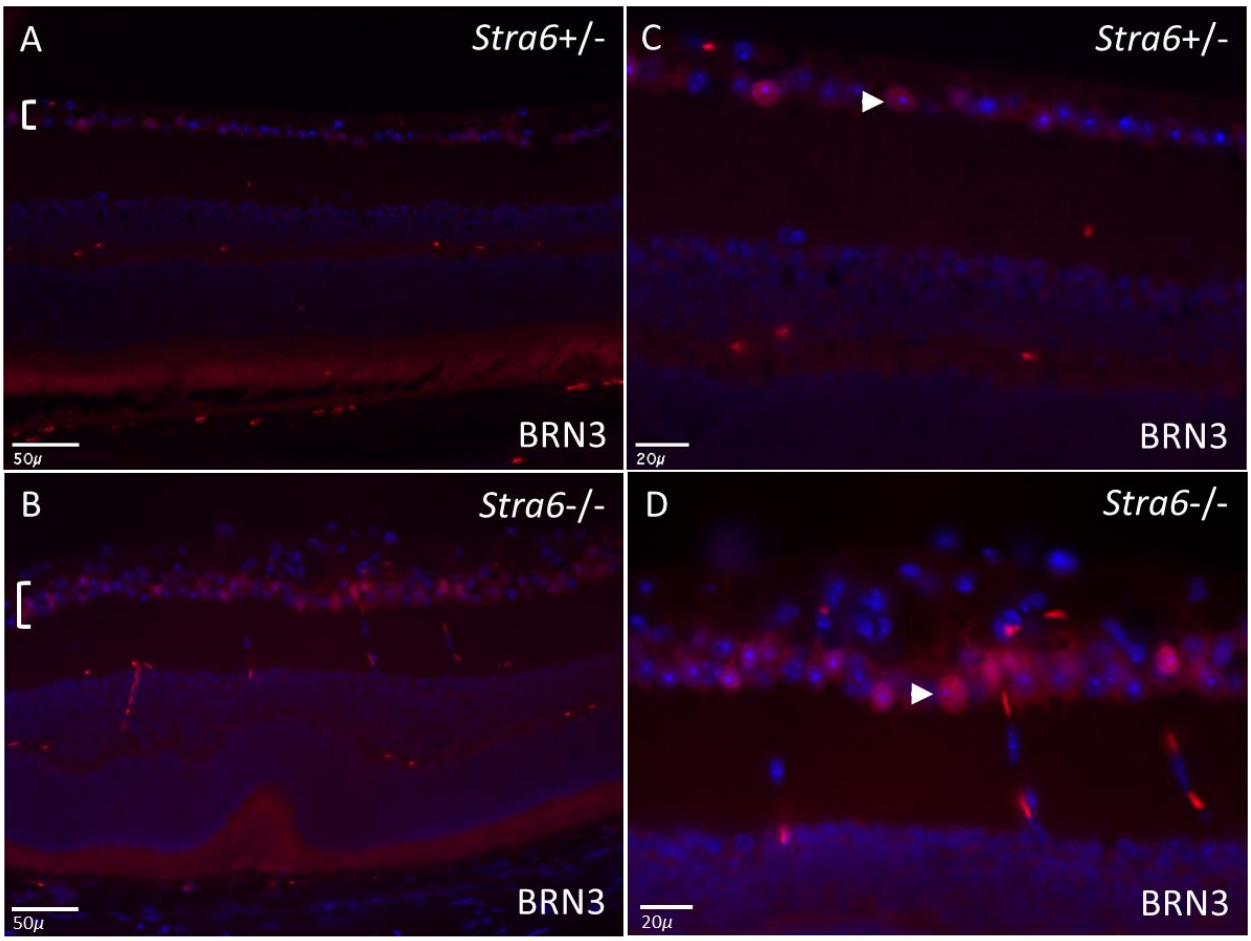

Figure 3.9: BRN3 positive cells are increased in the *Stra6-/-* retina.

Low magnification images of *Stra6+/-* (A) and *Stra6-/-* (B) retinas highlight increase in the thickness of the BRN3 positive layer (white bracket) in *Stra6-/-* animals (n=2) compared to *Stra6+/-* littermates (n=2). High magnification images show the increase in the number of BRN3 positive cells (white arrowhead) in *Stra6-/-* (D) compared to *Stra6+/-* (C) ganglion cell layer.

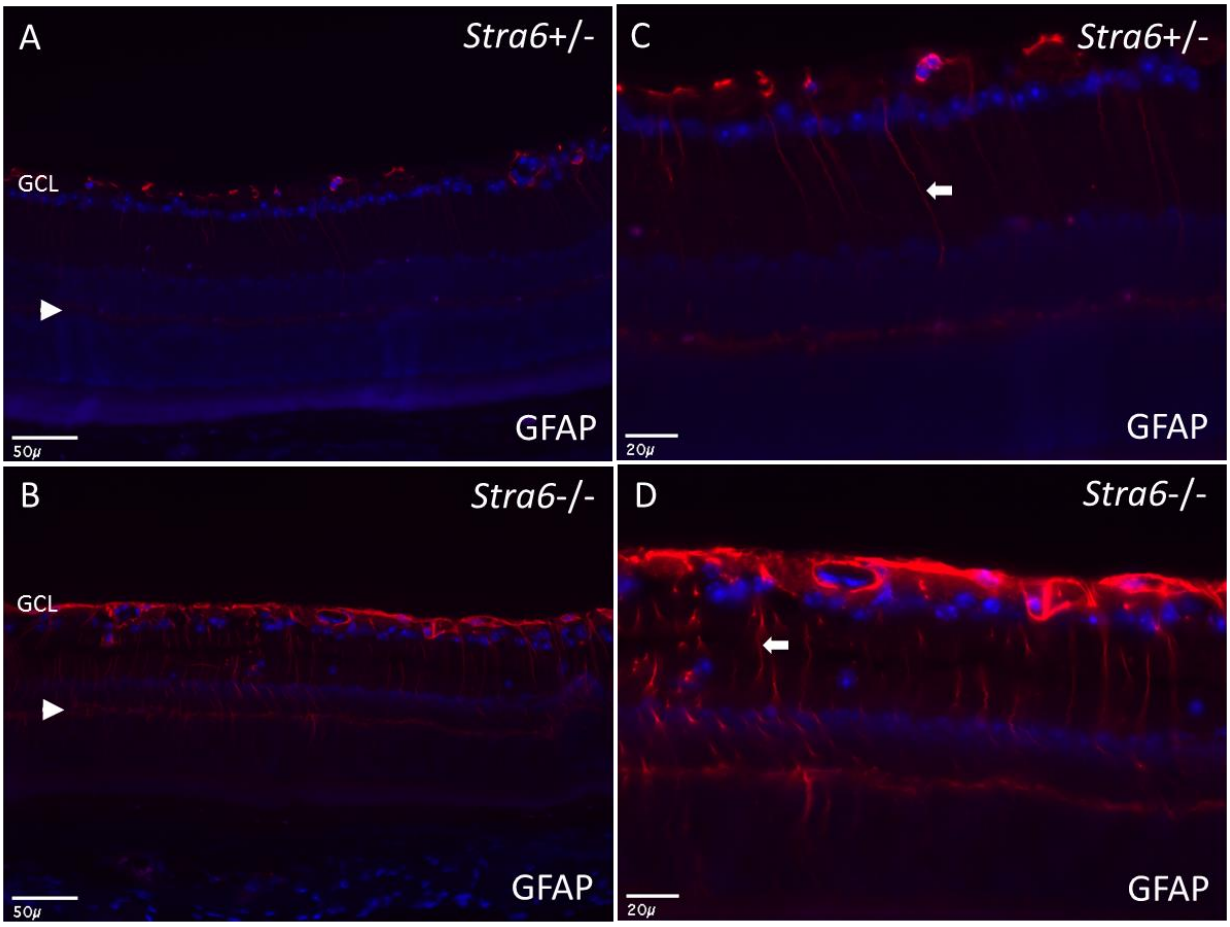

Figure 3.10: *Stra6-/-* retinas show sign of stress and changes to astrocyte projections.

Low magnification images indicate the location of GFAP positive (red) cells within the *Stra6+/-* (A) and *Stra6-/-* (B) retina. GFAP positive cells are found throughout the ganglion cell layer (GCL) in both *Stra6+/-* (n=2) and *Stra6-/-*(n=2) animals, but the Muller cell layer (white arrowhead) is only positive in *Stra6-/-* retinas. High magnification images focus on the astrocyte projections (white arrow) in the *Stra6+/-* (C) and *Stra6-/-* (D) retina highlighting the difference in projection morphology from smooth lengths to more feathered and disorganised lengths respectively.

Astrocytes are known to be associated with the vasculature of the retina and they induce vessel formation during development. Blood vessels within the retina are positive for Collagen IV and staining for Collagen IV appears to highlight changes to retinal vascularisation in homozygous mutant animals although further control experiments are required to confirm this. *Stra6+/-* controls showed staining of end-profile cross-sectional vessels within both the inner and outer plexiform-nuclear layer boundary and in the GCL (white arrowhead, Figure 3.11 A & C). In contrast, staining of *Stra6-/-* retinas for Collagen IV mainly highlights vessels with a longitudinal cross-section between the inner and outer plexiform layers. This type of vessel morphology not observed in *Stra6+/-* littermates. This indicates that vessels in *Stra6-/-* animals do not have the normal horizontal position within the retina and instead often form vertical paths across the plexiform layers (white arrowhead, Figure 3.11 B & D).

Light sensing within the eye is performed by the photoreceptors – specialised cells which contain light sensitive pigments containing retinal. Rhopdopsin was used as a marker of photoreceptor cells and to investigate retinal degeneration in *Stra6-/-* animals. Rhodopsin appeared to be observed only within the photoreceptor layer of the retina in *Stra6+/-* (Figure 3.12 A) and *Stra6-/-* (Figure 3.12 B) animals, although further control experiments are required to confirm this. Rhodopsin specifically stained the outer segment of the photoreceptor layer in *Stra6+/-* animals (white bracket, Figure 3.12 C) but not the inner segment (white double arrow, Figure 3.12 C). Rhopdopsin levels may be reduced in *Stra6-/-* animals with less intense staining seen (Figure 3.12 B) compared to *Stra6+/-* littermates (Figure 3.12 A) although this difference was not quantified. Photoreceptor integrity was good and rhodopsin did not appear to be mis-localised to the inner segment; a known marker of photoreceptor degeneration (white double arrow, Figure 3.12 D). Photoreceptor degeneration does not seem to be a feature of the *Stra6-/-* diet study phenotype, at least in younger *Stra6-/-* mice.

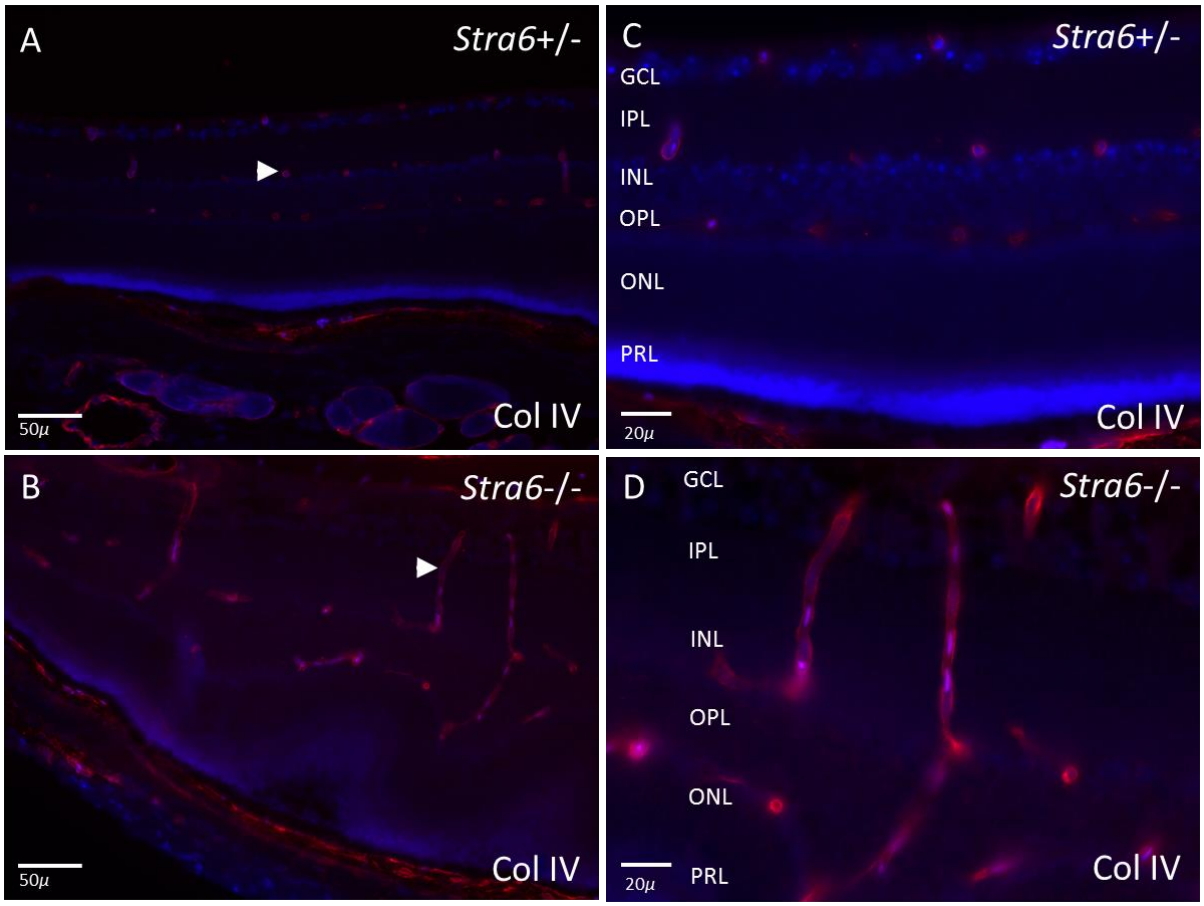

Figure 3.11: Vessel morphology and arrangement in the *Stra6-/-* retina is abnormal.

Low magnification images indicate the location and arrangement of Collagen IV (Col IV) positive (red) blood vessels (white arrowhead) within the retina of *Stra6+/-* (A) and *Stra6-/-* (B). High miagnification images reveal the location and direction of blood vessels within the retina in relation to the layers of the retina; the ganglion cell layer (GCL), inner plexiform layer (IPL), Inner nuclear layer (INL), outer plexiform layer (OPL), outer nuclear layer (ONL) and the photoreceptor layer (PRL). Vessels within *Stra6+/-* animals (C) are found at the intersection of both the inner and outer plexiform and nuclear layers. However, in *Stra6-/-* retinas (D), the vessels span the plexiform layers and can be seen in their longitudinal cross-section. *Stra6+/-* n=2, *Stra6-/-*n=2.

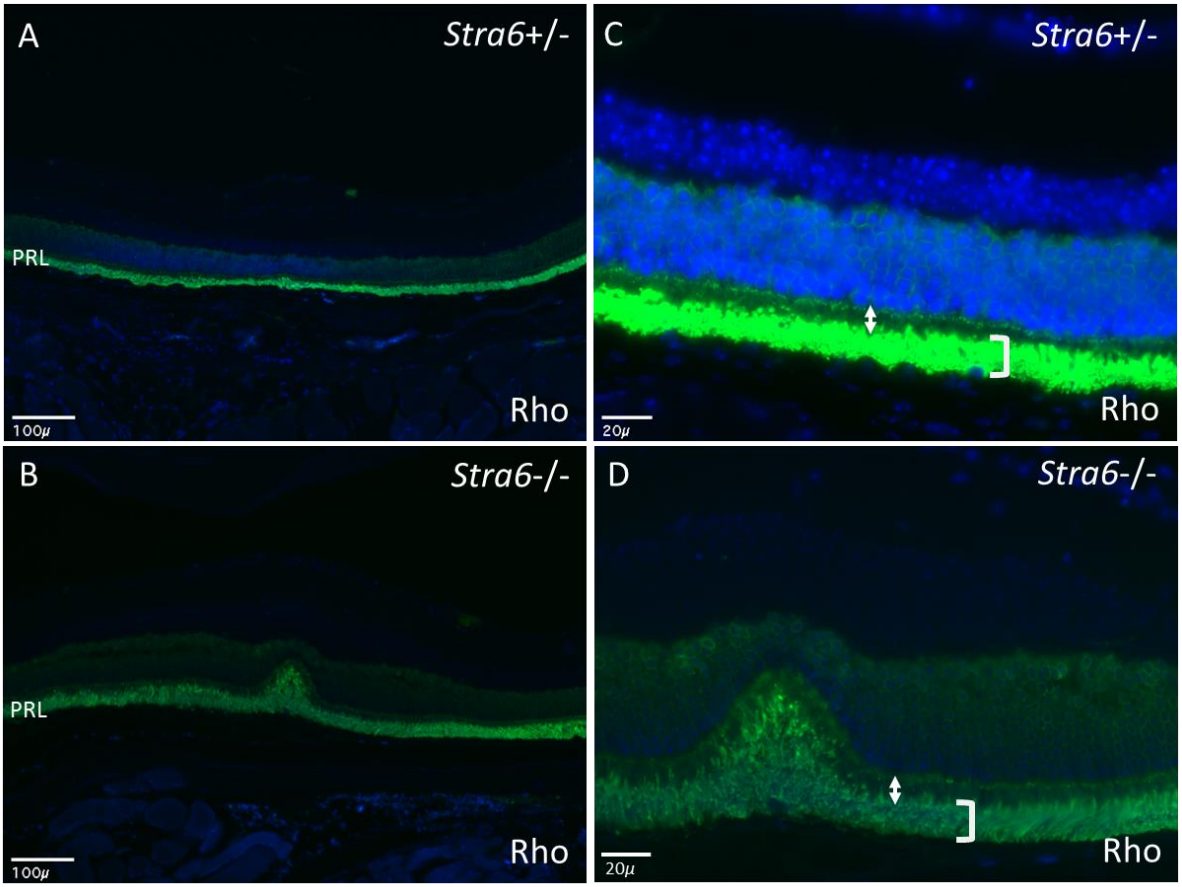

Figure 3.12: *Stra6* is not required for photoreceptor integrity or development.

Low magnification images show that Rhodopsin (Rho) is localised only to the photoreceptor layer (PRL) of the retina in *Stra6*+/- (A) and *Stra6*-/- (B) animals. High magnification images indicate that Rhodopsin (green) is localised only to the outer segment (white bracket) and not the inner segment (white double arrow) of the photoreceptor layer of the retina in both *Stra6*+/- (C) and *Stra6*-/- (D) animals. *Stra6*+/- n=2, *Stra6*-/-n=2.

3.2.3.2 The susceptibility of the developing eye to changes in maternal dietary retinoid provision appears to be temporally variable.

The critical period for the requirement of maternal retinoid provision in order to maintain eye development in the absence of *Stra6* was investigated via provision of a retinoid-free diet for 10-day windows during pregnancy (Figure 3.4). The temporal requirement for *Stra6* in eye development may therefore be further defined. The data collected in order to investigate the critical period is preliminary and further animals need to be collected and investigated in order to solidify the initial conclusions drawn.

3.2.3.2.1 A *Stra6-/-* $^{E0.5\text{-}10.5}$ diet study animal has no defects in eye development.

Eye weight was not significantly different between *Stra6-/-* diet study animals from dams fed a retinoid free diet from plug discovery until E10.5 (*Stra6-/-* $^{E0.5\text{-}10.5}$) to the average eye size of *Stra6+/-* animals from dams fed a retinoid-free diet for 10-day windows during pregnancy (Table 3.7). Only one animal was obtained for this time point and this required the comparison to the average eye size of animals from different dietary windows, therefore data presented is only preliminary observations.

Eye morphology of the *Stra6-/-* $^{E0.5\text{-}10.5}$ diet study animal was normal. The lens was the normal spherical shape expected with no indication of cataract formation. The posterior of the eye was free from PHPV (Figure 3.13 A); a histological finding noted in all eyes from *Stra6-/-*$^{E0.5\text{-}birth}$ diet study animals (Figure 3.7 B-C). The retina was well structured and the photoreceptor layer was associated with the RPE. The retina did not contain any folds or 'waves' and the ganglion cell layer was uniform across its length (Figure 3.13 B).

3.2.3.2.2 A *Stra6-/-* $^{E5.5\text{-}15.5}$ diet study animal has defects in eye development.

The eye weight was notably reduced in a *Stra6-/-* diet study pup from a dam fed a retinoid-free diet from day E5.5-15.5 compared to a control *Stra6+/-* littermate (Table 3.8).

Stra6-/- $^{E5.5\text{-}15.5}$ eye morphology differed from the *Stra6+/-* $^{E5.5\text{-}15.5}$ littermate eye with defects observed in the retina. The retina formed 'waves' indicating folding of the

retinal sheet as observed for *Stra6-/-* $^{E0.5\text{-}birth}$. The photoreceptor layer was also dissociated from the RPE layer. The ganglion cell layer was, however, fairly even along the length of the section (Figure 3.13 C & E). The lens was normal in appearance and shape indicating no formation of cataract in *Stra6-/-* $^{E5.5\text{-}15.5}$ eyes (Figure 3.13 C). Cataract was not observed in all *Stra6-/-* $^{E0.5\text{-}birth}$ animals and therefore the absence of cataract in this animal is not conclusive to the lack of cataract in all *Stra6-/-* $^{E5.5\text{-}15.5}$ animals. PHPV was observed bilaterally as a small vascular prominence from the back of the eye in the region of the optic nerve entrance in *Stra6-/-* $^{E5.5\text{-}15.5}$ eyes. The vascular tissue is, however, not pigmented and was less extensive compared to *Stra6-/-* $^{E0.5\text{-}Birth}$ eyes (Figure 3.13 D).

3.2.3.2.3 A *Stra6-/-* $^{E10.5\text{-}Birth}$ diet study animal has defects in eye development.

Eyes from the *Stra6-/-* $^{E10.5\text{-}birth}$ animal weighed notably less than their Stra6+/- $^{E10.5\text{-}birth}$ counterpart (Table 3.9).

The lens of the *Stra6-/-* $^{E10.5\text{-}birth}$ animal was normal and spherical in appearance with no vacuoles indicative of cataract formation (Figure 3.13 F). The retina of the *Stra6-/-* $^{E10.5\text{-}birth}$ animal showed some defects with the photoreceptor layer separated from the RPE and the size of the inner and outer nuclear layers was not even across the length of the section. The ganglion cell layer also varied in thickness slightly across the length of the section (Figure 3.13 G). PHPV was also observed bilaterally in the *Stra6-/-* $^{E10.5\text{-}birth}$ animal as a region of vascular tissue in the posterior of the eye (Figure 3.13 F). As for the *Stra6-/-* $^{E5.5\text{-}10.5}$ animal and in contrast to *Stra6-/-* $^{E0.5\text{-}birth}$ animals, the PHPV in these eyes is small and is not pigmented.

E0.5-10.5		Eye Weight	
		%	g
Stra6	+/- *	0.084%	0.0198
	-/-	0.078%	0.0217

Table 3.7: *Stra6-/-*$^{E0.510.5}$ do not show a reduction in eye size compared to diet study *Stra6+/-.*

g: eye weight in grams, %: eye weight as a percentage of body weight. * indicates that these values are an average of *Stra6+/-* eyes from animals from dams fed a retinoid deficient diet for 10-day windows during pregnancy. *Stra6+/-* n=2, *Stra6-/-* n=1.

E5.5-15.5		Eye Weight	
		%	g
Stra6	+/-	0.101%	0.0223
	-/-	0.075%	0.0200

Table 3.8: *Stra6-/-*$^{E5.5\text{-}15.5}$ show a reduction in eye size compared to a *Stra6+/-* littermate.

g: eye weight in grams, %: eye weight as a percentage of body weight. *Stra6+/-* n=1, *Stra6-/-*n=1.

E10.5-Birth		Eye Weight	
		%	g
Stra6	+/-	0.109%	0.0226
	-/-	0.094%	0.0196

Table 3.9: *Stra6-/-*$^{E10.5\text{-}Birth}$ show a reduction in eye size compared to a *Stra6+/-* littermate.

g: eye weight in grams, %: eye weight as a percentage of body weight. *Stra6*+/- n=1, *Stra6-/-*n=1.

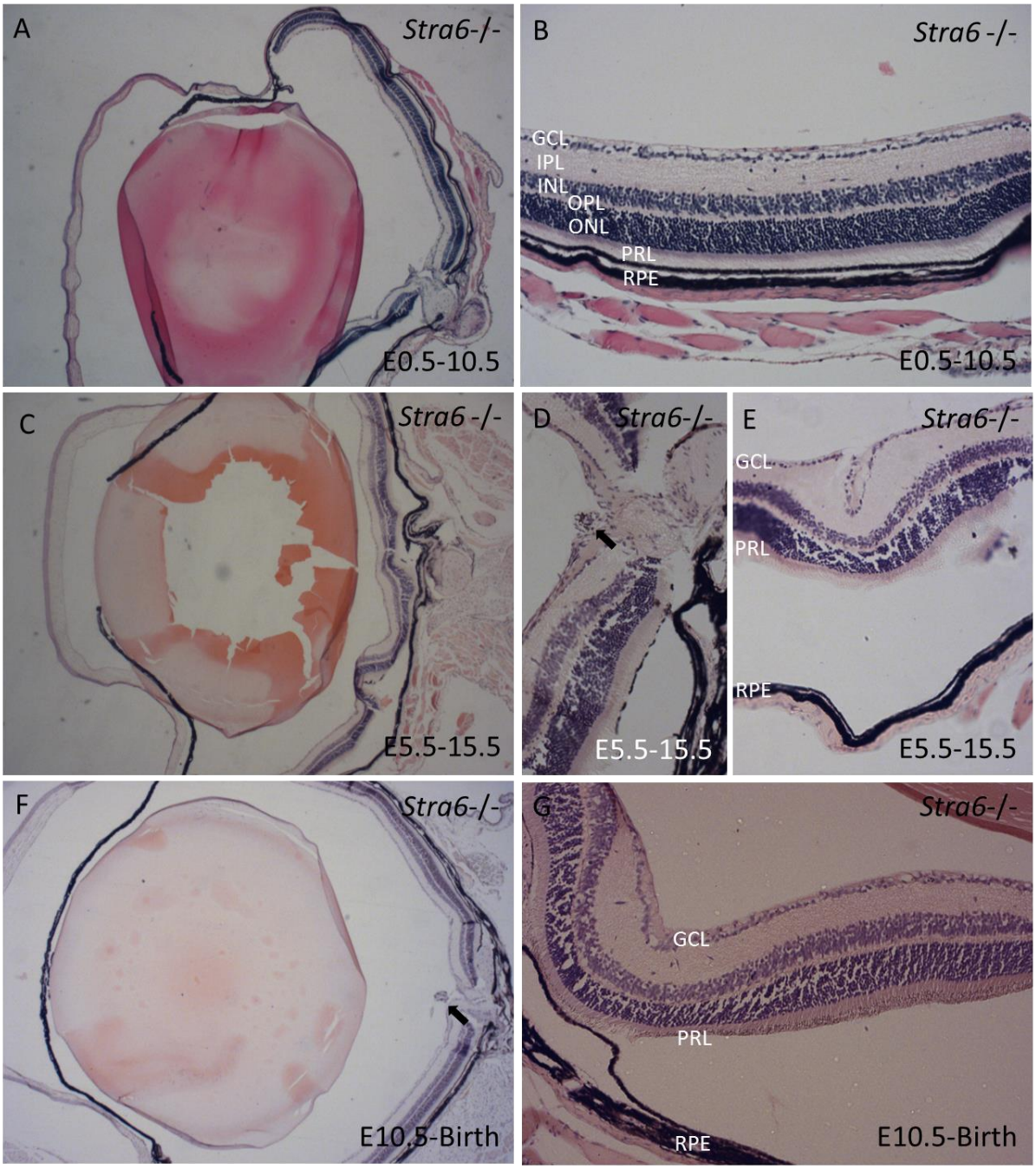
A
Stra6-/-
E0.5-10.5
B
Stra6 -/-
GCL
IPL
INL
OPL
ONL
PRL
RPE
E0.5-10.5
C
Stra6 -/-
E5.5-15.5
D
Stra6-/-
E5.5-15.5
E
Stra6-/-
GCL
PRL
RPE
E5.5-15.5
F
Stra6-/-
E10.5-Birth
G
Stra6-/-
GCL
PRL
RPE
E10.5-Birth

Figure 3.13: The requirement for *Stra6* in eye development is temporally dependent.

The *Stra6-/-*$^{E0.5-10.5}$ eye (A) is normal with no folds of the retina observed and normal lens size and shape noted. The retina of *Stra6-/-*$^{E0.5-10.5}$ (B) consists of the expected layers (inner plexiform layer -IPL, Inner nuclear layer - INL, outer plexiform layer - OPL, outer nuclear layer - ONL), the photoreceptor layer is associated with the retinal pigmented epithelium (RPE) and the ganglion cell layer (GCL) is consistent throughout the section. The *Stra6-/-*$^{E5.5-15.5}$ eye (C) has a normal lens in both morphology and size; however a small remnant of vascular tissue (black arrow) remains to the posterior of the eye (D). The *Stra6-/-*$^{E5.5-15.5}$ retina contains 'waves' and folds and the photoreceptor layer (PRL) is dissociated from the retinal pigmented epithelium (RPE, E). The ganglion cell layer (GCL) is, however, consistent along the length of the retina. The *Stra6-/-*$^{E10.5-Birth}$ eye has a normal lens structure and shape (F). PHPV (black arrow) is observed to the posterior of the eye and the retina was found to be folded in some regions (G). The phoreceptor layer (PRL) is dissociated from the retinal pigmented epithelium (RPE) and the ganglion cell layer (GCL) is uneven.

3.2.3.3 *Stra6-/-* diet study animals have defects in visual acuity.

Visual capacity of *Stra6-/-* and *Stra6+/-* *Stra6*-diet study animals from dams fed a retinoid-free diet from plug discovery to birth was tested by detecting head tracking movements in response to a moving grating, as for non-diet study animals.

Visual acuity was reduced in *Stra6-/-* animals but vision in *Stra6+/-* animals was identical to wild type. The moving grating in the visual testing drum can be varied to different degrees with the lower degrees indicating finer visual ability. Animals were initially tested at 4° at which all *Stra6+/-* animals and most *Stra6-/-* animals (2/3) were noted to head track in response to the drum. The one *Stra6-/-* animal that showed no head tracking response was also un-responsive at 8° and the eye surface appeared bilaterally cloudy indicating that this animal was probably blind. Animals were then tested at 2°, a spacing that wild type animals were comfortably able to distinguish and track. *Stra6+/-* animals tracked movement at 2° but *Stra6-/-* animals showed no head tracking responses to grating at this spacing. *Stra6-/-* diet study animals have vision, as head tracking is seen at 4°, but fine visual acuity is compromised in *Stra6-/-* diet study animals, indicated by a lack of head tracking response at 2° (Table 3.10).

		Stra6 DS	
		+/-	-/-
Sight at 2°	response	4	0
	no reponse	0	3
Sight at 4°	response	4	2
	no reponse	0	1

Table 3.10: *Stra6-/-* $^{E0.5\text{-}Birth}$ animals have an altered visual response.

Stra6+/-$^{E0.5\text{-}Birth}$ animals show normal head tracking (response) in response to both 4° and 2° grating. *Stra6-/-*$^{E0.5\text{-}Birth}$ failed to head track (no response) in response to 2° and response to 4° was variable between animals. *Stra6+/-* n=4, *Stra6-/-*n=3.

3.2.3.4 Male *Stra6-/-* animals show changes to spleen morphology compared to *Stra6+/-* control littermates.

During comparative pathology of homozygous/heterozygous same-sex littermate pairs, the visceral organs were weighed in order to highlight organs which may be affected in *Stra6-/-* diet study animals. In addition to the reduction in eye size observed in *Stra6-/-* animals, the spleen was also found to be significantly smaller in *Stra6-/-* animals compared to their control littermates in terms of total weight but not as a percentage of body weight (Figure 3.14 A & B, Table 3.11). Analysis was then split by sex and the spleen in male *Stra6-/-* was significantly smaller in grams than in male *Stra6+/-* littermates but was not significantly smaller as a percentage of body weight (Table 3.8, Figure 3.14 C & D). No difference in spleen weight was observed between female diet study *Stra6+/-* and *Stra6-/-* animals (Table 3.12, Figure 3.14 E & F). The shape of the spleen was markedly different between male *Stra6-/-* and *Stra6+/-* animals, with the *Stra6-/-* spleen being shorter in length and more 'triangular' compared to the *Stra6+/-* spleen which had a more elongated 'rectangular' appearance (Figure 3.15 A & B). Histological sectioning of the spleen showed a reduction in the size of the white pulp regions in the *Stra6-/-* animals compared to *Stra6+/-*animals (white asterisk, Figure 3.15 C & D); although histology of the white and red pulp appeared normal (Figure 3.15 E & F).

Due to the changes in spleen morphology, immune cell distribution was investigated using FACS. Both spleen and bone marrow were analysed for changes in erythrocyte maturation, B-cell/T-cell ratio or T-cell type between *Stra6-/-* and *Stra6+/-* littermates.

B-cell/T-cell ratio was analysed by investigating the distribution of cells positive for Thy-1, a marker of T-cells and B220, a marker of B-cells. There was a trend to a greater number of B-cells in the *Stra6-/-* spleen and a reduction in T-cell number, compared to the *Stra6+/-* spleen (Figure 3.16, Table 3.13). No difference was observed between T-/B-cell number in the *Stra6-/-* bone marrow (Figure 3.16, Table 3.13).

Erthrocyte differentiation was assessed by comparing the relative levels of CD71 and Ter119 in order to follow the differentiation to mature erythrocytes (Figure 3.17). Erthrocyte maturation profile did not differ significantly between *Stra6-/-* and *Stra6+/-* spleen and bone marrow although the number of mature erythrocytes showed a trend towards reduction in *Stra6-/-* animals in both spleen and bone marrow (Figure 3.18, Table 3.14). The percentage of mature erythrocytes was highly variable between biological replicates however, and therefore it is difficult to definitively make a conclusion on the effect of *Stra6* on mature erythrocyte number.

The distribution of CD45+ T-cells into CD4+ and CD8+ was analysed in order to understand any requirement for *Stra6* in T-cell lineage choice and differentiation. The distribution of CD-45+ T-cells between CD4+ and CD8+ lineages did not significantly differ between *Stra6-/-* and *Stra6+/-* bone marrow or in the spleen (Figure 3.19, Table 3.15). No physiological significant changes were seen to any of the cell populations tested and therefore the histological changes observed in *Stra6-/-* spleens cannot be explained by changes in the cell populations investigated.

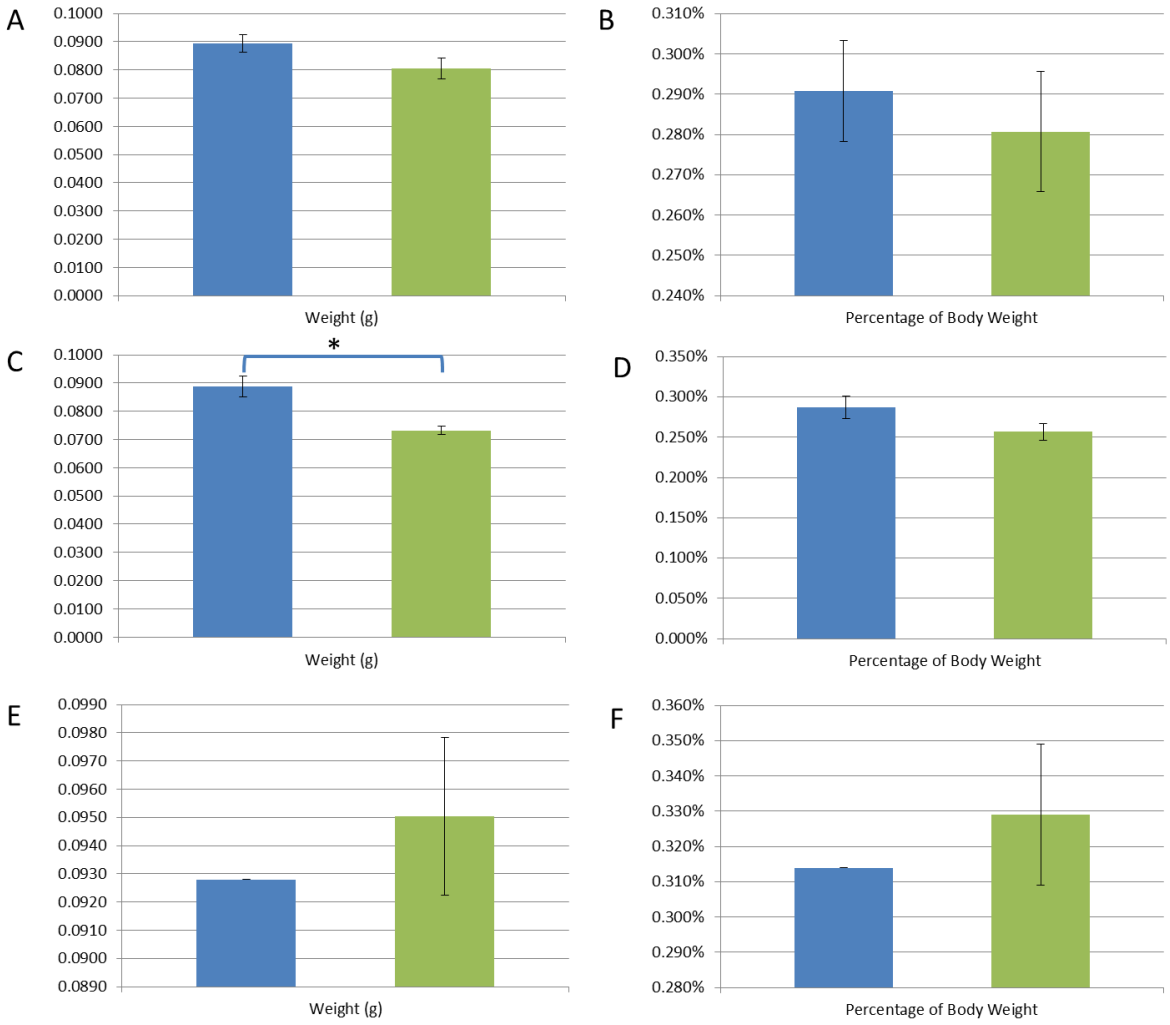

Figure 3.14: Spleen size is reduced in male *Stra6-/-*$^{\text{E0.5-Birth}}$.

Spleen weight was not significantly reduced in *Stra6-/-* (green) animals compared to *Stra6-/-* littermates (blue) either in terms of grams (A) or as a percentage of body weight (B). The reduction in spleen size is observed only in male animals (C & D) and only in terms of grams (C). Female animals (E & F) show no significant difference in spleen size. Significant differences in weight highlighted by an asterisk.

		Spleen Weight	
		%	g
Stra6	+/-	0.291%	0.0894
	-/-	0.281%	0.0805

Table 3.11: *Stra6-/-*$^{E0.5\text{-}Birth}$ spleens do not weigh significantly less than *Stra6-/-*$^{E0.5\text{-}Birth}$.

g: spleen weight in grams, %: spleen weight as a percentage of body weight. Values shown are averages. P= 0.1059, Student t-test. *Stra6*+/- n=7, *Stra6-/-*n=8.

Male		Spleen Weight	
		%	g
Stra6	+/-	0.287%	0.0888
	-/-	0.256%	0.0733

Table 3.12: *Stra6-/-*$^{E0.5\text{-}Birth}$ male spleens weigh significantly less than *Stra6-/-*$^{E0.5\text{-}Birth}$.

g: spleen weight in grams, %: spleen weight as a percentage of body weight. Values shown are averages. P= 0.0024, Student t-test. *Stra6*+/- n=6, *Stra6-/-*n=6.

Female		Spleen Weight	
		%	g
Stra6	+/-	0.314%	0.0928
	-/-	0.329%	0.0950

Table 3.13: *Stra6-/-*$^{E0.5\text{-}Birth}$ female spleens do not weigh significantly less than *Stra6-/-*$^{E0.5\text{-}Birth}$.

g: spleen weight in grams, %: spleen weight as a percentage of body weight. Values shown are averages. P= 0.5798, Student t-test. *Stra6*+/- n=1, *Stra6-/-*n=2.

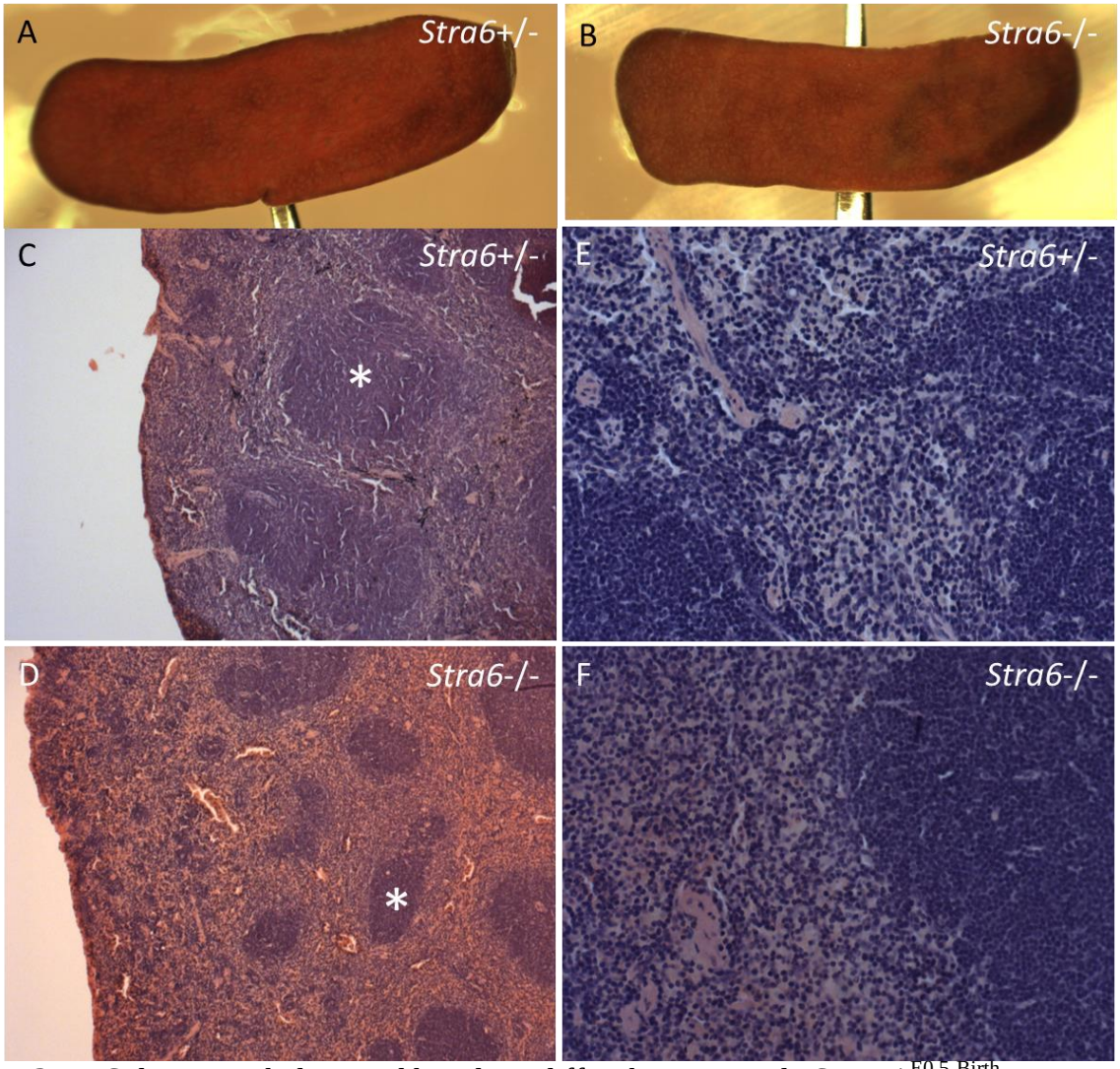

Figure 3.15: Spleen morphology and histology differs between male *Stra6-/-*$^{E0.5\text{-}Birth}$ and *Stra6+/-*$^{E0.5\text{-}Birth}$.

The spleen in *Stra6+/-*$^{E0.5\text{-}Birth}$ (A) is rectangular and elongated whereas the spleen in *Stra6-/-*$^{E0.5\text{-}Birth}$ (B) is more triangular and shorter in length (*Stra6+/-* n=6, *Stra6-/-* n=6). Histological sections of the spleen highlights the normal morphology of the spleen in *Stra6+/-*$^{E0.5\text{-}Birth}$ males (C) with white pulp regions (white asterix) located within the red pulp (*Stra6+/-* n=2, *Stra6-/-*n=2). The regions of white pulp are reduced in size and number in *Stra6-/-*$^{E0.5\text{-}Birth}$ males (D). High magnification images of the white and red pulp regions in *Stra6+/-*$^{E0.5\text{-}Birth}$ (E) and *Stra6-/-*$^{E0.5\text{-}Birth}$ (F) revealed no difference in the morphology of these regions of their borders.

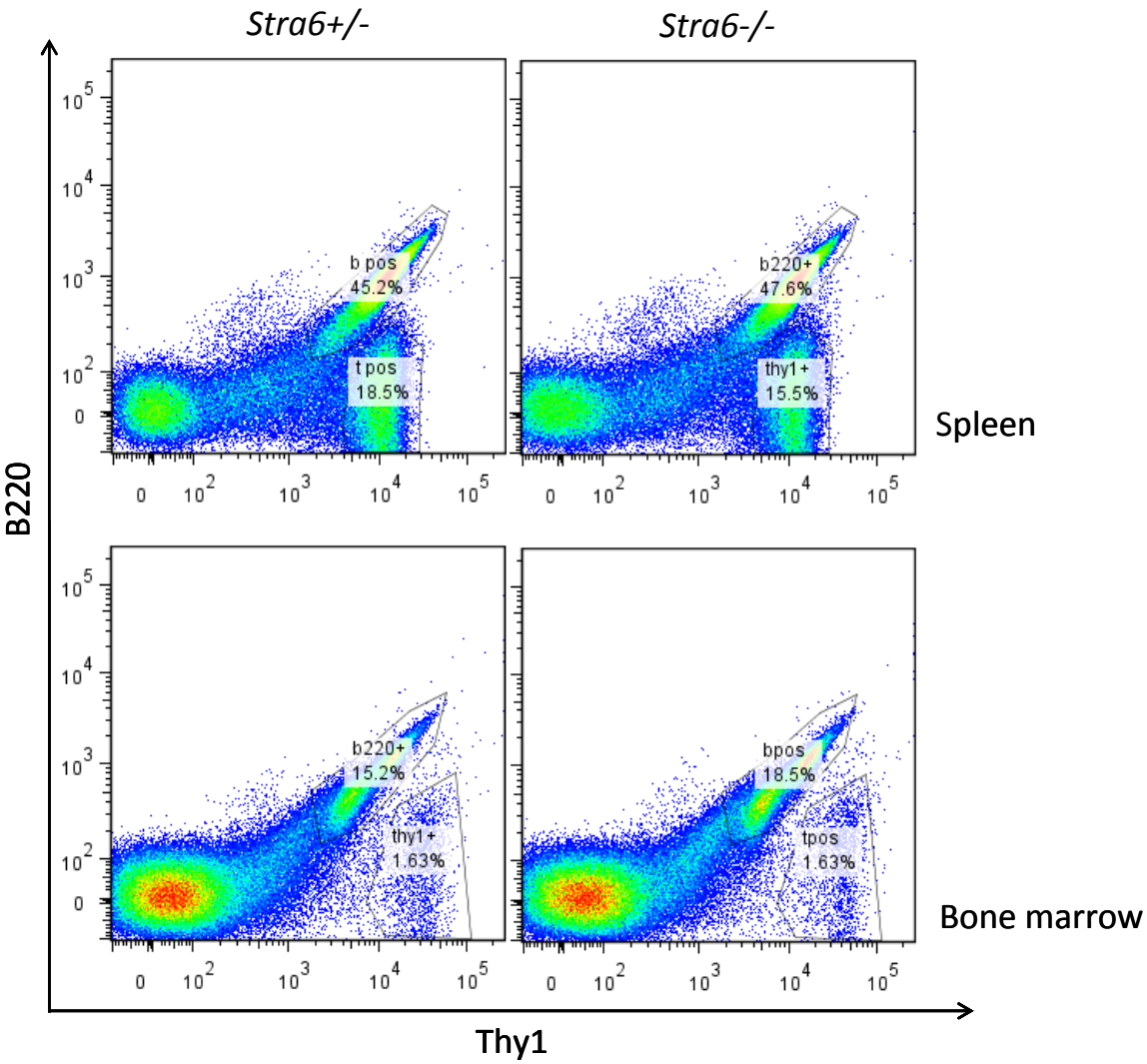

Figure 3.16: T-cell/ B-cell ratio determination is not dependent on *Stra6*.

Representative FACS plots of Thy-1 positive vs. B220 positive spleen and bone marrow cells from *Stra6*+/- and *Stra6*-/- animals. *Stra6*+/- n=2, *Stra6*-/-n=2.

		Thy1 +, B220 -	Thy1 -, B220 +
Spleen	*Stra6 +/-*	25.8	58.9
	Stra6 -/-	22.6	63.2
Bone marrow	*Stra6 +/-*	3.0	35.4
	Stra6 -/-	3.0	34.9

Table 3.14: T-cell/ B-cell ratio determination is not dependent on *Stra6*.

Average percentage of Thy-1 negative, B220 positive B-cells (Thy-1 -, B220+) and Thy-1 positive, B220 negative T-cells (Thy-1+, B220-) in spleen and bone marrow samples analysed by FACS. *Stra6*+/- n=2, *Stra6*-/-n=2.

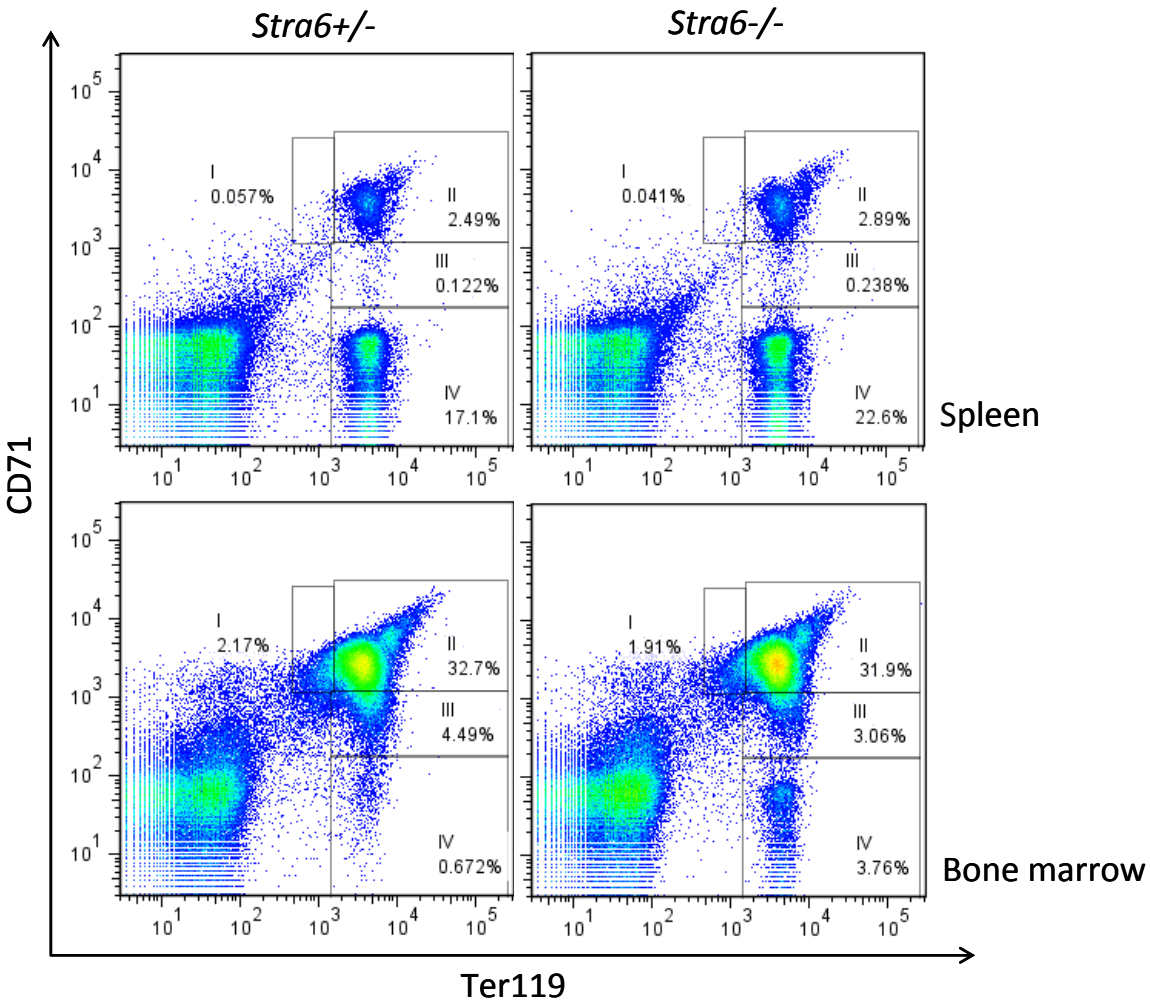

Figure 3.17: Erythrocyte maturation is independent of *Stra6*.

Representative FACS plots of CD71 positive vs. Ter119 positive spleen and bone marrow cells from *Stra6*+/- and *Stra6*-/- animals. Stages of erythrocyte maturation are represented by the ratio between CD71 and Ter119 expression and each gated stage is labelled I, II, III or IV for the most immature to mature erythrocytes respectively. *Stra6*+/- n=2, *Stra6*-/-n=2.

		I	II	III	IV
Spleen	Stra6 +/-	0.0	2.8	0.2	24.5
	Stra6 -/-	0.0	2.2	0.1	11.0
Bone marrow	Stra6 +/-	2.4	27.3	4.5	14.4
	Stra6 -/-	1.8	25.9	3.5	1.4

Table 3.15: Erythrocyte maturation is independent of *Stra6*.The average percentage of cells at erythrocyte differentiation stage I-IV in spleen and bone marrow samples from *Stra6+/-* and *Stra6-/-* animals analysed by FACS. *Stra6+/-* n=2, *Stra6-/-*n=2.

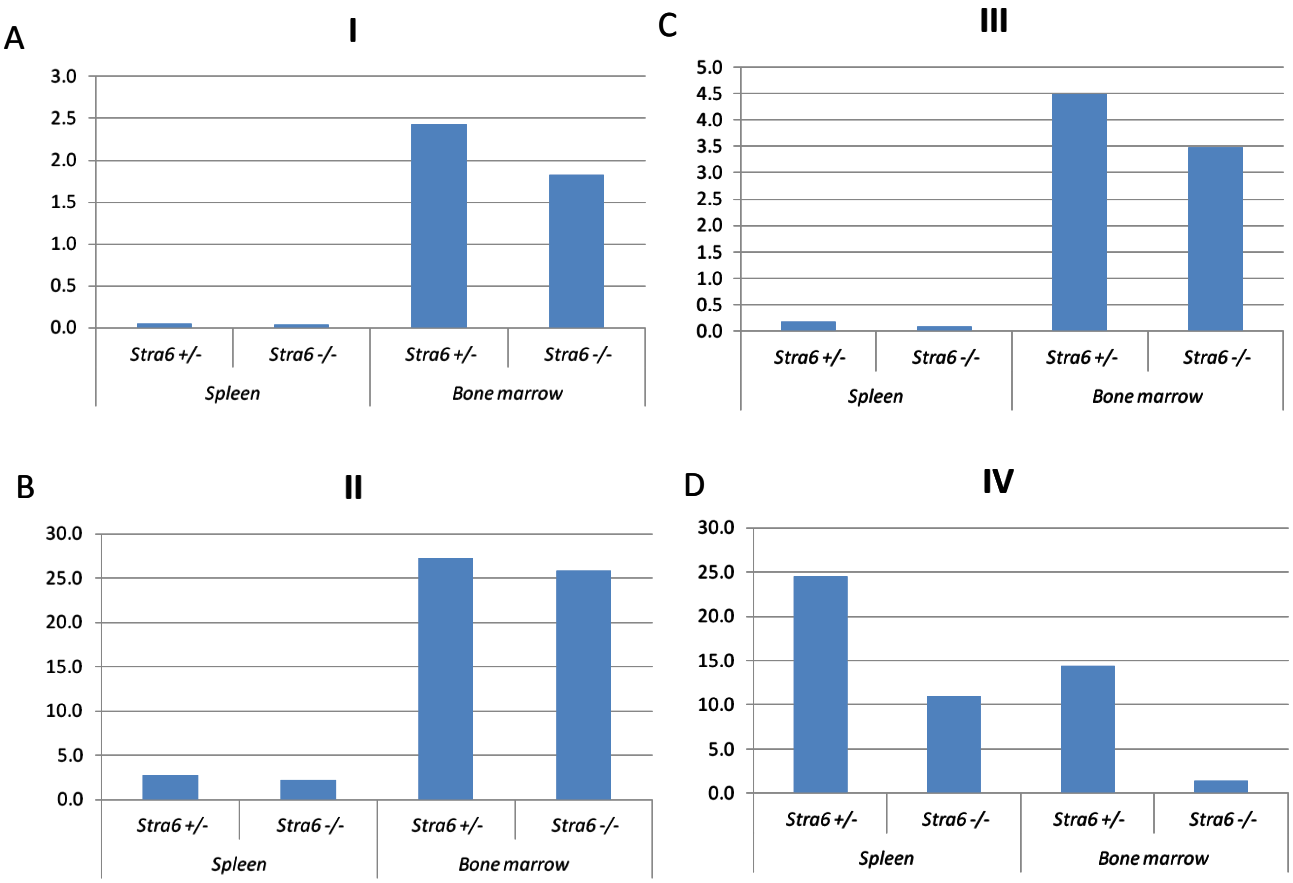

Figure 3.18: Erythrocyte differentiation profile of *Stra6*+/- and *Stra6*-/- animals is undistinguishable.

Average percentage of spleen and bone marrow cells at each stage of erythrocyte differentiation from I (A), II (B), III (C) to IV (D). *Stra6*+/- n=2, *Stra6*-/-n=2.

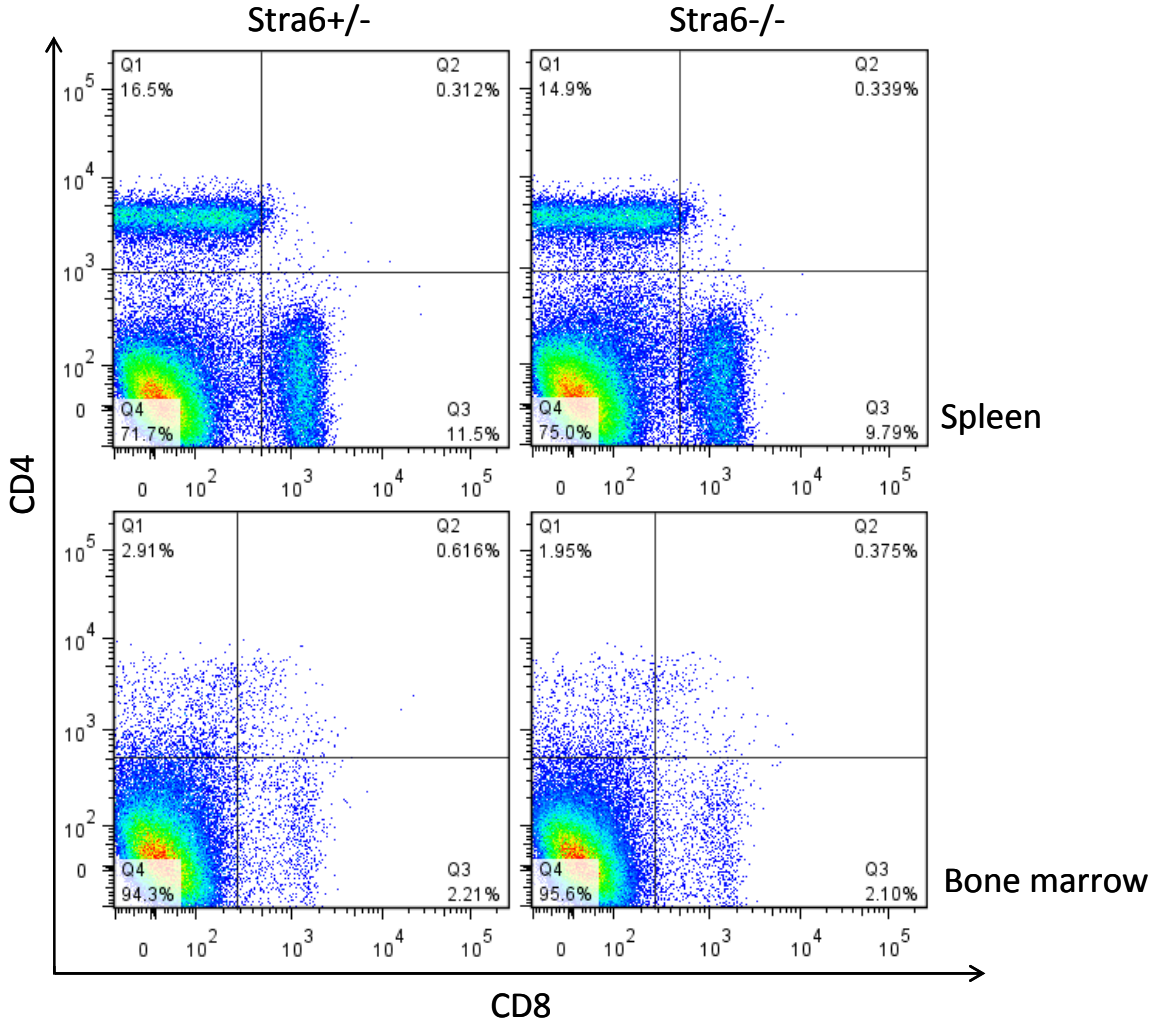

Figure 3.19: The ratio between CD8+ and CD4+ CD45+ T-cells is unaffected by -*Stra6* loss.

Representative FACS plots of CD8 positive vs. CD4 positive spleen and bone marrow cells from *Stra6*+/- and *Stra6*-/- animals. Only cells positive for CD45 have been represented on this plot in order to examine only the CD4/CD8 profile of T-cells. *Stra6*+/- n=2, *Stra6*-/-n=2.

		CD8-, CD4-	CD8+, CD4+	CD8+, CD4-	CD8-, CD4+
Spleen	Stra6 +/-	72.4	0.2	10.5	16.8
	Stra6 -/-	74.9	0.2	9.5	15.4
Bone marrow	Stra6 +/-	96.3	0.3	1.6	1.9
	Stra6 -/-	96.3	0.2	1.7	1.8

Table 3.16: The ratio between CD8+ and CD4+ CD45+ T-cells is unaffected by -*Stra6* loss.

Average percentage of CD4 negative, CD8 positive (CD4 -, CD8+), CD4 positive, CD8 negative (CD4+, CD8-), double negative (CD4-, CD8-) and double positive (CD4+, CD8+) in spleen and bone marrow samples analysed by FACS. Only cells positive for CD45 have been represented in this table in order to examine only the CD4/CD8 profile of T-cells. *Stra6*+/- n=2, *Stra6*-/-n=2.

3.3 Discussion

Stra6-/- mice do not represent the expected model of Matthew-Wood syndrome. *Stra6-/-* animals are not anophthalmic, nor do they have any heart, lung or diaphragmatic defects consistent with the human condition. The knockout animal, produced by removal of two exons by homologous recombination, should result in the production of a truncated transcript due to the production of a premature stop codon and therefore a truncated protein. The removal of the exons was confirmed during production of this knockout allele prior to the commencement of the work described in this thesis and animals were genotyped on the basis of the absence of an exon removed by the targeting construct; however the loss of protein production was not confirmed via western blotting. The lack of phenotype in *Stra6-/-* animals may therefore be the result of production of wildtype protein from the targeted knockout allele, although this scenario is unlikely. The lack of correlation between the human and mouse phenotypes could be explained, assuming the lack of STRA6 protein in *Stra6-/-* animals, by two scenarios; a) complete loss of the protein is less deleterious than the production of a mutant protein, b) a second gene in mouse is able to compensate for the function of STRA6, but this gene is not functional in the human thereby resulting the severe developmental phenotype observed. The first scenario is supported by the continued survival of a human Matthew-Wood patient into late childhood, who is effectively STRA6-null, compared to the normal prognosis of Matthew-Wood patients who typically die within the first year of life (Pasutto 2007). The mutant protein produced in other Matthew-Wood patients could, in addition to minimal retinol transport potential, result in either novel functions which are deleterious to normal development or act in a dominant negative manner in interaction with other genes or pathways in order to cause the observed developmental defects and mortality. The second scenario is further discussed in the subsequent chapter (See 4.0) as a second gene is present in mouse, and other mammals, but is disrupted in humans and other great apes and this may provide a mechanism by which *STRA6* mutations in human result in Matthew-Wood syndrome, but *Stra6-/-* mice are normal.

The retinoid pathway has many inbuilt 'checks and balances' in order to ensure that this most important developmental pathway is functional. Study of various genes of the retinoid pathway have shown that most either form part of functionally redundant families able to compensate for each other's function or are not required unless the animal or embryo is subject to low-retinoid conditions. Due to the lack of any developmental or adult phenotype in *Stra6-/-* mice, *Stra6-/-* dams were fed a low-retinoid diet during pregnancy in order to discern if STRA6 is required under conditions of low-retinoid supply. This has previously been undertaken for *Crbp*, *Rbp4* and *Lrat* knockout mice and resulted in developmental phenotypes under the dietary regime when none were observed under normal dietary retinoid supply. *Stra6-/-* offspring of *Stra6-/-* dams fed a retinoid-free diet during pregnancy had significantly smaller eyes than *Stra6+/-* littermates and also demonstrated various defects in the retina, lens and the vasculature of the eye.

Stra6-/- animals are microphthalmic rather than clinically anophthalmic as observed in Matthew-Wood patients and therefore even with a retinoid-free diet *Stra6-/-* animals are not a model of the eye defects in the Matthew-Wood syndrome. Vitamin-A depleted females, whose growth and fertility was maintained by provision of RA, gave birth to microphthalmic offspring when a rapid and temporally controlled vitamin-A deficiency was induced by removal of the supportive RA during pregnancy (Dickman 1997). The microphthalmia observed in all *Stra6-/-* animals is therefore likely to be the result of a lack of retinoid provision to the developing eye to ensure normal growth.

Persistent hyperplastic primary vitreous (PHPV) was observed bilaterally in all *Stra6-/-* diet study animals and has been described as a feature of other retinoid gene knockouts, such as *Rarβ* (Kastner 1997) and *Raldh3* (Dupe 2003), and also of RA-excess treatment during development between E7-E11 in mouse (Ozeki 1999). The mechanism for this defect in diet study *Stra6-/-* animals is likely to be due to a lack of retinoids, perhaps retinoic-acid. Retinoic acid appears to be required for correct control of apoptosis within the eye possibly through the regulation of apoptosis-effector gene *Eya2* (Matt 2005), which is up-regulated in response to retinol (Ali-Khan 2006). Apoptosis is required for the correct regression of the hyoid vasculature,

which provides nutrients to support the developing eye, before regressing upon the formation of the retinal vasculature which supports the adult eye. In the case of *Stra6-/-*, the lack of retinoids may result in a persistence of the primary vitreous due defects in the normal apoptosis process which would cause regression of the primary vitreous at the appropriate time during development (McKeller 2002). PHPV is known to be associated with an increased occurrence of cataracts in both humans (Silbert 2000) and mice (Reichel 1998). The increased occurrence of cataract with PHPV is possibly due to the connection of the persistent vasculature to the posterior lens surface via a fibrous membrane resulting in the formation of a fibrovascular plaque which in turn leads to cataract (Reichel 1998).

The retina of *Stra6-/-* diet study animal is also disrupted with 'waves' and folds observed in histological sections. Expression of *Stra6* during development was not observed in the developing retina but rather in the RPE and the periocular mesenchyme. The RPE is known to function in the correct specification of the neural retina through expression of various neurotrophic factors. *Stra6* may therefore have a role in the expression of these neurotrophic factors and in its absence the formation of the neural retina becomes disrupted. The retina has a specific pattern of RA activity during development but the retina does not require the RA to be autonomously provided as seen by the lack of retinal layering or folding defects in *Raldh1-/-* and *Raldh3-/-* animals (Matt 2005). STRA6 may therefore have a role in providing RA for retina formation through paracrine signalling from the neural crest-derived periocular mesenchyme. *Rarα/β/γ* triple knockout specifically in the neural crest cells recapitulates the eye defects observed in complete *Rarα/β/γ* knockout and therefore the neural crest cells are the only source of RA required during eye development (Matt 2008).

Stra6-/- diet study retinas have an increase in the number cells in the retinal ganglion cell layer and these additional cells are positive for markers of this cell layer, GFAP and BRN3. GFAP marks astrocytes and, in addition to staining the extra cells, also stains the axons which in *Stra6-/-* are 'feathered' in appearance and some seem to have not made the correct contacts with the inner nuclear layer. *Vax2* controls intraretinal RA metabolism and *Vax2* loss in mouse results in an expansion of the

RA-free zone in the developing retina. *Vax2-/-* animals show an increase in the thickness of the nerve fibre layer, i.e. the astrocytes of the ganglion cell layer, and a disorganisation of the nerve fibre bundles (Alfano 2011). Therefore in *Stra6-/-* animals, an increase in the RA-free region of the developing eye could result in expansion of the astrocytes of the ganglion cell layer resulting in the observed increase in thickness of the GCL. Astrocytes migrate into the eye guided by the secreted chemoattractant PDGF. PDGF and its receptor are negatively regulated by RA in the developing branchial arch (Han 2006), although the relationship between RA and PDGF expression is not clear with both positive and negative regulatory mechanisms reported. Disruption of RA signalling via the loss of *Stra6* may therefore cause an increase in PDGF levels resulting in greater migration of astrocytes into the developing retina.

Embryos from the *Stra6-/-* diet study, as for those *Stra6-/-* born to dams on a retinoid-sufficient diet, do not represent a model for Matthew-Wood syndrome. No defects were observed in the diaphragm, heart or lungs and in the eye only microphthalmia occurred rather than anophthalmia. A recent report has however described homozygous *STRA6* mutations in a consanguineous Irish Traveller family with autosomal recessive non-syndromic colobomatous micro-anophthalmia. *Stra6-/-* diet study animals may in fact be a good model for a subset of human STRA6 mutants which affect only the development of the eye and spare the other organs affected in Matthew-Wood patients. One of the patients with isolated eye defects had a sibling with a typical Matthew-Wood presentation and therefore the penetrance of *STRA6* mutations may be dependent on genetic background or environmental factors in humans (Casey 2011). *Stra6-/-* offspring of dams exposed to a retinoid-free diet for longer periods before pregnancy or on other inbred mouse backgrounds therefore may result in a Matthew-Woods model. The ‘waves’ and folds of the retina observed in diet study *Stra6-/-* animals could be interpreted as signs of coloboma in the mouse; being similar in appearance to the defects observed in the colobomatous *Vax2*-inactivated mouse (Barbieri 2002), further adding to the possibility of using these animals as a model for isolated *STRA6*-related eye defects. This overlap of phenotype between *Vax2-/-* and *Stra6-/-* diet study animals, in the observation of coloboma and

nerve fibre expansion, indicates that *Stra6* loss causes a reduction in RA signalling in the eye incompatible with normal eye development (Alfano 2011).

Stra6-/- dams were transferred to a retinoid-free diet for 10-day windows, E0.5-E10.5, E5.5-15.5 and E10.5-birth, during pregnancy in order to pinpoint the temporal requirement for STRA6 in eye development by studying their *Stra6-/-* offspring. *Stra6-/-* animals from dams transferred between E0.5-E10.5 had normal eye development and consistent with this observation eye development during this period is minimal. Specification of the retinal anlage occurs at the end of gastrulation and at E9.5 the specified eye field splits into symmetrical retinal primordium which evaginate from the forbrain to form optic vesicles (Donner 2004). STRA6 is therefore not likely to be required for the specification of the retinal analage or the later specification of the optic vesicles from the eye field. Development of the eye is rapid and complex between E10-15 with lens formation from the surface ectoderm, optic cup formation, vessel invasion and orientation, and eyelid formation and eventual fusion. Consistent with this intense period of eye development, *Stra6-/-* animals from dams transferred between E5.5-E15.5 and E10.5-birth both show microphthalmia and PHPV consistent with, although not identical to, the phenotype of *Stra6-/-* animals from E0.5-birth dams. This therefore highlights the period between E10.5-E15.5 as a period of eye development with a critical requirement for STRA6. During this period the optic cup closes and the lens vesicle is budded from the surface ectoderm. The hyaloid artery also enters the developing eye at E11-13 and then proceeds to form the posterior region of the vascular tunic surrounding the lens. The vessels of the eye, which surround the optic cup at E10-11, orientate themselves between E12-13 and then begin to regress at E14-15 (Pei 1970). The observation of PHPV in *Stra6-/-* animals from dams transferred between E5.5-E15.5 and E10.5-birth is consistent with the vessel development, morphogenic movement and regression of the embryonic vessels during the defined critical STRA6-requirement period of E10.5-E15.5. The critical window of STRA6 requirement that has been defined suggests that STRA6 is required either to suppress excess vessel formation during early eye development or to stimulate apoptosis aiding vessel regression or possibly a combination these.

3.4 Further Work

The conclusions drawn within this chapter as to the phenotype of *Stra6-/-* animals are based on the assumption that the knockout allele produces an out-of-frame transcript and therefore no STRA6 protein. In order to confirm these observations the presence or absence of STRA6 protein in knockout animals should be investigated via western blotting with a STRA6 specific antibody in protein extracts from *Stra6-/-* animals compared to controls.

Immunohistochemistry performed for markers of various components of the eye, in order to investigate the phenotype of *Stra6-/-* offspring from dams fed a retinoid-deficient diet during pregnancy (Figures 3.7, 3.9, 3.10, 3.11 3.12) requires further controls to be included in order to confirm the observations made. Absorption controls, in which the primary antibody is pre-absorbed with the specific antigen before incubation with the tissue, would allow non-specific staining to be identified as specific staining should be greatly reduced or abolished as they antibody has been bound to the pre-incubated antigen. Isotype controls could also be utilised in order to eliminate the possibility of non-specific interactions between immunoglobulins and the sample.

Stra6-/- dams fed on a retinoid-free diet through pregnancy give birth to *Stra6-/-* offspring with microphthalmia and defects of the retina, lens and vasculature. In order to understand the contribution of maternal genotype of this phenotype it would be interesting to look at *Stra6-/-* offspring from *Stra6+/-* dams, mated to *Stra6-/-* males, fed the retinoid-free diet throughout pregnancy. The contribution of maternal genotype to the phenotype of the pups from dams fed retinoid-free diet depends on the gene; *Rbp4+/-* females have no malformed *Rbp4-/-* pups compared to all of the *Rbp4-/-* pups from a *Rbp4-/-* females (Quandro 2005), Neonatal mortality rate of *Crbp2+/-* pups was dependent on maternal genotype with 79% of pups from *Crbp2-/-* dams versus 29% of pups from *Crbp+/+* dams dying in the neonatal period (Xueping 2002). *Stra6-/-* dams could be normal in terms of retinol storage and the ability to make RBP-ROH for provision of retinol to the embryo. STRA6 would only be required on the part of the embryo in order to access the maternal provision of retinoids provided as RBP-ROH. In this case, *Stra6+/-* embryos will be able to

utilise this RBP-ROH by uptake through the placenta, however *Stra6-/-* embryos will be unable to access this supply but would support development by obtaining retinol from chylomicrons or albumin-bound retinol. This supply of retinoids would maintain normal development of the *Stra6-/-* embryos during normal maternal dietary provision of retinoids, but maternal transfer to a retinoid-free diet would result in minimal non-specifically bound retinoid provision to *Stra6-/-* embryos but relatively normal RBP-ROH provision to *Stra6+/-* littermates. In this case, *Stra6+/-* dams fed retinoid-free diet during pregnancy would also result in the same *Stra6-/-* phenotype as chylomicron or albumin-bound retinoids are provided directly from dietary retinoids. If STRA6 is required in the dam to store retinoids, *Stra6-/-* dams fed a retinoid-free diet would become rapidly VAD. *Stra6+/-* embryos may be able to access the minimal retinoids available more successfully than *Stra6-/-* embryos. In this case *Stra6+/-* dams fed retinoid-free diet during pregnancy would have normal *Stra6-/-* offspring as they would have retinoid stores and therefore not become VAD upon eating the retinoid-free diet.

Stra6-/- dams fed on a retinoid-free diet for various 10-day 'windows' during pregnancy has allowed an initial survey of the likely timing of the occurrence of the developmental defects observed in *Stra6-/-* diet study eyes. In order to fully appreciate the difference, it would be useful to investigate further litters from the diet study windows at E0.5-10.5 E5.5-E15.5 and E10.5-birth compared with the phenotype of the E0.5-birth diet study animals. If the observations previously made hold, investigation of both vessel proliferation and apoptosis between E10.5-15.5 may highlight the cause of PHPV in *Stra6-/-* animals from retinoid-free diet fed dams.

Male and female animals from the *Stra6-/-* diet study have been bred to a C57BL6 female and male, respectively, in order to determine if these animals are fertile and able to produce offspring. Due to time constraints only one breeding was observed. The *Stra6-/-* diet study male was able to plug a female and one surviving pup was observed. The female *Stra6-/-* diet study animal became pregnant but no live pups were observed. Further breeding of *Stra6-/-* diet study males and females is required to gain a full picture of the fertility of *Stra6-/-* diet study animals. At present it seems

likely that *Stra6-/-* males are fertile but may be less so than a non-diet study *Stra6-/-* animal and *Stra6-/-* females are able to become pregnant but it is unknown if they are able to give birth to live pups.

HPLC analysis of the levels of various retinoids within the liver, eye and plasma of *Stra6-/-* animals fed either a retinoid-sufficient or a retinoid-free diet would allow a better understanding of the mechanism of STRA6 action and the effect STRA6 loss has on retinoid equilibrium. Liver and, perhaps, adipose retinoid levels will address questions of the ability of *Stra6-/-* to store retinoids or utilise stored retinoids. If STRA6 is required for retinoid storage, the liver level of retinyl esters will be low and if STRA6 is required to utilise stored retinoids then the liver retinyl ester levels will be likely be higher compared to WT and will not decrease upon transferral to retinoid-free diet.

Chapter Four

A role in zebrafish development for *stra6.2*: a paralogue of *stra6*.

4.0 Introduction

Matthew-Wood syndrome is a human birth defect caused by mutations in *STRA6* and it would be predicted that the *Stra6* knockout mouse would be the ideal candidate for a mouse model of this condition. However, as shown in the previous chapter, this is not the case and *Stra6*-knockout mice are viable and healthy. Modification of the retinoid content of the dams diet during pregnancy did produce offspring with microphthalmia and defective eye development but this was not an accurate model of Matthew-Wood syndrome, although it may be a good model of isolated anophthalmia/ microphthalmia associated with *STRA6* mutations (Casey 2011). The identification of a paralogue of *Stra6*, discussed in this chapter, may explain the developmental disparity between *Stra6*-knockout mice and Matthew-Wood patients.

The morpholino knockdown technique in zebrafish has been previously used in order to study the role in development of *stra6* and attempt to create a model of Matthew-Wood syndrome in the zebrafish (Isken 2008). The morpholino knockdown technique was therefore used to investigate *stra6.2* function as discussed below. Morpholinos are 20-25 base pair single stranded anti-sense oligonucleotides with modified backbones. The deoxyribose rings are replaced with 6-membered morpholine rings and non-ionic phosphorodiamidate linkages replace the anionic phophodiester linkages resulting in un-charged morpholino molecules (Wikipedia 2011). The modified backbone is not recognised by nucleases and they are therefore not degraded. Morpholinos also do not activate the innate immune response or toll-like receptors, a common problem encountered with 'natural' antisense oligonucleotides used previously to knockdown gene expression in the zebrafish. The morpholinos are designed to bind either at the translation intiation codon preventing protein translation from the target mRNA (Summerton 1999) or to a splice-acceptor or –donator site causing defective splicing resulting in modified and/or prematurely terminated protein (Draper 2001).

stra6 is expressed within the developing zebrafish embryo, being observed in the pineal gland, eye, anterior somites and the yolk syncetium at the 12-somite stage (Isken 2008). By 24hpf, expression is still observed in the pineal gland, eye and anterior somites with expression also observed in the anterior hindbrain. Later in

development expression is still observed in the eye and pineal gland and becomes restricted to the RPE of the eye by 4dpf. *stra6* morphants had developmental defects reflective of those observed in human patients, namely microphthalmia, heart edema and jaw defects (Isken 2008). The eyes of *stra6* morphants, despite being microphthalmic, were histologically normal with all the cell types specified correctly and retinal lamination indistinguishable from controls (Isken 2008). RA signalling within *stra6* morphants was increased, with the expression of *cyp26a1* increased in morphants compared to controls (Isken 2008). Reduction of Rbp4 levels within the morphant embryos rescued their developmental phenotypes indicating that Rbp4, in the absence of *stra6*, is toxic to normal development (Isken 2008). *stra6* in the zebrafish appears to function in an Rbp4-dependent manner in order to regulate vitamin A homeostasis during development. Loss of *stra6* during development causes an excess of RA signalling due to a non-specific increase in vitamin A caused by holo-Rbp4 in several embryonic tissues, with the exception of the eye which shows a decrease in retinoid content. *stra6* may therefore function differentially with some tissues requiring *stra6* to provide retinoids, i.e. the eye, and other tissues requiring its function in order to regulate the effects of circulating holo-Rbp4.

Many thanks to Philippe Gautier for assistance with the work described in section 4.1.

4.1 *Stra6.2* is a paralogue of *Stra6*

4.1.1 Identification of *Stra6.2*

Stra6.2 was identified as a paralogue of *Stra6* within the mouse genome by Blast. Protein identity between STRA6 and STRA6.2 is relatively low at around 18%; however the conserved residues do appear to be those important to STRA6 function. By mapping the STRA6 residues mutated in Matthew-Wood syndrome onto to the mouse protein and then comparing these to the equivalent residues in mouse STRA6.2 revealed that over half of these were conserved with almost all of the residues affected by missense mutation identical between the proteins (Figure 4.1 A). The binding site for RBP4 previously identified within STRA6 was, however, not

conserved between the proteins with only one of the three essential residues being conserved (Figure 4.1 A).

4.1.2 Evolutionary conservation of *Stra6.2*

The origin of *Stra6.2* and the relationship between *Stra6* and *Stra6.2* was investigated by identifying *Stra6*-like homologues in diverse species. *Stra6*-like homologues appear to have arisen before the proposed appearance of retinoic acid signalling in the deuterosomes (Albalat 2009). A *Stra6*-like homologue was identified in the simple eumetazoan *Trichoplax adhaerens*, but retinoic acid signalling is thought to have arisen in the deuterostomes (Marletaz 2006). *Stra6*-like homologues could not be identified in all bilaterians, however, and was absent in *Caenorhabditis elegans* and *Drosophila melanogaster*. These species are known to be missing other members of the RA pathway and do not use RA as a signalling molecule (Albalat 2009). In contrast, the *Trichoplax* genome also contains orthologues of *Rdh*, *Raldh2* and *RXR* orthologues suggesting a functional RA signalling pathway in this primative organism.

Comparison of STRA6-like homologues identified in invertebrates and basal vertebrates were found to sit between the STRA6 and STRA6.2 branches within a phylogenetic tree of STRA6-like homologues (Figure 4.1 B). Sequence comparison and their branching position within the tree revealed that they shared a greater similarity with STRA6.2. In the vertebrates proper, as represented by lamprey (*Petromyzon marinus*), definitive *Stra6* and *Stra6.2* homologues are observed (Figure 4.1 B). The observation of both a *Stra6* and *Stra6.2* homologue is the vertebrate norm with both genes observed in all, but two, groups. In all sequenced birds investigated, chicken (*Gallus gallus*) and zebrafinch (*Taeniopygia guttata)*, no *Stra6.2* homologue was observed and this loss was specific to the bird lineage with a *Stra6.2* homologue observed in a representative from the reptile lineage, *Anolis carolinensis*. The second deviation from the vertebrate norm is discussed below.

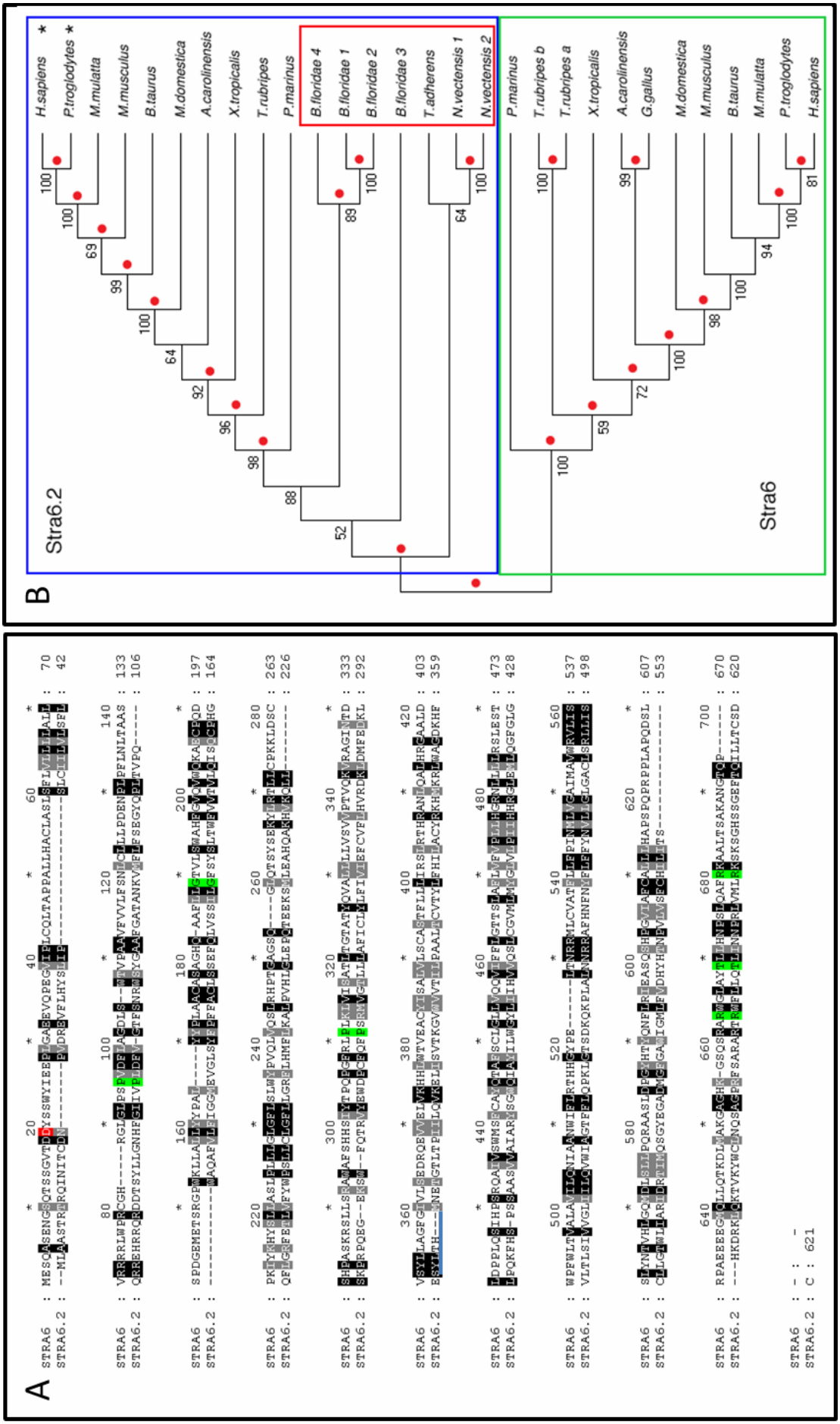
A
B
Stra6.2
Stra6
H.sapiens
P.troglodytes
M.mulatta
M.musculus
B.taurus
M.domestica
A.carolinensis
X.tropicalis
T.rubripes
P.marinus
B.floridae 4
B.floridae 1
B.floridae 2
B.floridae 3
T.adherens
N.vectensis 1
N.vectensis 2
T.rubripes b
T.rubripes a
G.gallus

Figure 4.1 Identification of *Stra6.2*.

Protein sequence alignment between mouse STRA6 and STRA6.2 highlights the low degree of conservation (A). Residues labelled black are identical between the proteins and grey-labelled residues indicate similar but not identical residues. Residues mutated in PDAC conserved between the proteins are labelled in green and those non-conserved are labelled red. The RBP4 binding site (underlined in blue) is not conserved between the two proteins. A phylogenetic tree indicates the relationship between *Stra6*-like homologues (B). Green box highlights *Stra6*-like homologues. Blue box indicates *Stra6.2*-like homologues. Red box highlights non-vertebrate sequences. ***** indicates homologues in which the disrupted gene has been artificially joined for tree construction. Bootstrap values are indicated for each branch. Branches which have been independently verified by Bayesian tree method are marked with a red dot.

4.1.3 Disruption to *STRA6.2* in humans and great apes

Stra6.2 forms part of a recognisable syntenic unit through a portion of mammalian evolution. In great apes, including humans, the *STRA6.2* coding region has become split across its resident chromosome with an associated break in synteny (Figure 4.2 A). The 5' region of the gene is found within the P-arm of chromosome 9 in humans with the genes normally 5' to *Stra6.2* residing in their normal position in relation to *STRA6.2* (Figure 4.2 B). The 5' region of the gene is not found in EST databases and appears not to be transcribed; however, its exonic structure does appear to be conserved. Analysis of evolutionary conserved regions, in addition to identifying the remains of exonic structure in the 5' region, also highlighted the likely split in the gene to have occurred within the intron between exons 7 and 8 (Figure 4.2 C). The 3' region resides within the Q-arm of chromosome 9 and maintains the synteny normally associated with the 3' of *Stra6.2*. The 3' region of the gene, representing the final transmembrane domain and the C-terminal tail of the protein, is transcribed and represented in EST databases from human. The EST databases do show the addition of a non *Stra6.2*-homologous portion to the 5' of the transcript and many of the ESTs also show additional transcribed regions 3' to the *Stra6.2*-homologous region. In non-human great apes in which *STRA6.2* is split, this 3' transcript appears to contain a premature stop codon although this codon is not observed in the human transcript.

4.1.4 Summary of *Stra6.2* in mouse, human and zebrafish

The paralogue of *Stra6*, *Stra6*.2, has an interesting evolutionary history in the species pertinent to the work discussed within this thesis. The paralogue was identified initially in the mouse genome and shows relatively low conservation overall, although the conservation of important amino acids within the protein appears to be good. The mouse genome contains both a *Stra6* and a *Stra6.2* gene and this situation is also replicated in the zebrafish with a single copy of both *stra6* and *stra6.2* also present within the zebrafish genome. A common feature of the zebrafish genome is the duplication of many genes, however *stra6* and *stra6.2* are present as single copies with no evidence of additional copies of either. The genomic situation in the human is somewhat different to that in the mouse and the zebrafish. The human genome

contains a ‘normal’ copy of *STRA6*, however *STRA6.2* has become disrupted compared to the mouse. The gene has become split, with the 5’ region of the gene appearing to be non-transcribed and non-functional, although enough conservation remains to allow the region to be identified. The 3’ region of the gene, however, does appear to be transcribed although the functional significance of this shorter transcript and protein is not clear at present. The conservation of the syntenic context of the split gene, with the 5’ genes associated with the 5’ portion and the 3’ genes associated with the 3’ portion, suggests that this disruption of the *STRA6.2* gene may be due to an evolutionary large scale genomic rearrangement.

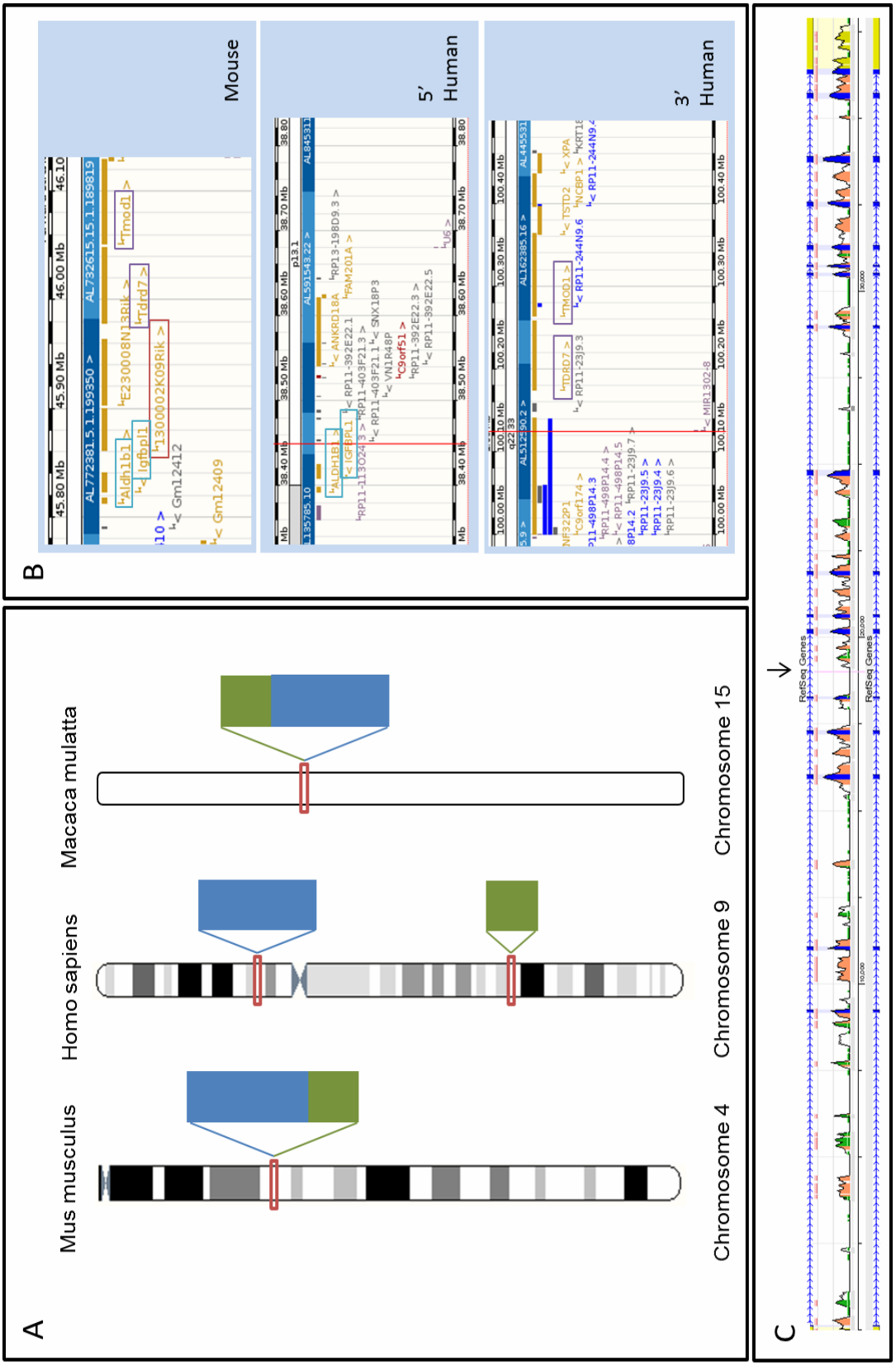
A
Mus musculus
Homo sapiens
Macaca mulatta
Chromosome 4
Chromosome 9
Chromosome 15
B
Mouse
5′ Human
3′ Human
C
RefSeq Genes

Figure 4.2 *STRA6.2* is disrupted in great apes.

The chromosomal location and arrangement of the *Stra6.2* gene in mouse, human and macaque (Macaca mulatta) highlights the disruption to the *STRA6.2* gene in humans (A). Blue indicates the N-terminal and green the C-terminal regions which highlight the chromosomal disruption of the gene that occurred in the hominids. Synteny 5' and 3' to *STRA6.2* is maintained despite the split across chromosome 9 (B). 5' genes (green boxes) and 3' genes (purple boxes) in their relative position compared to Stra6.2 (red box) in mouse. The 5' and 3' syntenic region is found correctly located with respect to the 5' and 3' portions of *STRA6.2* in human. (C) All exons (blue) of STRA6.2 are maintained despite the split and can be identified by using the ECR browser comparing human to mouse. The mouse reference gene is shown at the top and bottom of the panel and a graphical representation highlights conservation to human across the region. The split in the gene is indicated by the black arrow.

4.2 *stra6.2* and zebrafish

4.2.1 *stra6.2* expression during zebrafish development.

4.2.1.1 RT-PCR

Temporal expression of *stra6.2* during zebrafish development was assessed using RT-PCR on RNA extracts from various developmental time-points between the fertilised egg and 48hpf (Figure 4.3). Expression of *stra6.2* by RT-PCR was detected in the fertilised egg indicating that *stra6.2* mRNA is deposited by the female into the egg as zygotic transcription does not begin until the mid-blastual transition at approximately 6hpf. *stra6* was also observed in the fertilised egg by RT-PCR. Expression was observed for both *stra6* and *stra6.2* at all the developmental time points assessed.

4.2.1.2 WISH

The spatial expression pattern of *stra6.2* was investigated using wholemount in situ hybridisation (WISH). Expression before 14hpf could not be definitively detected using WISH with diffuse staining observed across the embryo (Figure 4.4 A). The eye was consistently positive for *stra6.2* throughout development and was often the strongest region of expression observed across the embryo. Expression at the 10-somite stage (approximately 14hpf) is seen within the horizontal crease of the developing eye (Figure 4.4 B). At 18hpf, in addition to expression within the developing eye (Figure 4.4 C), expression was also observed faintly within the notochord and in the tail bud (Figure 4.4 D). Expression at 24hpf was restricted only to the anterior of the embryo (Figure 4.4 E) within the eye, brain and the endoderm above the yolk (Figure 4.4 E, G-H). The anterior region, specifically the tail, was devoid of staining. Staining at 48hpf was observed in the anterior somites (Figure 4.4 I), in RPE of the eye (Figure 4.4 K) and in the posterior notochord (Figure 4.4 L).

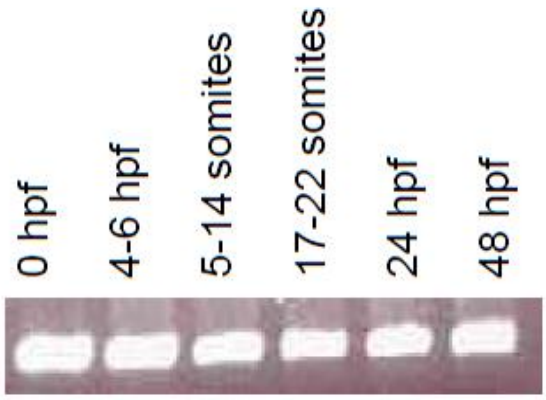

Figure 4.3 *stra6.2* is expressed from the earliest stage of zebrafish development.

Expression of stra6.2 can be detected by RT-PCR at various developmental stages from the fertilised (0hpf) to 48hpf as shown by gel electrophoresis.

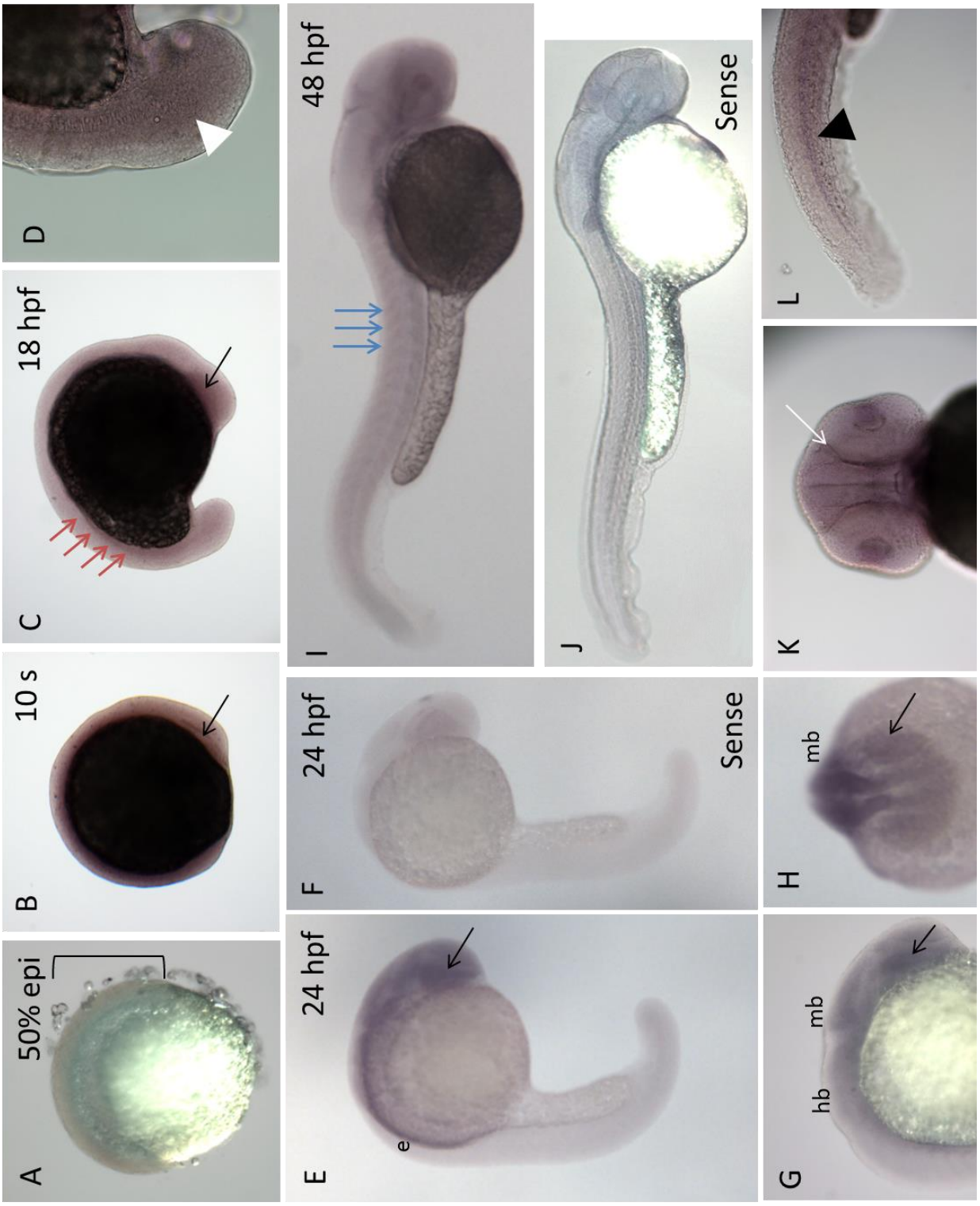
A
50% epi
B
10 s
C
18 hpf
D
E
24 hpf
e
F
24 hpf
Sense
G
mb
hb
H
mb
I
48 hpf
J
Sense
K
L

Figure 4.4 *stra6.2* is expressed in a tissue specific manner during zebrafish development.

Expression of *stra6.2* (purple) was assessed by WISH from gastrulation at 50% epiboly (A) where expression was diffusely observed throughout the embryonic tissue (bracket). *stra6.2* expression was observed in the eye (black arrow) throughout development from the 10 somite stage (B). At 18hpf (C), expression is additional observed in the notochord (red arrows) and within the tailbud (white arrowhead, D). The anterior of the embryo is positive at 24hpf (E) specifically within the endoderm above the yolk (e) and within the brain (G&H), namely the midbrain (mb) and hindbrain (hb). The somites (blue arrows) at 48hpf (I) are positive for *stra6.2* expression and expression within the eye has become restricted to the RPE (K, white arrow). The posterior notochord (black arrowhead) is also positive for *stra6.2* at 48hpf (L). The yolk in B-D and I appears dark as embryos are flatmounted and illuminated from below. Sense control embryos at 24hpf (F) and 48hpf (J) are shown for comparison.

4.2.2 *stra6.2* is required for normal zebrafish development.

4.2.2.1 *stra6.2* targeting morpholinos

The developmental requirement for *stra6.2* was investigated using the morpholino knockdown approach. *stra6.2* expression was knocked-down and depleted using three morpholinos; two translation blocking morpholinos which prevent the translation of the target mRNA and one splice-blocking morpholino which targets a splice-junction resulting in aberrant splicing leading to exon-skipping and intron-inclusion (Figure 4.5). The translation blocking morpholinos overlap only at the initiation codon ATG and target up-stream and down-stream of this in MO1 and MO2 respectively. The splice blocking morpholino targets the junction between intron 4-5 and exon 5. RT-PCR of RNA from phenotypic morphants injected with this morpholino identified both exon skipping and intron inclusion of single or multiple introns downstream of the target region (Figure 4.6).

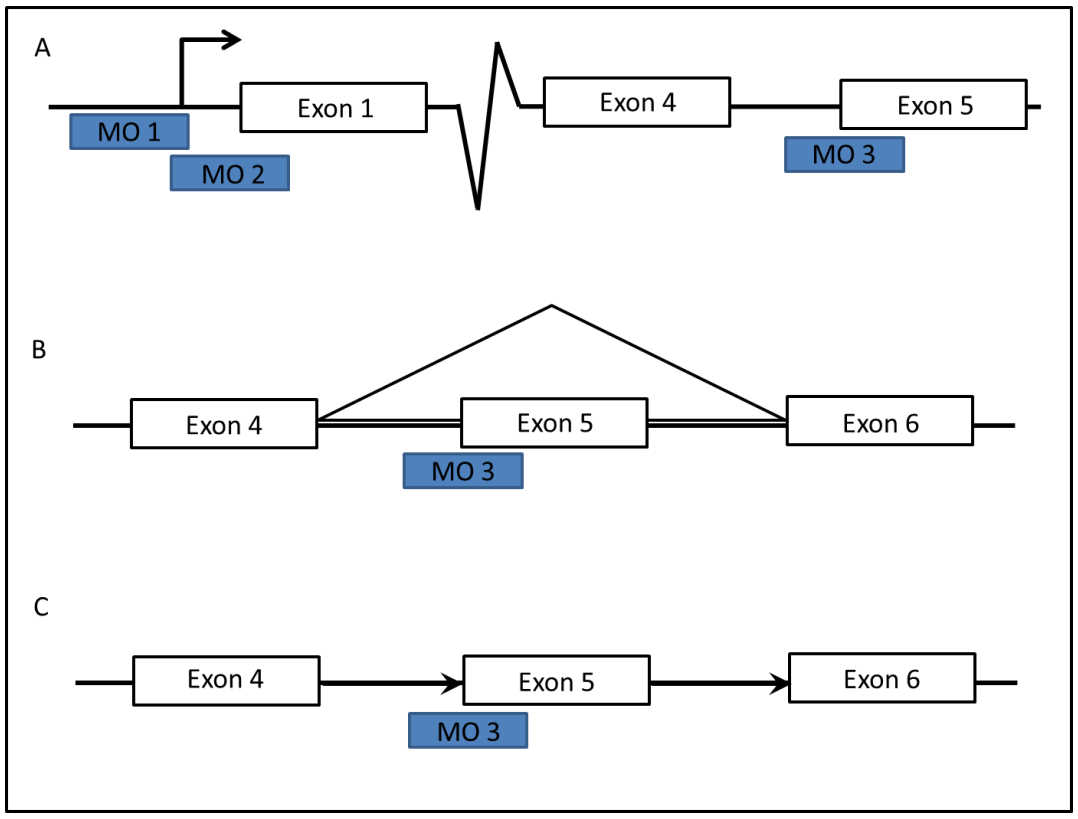

Figure 4.5 Morpholinos targeted to both the translational start and a splice junction of *stra6.2*.

Morpholinos (MO1, 2 & 3) were directed towards the stra6.2 gene at the indicated positions (A). Splice blocking morpholino (MO3) can alter pre-mRNA splicing by causing exon skipping (B) and intron inclusion (C).

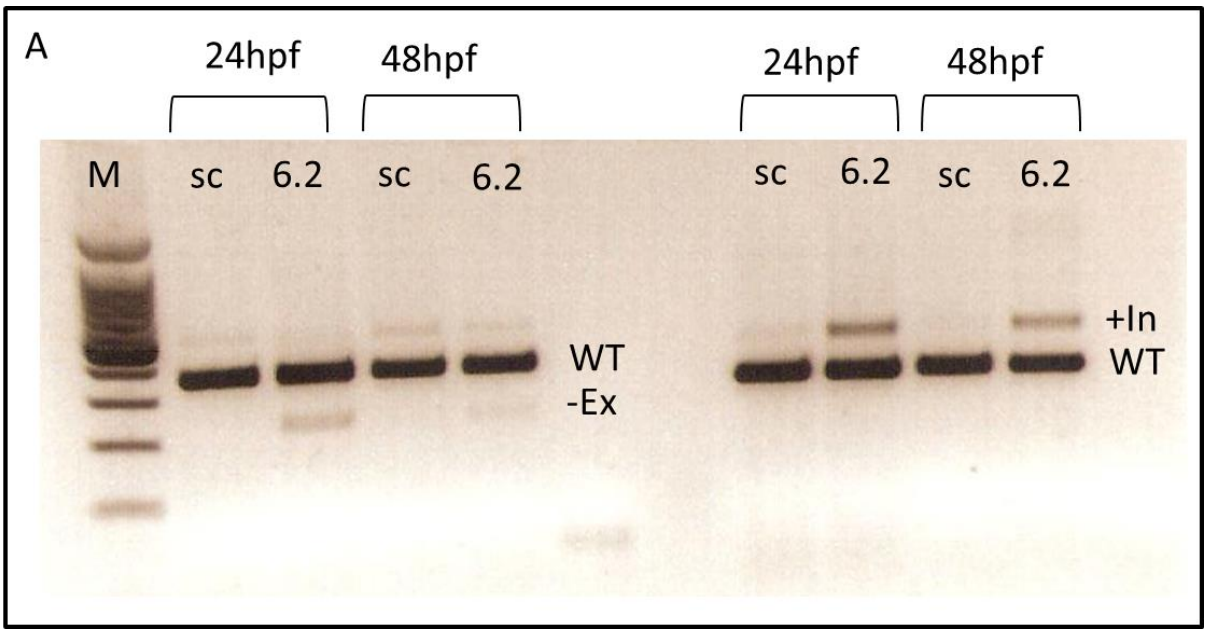

Figure 4.6 Splice blocking morpholino (MO3) causes both intron-inclusion and exon-skipping.

RT-PCR identifies both exon skipping (-Ex) and intron inclusion (+In) in mRNA collected from splice morpholino injected *stra6.2* morphants (s6.2) at both 24hpf and 48hpf. The expected normal size band (WT) was the only product observed in standard control (sc) mRNA but was also observed in the morphant lane.

4.2.2.2 *stra6.2* morphant phenotype

stra6.2 knockdown using any of the three described morpholinos resulted in an identical phenotype (Figure 4.7 E-F) and further experiments were performed using morpholino one (MO1). stra6.2 MO1 was also injected into *p53*-null zebrafish in order to control for off-target effects caused by activation of the p53 apoptosis pathway, which has been reported for some other morphants (Robu 2007). A comparable level of phenotype was observed between those morphants on a WT or *p53*-null background.

Defects observed in *stra6.2* morphants later in development (discussed below) resemble those observed in mutants with defects in convergent-extension and early axis elongation, such as the *frizzled*-2 morphant (Sumanas 2001). In order to ascertain if the *stra6.2* morphant phenotype was due to defects in convergent-extension or axis elongation and identify the earliest aberrations in development in these morphants, early development of *stra6.2* morphants (n=10) compared to standard control morphants (n=10) was monitored. *stra6.2* morphants could be distinguished from standard control injected embryos at the 10-somite stage, at which stage the distance between the head and tail across the yolk was increased in *stra6.2* morphants compared to standard control injected embryos (P=0.0006, Figure 4.8 C-D). *stra6.2* morphants were also slower to develop at this time with embryos reaching the 10-somite stage later temporally than the equivalent standard control injected embryos (Figure 4.8 A-B). *stra6.2* morphants could also be distinguished later in development at 18hpf, at which point development of the *stra6.2* morphants appeared to be of an equivalent stage to the development of standard control injected embryos of the same age (Figure 4.8 A-B). The developing tail of *stra6.2* morphants has not disengaged from the yolk extension as for standard control morphants, although this detachment does occur later in development (Figure 4.8 E-F). *stra6.2* morphants can be readily distinguished at both 24hpf (Figure 4.7 A-B) and 48hpf from standard control injected embryos. *stra6.2* morphants at 48hpf are significantly shorter along their anterior-posterior axis and also curved ventrally in respect to standard control embryos (Figure 4.7 C-D). Many *stra6.2* morphants also fail to spontaneously dechorinate and require manual dechorination. Upon dechorination movement of the *stra6.2* morphants is impaired with reduced startle response to

stimuli and movement restricted to stationary rotation about the yolk. *stra6.2* morphants at 48hpf are also microphthalmic with a significant reduction in eye size as a ratio of body length compared to standard control embryos ($P<0.0001$, Figure 4.7 C-D). Somite morphology in *stra6.2* morphants, as analysed by histological sections (Figure 4.9 A-B) and in intact embryos (Figure 4.9 C-D), is disrupted with an increase in somite angle resulting in a flattened somite appearance compared to standard control embryos. Somite size and number is however comparable between *stra6.2* and standard control morphants.

A
SC
B
stra6.2
C
10s
SC
D
10 s
stra6.2
E
18hpf
SC
F
18hpf
stra6.2

Figure 4.7 *stra6.2* morphants have defects in axis elongation and tail formation.

Development of standard control injected embryos (A, n=10) and stra6.2 morphants (B, n=10) was observed at 1-hourly intervals (each image is plus 1 hour compared to the previous image) in order to investigate axis elongation and tail formation between 13-18hpf. Head-tail distance (double-headed arrow) is a measure of axis elongation and was smaller in standard control embryos (C) compared to *stra6.2* morphants (D). Tail formation is also defective compared to standard control embryos (E) at 18hpf. Disengagement of the tailbud (black arrow) from the yolk extension has not occurred in *stra6.2* morphants (F).

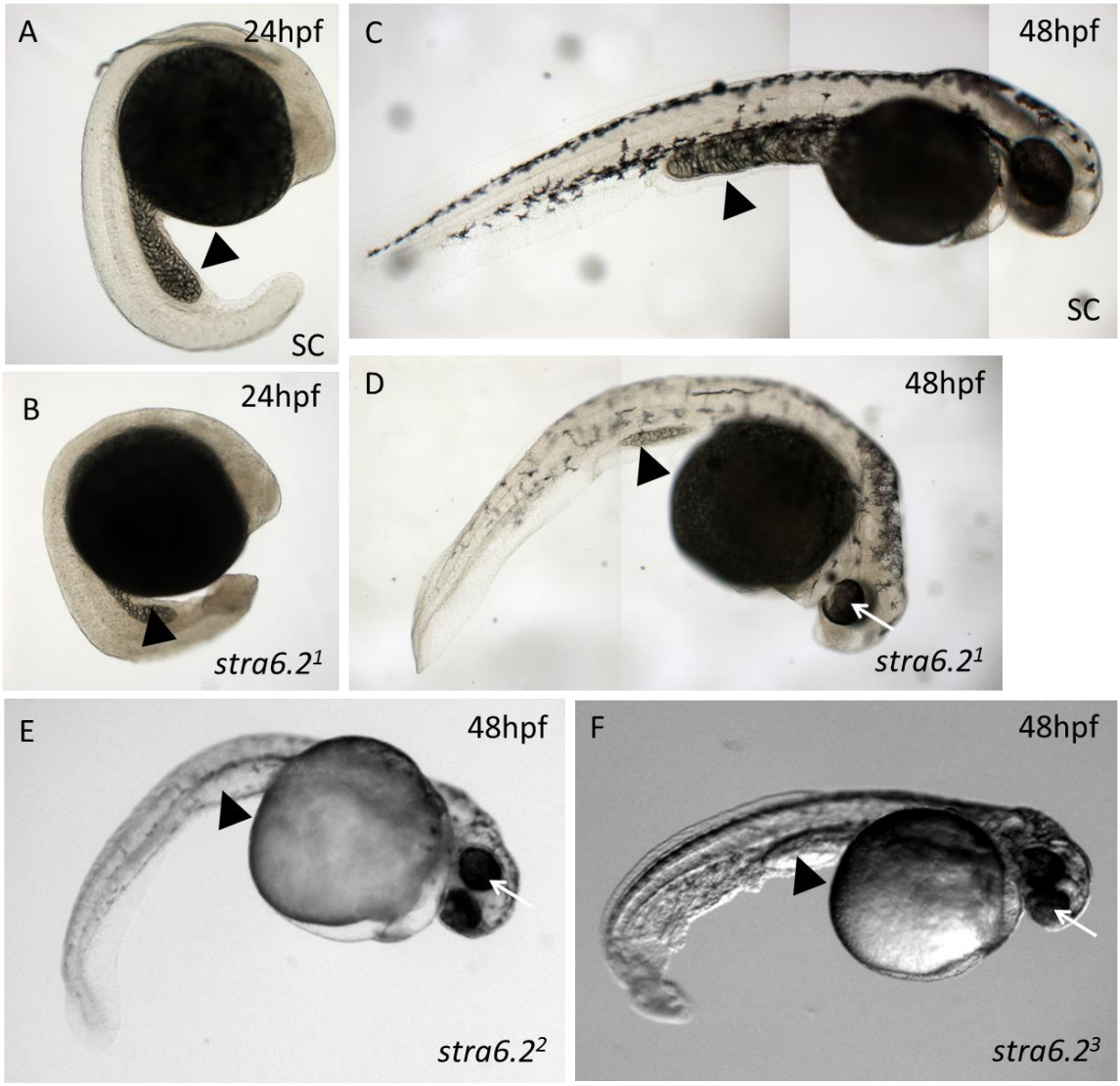

Figure 4.8 *stra6.2* morphants are also distinguishable at 24hpf and 48hpf.

Standard control embryos (A) are longer along their body axis and have yolk extensions (black arrowhead) which are relatively even in width along their length compared to *stra6.2* morphants (B) at 24hpf. At 48hpf, compared to standard control embryos (C), *stra6.2* morphants of each of MO1 (D), MO2 (E) and MO3 (F) are shorter along their body axis, microphthalmic (white arrow) and have shorter, uneven yolk extensions (black arrowhead). The yolk in A-D appears dark as embryos are flatmounted and illuminated from below. Multiple images of the same embryo have been used in C and D in order to maintain focus across the embryo.

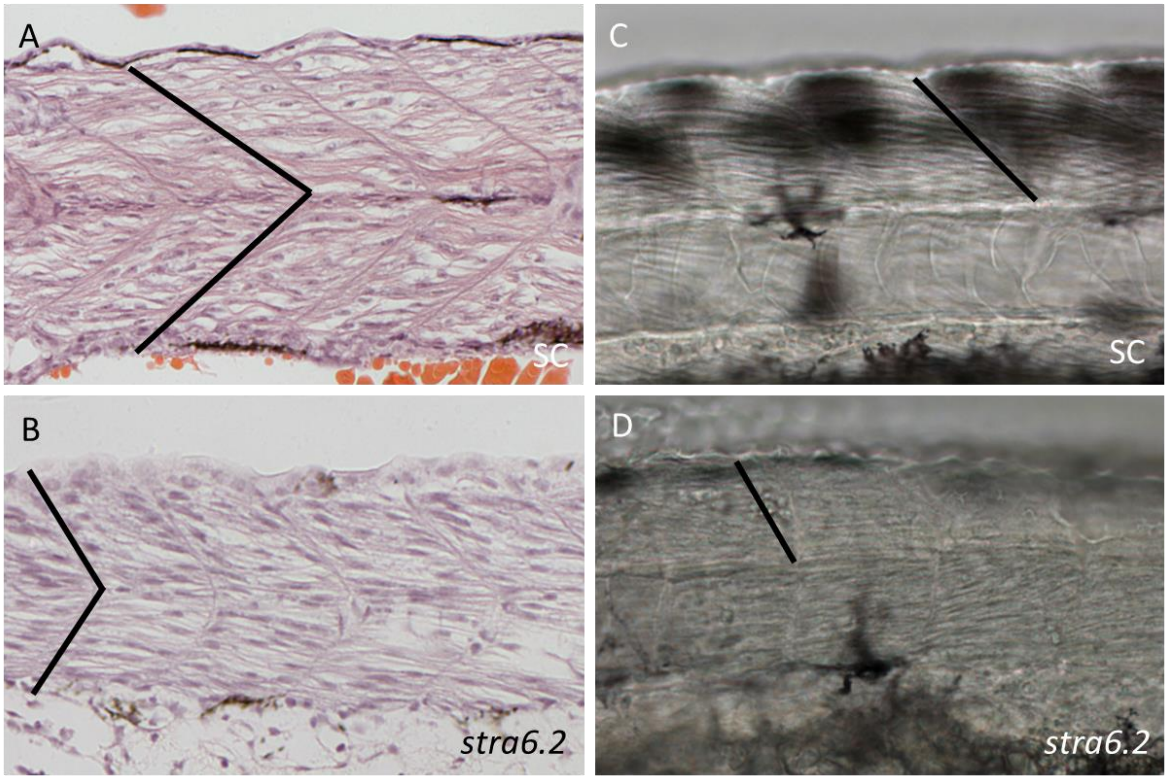

Figure 4.9 Somite angle is increased in *stra6.2* morphants.

Somite angle, compared to standard control (A&C), is larger in *stra6.2* morphant (B&D) at 48hpf. Black lines outline the edge of one somite on H&E section (A-B) and in the intact embryo (C-D).

4.2.2.3 Eye defects in *stra6.2* morphants

Due to the microphthalmia observed in *stra6.2* morphants, eye morphology was histologically investigated. The eye in standard control embryos at 3dpf was fully laminated with the cells of the retina arranged into the stereotypical pattern of cell type and position required for normal vision. The *stra6.2* morphant eye was more akin to a control eye at 48hpf with no lamination observed within the retina in stark contrast to the control histological findings. The *stra6.2* eye does appear to be delayed in development between 2-3dpf with some *stra6.2* morphant eyes demonstrating a degree of lamination by 4dpf. The retinal level of lamination in *stra6.2* morphants was variable however, with some morphant eyes still histologically equivalent to 48hpf control eyes (Figure 4.10 A-B&F). In contrast, some *stra6.2* eyes were completely normal with the retina fully and correctly laminated but a percentage of these still had nuclei present within the lens, a histological finding not observed past 48hpf in control eyes (Figure 4.10 C). In between these extremes, various levels of lamination were observed in the *stra6.2* morphant eye with specification of cell types but minimal layering (Figure 4.10 E) to a specification of all the cells arranged into layers but a lack of nuclei-free plexiform layers (Figure 4.10 D).

4.2.2.4 Cartilage defects in *stra6.2* morphants

The head of *stra6.2* embryos is smaller and defective in shape compared to standard control embryos and therefore cartilage morphology was assessed by alcian blue staining at 5dpf (Figure 4.11). Standard control morphants had well developed head and jaw cartilages at this stage (Figure 4.11 A-B). The lower jaw consisted of Meckel's cartilage, extending anterior to the eyes, and the ceratohyates meeting at an approximately 90° angle with the point facing towards the anterior of the embryo. The 6 ceratobranchials, which will later form the gill arches, were also similarly angled as the ceratohyates. *stra6.2* morphants, however, had defective jaw morphology (Figure 4.11 C-D). Meckel's cartilage did not extend anterior to the eyes as for the control embryo and the ceratohyates were not angled and lay either flat or in some cases angled posteriorly. The ceratobranchials were reduced in number and those which remained were malformed. In contrast the cartilages of the head were

not affected by the knockdown of *stra6.2* indicating that this was not a generalised affect upon all cartilages. Alcian blue staining also highlighted a change to the shape of the pectoral fins, in which rather than forming a gentle curve to be held in proximity to the body as for control embryos, are held at right angles to the body with the distal half then bent back into plane with the body axis (Figure 4.11).

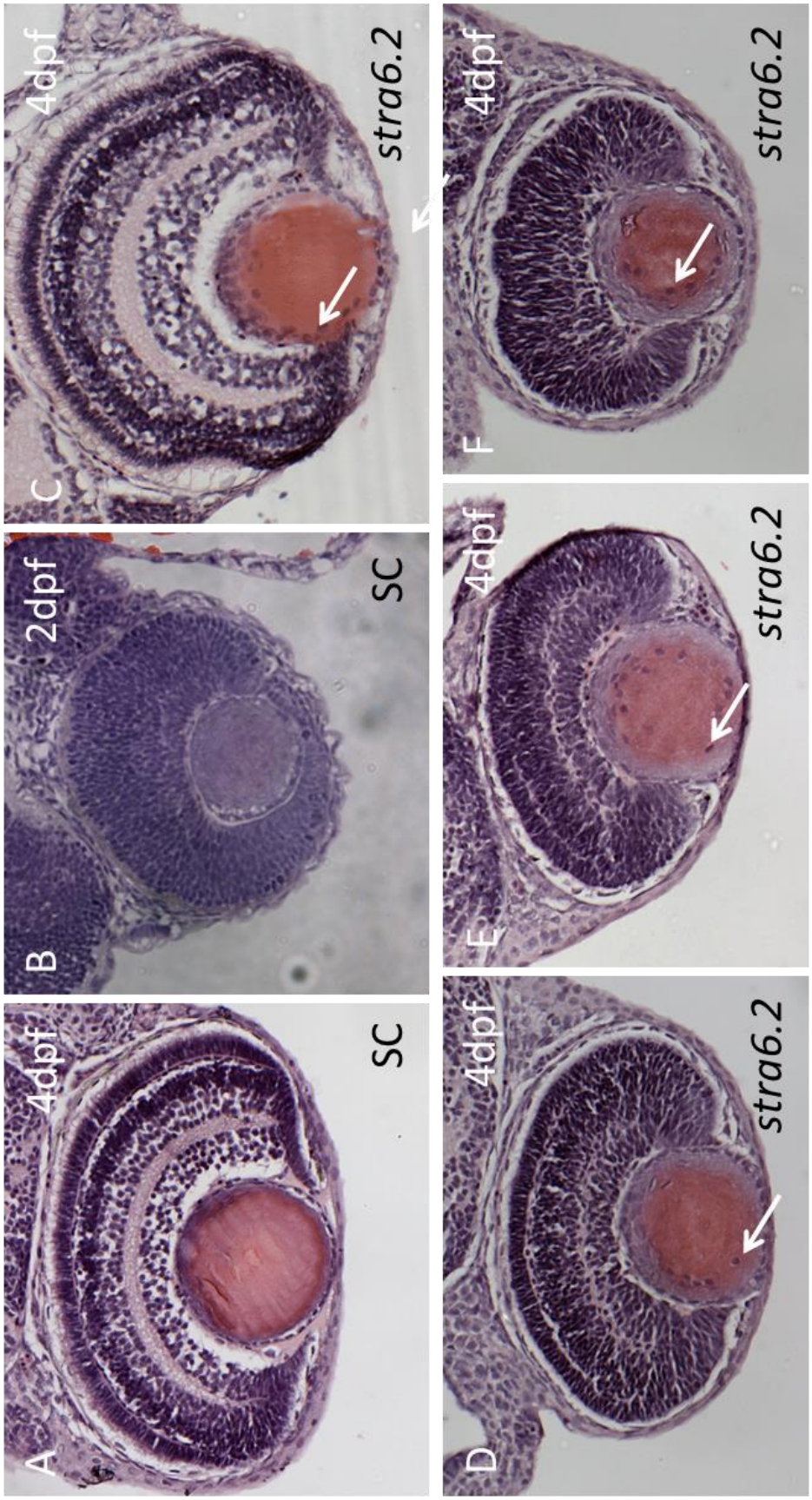
A
4dpf
SC
B
2dpf
SC
C
4dpf
stra6.2
D
4dpf
stra6.2
E
4dpf
stra6.2
F
4dpf
stra6.2

Figure 4.10 *stra6.2* morphants have defects in retinal cell specification and lamination.

By 4dpf, standard control embryos (A) show specification of the various cell types of the retina and lamination into the stereotypical layered structure of the retina. Standard control eyes at 2dpf (B) do not have any specification of retinal cell type or lamination of the retina. stra6.2 morphants at 4dpf (C-F) show a range of defects in lamination and retinal cell specification from full specification and lamination but the persistence of lens nuclei (white arrow, C), to specification and some lamination (D), to no lamination and some specification (E) and in some cases complete lack of retinal specification or lamination (F) resulting in an eye akin to a control at 2dpf (B).

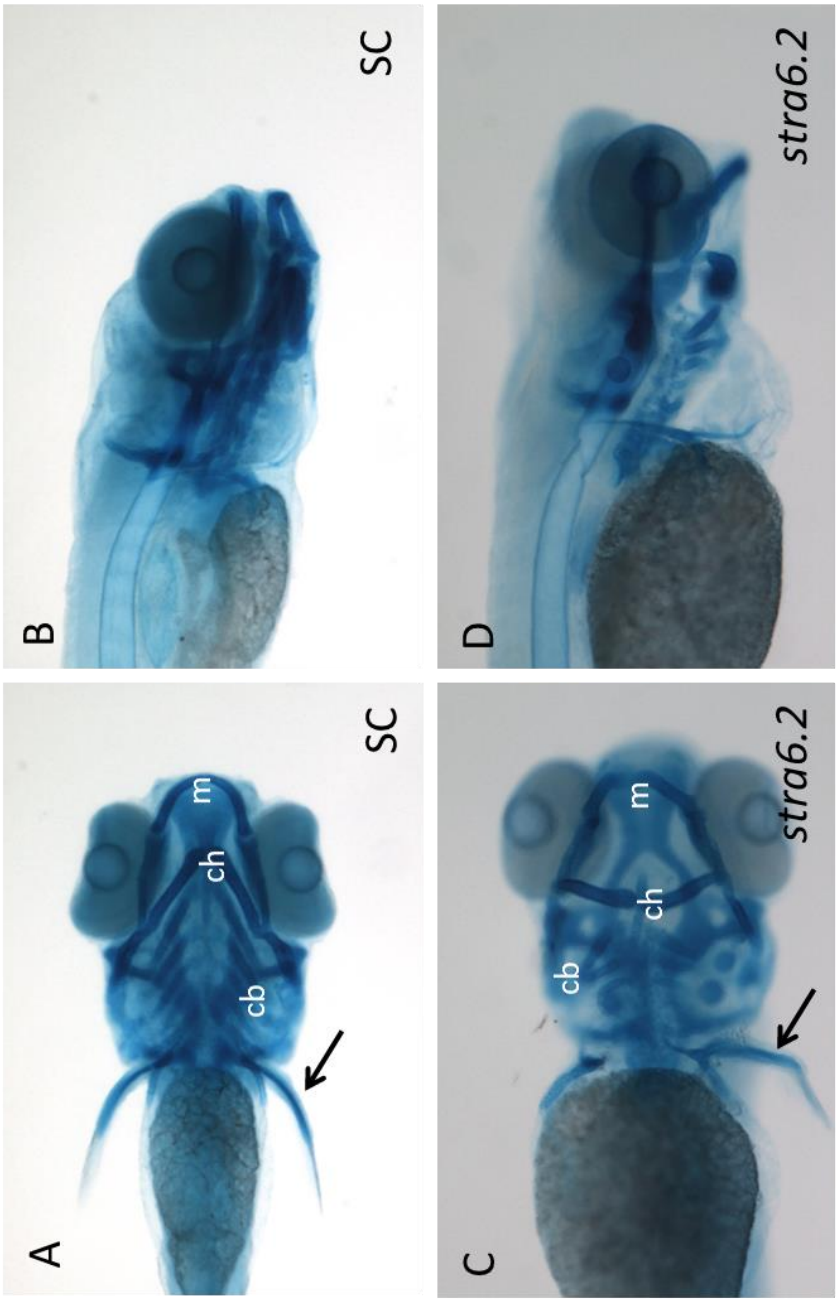

Figure 4.11 *stra6.2* morphants have defects in the jaw and fin cartilage.

The jaw of standard control embryos (A-B) consists of Meckel's (m), ceratohyalate (ch) and ceratobranchial (cb) cartilage elements. stra6.2 morphants (C-D) show defects in all of the these jaw elements. The fin (black arrow) shape is also malformed compared to standard control.

4.2.2.5 Gene expression within the zebrafish pronephros is not affected in *stra6.2* morphants.

The zebrafish pronephros contains discrete segments, akin to the tubule segments of the metanephric nephrons of mammalian kidneys, which have a unique gene expression profile. The specification of these segments is affected by RA, such that RA treatment inhibits the formation of distal fates and inhibition of RA-signalling will rescue distal fate formation in a mutant which lacks them (Wingert 2007). The expression of several genes, known to be expressed in discrete regions of the developing pronephros were investigated in *stra6.2* morphants, namely, *cdh17* for the neck, tubule and pronephretic duct (Figure 4.12 A-B); *slc12a3* for the distal late region (Figure 4.12 C-D); *gata3* for the pronephretic duct (Figure 4.12 E-F). All markers stained the expected regions in standard control embryos as previously reported for WT and staining was also observed in *stra6.2* morphants. Upon initial inspection, the expression domain of several of these genes appeared to be shortened. However, the length of the expression domain as a ratio of the embryo length was calculated and this revealed that no significant difference was observed between pronephros of control and *stra6.2* morphants (*slc12a3* p= 0.3440, *cdh17* P= 0.1931).

4.2.2.6 Tail bud and notochord morphology is affected in *stra6.2* morphants.

The notochord of *stra6.2* morphants was observed to be undulated in its dorsal ventral axis. Markers for notochord were investigated in order to confirm this observation. *ntl*, the zebrafish homologue of brachyury, is expressed in the notochord during development. The *ntl* expression domain in *stra6.2* morphants is increased compared to control morphants and the staining within the tail-bud is more intense. The undulation of the notochord can be visualised by the *ntl* expression domain and the notochord appears thicker in its dorsal-ventral plane (Figure 4.13 A-B). Notochord morphology was also investigated using the *shha*-GFP transgenic line. The undulated morphology and notochord thickening was again highlighted and the staining within the brain was not as intense in *stra6.2* morphants compared to controls (Figure 4.13 C-E). Tail development in stra6.2 morphants is disrupted with failure of the tailbud to disengagae from the yolk extension in the early stages. Staining with ntla marks the tailbud and is increased in expression within the tail bud

compared to a standard control injected embryo. *eve1* expression, a marker of tailbud, is more intense and observed further round the tailbud in *stra6.2* morphants at 15hpf compared to standard control embryos (Figure 4.13 F-G).

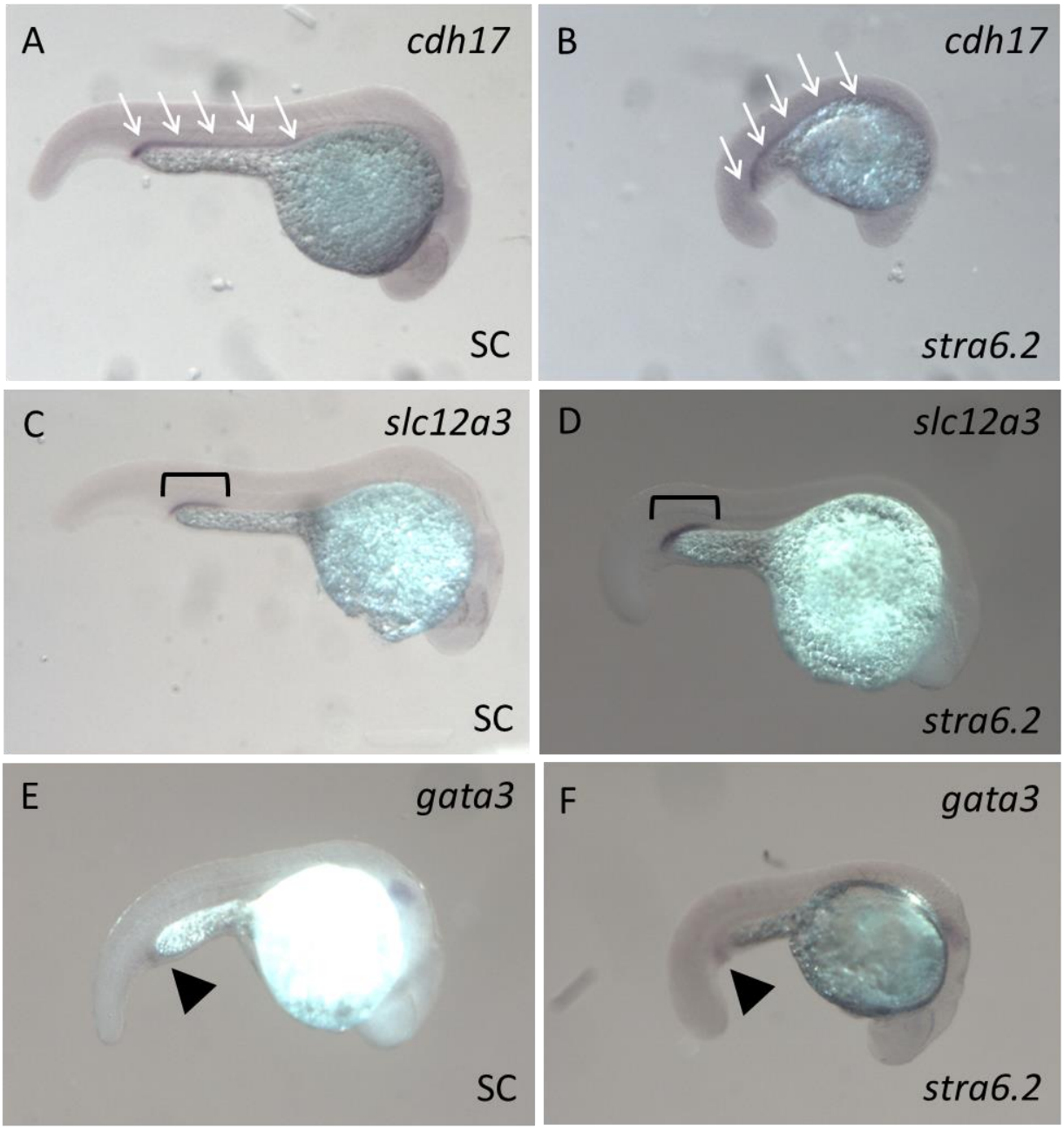

Figure 4.12 Markers of the pronephros are unaffected in *stra6.2* morphants.

Standard control embryos (A,C & E) are indistinguishable from *stra6.2* morphants (B, D & F) in respect to the expression of various markers of the pronephros (purple). *cdh17* (A-B) is a marker for the neck, tubule and pronephretic duct (white arrows), *slc12a3* is a marker for the distal late region (black bracket) and *gata3* is a marker for pronephetic duct (black arrowhead).

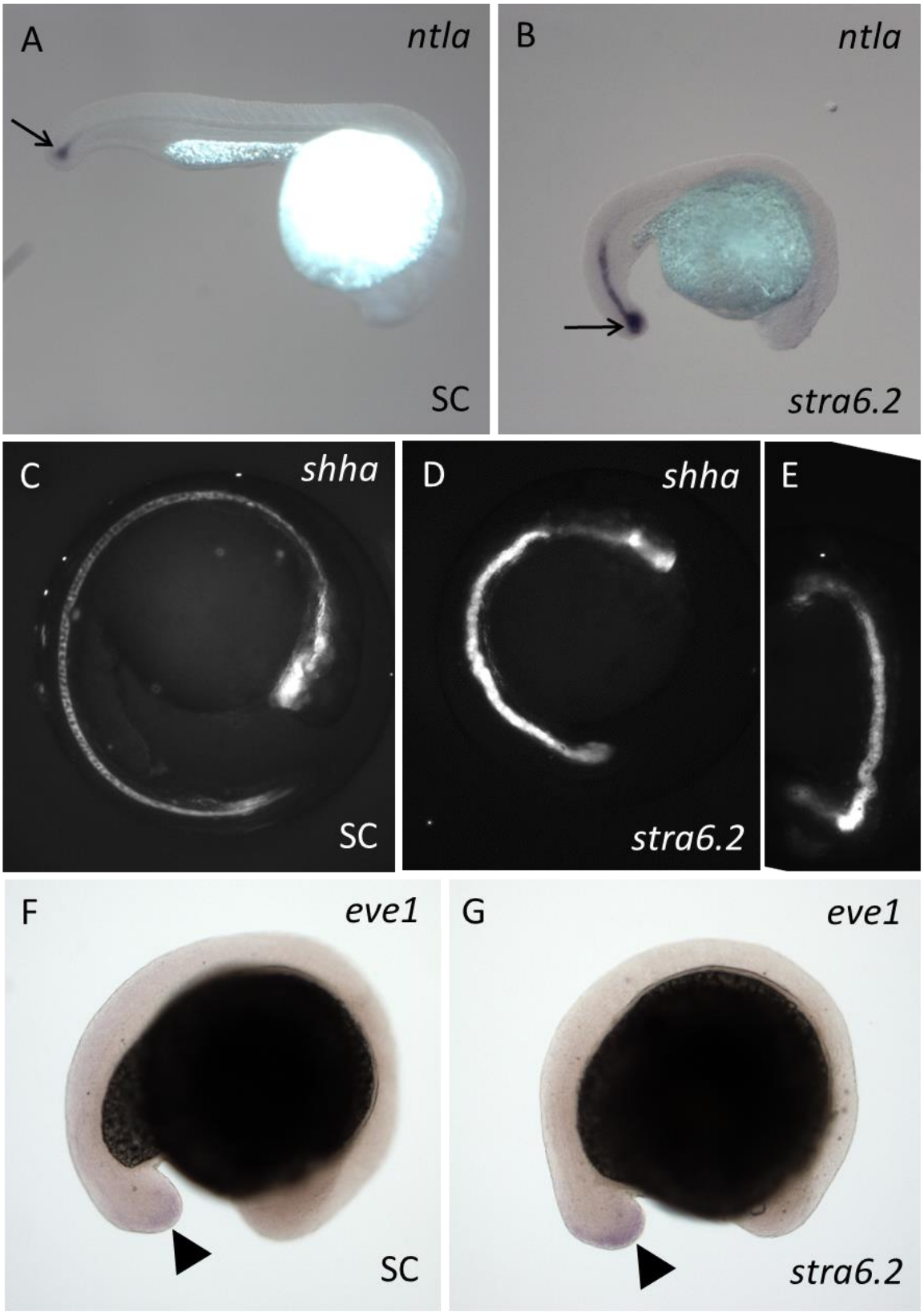
A
ntla
SC
B
ntla
stra6.2
C
shha
SC
D
shha
stra6.2
E
F
eve1
SC
G
eve1
stra6.2

Figure 4.13 Expression of marker genes for the notochord and tail are altered in *stra6.2* morphants.

ntla is a marker for notochord and the tailbud (black arrow) in standard control (A) and stra6.2 morphant embryos (B) and highlights the undulation of the notochord in *stra6.2* morphants. The expression of *ntla* (purple) extends further into the notochord in *stra6.2* morphants and stains a larger region of the tailbud. Undulation of the notochord is also highlighted by GFP signal (white) from the *shha*-GFP reporter line in *stra6.2* morphants in both the lateral (D) and dorsal view (E) compared to standard control embryos (C). *eve1* is a marker for the tailbud (black arrowhead) in standard control (F) and *stra6.2* morphants (G) and the domain of expression is expanded in *stra6.2* morphants.

4.2.2.7 The pancreas is correctly specified in *stra6.2* morphants.

Pancreas development in the zebrafish requires RA in order to specify pancreatic cell types at the end of gastrulation. Neither embryos treated with a Raldh inhibitor, BMS493, or *neckless* (*nls*) mutants, which harbour a mutation in *raldh2*, showed any pancreatic tissue positive for endocrine markers. Exocrine markers were also missing or greatly reduced (Stafford 2002). *islet1* marks the pancreas in addition to regions of the telencephalon, pharyngeal arches and dorsal spinal chord neurons (Thisse 2005) and is undetected in the pancreas of the absence of *raldh2* (Alexa 2009). *islet1* expression in the developing pancreas, as assayed by WISH, is unaffected by *stra6.2* knockdown and specification of the pancreas appears not to be perturbed by loss of *stra6.2*. Analysis of *islet1* expression within the dorsal spinal chord neurons indicate that this region is also unaffected in *stra6.2* morphants indicating that innervation of the dorsal region by the spinal chord nerves does not require *stra6.2*. *islet1* expression also marks several regions of the brain, namely the dorsal-rostral cluster of the telecephalon, ventral-rostral cluster of the diencephalon, the dorsal diencephalon and the epiphysis (Thisse 2005). These regions are not positive for *islet1* in *stra6.2* morphants indicating that these regions of the brain may be malformed or absent in *stra6.2* morphants (Figure 4.14 A-B).

4.2.3 *stra6* and *stra6.2* morpholinos act synergistically.

stra6 and *stra6.2* morphants share a similar phenotypic constellation and the STRA6 and STRA6.2 proteins conserve a number of residues likely to be important for functionality therefore they may have similar functions and interact in development. In order to understand interactions between *stra6.2* and *stra6*, the morpholinos were co-injected into the same embryo. *stra6;stra6.2* double morphants were more severely affected (Figure 4.15 A) than either single morphant injected individually and within a group of injected embryos those exhibiting phenotype formed a larger proportion of the group. In addition to co-injecting at a similar dose per morpholino as when injected singularly, embryos were also co-injected with morpholinos which when injected singularly gave a low percentage of mildly affected morphants. This revealed an interaction between the morpholinos with the percentage of morphants in the co-injected group being more than additive for the single morpholino injected

embryo (Figure 4.15 C). The severity of these co-injected morphants was also greater than the phenotype of single injected embryos (Figure 4.15 B). Synergistic action of *stra6* and *stra6.2* morpholinos indicates that *stra6* and *stra6.2* function co-operatively within the same pathway; in this case this is likely to be the retinoid pathway. The knockdown of both genes results in a knockdown of the function of the same pathway thereby resulting in a larger number of more severely affected embryos. If the genes had independent functions the number of affected embryos would be at maximum the total of both of the individually injected group and the severity of the phenotype would not be increased. Stra6.2 is therefore likely to also function as a retinoid transporter.

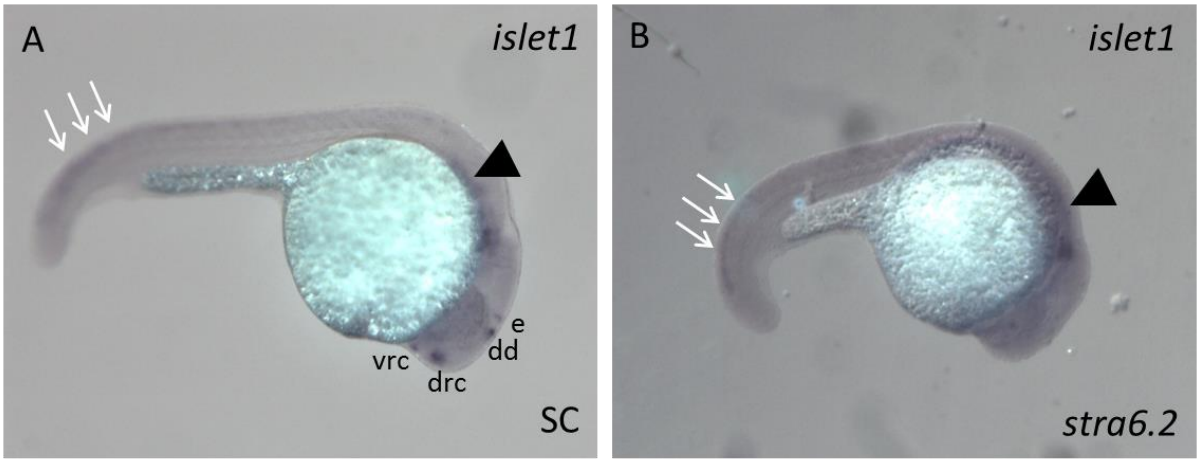

Figure 4.14 *islet1*expression is unaffected in the pancreas but highlights defects in the brain of *stra6.2* morphants.

islet1 is a marker for spinal chord neurons (white arrows), pancreas (black arrowhead) and within the brain, namely the ventral-rostral cluster (vrc), dorsal-rostral cluster (drc), epiphysis (e) and the dorsal diencephalon (dd), in standard control embryos (A). *stra6.2* morphants show no changes to the expression of *islet1* in the spinal neurons or the pancreas but do not show staining within the brain.

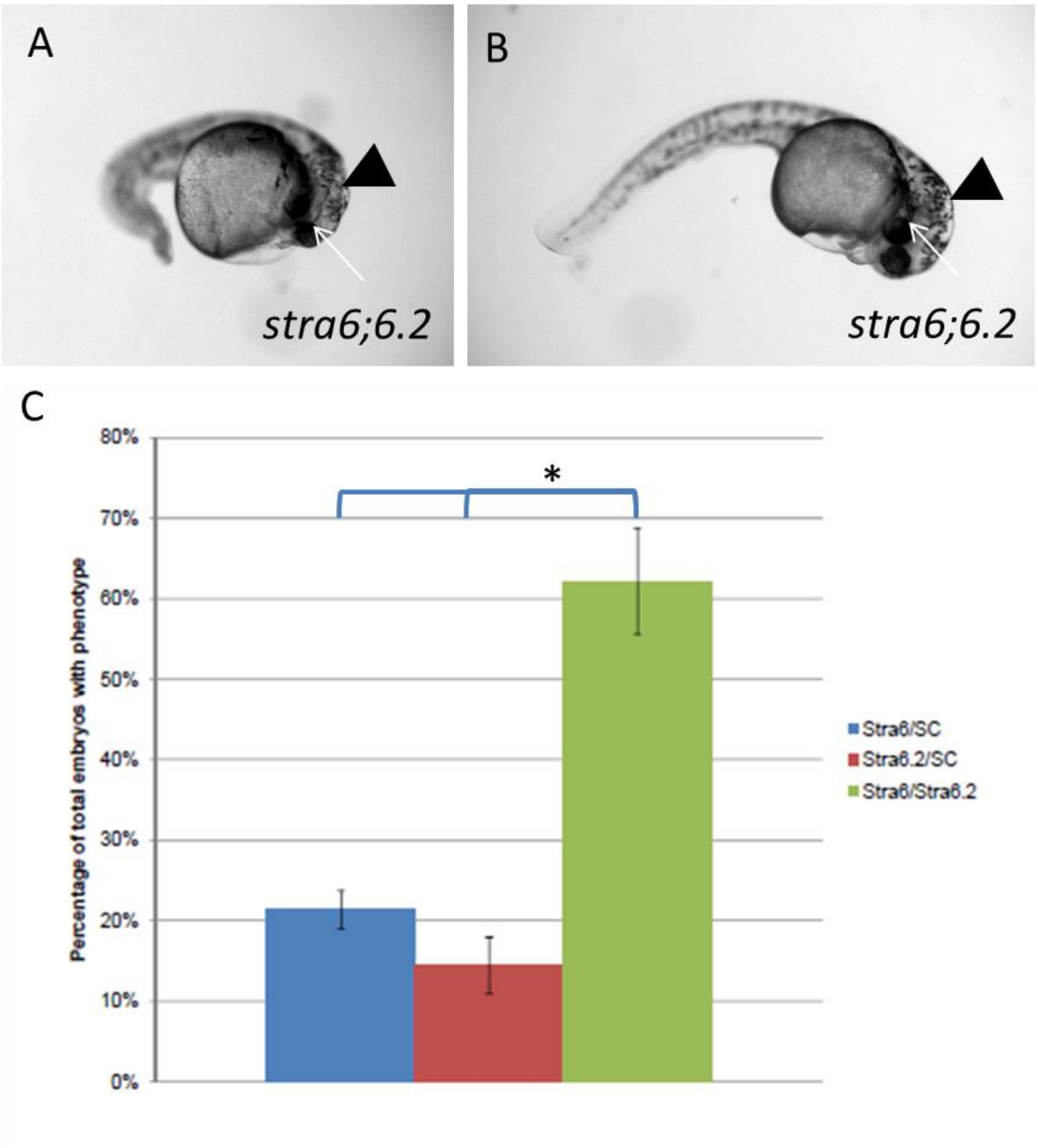
A
stra6;6.2
B
stra6;6.2
C
80%
70%
60%
50%
40%
30%
20%
10%
0%
Percentage of total embryos with phenotype
*
Stra6/SC
Stra6.2/SC
Stra6/Stra6.2

Figure 4.15 *stra6* and *stra6.2* morpholinos function synergistically.

Co-injection of *stra6* and *stra6.2* morpholinos at the normal injection concentration results in a severely phenotypic embryo (A) with microphthalmia (white arrow) and brain edema (black arrowhead). Co-injection at a concentration which, when injected singularly gives a low degree of mild phenotype, results in a more severely affected morphant (B). The low percentage of mildly-phenotypic morphants in low-dose single morpholino injected groups can be seen in the graph (C) as stra6/SC and stra6.2/SC. The percentage of co-injected (stra6/stra6.2) morphants with phenotype is more than additive of the percentages of singularly injected morphants ($P<0.0001$). *stra6*/SC n=205, *stra6.2*/SC n= 188, *stra6/stra6.2* n=247.

4.2.4 Reduction of Rbp4 rescues morphants.

Previously published work on *stra6* morphants revealed that reduction in Rbp4 level through either morpholino co-injection or chemical treatment with PTU was able to rescue the *stra6* morphant phenotype (Isken 2008). The *stra6* morphant phenotype was hypothesised to be caused by a nonspecific vitamin A excess within the embryo, provoked by holo-Rbp4 (Isken 2008). Reduction of Rbp4 level within *stra6.2* morphants using both an *rbp4* morpholino co-injected and the drug PTU was able to rescue 52% and 42% of morphants respectively and resulted in a significant increase in the percentage of normal embryos (Figure 4.16). PTU was also able to rescue *stra6; stra6.2* double morphants and decreased the percentage of phenotypic embryos (Figure 4.16).

4.2.5 Increase in RA-responsive gene expression in morphants compared to controls.

stra6 morphants have an increase in the expression of the RA-inducible *cyp26a1* (Isken 2008). The indication that *stra6.2* may have a similar function to *stra6* within the retinoid pathway led to the investigation of the possible changes in retinoid signalling in *stra6.2* and *stra6; stra6.2* double morphants.

4.2.5.1 *cyp26a1* expression is increased in morphants compared to controls.

cyp26a1 expression is regulated by RA through two RAREs within 2.5kb of the promoter (Hu 2008). WISH for *cyp26a1* in *stra6*, *stra6.2* and *stra6; stra6.2* morphants revealed an up-regulation in gene expression in *stra6*, *stra6.2* and *stra6; stra6.2* morphants compared to control morphants. The upregulation of *cyp26a1* in *stra6* morphants was previously reported (Isken 2008) and the current study replicated those results showing an increase in the length of the expression domain within the posterior notochord (Figure 4.17 A-B). The upregulation of *cyp26a1* in *stra6.2* morphants (Figure 4.17 C) was greater than in *stra6* morphants (Figure 4.17 B) with a larger expansion in the posterior notochord and an increase in the intensity of expression within the tailbud. *stra6; stra6.2* morphants have a generalised increase in *cyp26a1* expression across the embryo and the intensity of the normal expression domains is again increased (Figure 4.17 D) compared to *stra6.2* morphants.

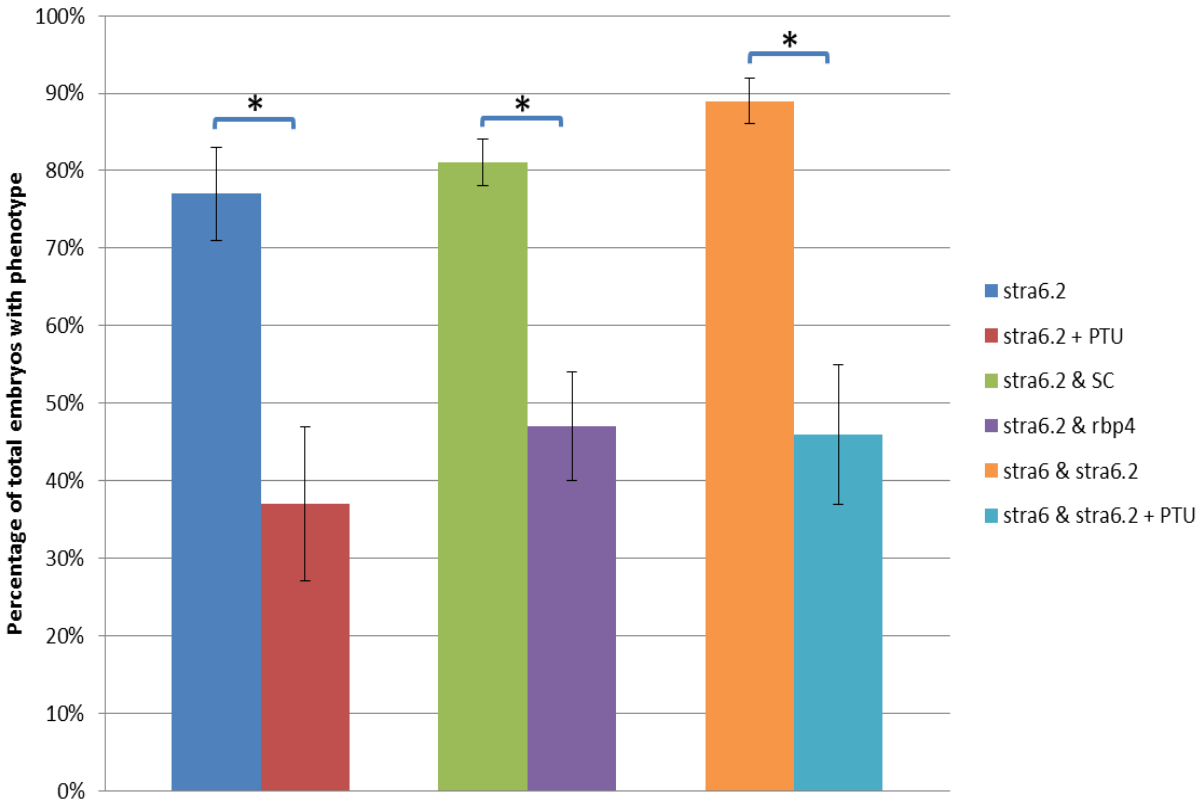

Figure 4.16 Reduction of Rbp4 level rescues *stra6.2* and *stra6; stra6.2* double morphants.

The percentage of embryos with phenotype from a *stra6.2* (stra6.2) or *stra6; stra6.2* (stra6 & stra6.2, P<0.0001) co-injected group is shown. When treated with PTU (+PTU, P<0.0001) or co-injected with *rbp4* morpholino (& rbp4, P<0.0001) this reduced the percentage of phenotypic embryos within the injected group. Error bars represent ±S.E.M. Asterisk highlight significant rescue of phenotypic embryos. *stra6.2* n=79, *stra6.2* + PTU n=68, *stra6.2* & SC n= 92, *stra6.2* & *rbp4* n= 101, *stra6 & stra6.2* n=69, *stra6 & stra6.2* +PTU n=60.

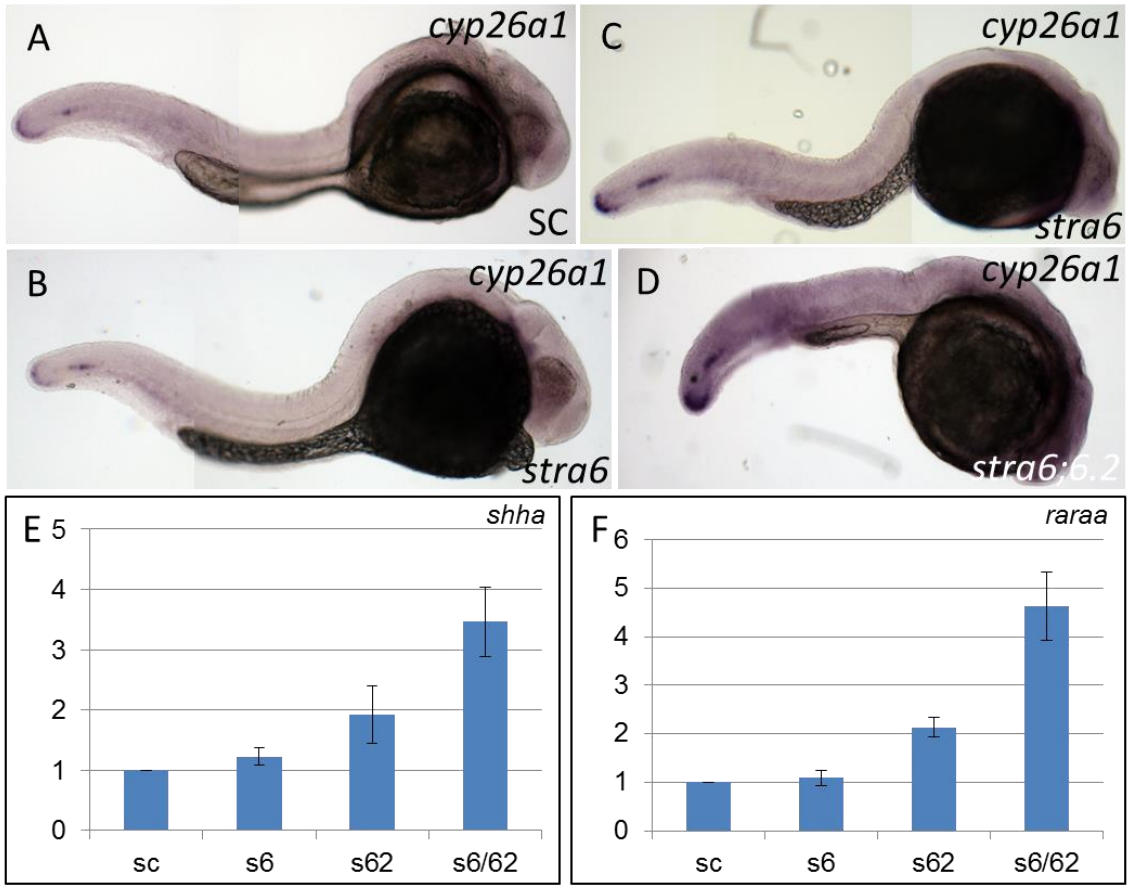

Figure 4.17 *stra6.2* morphants have excessive RA signalling.

Expression of the RA responsive genes *cyp26a1* (A-D), *shha* (E) and *raraa* (F) were analysed. *In situ* hybridisation analysis of *cyp26a1* expression (purple) in 30hpf flatmounted embryos was analysed in control injected (A), *stra6* morphant (B), *stra6.2* morphant (C) and the double *stra6/stra6.2* morphant (D). The yolk in A-D appears dark as embryos are flatmounted and illuminated from below. qRT-PCR for *shha* (E) and *raraa* (F) expression levels is shown (standard control (SC), *stra6* (S6), *stra6.2* (S6.2) and double morphant (S6/62) embryos). Error bars show ±SEM.

4.2.5.2 *shha* and *raraa* expression is increased in *stra6.2* and double morphants.

In order to gain a quantitative measure of the RA-responsive gene upregulation and to understand if this observation was applicable to other RA-responsive genes, qRT-PCR for the mRNA levels of *raraa* and *shha* was performed. *shha* (Figure 4.17 E) (Chang 1997) and *raraa* (Figure 4.17 F) (Wentworth 1999) both contain RAREs upstream of their promoters and are responsive to RA *in vivo*. Both genes showed upregulation in both *stra6.2* and *stra6; stra6.2* morphants compared to control morphants. The level of the housekeeping gene, *beta-actin*, was used as a standard. *stra6* morphants do not show a significant increase in the expression of either of these genes compared to control embryos.

4.2.6 *raldh2* expression is increased in the eye of *stra6.2* morphants.

raldh2 expression was assessed in order to investigate if *stra6.2* may be involved in the regulation of expression of *raldh2*. Expression of *raldh2* at 24hpf in *stra6.2* morphants is similar to that in standard control embryos being observed in the temporal retina of the developing eye and within the somites (Figure 4.18 A-B). However, *raldh2* expression within the dorsal portion of the eye at 48hpf is expanded in *stra6.2* morphants both within the dorsal-ventral and anterior-posterior axis. The intensity of the staining also seems increased in this region bordering the lens (Figure 4.18 C-D). *raldh2* expression within the 48hpf eye is affected in *stra6.2* morphants indicating that *stra6.2* either directly regulates *raldh2* expression or the perturbations in RA-signalling in *stra6.2* morphants affect the expression of *raldh2* within the eye.

4.2.7 Inhibition of RA synthesis rescues *stra6.2* morphants.

In order to investigate the mechanism behind the upregulation of RA-responsive gene expression in *stra6.2* morphants, Raldh-dependent RA synthesis was inhibited using DEAB (Begemann 2004). Treatment of *stra6.2* morphants with DEAB from the end of gastrulation until analysis at 48hpf rescued a significant number of morphants increasing the percentage of normal embryos (Figure 4.19).

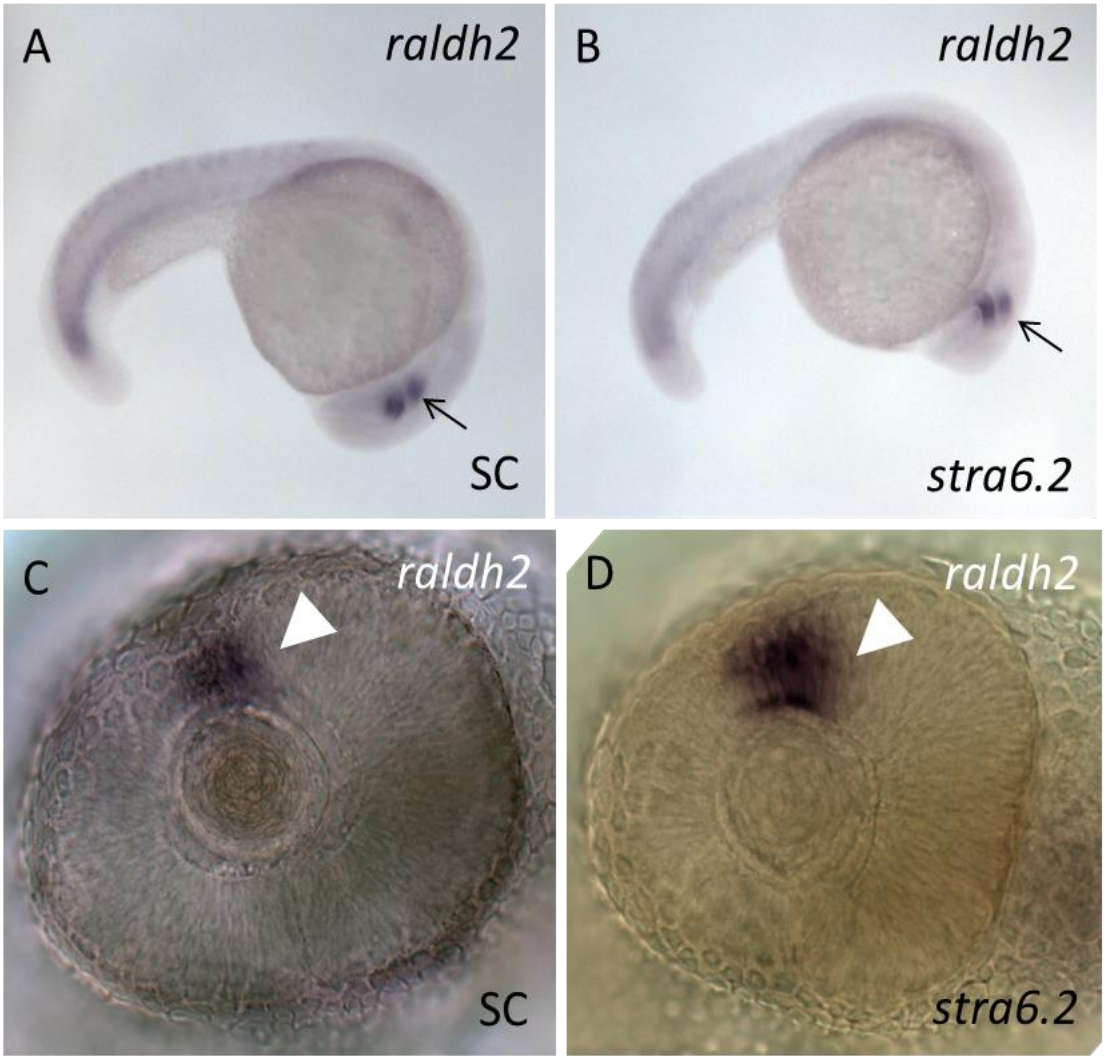

Figure 4.18 *raldh2* domain is expanded within the eye at 48hpf but not at 24hpf.

raldh2 expression (purple) was analysed by WISH at 24hpf (A-B) and in the eye at 48hpf (C-D). Expression levels and domains, namely the eye (black arrow) and the somites, were identical between standard control (A) and *stra6.2* morphants (B) at 24hpf. *raldh2* marks the dorsal retina (white arrowhead) of the eye at 48hpf in standard control embryos (C) but this domain of expression is expanded in both the dorsal-ventral and anterior-posterior axis in *stra6.2* morphants (D).

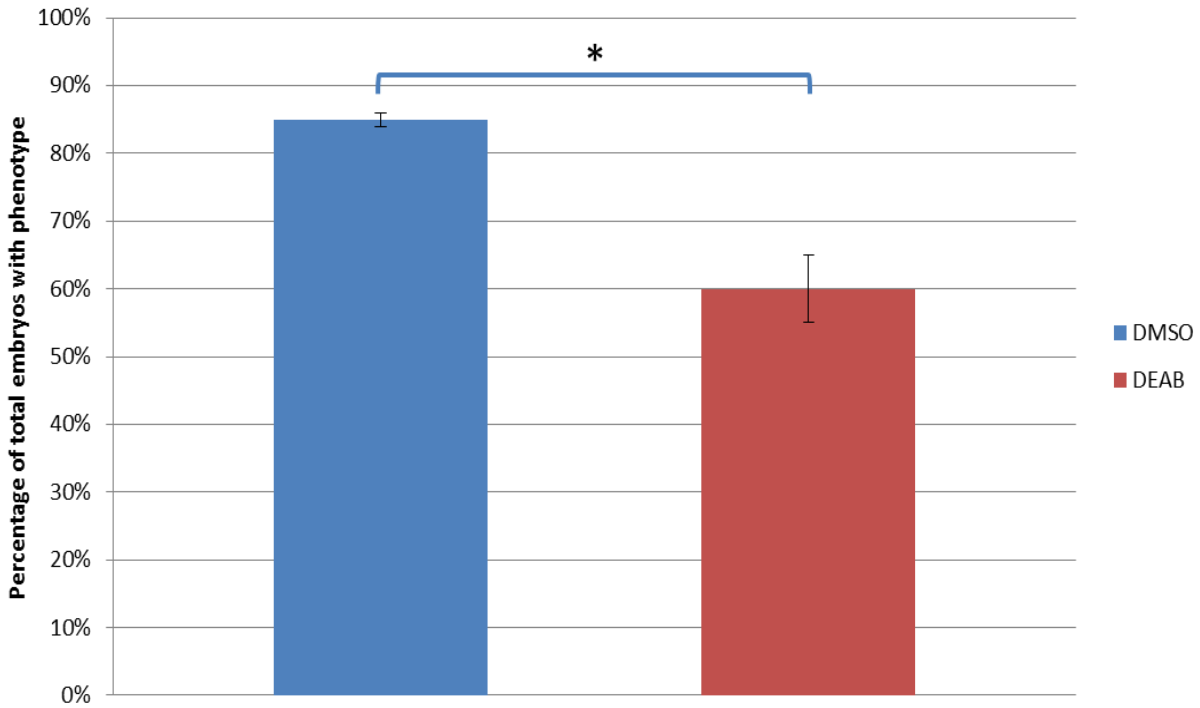

Figure 4.19 Inhibition of Raldh enzymes rescues *stra6.2* morphants.

stra6.2 morphants treated with the Raldh-inhibitor DEAB decreases the percentage of phenotypic embryos compared to *stra6.2* moprhants treated with only the solvent, DMSO. P<0.0001, Chi-square test. +DMSO n=282, +DEAB n=224.

4.3 Discussion

Stra6-like homologues are represented through evolution, from the simple eumetazoan *Trichoplax*, and are likely to have an ancient origin previous to the cnidarians and the bilaterians. The presence of a *Stra6*-like homologue in *Trichoplax*, in addition to homologues of other members of the retinoid pathway; *Rdh*, *Raldh* and *RXR*, indicate an ancient requirement for retinoid signalling in even morphologically simple organisms. The requirement for a functional retinoid signalling is not universal, with *Drosophila* and *C.elegans* both lacking any *Stra6*-like homologues and most of the components of the retinoid signalling pathway. *Drosophila*, however, require retinoids only for the visual cycle (Giovannucci 1999) with the developmental function of the retinoids replaced by edycosone (Garen 1977; Hall 1998). The lack of *Stra6*-like homologues in these species is, therefore, unsurprising as the retinoid signalling pathway is replaced with an alternative, which does not require the regulated provision of retinoids.

The appearance of two *Stra6*-like genes in vertebrates appears to have occurred early in their evolutionary history and may have occurred during the duplication events proposed to pre-date the fish-tetrapod split. The known duplication and divergence of many genes in the basal vertebrate (Dehal 2005) indicate that *Stra6* could possibly have originated from the duplication and divergence of *Stra6.2*. The vertebrate genome-norm for a single copy of both *Stra6* and *Stra6.2* is broken in the bird lineage and in the great apes, including humans. The bird lineage have only a copy of *Stra6* and no remnant of *Stra6.2* and in the great apes, *Stra6.2* has become split across the chromosome with only part of the gene still actively transcribed. The loss of *Stra6.2* in birds and great apes may be tolerated due to functional redundancy between *Stra6* and *Stra6.2*, a common feature of genes within the retinoid pathway. Differences in retinoid metabolism or signalling between species with and without an intact *Stra6.2* are also a possible explanation for the tolerated loss of this gene. Dietary provision of retinoids may also account for the loss of *Stra6.2*; however, it is difficult to identify the dietary differences which would allow tolerance of *Stra6.2* loss.

Stra6.2 was identified as a paralogue of *Stra6*, however, the conservation of the proposed RBP4 binding site was low with only one of the three residues required conserved. The proposed site was identified by mutational analysis of STRA6 and changes to these residues individually resulted in a dramatic reduction in intracellular retinol accumulation. However, a human polymorphism within this domain, which *in vitro* abolishes transport function, was found within the general population. There is no evidence that those people with this polymorphism had any gross developmental defects or overt retinoid deficiencies postnatally. Co-injection of *stra6* and *stra6.2* morpholinos into zebrafish embryos indicates that *stra6* and *stra6.2* interact synergistically and are likely to function in the same pathway. Furthermore, reduction of Rbp4 level in *stra6.2* morphants rescues their phenotype as has been previously shown for *stra6* morphants (Isken 2008). These observations lead to the conclusion that STRA6.2 is also likely to function as a RBP4-dependent retinoid transporter. The lack of conservation of the RBP4 binding domain in STRA6.2, however, makes it likely that either STRA6.2 has an RBP4 binding site made up of alternative amino acids or binds RBP4 through an alternative protein interaction mechanism. STRA6.2 may also function to transport retinol, although RBP4 is known to be promiscuous in its retinoid binding potential making it possible that it may function to transport other retinoids bound to RBP4.

Morpholino knockdown of *stra6.2* results in defects affecting the eye, notochord, somites, jaw and fin. A transgenic zebrafish reporter line, which links three copies of the RARE from mouse RARβ to GFP or YFP, highlights regions of the embryo in which RA signalling is active. Fluorescence is detected in the neural tube, notochord, somites, retina, pronephric duct, heart, branchial arches and forebrain indicating that these areas of the embryo have active retinoic acid signalling. Upon treatment with RA, more regions of the embryo become fluorescent including the fin and the fluorescence within the retina becomes more extensive. These regions of RA signalling significantly overlap with the defects observed in *stra6.2* morphants. *stra6.2* morphants are likely to have an increase in RA levels within the embryo due to an increase in RA synthesis. Regions, which normally have active RA signalling, contain the necessary components for RA synthesis. These regions are therefore likely to be more sensitive to excessively synthesising RA, due to the ready

availability of RA pathway enzymes, thereby resulting in the *stra6.2* morphant phenotype preferentially affecting these regions.

stra6.2 morphants are microphthalmic and, in addition, also have defects in lamination which are observed from 3dpf with no lamination or cellular specification observed in morphant retina. This progresses to a variable degree of lamination and cellular specification in the retina by 4dpf. The phenotype has some morphological overlap with *young* mutants who show no lamination of the retina due to a non-cell autonomous defect in differentiation, but not molecular specification, of the retinal cell types (Link 2000). The *young* mutant harbours a mutation in brahma related gene 1, *brg1*, a member of the chromatin remodelling complex SWI/SNF (Gregg 2003). Brg1 is known to function as transcriptional co-activators with retinoic acid receptors (Chiba 1994) and conversely also form part of the nuclear receptor corepressor complex, NCoR (Underhill 2000). *stra6.2* morphant eye defects may be the result of changes in RAR/RXR-dependent RA signalling causing a defect in the differentiation of some retinal cell types.

Development of the jaw in *stra6.2* morphants is severely affected with all the major cartilage elements showing some degree of aberration from the WT norm. The jaw cartilages develop from cranial neural crest cells which migrate into the visceral arch primordial, namely the mandibular arch, hyoid arch and branchial arches. Each arch forms a defined set of cartilage elements which make up the jaw. The mandibular arch forms the palatoquadrate and Meckel's cartilages. The hyoid arch forms the ceratohyal, basihyal and hyosymplectic cartilages. The branchial arch forms the ceratobranchial and basibranchial cartilages (Ellies 1997). Retinoic acid treatment of zebrafish embryos is known to disrupt jaw cartilage development; with Meckel's cartilage positioned behind the eyes, the ceratohyals flattened and the ceratobranchials malformed and reduced in number. The jaw defects seen in stra6.2 morphants significantly overlap with the defects observed in retinoic acid treated embryos (Alexandre 1996). Retinoic acid treatment is known to reduce the expression of *dlx* genes in cranial neural crest (Ellies 1997), where they are required to specify jaw cartilage elements (Depew 2002). Several *dlx* genes in zebrafish have

possible RAREs within their regulatory regions. Retinoic acid treatment is also known to cause ectopic accumulation of *hoxa1* in the head region and injection of *hoxa1* RNA into zebrafish embryos results in similar jaw cartilage defects as treatment with RA (Alexandre 1996). *stra6.2* morphants may therefore accumulate excess RA, which affects the expression of genes required for jaw specification, resulting in the developmental jaw defects observed.

Notochord and tail morphology are disrupted in *stra6.2* morphants and this is consistent with the expression of *stra6.2* in these tissues at various developmental stages. The notochord is undulated in respect to the dorsal ventral axis and this, along with the increase in head-tail distance and shorter embryos, indicates a defect in body axis elongation. The notochord, in addition to being undulated, also appears thicker which is a feature observed in body axis elongation-defective morphants, such as *frizzled-2* (Sumanas 2001). Tail morphology is also disrupted at 18hpf when the tailbud fails to disengage from the yolk extension. The tailbud marker *eve1* is upregulated along with an increase in the expression of *ntla*. *eve1* is known to be positively regulated by *ntla* (Joly 1993) and it is therefore likely that the excess *ntla* expression increases *eve1* expression within the tailbud. *eve1* expression within the tailbud reduced with age and it is therefore possible the tailbud remains immature for longer due to the increase in *eve1* expression.

The expression pattern of *stra6.2* at 24hpf, restricted only to the anterior of the embryo within the eye, brain and endoderm above the yolk, is broadly similar to that of *lrat* and significantly different to *raldh2*. Lrat is required to esterify retinol for storage as retinyl esters and Raldh2 to convert retinol to form retinal in the synthetic pathway to retinoic acid. *stra6.2* and *lrat* morphants are morphologically similar with a wavy notochord, defects in the eye and flattening of the somites observed in both (Isken 2007). The overlap between the expression pattern and morphant phenotype of *stra6.2* and *lrat* indicates that *stra6.2* may be required to direct retinoids to the storage pathway instead of retinoic acid synthesis. The upregulation of RA-dependent gene expression and the rescue of the *stra6.2* morphant phenotype with the Raldh-inhibitor DEAB add further weight to this conclusion. It can therefore be

postulated that in the absence of *stra6.2*, retinoids are no longer directed to the storage pathway but instead become metabolised to form RA which changes the levels of RA-responsive genes thereby resulting in the morphant phenotype observed. *stra6.2* is therefore likely to function to regulate the retinoid pathway through storage of retinoids in order to regulate intracellular free retinoid levels to prevent excess synthesis of RA.

4.4 Further work

In order to truly define the role of *Stra6.2*, a cellular based investigation of its function is required. The function of STRA6 has previously been defined by transfecting *Stra6* into COS cells, in addition to *Lrat* in order to 'trap' the transported retinoids intracellularly in a measurable form. The cells are then treated with RBP4-bound retinoids, in the case of STRA6 – retinol, for a defined period and the cells were then washed to remove any retinoids associated with the extracellular surface. The cells were lysed and the retinoid profile of the contents analysed by HPLC. Transfection with *Stra6* and *Lrat* results in an accumulation of retinyl esters compared to un-transfected cells (Kawaguchi 2007; Kawaguchi 2008). *Lrat* is required for significant accumulation of retinoids by STRA6 due to the newly proposed mechanism for STRA6 action. This mechanism proposes that any transported retinol will be re-loaded onto RBP4 if the retinol is not met by LRAT or CRBP, in order to regulate the level of free retinol within the cell (Kawaguchi 2011). Defining the retinoid transport potential of STRA6.2 would require transfection of *Stra6.2* alone and in conjunction with other genes, such as *Lrat*, *Crbp* and *Crabp*, to process the transported retinoids into cells. Unbound and RBP4-bound retinol, retinal and retinoic acid need to be applied to these transfected cells in order to define the preferred transport ligand of STRA6.2. The retinoid-treated transfected cells, after washing to remove extracelluarly associated retinoids, would then be analysed by HPLC in order to detect any changes to the retinoid profile compared to un-transfected cells. Hopefully this methodology would successfully identify the transport actions of STRA6.2.

The role of STRA6 in signalling through the JAK-STAT pathway in an RBP4-retinol dependent manner has been recently defined (Berry 2011). The YTLL domain within the C-terminal tail of STRA6 become phosphorylated in response to RBP-bound retinol and in turn recruits STAT5 and JAK2. The association between these proteins phosphorylates STAT5 allowing its translocation to the nucleus and activation of the transcription of STAT5 dependent gene expression (Berry 2011). The conservation of part of this YTLL phosphorylation domain in STRA6.2 indicates that STRA6.2

may also act as part of the JAK/STAT signalling pathway. Upon identification of the preferred transport ligand of STRA6.2, the level of tyrosine phosphorylation within STRA6.2 could be measured upon exposure to the transportable retinoid. The activation of known STAT5 target genes, such as SOCS3 and PPARγ, or a STAT5-activated luciferase reporter could also be quantified in the presence of the preferred transportable retinoid. Microarray analysis between retinoid treated and un-treated cells may also help define possible signalling pathways activated.

The phenotypes observed in *stra6.2* morphants are unlikely to be the result of off-target effects of morpholinos due to the rescue of the phenotype by both co-injection with a *rbp4* morpholino and chemical reduction of Rbp level with PTU. The morpholinos also result in intron-inculsion and exon-skipping within the target transcript, as shown in figure 4.6. However, the level of wild-type transcript observed by this method does not seem to be reduced despite the appearance of the additional bands indicative of changes to the transcript produced. This is possible due to saturation of the PCR reaction which does not allow the reduction in wild-type transcript to be observed and therefore qRT-PCR may be an appropriate method in order to investigate and quantify any reduction in wild-type transcript level. The use of primers specific to the 'skipped' exon would allow quantification of any reduction in morphant compare to wild-type embryos. In order to quantify intron-inclusion, primers directed towards the intron would be used, in conjunction with no-RT controls in order to distinguish any genomic contamination from the presence of intronic sequences within the mRNA transcripts.

Chapter Five

In search of a mouse model of Matthew-Wood syndrome.

5.0 Introduction

Matthew-Wood syndrome results from homozygous and compound heterozygous mutations in *STRA6*, however, *Stra6-/-* mice do not represent a model of Matthew-Wood syndrome. This disparity between the phenotype of Matthew-Wood patients and *Stra6-/-* mice could be due to the presence of second gene in mice compared to humans, *Stra6.2*. Investigations in the previous chapter highlight a developmental role for *stra6.2* in zebrafish development and therefore *Stra6.2-/-* mice or loss of both *Stra6* and *Stra6.2* in mice may result in a similar genetic and phenotypic situation to that of human Matthew-Wood patients.

5.1 *Stra6.2* knockout-first mice

KOMP knockout-first ES-cells were obtained in order to create *Stra6.2-/-* animals. The *Stra6.2* locus has been manipulated in order to maintain all of the coding material but has been altered to include a lacZ insertion followed by a strong stop codon in order to tag expression of the *Stra6.2* gene. This construct also introduces loxP sites surrounding one exon allowing, after removal of the lacZ by the integrated Flp sites, the creation of a conditional allele for further investigation of the function of *Stra6.2* (Figure 5.1). The position of the construct was confirmed with long-range PCR between construct and gene specific primers.

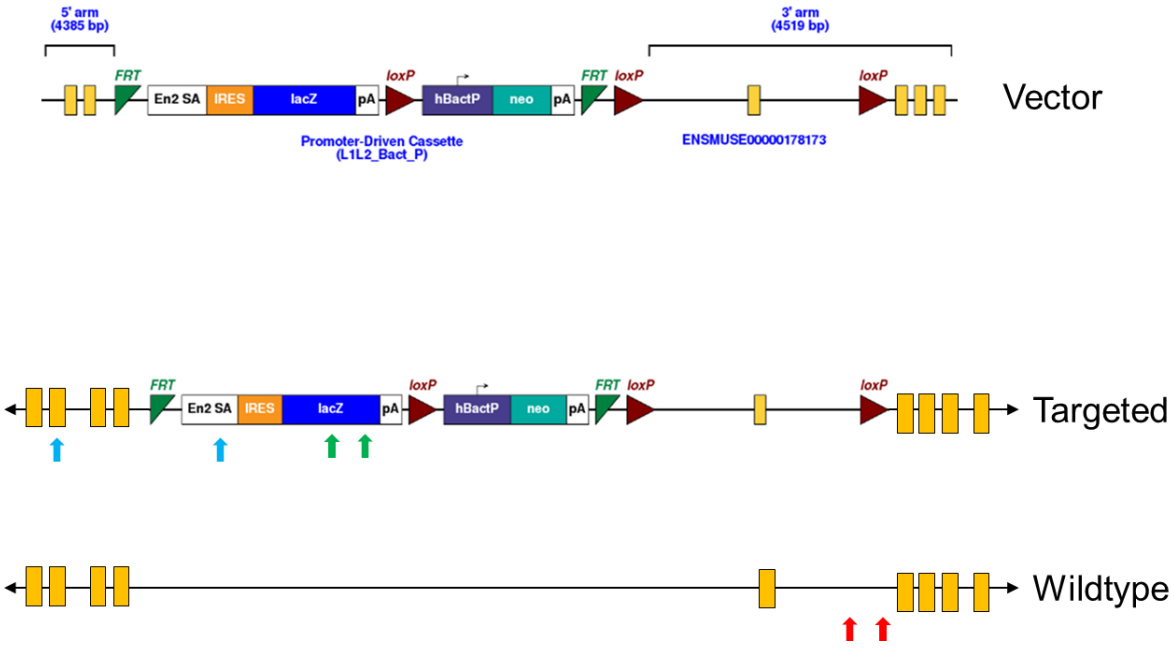

Figure 5.1: Diagram of the *Stra6.2* knockout-first allele within the *Stra6.2* gene.

The knockout first construct is located within intron 6-7 and consists of a promoter driven lacZ gene (lacZ, blue rectangle) with a strong stop (pA, white rectangle) and a neomycin-resistance gene (neo, turquoise rectangle) to enable cell selection. The construct also surrounds exon-7 with loxP sites (red triangles) in order to create a cre-sensitive conditional allele after removal of the expression tagging and selection cassette through activation of the FRT sites (green triangles). The position of the vector within the genome was confirmed via long range PCR with a primer pair directed to regions in- and outside the targeting construct (blue arrows). The targeted locus is genotyped using primers directed to the inserted lacZ gene (green arrows). The wildtype locus is genotyped using a pair of primers in which the forward sequence is present in both the wildtype and targeted loci with a reverse primer located in a small portion of sequence lost during the targeting event (red arrows).

5.2 *Stra6.2* is expressed during mouse development.

Expression of *Stra6.2* in the developing embryo was investigated by staining for β-galactosidase function of the integrated lacZ construct within the *Stra6.2* gene. The expression of *Stra6.2* was investigated through the expression of the integrated lacZ construct due to the failure of whole mount *in situ* hybridisation (WISH) to identify a specific expression pattern in embryos between E9.5-E12.5.

Expression of *Stra6.2* via the activity of the integrated lacZ construct could not be detected until E9.5 with no expression observed at E7.5. Embryos at E7.5 showed no blue staining in either the embryonic or extra-embryonic compartment (Figure 5.2 A & B) despite additional staining time compared to other stages. The small size and tissue volume of E7.5 embryos may make visualising the stain difficult and therefore these stages may express *Stra6.2* at low levels undetectable under this protocol.

Expression at E9.5 is restricted only to the tail region of the embryo (Figure 5.2 A, Figure 5.3 A) within the open neural tube mesenchyme and the epithelial edge adjacent to this (Figure 5.3 B). Expression also extends further into the neural tube restricted only to the internal edge of the epithelium (Figure 5.2 D, Figure 5.3 B). *Stra6.2* expression is also restricted to the tail region later in development (Figure 5.2 E, F & J). Expression within the tail region at E10.5 is restricted to the circular tail-bud (Figure 5.2 E) and into the posterior neural tube (Figure 5.3 C). Neural tube expression is found only within the ventral portion close to the edge (Figure 5.3 D). In addition to the consistent expression within the tail (Figure 5.2 F, H & I), expression is also observed within the somites posterior to the hind-limb bud at E11.5 (Figure 5.2 G). Somite expression at E11.5 is restricted mainly to the ventral edge only, although at E12.5 expression is observed punctately throughout the somite (Figure 5.2 K). Expression in addition to being observed within the neural tube (Figure 5.2 J) and tail-bud (Figure 5.2 L) is also noted within the umbilicus (Figure 5.2 M).

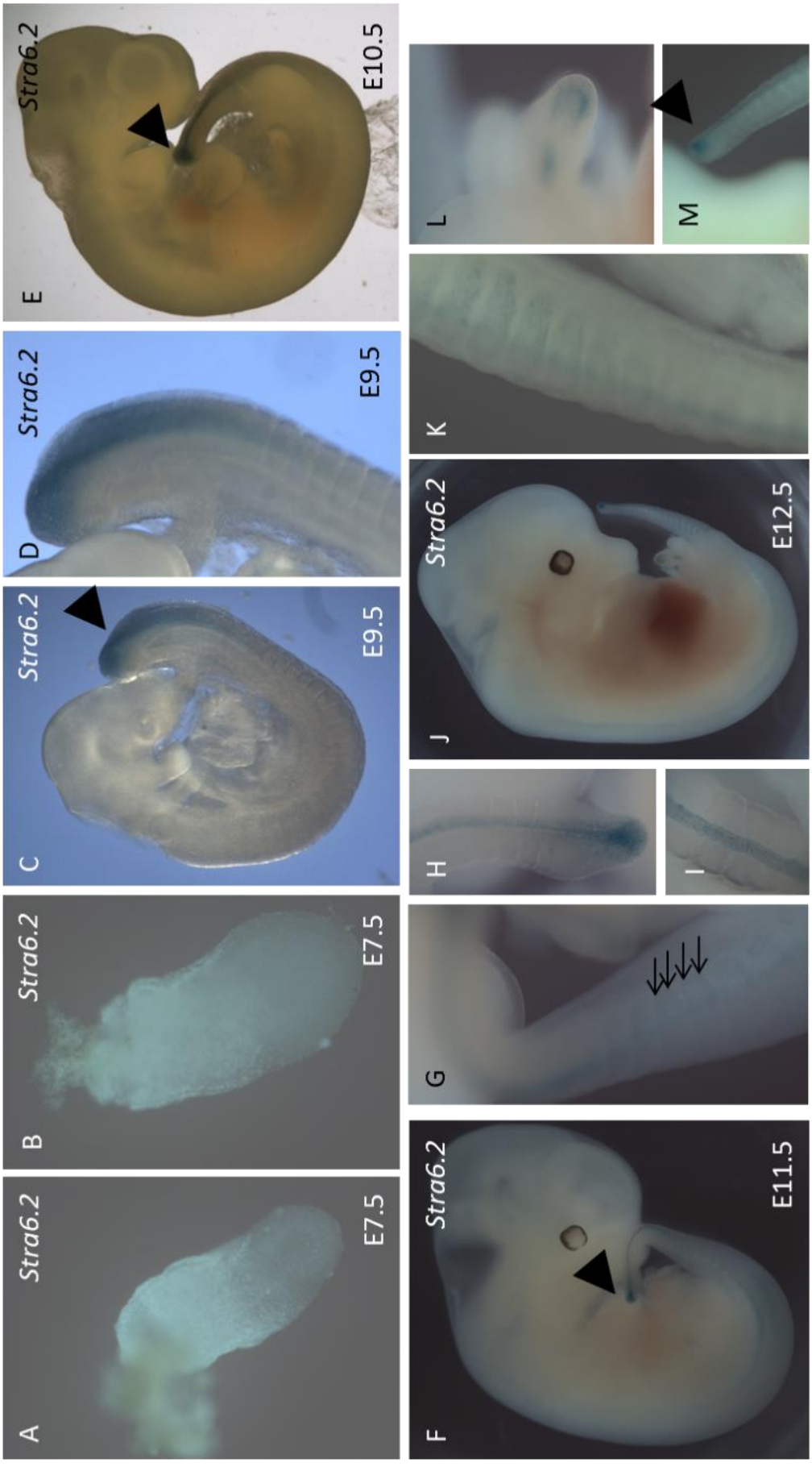
A
Stra6.2
E7.5
B
Stra6.2
E7.5
C
Stra6.2
E9.5
D
Stra6.2
E9.5
E
Stra6.2
E10.5
F
Stra6.2
E11.5
G
H
I
J
Stra6.2
E12.5
K
L
M

Figure 5.2: *Stra6.2* is expressed during embryonic development from E9.5.

Expression of *Stra6.2* marked by staining for the activity of the lacZ marker integrated into the *Stra6.2* locus. Expression could not be observed at E7.5 in either early (A) or late streak (B) embryos. *Stra6.2* expression (blue) was restricted to the tail region (black arrowhead) of the embryo at E9.5 (C). The expression within the tail was restricted to the open neural tube of the posterior region of the embryo (D). At E10.5, expression is also restricted to the tail region (E) specifically the tail bud (black arrowhead) and this is consistent at E11.5 (F). The ventral edge of the somite (G, black arrows), the tailbud(H) and neural tube (I). Expression is broadly similar at E12.5 (J) and is observed throughout the somites (K) and the tailbud (black arrowhead, L). In addition expression is also observed in the umbilicus (M).

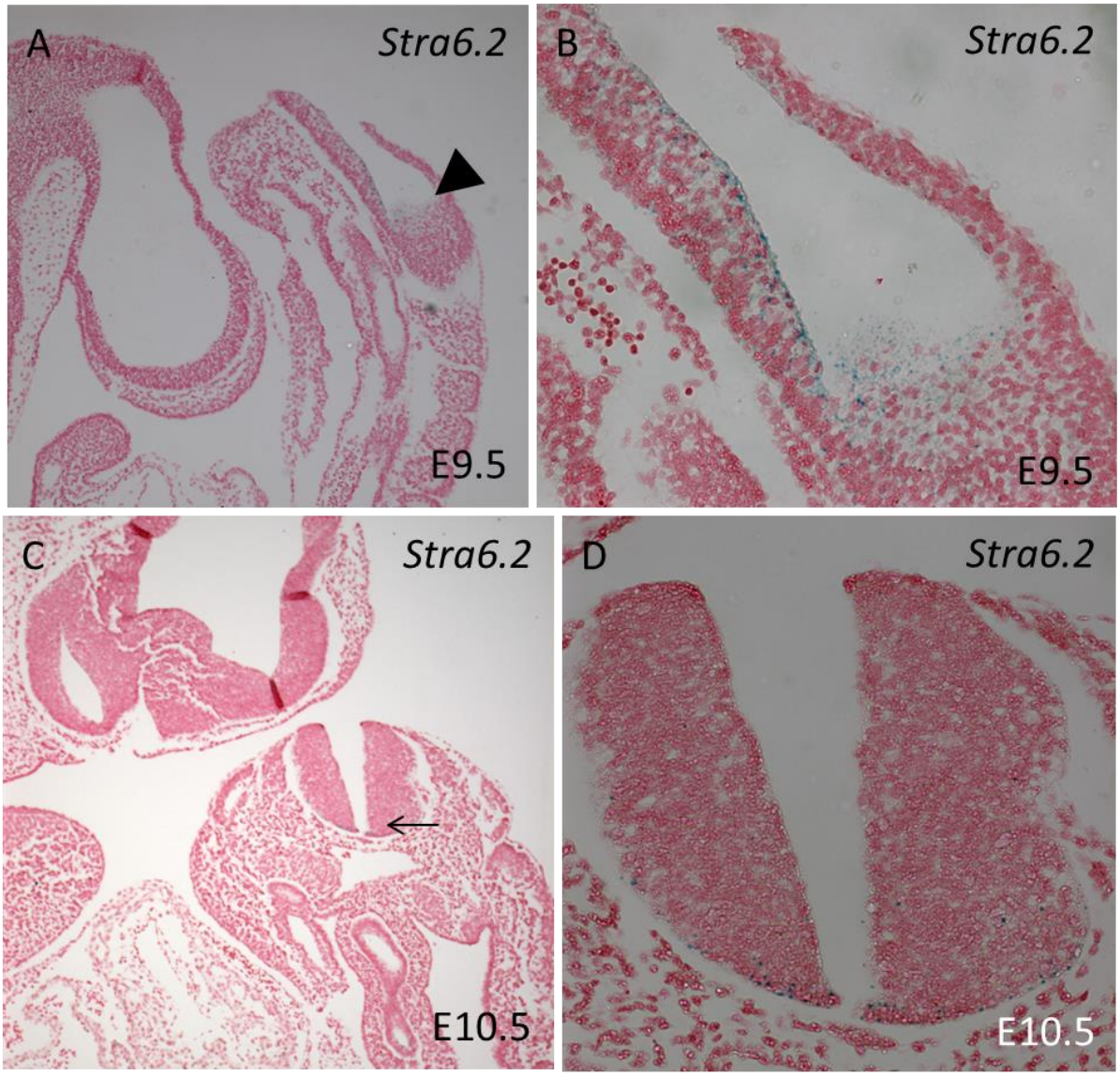

Figure 5.3: Histological sections reveal specific regions of *Stra6.2* expression.

Sagittal sections of embryos have been counterstained with nuclear fast red (pink) after β-gal staining for *Stra6.2* expression (blue). At E9.5, expression is found only in the tail region (black arrowhead, A) within the mesenchyme of the open neural tube of the tail and along the epithelial edge of this region (B). Expression at E10.5 is also observed further into the neural tube (black arrow, C) and is restricted to a subset of cells on the ventral border (D).

5.2.1 *Stra6.2-/-* animals are not a model of Matthew-Wood syndrome.

Stra6.2 knockout mice have no gross developmental defects. *Stra6.2* knockout mice were indistinguishable for their heterozygous and wildtype littermates when viewed in the cage. *Stra6.2* knockout animals also have normal eye size and appearance compared to their littermates in the cage. *Stra6.2-/-* animals did not have an increased mortality rate compared to heterozygous and wild type littermate. *Stra6.2* is a paralogue of *Stra6* and mutations in *STRA6* in humans result in Matthew-Wood syndrome. *Stra6-/-* mice do not represent a model of Matthew-Wood syndrome showing no detectable defects in the heart, lungs, eyes or the diaphragm (See Chapter 3). *Stra6.2* knockout mice, also, do not represent a model of Matthew-Wood syndrome with no reduction in eye size or increase in mortality.

Stra6.2-/- animals were observed in the expected ratio when routinely genotyped at 2-3 weeks of age indicating that *Stra6.2* is not required for survival through the embryonic or neonatal period (Table 5.1). Depression of the number of homozygotes would be expected if *Stra6.2* affected the survival threshold.

5.2.2 *Stra6.2-/-* animals have normal visual function and acuity.

Stra6.2 knockout animals had normal sized eyes with eye shape and position indistinguishable from littermates. Vision was tested using a moving grating in a visual testing drum and head tracking was monitored in response to this. The vision of *Stra6.2* knockout animals was normal with head tracking observed in response to moving grating at both 4° and 2° indicating visual acuity was normal (Table 5.2) and comparable to wildtype animals.

	Stra6.2		
	+/+	+/-	-/-
Observed	17	23	15
Expected	13.75	27.5	13.75

Table 5.1: *Stra6.2-/-* are observed at the expected genetic ratio.

No significant difference in the number of *Stra6.2+/+*, *Stra6.2+/-* and *Stra6.2-/-* animals between the expected and observed values was seen. P=0.4453, Chi-square test.

		Stra6.2	
		+/-	-/-
Sight at 2°	response	1	2
	no reponse	0	0
Sight at 4°	response	1	2
	no reponse	0	0

Table 5.2: *Stra6.2+/-* and *Stra6.2-/-* animals demonstrate a normal visual response.

Stra6.2+/- and *Stra6.2-/-* animals showing normal head tracking (response) to both 4° and 2° grating. No animals failed to head track (no response).

5.3 *Stra6.2* diet study

Stra6.2 knockout animals have no developmental or postnatal phenotypes. *Stra6* knockout animals also have no developmental defects under normal dietary conditions, but when *Stra6*-/- dams are fed a retinoid-free diet during pregnancy the *Stra6*-/- offspring are microphthalmic and have defects in the retina, lens and vasculature of the eye (See Chapter 3). *Stra6.2* dams were therefore transferred to a retinoid-free diet during pregnancy in order to understand the contribution of diet to the requirement for *Stra6.2*. *Stra6.2*-/- females were mated to *Stra6*+/- males in order to produce litters with a mixture of homozygous experimental (*Stra6.2-/-*$^{E0.5\text{-}Birth)}$ and heterozygous (*Stra6.2+/-*$^{E0.5\text{-}Birth)}$ control animals. Dams were transferred to the retinoid-free diet from plug discovery, at approximately E0.5, till birth of the pups.

5.3.1 *Stra6.2-/-* diet study animals are also not a model of Matthew-Wood syndrome.

Stra6.2 knockout mice have no gross developmental phenotypes and do not represent the multisystem developmental disorder Matthew-Wood syndrome. *Stra6.2-/-* animals born to dams fed a retinoid-free diet from plug discovery to birth did not represent an animal model of the human condition with no discernable developmental defects of the eyes, heart, lung or diaphragm.

Stra6.2-/- $^{E0.5\text{-}Birth}$ animals have normal eye morphology when viewed in the cage and upon weighing of the eyes were found not to differ substantially in weight compared to other animals from dams maintained on a retinoid-free diet for the same gestational period (Table 5.4). Histological sections were taken through the eye of *Stra6.2-/-*$^{E0.5\text{-}Birth}$ and eye morphology was normal with no defects of the lens, cornea (Figure 5.4 A) or retina (Figure 5.4 B). *Stra6.2* is therefore not required, even under conditions of low-retinoid stress, for the development or maintenance of the eye.

Heart defects are commonly observed in Matthew-Wood patients and form part of the constellation of symptoms diagnostic for the condition. *Stra6.2-/-* $^{E0.5\text{-}Birth}$ animals were active in the cage. No gross defects in heart morphology were observed (Figure 5.4 C) and upon histological analysis normal ventricular walls and intact ventricular septum were noted (Figure 5.4 D).

Stra6.2-/- $^{E0.5\text{-}Birth}$ animals did not experience respiratory distress at birth indicating that the severe lung hypoplasia associated with Matthew-Wood syndrome are not replicated in *Stra6.2-/-* $^{E0.5\text{-}Birth}$ animals. Normal lung morphology, with the expected number of lobes noted appropriate for laterality, was found upon pathological analysis of *Stra6.2-/-* $^{E0.5\text{-}Birth}$ animals (Figure 5.4 E). Histological sectioning of adult lungs from *Stra6.2-/-* $^{E0.5\text{-}Birth}$ animals showed no major defects in alveoli size or shape (Figure 5.4 F).

Pathological investigation of *Stra6.2-/-*$^{E0.5\text{-}Birth}$ animals did not find any signs of diaphragmatic hernia, another defining morphological finding of Matthew-Wood syndrome. The diaphragm was intact with no signs of eventration of the liver or any other thoracic organs.

Stra6.2-/- offspring of *Stra6.2-/-* dams fed a retinoid-free diet were found in the expected ratio (Table 5.3). Although the numbers are still low, the requirement for *Stra6.2* is therefore likely to not be dependent on dietary retinoid supply.

5.3.2 *Stra6.2-/-* diet study animals have normal visual function and acuity.

Stra6.2-/-$^{E0.5\text{-}Birth}$ animals showed no reduction in eye size nor were any morphological defects observed upon histological sectioning. Consistent with this observation no defects in vision were noted in *Stra6.2-/-* $^{E0.5\text{-}Birth}$ animals when tested for a head-tracking response to a moving grating. *Stra6.2-/-* $^{E0.5\text{-}Birth}$ animals responded to both 4° and 2° grating indicating no defects in vision or visual acuity are detectable in these animals (Table 5.4).

	Stra6.2	
	+/-	-/-
Observed	2	4
Expected	3	3

Table 5.3: *Stra6.2-/-* animals born to dams under dietary retinoid stress are observed at the expected genetic ratio.

No significant difference in the number of *Stra6.2+/-* and *Stra6.2-/-* animals between the expected and observed values was seen. P= 0.4142, Chi-square test.

		Stra6.2
		-/-
Sight at 2°	response	4
	no reponse	0
Sight at 4°	response	4
	no reponse	0

Table 5.4: *Stra6.2-/-*$^{E0.5\text{-}Birth}$ animals demonstrate a normal visual response.

Stra6.2-/- $^{E0.5\text{-}Birth}$ animals showing normal head tracking (response) to both 4° and 2° grating. No animals failed to head track (no response).

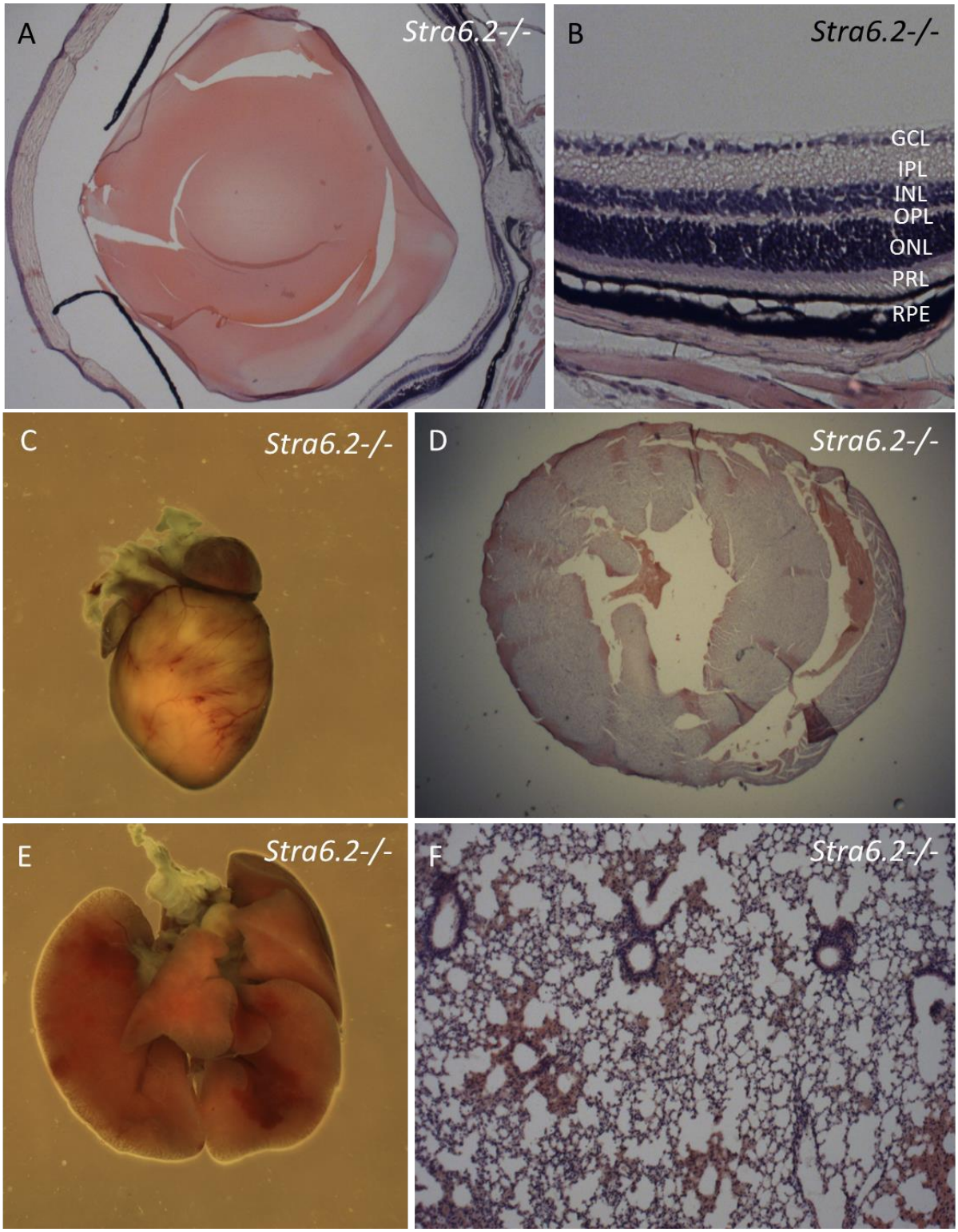
A
Stra6.2-/-
B
Stra6.2-/-
GCL
IPL
INL
OPL
ONL
PRL
RPE
C
Stra6.2-/-
D
Stra6.2-/-
E
Stra6.2-/-
F
Stra6.2-/-

Figure 5.4: *Stra6.2-/-* animals show none of the defects associated with Matthew-Wood syndrome.

Eye morphology is normal in *Stra6.2-/-* animals (A) with lens, cornea and retina intact and correctly arranged. The retina is made up of the expected layers (B); namely the ganglion cell layer (GCL), inner plexiform layer (IPL), Inner nuclear layer (INL), outer plexiform layer (OPL), outer nuclear layer (ONL), photoreceptor layer (PRL) and retinal pigmented epithelium (RPE). The heart of *Stra6.2-/-* $^{E0.5\text{-}Birth}$ is morphologically normal (C). Histological sections through the ventricular region of the heart show normal thickness of both the right- (RV) or left ventricle (LV)with no sign of ventricular septal defects (D). Gross morphology of the lung is normal with the expected lobes observed (E) and histological sections of the lung show normal alveoli size or shape (F).

5.4 *Stra6; Stra6.2*: the key to a mouse model of Matthew-Wood syndrome?

Stra6 and *Stra6.2* appear, in mouse, to be functionally redundant and able to compensate for each other's function, such that individual knockouts for either gene are unable to recapitulate Matthew-Wood syndrome. Matthew-Wood syndrome is caused, in humans, by mutations within *STRA6*, however loss *STRA6.2* gene function in humans may account for the differences between mouse and human in developmental phenotype. In order to create a possible mouse model for Matthew-Wood syndrome, *Stra6* and *Stra6.2* knockout animals were bred together in order to produce *Stra6+/-; Stra6.2-/-*, *Stra6-/-; Stra6.2+/-* and *Stra6-/-; Stra6.2-/-* animals as possible models.

5.4.1 *Stra6+/-; Stra6.2-/-* do not represent a model of Matthew-Wood syndrome.

Stra6+/-; Stra6.2-/- animals are viable and fertile. Eye size is normal with no discernable difference in size of shape of the eye when viewed in the cage. These animals were found in excess of the expected genetic ratio with no suppression of this genotype in multiple litters (Table 5.5). Visual testing of the animals with the head tracking response to moving grating highlighted no visual defects or reduction in visual acuity (Table 5.6). *Stra6+/-; Stra6.2-/-* animals therefore do not represent a model for Matthew-Wood syndrome. The viability, normal vision and fertility of these animals indicate that a single copy of *Stra6* is sufficient to support embryonic development and maintenance of the retinoid-dependent visual and reproductive systems.

	Stra6; Stra6.2		
	- - ; + -	+ - ;- -	- - ; - -
Observed	4	24	0
Expected	6.00	12	15.25

Table 5.5: *Stra6+/-;Stra6.2-/-, Stra6-/-;Stra6.2+/-* and *Stra6-/-;Stra6.2-/-* are not observed in the expected genetic ratio.

A significant increase in the number of *Stra6+/-;Stra6.2-/-* animals observed was noted compared to a loss of all *Stra6-/-;Stra6.2-/-* and a slight reduction in the number of *Stra6-/-;Stra6.2+/-* animals compared to the expected values predicted

		Stra6; Stra6.2	
		+/-; -/-	-/-; +/-
Sight at 2°	response	3	2
	no reponse	0	0
Sight at 4°	response	3	2
	no reponse	0	0

(P<0.0001, Chi-square test).

Table 5.6: *Stra6+/-;Stra6.2-/-* and *Stra6-/-;Stra6.2+/-* animals demonstrate a normal visual response.

Stra6.2-/- $^{E0.5\text{-}Birth}$ animals showing normal head tracking (response) to both 4° and 2° grating. No animals failed to head track (no response).

5.4.2 A single copy of *Stra6.2* is able to support normal development and postnatal survival in some cases.

Stra6-/-; Stra6.2+/- animals are variable in their phenotype and survival. *Stra6-/-; Stra6.2+/-* animals are observed less than expected at 2-3 weeks (Table 5.5) and appear to have a higher mortality rate with 2 of 4 *Stra6-/-;Stra6.2+/-* animals lost around weaning. One such animal which died around the time of weaning was found to have fused eyelids (Figure 5.5 A), however, ocular tissue was noted within the orbits and histological sections of this tissue showed mass disorganisation of the retina but a reasonably well developed lens bilaterally (Figure 5.5 B & C). Those *Stra6-/-;Stra6.2+/-* animals which died at weaning were runted compared to littermates, however a surviving *Stra6-/-; Stra6.2+/-* animals also appeared runted at weaning (1/2). In this *Stra6-/-; Stra6.2+/-*animal, eye size was reduced when compared to *Stra6+/-; Stra6.2-/-* littermates. One *Stra6-/-; Stra6.2+/-* animal was, however, normal and indistinguishable from littermates in terms of body and eye size.

Despite the small eye size observed in 1 of the 2 surviving *Stra6-/-; Stra6.2+/-* animals, visual function is normal with a normal head tracking response to moving grating (Table 5.6) in both surviving animals. Initial experiments suggest that both male and female *Stra6-/-; Stra6.2+/-* animals are fertile and able to produce viable pups when bred to C57Bl6 animals. A single copy of *Stra6.2* is therefore sufficient for survival and will support normal development in some animals, but in others development appears to fail or is affected. *Stra6.2* appears to be stochastically sufficient for normal development in some animals but not all and is therefore likely to have a lower functional capacity than *Stra6*.

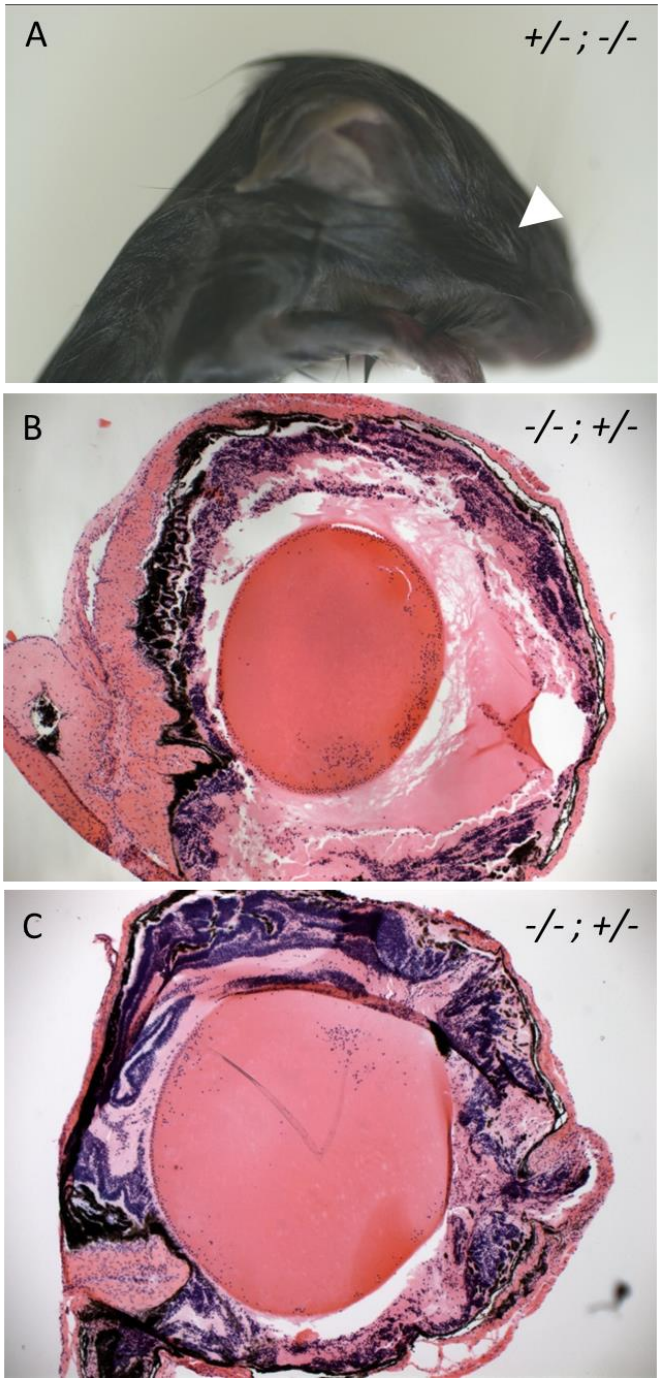

Figure 5.5: *Stra6-/-;Stra6.2+/-* animal died around weaning with fused eyelids and under-developed eyes.

A *Stra6-/-;Stra6.2+/-* animal died around weaning with fused eyelids (white arrowhead, A). Histological sectioning of the small volume of eye tissue present within the orbits upon dissection revealed mass disorganisation of the retinal tissue but relatively normal lens morphology (B & C).

5.4.3 *Stra6-/-; Stra6.2-/-*: a model for Matthew-Woods?

Stra6-/-; Stra6.2-/- pups were not observed in any litters born to either *Stra6+/-; Stra6.2-/-* or *Stra6+/-; Stra6.2+/-* dams indicating that regardless of maternal genotype *Stra6-/-; Stra6.2-/-* pups are not viable postnatally. No *Stra6-/-; Stra6.2-/-* pups were observed for all matings compared to the expected 11.68 *Stra6-/-; Stra6.2-/-* pups which should be observed in accordance with expected genetic ratios calculated from parental genotype.

Plugs from were taken from *Stra6+/-; Stra6.2-/-* or *Stra6+/-; Stra6.2+/-* dams at various embryonic stages in order to investigate the loss of *Stra6-/-; Stra6.2-/-* embryos during gestation. At E7.5, the expected number of *Stra6-/-; Stra6.2-/-* embryos was observed in a single plug from a *Stra6-/-; Stra6.2-/-* dam (Table 5.7, Figure 5.7 A). The *Stra6-/-; Stra6.2-/-* embryos appeared morphologically normal with development of the ectoderm appearing normal within the embryo and no gross morphological differences observed between *Stra6+/-; Stra6.2-/-* (Figure 5.6 A) and *Stra6-/-; Stra6.2-/-*embryos (Figure 5.6 B). Sections of the embryos were not taken in this initial investigation as the whole embryo (with any extra-embryonic tissue removed) was used for DNA extraction for genotyping to ensure an accurate assessment of *Stra6-/-; Stra6.2-/-* embryo survival.

Stra6-/-; Stra6.2-/- embryos were not observed in their expected ratio at E8.5 from plugs from either *Stra6 +/-; Stra6.2-/-* or *Stra6+/-; Stra6.2+/-* dams (Table 5.8). An individual *Stra6-/-; Stra6.2-/-* embryo was also observed at E8.5 (Figure 5.6 E) and the development of this embryo appeared consistent with the development of other E8.5 embryos from the same litter with no gross morphological defects observed externally (Figure 5.6 C & D). The number of reabsorptions observed at this stage accounts for the loss of *Stra6-/-; Stra6.2-/-* embryos (Table 5.7) and it is therefore reasonable to assume that these reabsorptions represent the fate of most *Stra6-/-; Stra6.2-/-* embryos by E8.5.

A single *Stra6-/-; Stra6.2-/-* embryo was observed at E9.5, significantly less than the expected number of *Stra6-/-; Stra6.2-/-* embryos from these matings (Table 5.7). The genotype of the dam, either *Stra6 +/-; Stra6.2-/-* or *Stra6+/-; Stra6.2+/-*, had no affect on the presence or absence of *Stra6-/-; Stra6.2-/-* indicating that maternal

genotype did not contribute to the survival of these embryos. The *Stra6-/-; Stra6.2-/-* embryo observed at E9.5 was not fully turned (Figure 5.6 G & H) and was more akin to a wildtype E8.5-9.0 embryo (Figure 5.6 D). The head and therefore brain appear under-developed compared to a *Stra6+/-; Stra6.2-/-* embryo of the same gestational age (Figure 5.6 F) and although the heart was present (Figure 5.6 G & H) it was also more consistent with an embryo of E8.5-9.0. The optic pit appears to be specified and present (Figure 5.6 G & H) although its development appears similar to that at E8.5-9.0. The *Stra6-/-; Stra6.2-/-* E9.5 embryos was also considerably smaller than other embryos (Figure 5.6 G & H) from the same litter consistent with a stalling in development between E8.5-9.0.

Stra6-/-; Stra6.2-/- embryos were never observed at E12.5 (Figure 5.7 B) and the number of reabsorbed embryos did not account for the missing *Stra6-/-; Stra6.2-/-* embryos (Table 5.7). *Stra6-/-; Stra6.2-/-* embryos appear to be promptly reabsorbed upon death between E7.5-E8.5 and most are completely removed from the uterus by E12.5. The presence of *Stra6-/-; Stra6.2-/-* embryos at E7.5 (Figure 5.7 A) and the number of reabsorptions noted at E8.5 indicate that loss of *Stra6* and *Stra6.2* severely limits viability at some point between E7.5 and E8.5 resulting in death of these embryos. Survival of a few embryos indicates that some embryos are able to overcome this block to development after E7.5 and continue development until approximately E8.5 and to survive until E9.5 but subsequently these embryos are also lost (Figure 5.7 C).

Stra6; Stra6.2	E7.5		E8.5		E9.5		E12.5	
	Obs	Exp	Obs	Exp ☆	Obs	Exp ☆	Obs	Exp ☆
++;- -	0	1.5	0	1.75	2	5.625	4	4.25
++;+ -	-	-	-	-	2	1.375		
+-;- -	3	3	12	8.25	17	12.25	13	8.5
- - ; + -	-	-	0	4.75	2	2.375	-	-
+ - ; + -	-	-	6	4.75	6	3.75	-	-
- -; - -	2	1.5	1	6.5	1	6.625	0	4.25
Reabsorbed	1	-	7	-	3	-	0	-

Table 5.7: *Stra6-/-;Stra6.2-/-* embryos are observed in the expected genetic ratio at E7.5 but are lost progressively through development before E12.5.

No significant difference in the number of *Stra6-/-;Stra6.2-/-* embryos between the expected and observed values was seen at E7.5 (P=0.4066, Chi-square test). A significant difference in the number of *Stra6-/-;Stra6.2-/-* embryos between the expected and observed values was observed at E8.5 and E9.5. The number of reabsorptions at E8.5 (P=0.0038, Chi-square test) and E9.5 (P=0.0471, Chi-square test) may account for the lost *Stra6-/-;Stra6.2-/-* embryos. No *Stra6-/-;Stra6.2-/-* embryos were observed by E12.5 (P=0.0360, Chi-square test). Star indicates significant deviations from the expected ratio.

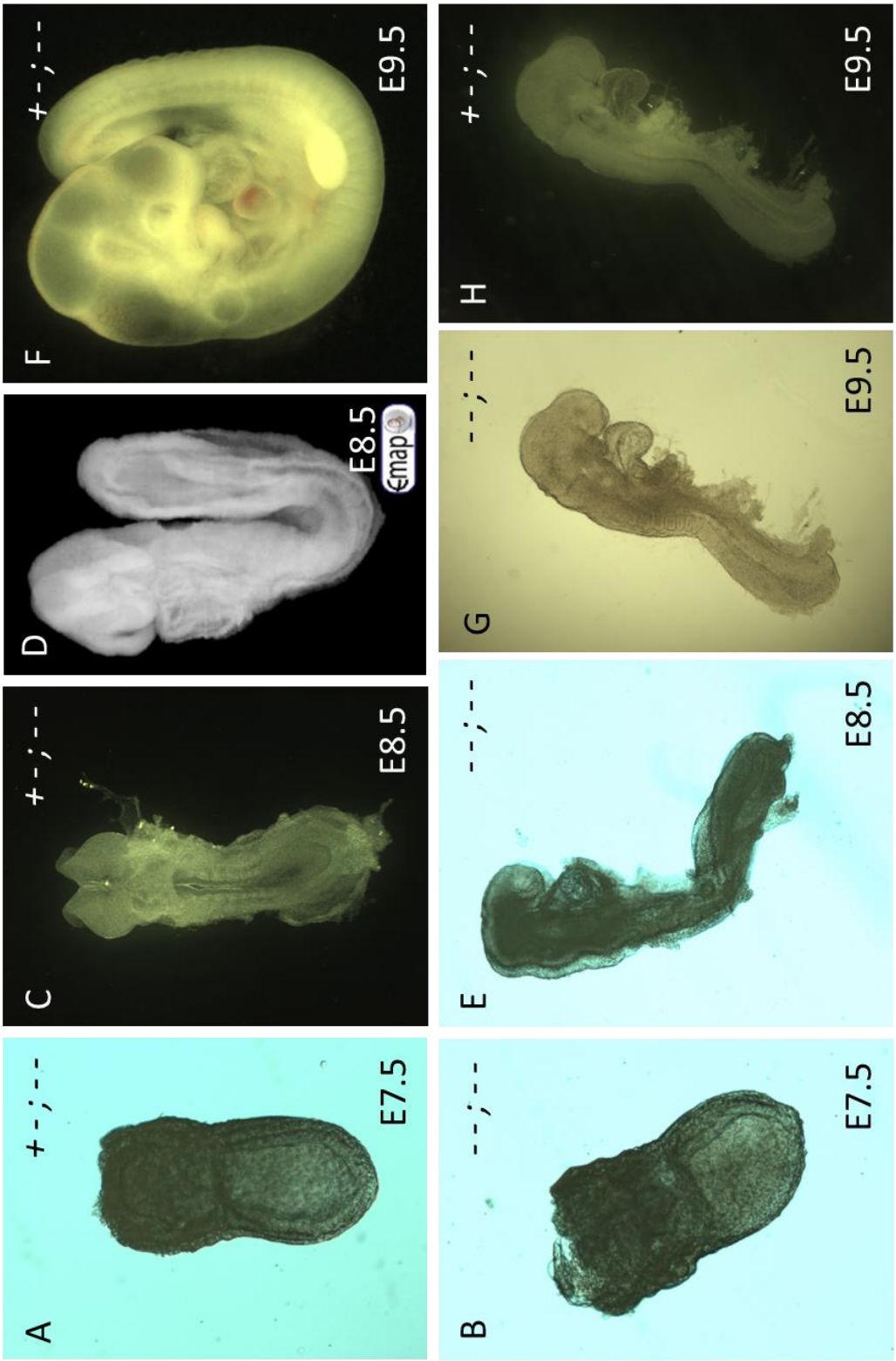
A
+-;--
E7.5
B
--;--
E7.5
C
+-;--
E8.5
D
E8.5
emap
E
--;--
E8.5
F
+-;--
E9.5
G
--;--
E9.5
H
+-;--
E9.5

Figure 5.6: *Stra6-/-;Stra6.2-/-* embryos show defects in embryonic development.

*Stra6+/-;Stra6.2-/- (*A) and *Stra6-/-;Stra6.2-/-* (B) are indistinguishable at E7.5. Dorsal view of *Stra6+/-;Stra6.2-/-* embryo at E8.5 (C) and a lateral view of an E8.5 embryo from EMAP (D) compared to a *Stra6-/-;Stra6.2-/-* E8.5 embryo (E) does not highlight any major difference in morphology at this stage. EMAP image included to show a lateral view due to lack of images of the lateral view of an E8.5 *Stra6+/-;Stra6.2-/-* embryo. *Stra6+/-;Stra6.2-/-* embryo at E9.5 (F) is fully turned; however *Stra6-/-;Stra6.2-/-* embryo (G & H) is unturned and appears developmentally retarded. G & H show the same embryo under differential illumination in order to highlight aspects of morphology.

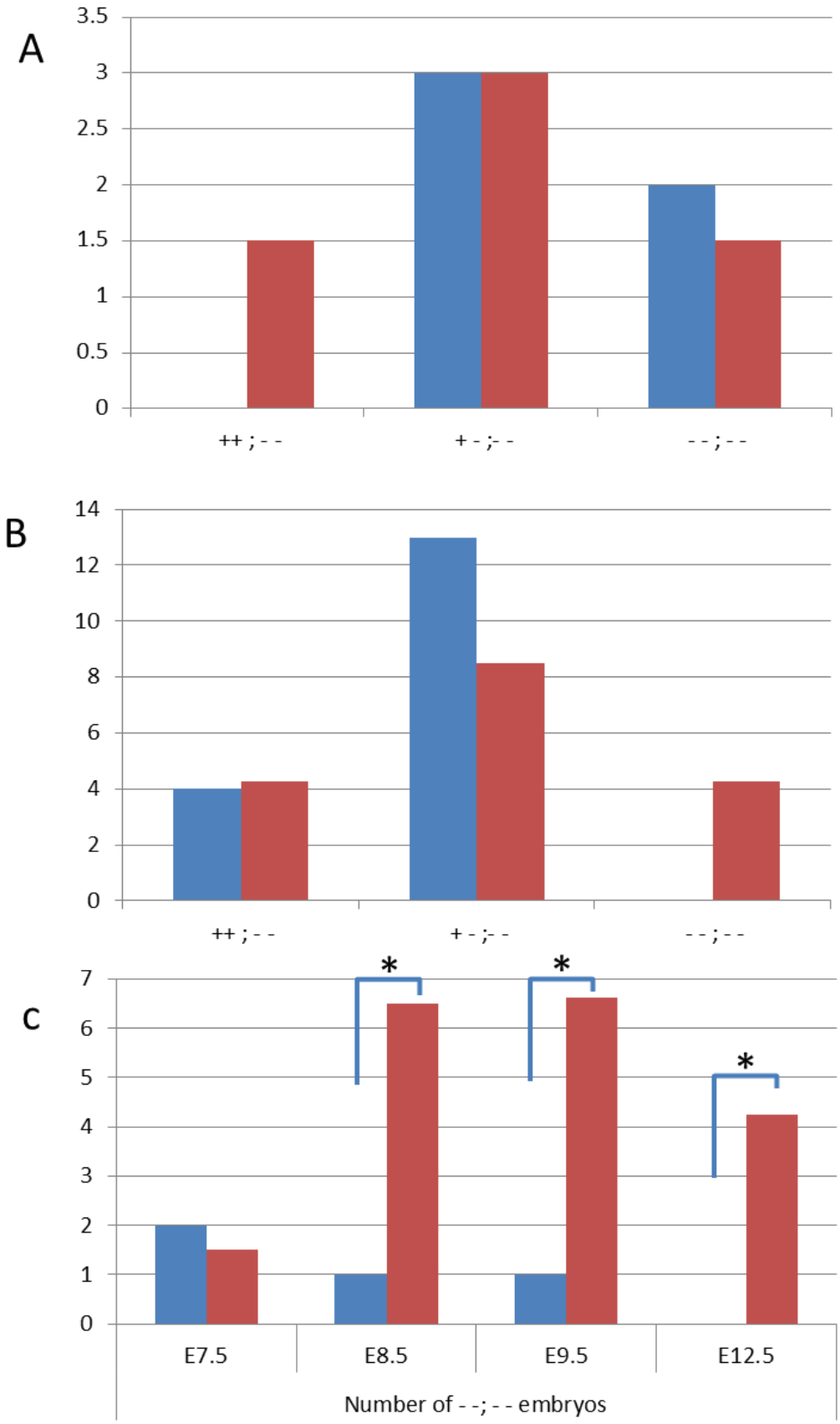
A
3.5
3
2.5
2
1.5
1
0.5
0
++ ; - -
+ - ; - -
- - ; - -
B
14
12
10
8
6
4
2
0
++ ; - -
+ - ; - -
- - ; - -
C
7
6
5
4
3
2
1
0
*
*
*
E7.5
E8.5
E9.5
E12.5
Number of - -; - - embryos

Figure 5.7: *Stra6-/-;Stra6.2-/-* animals are lost after E7.5.

The observed (blue) and expected (red) number of embryos for each genotype is graphical represented at E7.5 (A) and E12.5 (B). The observed (blue) and expected (red) number of *Stra6-/-;Stra6.2-/-* embryos is graphically represented at E7.5, E8.5, E9.5 and E12.5 (C) to highlight the loss of these embryos after E7.5. Asterisk indicates significant loss of *Stra6-/-;Stra6.2-/-* embryos.

5.5 Discussion

The recessive Matthew-Wood syndrome is the result of mutations within *STRA6* in humans (Pasutto 2007). The *Stra6-/-* mouse, however, does not represent a model of the human condition with no overt defects observed in the eye, heart, lung or diaphragm. In mouse, and other mammals, a paralogue of *Stra6* was noted and named *Stra6.2*. However, this paralogue in human has become split across its resident chromosome (as discussed in Chapter 4) and is therefore no likely to be entirely functional.

The differences in gene complement between mouse (and other mammals) and human may explain the disparity in phenotype. *Stra6.2-/-* animals were therefore investigated in order to assess possible interaction between *Stra6* and *Stra6.2* in supporting development in the mouse or the possibility that *Stra6.2-/-* may represent a model of Matthew-Wood syndrome. *Stra6.2-/-* animals having no developmental phenotypes even when born to *Stra6.2-/-* dams fed a retinoid-free diet during pregnancy and are therefore not a model of Matthew-Wood syndrome. *Stra6+/-;Stra6.2-/-* animals which are viable, fertile and have normal vision indicating development and adult visual and reproductive function can be maintained by only one copy of *Stra6*. However, *Stra6.2* in addition appearing dispensable for normal development to a degree in the presence of *Stra6*, also appears to be less able to support development in the absence of *Stra6*. *Stra6-/-;Stra6.2+/-* animals are variable in their viability and development, with a reduced number of these animals observed at genotyping and an increased incidence of death around weaning in these animals. Some animals were runted compared to littermates and appeared to have smaller eyes when compared to them, although vision and fertility were normal. Therefore it can be concluded that *Stra6.2*, although able in some cases to support normal development, is not equal to *Stra6* and may perform a similar or complementary role not as effectively as *Stra6*. *Stra6-/-; Stra6.2-/-* animals, however, not viable and are lost early in development between E7.5 and E8.5 in most cases with no *Stra6-/-; Stra6.2-/-* embryos surviving to E12.5. *Stra6* and *Stra6.2* are therefore likely to be redundant with loss of both genes incompatible with normal development and life but with a single copy of either able to support normal development. If *Stra6* and *Stra6.2* were to be functionally independently, the *Stra6-/-*

; Stra6.2-/- animal should be viable as *Stra6-/-* and *Stra6.2-/-* animals are individually viable.

Stra6-/-; Stra6.2-/- mice could be considered to be the most appropriate model for Matthew-Wood syndrome with a loss of all *Stra6*-like genes in both organisms. However, Matthew-Wood patients survive until birth (Pasutto 2007), and in some cases into adulthood (Chassainq 2009), in contrast to the early embryonic lethality observed in *Stra6-/-; Stra6.2-/-* embryos. The disruption of the *STRA6.2* gene in humans may not result in complete loss of STRA6.2 function and it may be able to support development to the postnatal stages. *Stra6-/-; Stra6.2+/-* animals may therefore hold the key to a model for Matthew-Wood syndrome with complete loss of *Stra6* in a background of reduced *Stra6.2* function. *Stra6-/-; Stra6.2+/-* animals appear to have a high mortality rate (2/4 died at weaning) and eye defects observed in one animal. The dietary provision of retinoids from standard mouse chow is high and therefore this may be supporting development and masking the possible Matthew-Wood type phenotype in *Stra6-/-; Stra6.2+/-* animals born to dams fed this retinoid-rich diet. The variability of the Matthew-Wood phenotype severity in patients could also be attributed to a similar mechanism by which sufficient maternal dietary retinoid provision may affect the phenotype of offspring. Evidence for this can be found in the family described by Chassainq *et al* (2009) in which the same mutational profile resulted in two surviving adult males with Matthew-Wood syndrome and a female infant who died within hours of birth. The apparent difference in phenotypic penetrance, even in the same mutational profile, suggests interaction with environmental factors, such as dietary retinoid content.

The interaction between *Stra6* and *Stra6.2* can be considered surprising due to the seeming lack of overlap between the expression domains of both genes during development. *Stra6* is expressed from E7.5 in the headfold mesoderm and is later observed in the prospective brain, eye, gut and the somites. In contrast, expression of *Stra6.2* cannot be observed before E9.5 and is primarily restricted to the posterior tail-region with later expression further observed within the somite, where it presumably overlaps with *Stra6* expression, and within the umbilicus. *Stra6.2* may be expressed at low levels within various tissues which also express *Stra6* as

published expression data of *Stra6* was collected through the use of radioactive *in situ* hybridisation with probes labelled with [^{35}S]-CTP and therefore is more sensitive than the methods used in this thesis. *Stra6.2* may also be able to compensate *Stra6*, despite being expressed in exclusive domains, through a non-cell autonomous effect perhaps relating to retinoid production.

The expression domains of *Stra6.2* appear to be greatly restricted compared to those of *Stra6* during development of the mouse, with only the posterior tail region, somites and umbilicus appearing to express *Stra6.2*. These differences in expression domains correlate with the phenotypes observed in knockout animals for each gene. *Stra6-/-* and *Stra6.2-/-* animals both show no discernible phenotypes under normal dietary retinoid provision. *Stra6.2-/-* offspring of *Stra6.2-/-* dams fed a retinoid-deficient diet during pregnancy also show no developmental or postnatal phenotypes. However, *Stra6-/-* offspring of *Stra6-/-* dams fed a retinoid-free diet during pregnancy demonstrate developmental eye defects correlating with the known expression of *Stra6* in the RPE and periocular mesenchyme of the developing eye. The expression of *Stra6.2* in later development and postnatally is not known and therefore the function of *Stra6.2* may be in these periods, perhaps in the provision of retinoids for the maintenance of adult tissues. Investigation of the expression of *Stra6.2* in late development and in adult organs, especially the eye and reproductive organs known to require retinoid provision for function and maintenance, may be enlightening.

Stra6-/-; Stra6.2-/- embryos are lost early in post-implantation development between E7.5 and E8.5. Some *Stra6-/-; Stra6.2-/-* embryos survive until E8.5-9.5 with some defects observed in the embryo at E9.5, such that the embryo had not turned. This is consistent with the phenotype of *Raldh2-/-* embryos, in which embryos never turn and are curved dorsally with an enlarged heart (Niederreither 1999). *Raldh2-/-* embryos die by E10.5 due to heart defects associated with defects in the development of the secondary heart field (Niederreither 2001). The rare *Stra6-/-; Stra6.2-/-* embryo observed at E9.5 appeared to be similar to *Raldh2-/-* embryos indicating that *Stra6* and *Stra6.2* are required to provide retinoids for the synthesis of RA later in development. However, an additional earlier role for the *Stra6* and *Stra6.2* seems

likely due the loss of *Stra6-/-; Stra6.2-/-* embryos prior to E8.5 in most cases compared to the survival of many *Raldh2-/-* embryos to E10.5.

The death of most *Stra6-/-; Stra6.2-/-* embryos between E7.5-8.5 highlights either heart or placental defects as the likely cause as this time in development is important in the development of both of these essential and interdependent organs. The placenta at this time (E8.0-8.5) undergoes chorioallantoic fusion in which the choronic epithelium contacts the allantois, arising from the mesoderm of the posterior of the embryo. This fusion results in the formation of folds in the chorion which mark the site of formation of the feto-placental blood vessels from the allantois (Rossant 2001). The formation of the trophoblast giant cells has been shown to be stimulated by retinoic acid (Yan 2001) and the formation of the chorion is linked to the development of the trophoblast giant cells (Rossant 2001). *Stra6-/-; Stra6.2-/-* embryos could be lost due to defects in the formation of the blood supply of the placenta resulting in death of the embryo as it is starved of oxygen and nutrients required for viability and development.

Heart defects could also be the cause of the early loss of *Stra6-/-; Stra6.2-/-* embryos as the heart is essential for normal development and in sustaining the embryo with other organs and tissues are generally dispensable until the later embryonic or the early post-natal period. The timing of embryonic death in *Stra6-/-; Stra6.2-/-* embryos could indicate a defect in heart specification (Conway 2003) and this is contemporary with the formation of the primordial heart and vascular system at E7.5 (Kaufman 1981) and the initiation of RA-synthesis within the embryo (Rossant 1991). Defects within the heart are also observed in Matthew-Wood patients although these defects allow the continued development of the embryo to birth.

5.6 Further work

Stra6-/-;Stra6.2+/- animals may hold the key to a model for Matthew-Wood syndrome. *Stra6-/-;Stra6.2+/-* animals are not observed in the expected number and some animals also died at weaning or were runted compared to littermates. One *Stra6-/-;Stra6.2+/-* animal which died around the time of weaning was found to have fused eyelids and a small volume of disorganised ocular tissue within the orbits. The variability of the developmental outcome in these animals may be resolved by feeding their dams a retinoid-free diet during pregnancy, initially from plug through to birth. The loss of retinoids throughout the whole pregnancy may result in the loss of all *Stra6-/-;Stra6.2+/-* pups and therefore smaller windows of treatment could be used if this proved to be the case. The birth of pups from such an experiment would need to be closely monitored as the pups would be likely to experience respiratory distress at birth if they did prove to be a model of Matthew-Wood syndrome. A model of Matthew-Wood would allow investigation of the development of the affected organ systems both anatomically through serial sectioning and also through marker analysis for important genes in the development of these organs. This approach may elicit the mechanism whereby the loss of *Stra6* in human results in Mathew-Wood syndrome and if this is solely due to a reduction in retinoid provision for the synthesis of RA in the embryo.

Stra6-/-;Stra6.2-/- embryos are lost early in post-implantation development between approximately E7.5 and E8.5, although a few embryos survive to E9.5. The timing of this embryonic lethality suggests a defect in heart or placental development and therefore it would be fortuitous to investigate via *in situ* hybridisation the expression of markers of placental and heart development in order to discern a possible reason and mechanism behind the early embryonic lethality in these animals.

The possibility of heart specification defects could be investigated in E7.5 *Stra6-/-; Stra6.2-/-* embryos by histological serial sectioning through entire embryos to highlight any anatomical abnormalities in the development of the heart (Conway 2003). Investigation of the expression of early markers of heart development via *in situ* hybridisation may also highlight the possible mechanism for any anatomical changes observed. *Nkx2.5* is a master regulator of cardiac specification (Tanaka

1999) and one of the earliest markers of the cardiac lineage therefore investigation of its expression in *Stra6-/-; Stra6.2-/-* embryos may highlights any defects. Other useful markers may be *dHAND* (Yamagishi 2001) and *eHAND* (Biben 1997) which interact with *Nkx2.5*, and *FGF4* and *Bmp2* both genes able to induce cardiac formation (Conway 2003). Inhibitory signals to cardiac development, such as *Wnt1* and *Wnt3a*, are also received from the neural tube therefore, the expression of these genes in *Stra6-/-; Stra6.2-/-* embryos should also be investigated (Conway 2003).

Defects in placental formation are another possibility for the loss of *Stra6-/-; Stra6.2-/-* embryos and therefore as for the investigation of heart defects serial sections through the embryo and the extra-embryonic tissues may provide insight as to the cause of the reduced viability of *Stra6-/-; Stra6.2-/-* embryos. Retinoic acid has been implicated in the differentiation of the trophoblast giant cells and therefore investigation of markers of this cell type may be fortuitous in understanding the role for *Stra6* and *Stra6.2* in this process. The investigation of the expression of *Hand1* and *Mdfi* may be enlightening for this purpose (Rossant 2001). The timing of the death of *Stra6-/-; Stra6.2-/-* embryos is contemporary with the initiation of chorioallantoic fusion and therefore investigation of markers of this process, such as *Bmp5*, *Bmp7* and *Dmnt1*, may indicate if any defects in this process are observed (Rossant 2001).

The early loss of *Stra6-/-; Stra6.2-/-* embryos, perhaps due to heart or placental defects, may mask the later roles and functions of *Stra6* and *Stra6.2*. Treatment of the mother with RA during early pregnancy may allow development of the *Stra6-/-; Stra6.2-/-* embryos to overcome the early block and continue past E8.5. A similar approach has been reported in order to investigate later roles for *Raldh2* (Mic 2002) and may allow more *Stra6-/-; Stra6.2-/-* embryos to make it to E9.5 in order to investigate the later developmental requirement for *Stra6* and *Stra6.2*. Additionally this approach would investigate if the only requirement for *Stra6* and *Stra6.2* is to facilitate the provision of retinoids for the synthesis of RA. The nature of the *Stra6.2* knockout construct also allows for creation of conditional *Stra6.2* alleles. These could be combined with either cell-type specific or Tamoxifen-inducible Cre-expressing alleles in order to cell-type specifically or temporally remove *Stra6.2* in a

Stra6-null background. This would allow early development to proceed normally before removal of *Stra6.2* at the appropriate time or place.

Chapter Six

Summary and final conclusions.

Matthew-Wood syndrome is a severe human birth defect condition resulting in death within the first months of life in most cases. Homozygous and compound heterozygous mutations in *STRA6* cause clinical anophthalmia, pulmonary hypoplasia, diaphragmatic hernia and cardiac defects in Matthew-Wood patients. STRA6 is known to function both as a transporter for retinol bound to RBP4, thereby forming part of the retinoid pathway, and as a transducer of signalling resulting in the phosphorylation of the insulin receptor in response to RBP-bound retinol. The mechanism by which mutations in *STRA6* result in Matthew-Wood syndrome is unknown, although the defects observed and the known functions of STRA6 suggest defects in the retinoid pathway, and therefore an animal model of Matthew-Wood syndrome was desired.

Stra6-/- mice, although being the logical genetic model of Matthew-Wood syndrome, do not replicate any of the phenotypic signs of the condition and are normal, viable and fertile. Published knockouts for some retinoid pathway genes are also normal when born to dams fed a retinoid-sufficient diet, however, when born to dams fed a retinoid-free diet during pregnancy develop abnormally. *Stra6-/-* dams were therefore fed a retinoid-free diet during pregnancy from plug discovery (E0.5) till birth. The *Stra6-/-* offspring of these dams was microphthalmic and their visual acuity was diminished compared to their *Stra6+/-* littermates. Persistent hyperplastic primary vitreous (PHPV) was observed in all *Stra6-/-* eyes and cataract was also observed in 27% of *Stra6-/-* eyes. Although *Stra6-/-* mice born to dams fed a retinoid-free diet do not represent a model of Matthew-Wood syndrome, they represent a model of isolated microphthalmia caused by mutations in *STRA6* in a consanguineous Irish-traveller family. The spleen of male *Stra6-/-* animals was abnormal in terms of shape and weighed less than that of male *Stra6+/-* littermates. Despite some changes histologically to the distribution of white and red pulp in the spleen, no significant defects could be observed by FACS analysis in the distribution of B-cells and T-cells, erythrocyte differentiation or CD8+/CD4+ T-cell profile.

The disparity between *Stra6-/-* mice and Matthew-Wood patients could be the result of functional redundancy in the mouse between *Stra6* and its paralogue, *Stra6.2*. *Stra6.2* was identified through a Blast search against the mouse genome and was

found to share 18% identity with *Stra6*. Although both *Stra6* and *Stra6.2* are present within the mouse, and most other vertebrate, genomes; the great apes, including humans, differ in this respect. The human orthologue of *Stra6.2* has become split across its native chromosome resulting in a both a pseudogene, representing the 5' region and a functional, yet significantly shorter, 3' region.

stra6.2 was found to have a developmental function in the zebrafish with *stra6.2* morphants having defects in axial extension, eye development, somite formation and jaw morphology. These defects were found to be caused by an increase in retinoic acid synthesis resulting in an increase in RA-responsive gene expression and this mechanism was Rbp4-dependent. Morpholinos to *stra6* and *stra6.2* were found to act synergistically suggesting that *stra6.2* was also likely to function within the retinoid-pathway, perhaps also as an Rbp4-dependent retinoid transporter. Morpholino knockdown of either *stra6* or *stra6.2* in the zebrafish results in developmental defects, although this is not the case in mouse with both *Stra6-/-* and *Stra6.2-/-* animals developing normally when born to dams fed a retinoid-rich diet during pregnancy. Nutrient provision to the developing embryo is significantly divergent between fish and mammals, with the fish provided with a nutrient store in the contents of its yolk and regulated only by the embryo itself, whereas the mammalian female regulates the provision of nutrients to her developing offspring through the placenta. The control of provision of retinoids by the maternal bloodstream across the placenta may allow greater compensation for fluctuations and defects in the retinoid metabolism of the developing mammalian embryo allowing normal development despite the loss of important gene functions.

Stra6.2-/- mice show no developmental defects even when born to *Stra6.2-/-* dams fed a retinoid-free diet throughout pregnancy. *Stra6* appears to be 'dominant' in developmental function compared to *Stra6.2* in the mouse. The lack of any phenotype associated with the loss of *Stra6.2*, even under conditions of retinoid-stress, and the higher mortality rate observed in *Stra6-/-;Stra6.2+/-* compared to *Stra6+/-;Stra6.2-/-* indicate that the requirement for *Stra6* is probably greater and this also supported by the loss of a part of *STRA6.2* in humans to no detrimental effect in the presence of *STRA6*. However, *Stra6.2* seems likely to have a

contributory role to play in the mouse and this redundancy is typical of the retinoid pathway with many functional steps in the pathway controlled by gene families with overlapping functions, such as *Raldh*1, 2 & 3 and *RAR*α, β & γ.

Stra6-/-;Stra6.2-/- animals could be thought of to be the ideal animal model of Matthew-Wood syndrome as these replicate the perceived total loss of *STRA6*-like gene function observed in human patients. *Stra6-/-;Stra6.2-/-* animals, however, represent an earlier and much more severe developmental phenotype resulting in death in most cases by E8.5 and survival of no *Stra6-/-;Stra6.2-/-* by E12.5. Matthew-Wood patients may reserve minimal functionality of STRA6 allowing development to proceed, although previous work suggests that all mutations resulting in Matthew-Woods result in severe compromisation of the retinol-transport function of STRA6. The remaining transcribed portion of *STRA6.2* in human may also function to allow development to the post-natal stages in most cases.

The loss of *Stra6-/-;Stra6.2-/-* embryos early in development, between E7.5 and E8.5 in most cases, highlights a fundamental requirement for retinol provision very early in development most likely in the formation of either the heart or placenta. *Stra6-/-;Stra6.2-/-* embryos die earlier than *Raldh2-/-* embryos, which survive to E10.5, indicating that retinol may have early developmental roles independent of being a precursor for retinoic acid synthesis. This observation may be interesting to investigate further in the future as the field is generally focussed on retinoic acid as the orchestrator of the developmental function of retinoids. Investigation into the role of retinol as an effector of development and the other future work avenues discussed in each of the chapters will hopefully be pursued by a future PhD student.

Chapter Seven

References

Abu-Abed, S., Dolle, P., Metzger, D., Beckett, B., Chambon, P., & Petkovich, M. (2001). "The retinoic acid-metabolizing enzyme, CYP26A1, is essential for normal hindbrain patterning, vertebral identity and development of posterior structures." Genes & Development **12**: 226-240.

Albalat, R. (2009). "The retinoic acid machinery in invertebrates: Ancestral elements and vertebrate innovations." Molecular & Cellular Endocrinology **313**: 23-35.

Albalat, R. C., C. (2009). "Identification of Aldh1a, Cyp26 and RAR orthologs in protosomes pushes back the retinoic acid genetic machinery in evolutionary time to the bilaterian ancestor." Chemico-Biological Interactions **178**(1-3): 188-196.

Alexa, K., Choe, S-K., Hirsch, N., Etheridge, L., Laver, E., & Sagerstrom, C.G. (2009). "Maternal and zygotic aldh1a2 activity is required for pancreas development in zebrafish." PLoS One **4**(12): e8261.

Alexandre, D., Clarke, J.D.W., Oxotoby, E., Yan, Y-.L., Jowett, T., & Holder, N. (1996). "Ectopic expression of Hoxa-1 in the zebrafish alters the fate of the mandibular arch neural crest and phenocopies a retinoic acid-induced phenotype." Development **122**: 735-745.

Alfano, G., Conte, I., Caramico, T., Avelino, R., Arno, B., Pizzo, M.T., Tantimoto, N., Beck, S.C., Huber, G., Dolle, P., Seeliger, M.W., & Banfi, S. (2011). "Vax2 regulates retinoic acid distribution and cone opsin expression in the vertebrate eye." Development **138**: 261-271.

Ali-Khan, S. E., & Hales, B.F. (2006). "Novel retinoid targets in the mouse limb during organogenesis." Toxicological Sciences **94**(1): 139-152.

Altschul, S. F., Madden, T.L., Schaffer, A.A., Zhang, J., Zhang, Z., Miller, W., & Lipman, D.J. (1997). "Gapped BLAST and PSI-BLAST: a new generation of protein database search programs." Nucleic Acids Research **25**: 3389-3402.

Ambrosio, D. N. D., Clugston, R.D., & Blaner, W.S. (2011). "Vitamin A metabolism: An update. ." Nutrients **3**: 63-103.

Bagavandoss, P., & Midgley, A.R. (1987). "Lack of difference between retinoic acid and retinol in stimulating progesterone production by luteinizing granulosa cells in vitro." Endocrinology **121**(1): 420-428.

Barbieri, A. M., Broccoli, V., Bovolenta, P., Alfano, G., Marchitiello, A., Mocchetti, C., Crippa, L., Bulfona, A., Marigo, V., Ballabio, A., & Banfi, S. (2002). "Vax2 inactivation in mouse determines alteration of the eye dorsal-ventral axis, misrouting of the optic fibres and eye coloboma." Development **129**: 805-813.

Batten, M. L., Imanishi, Y., Maeda, T., Tu, D.C., Moise, A.R., Bronson, D., Possin, D., van Gelder, R.N., Baehr, W., & Palczewski, K. (2004). "Lecithin-retinol

acyltransferase is essential for accumulation of all-trans-retinyl esters in the eye and in the liver." The Journal of Biological Chemistry **279**(11): 10422-10432.

Begemann, G., Marx, M., Mebus, K., Meyer, A., & Bastmeyer, M. (2004). "Beyond the neckless phenotype: influence of reduced retinoic signalling on motor neuron development in the zebrafish hindbrain." Developmental Biology **271**(1): 119-129.

Berry, D. C., Jin, H., Majumdar, A., & Noy, N. (2011). "Signalling by vitamin A and retinol-binding protein regulates gene expression to inhibt insulin responses." PNAS **108**(11): 4340-4345.

Beurskens, L. W. J. E., Tibboel, D., Lindemans, J., Duvekot, J.J., Cohen-Overbeek, T.E., Veenma, D.C.M., Klein, A., Greer, J.J., & Steegers-Theunissen, R.P.M. (2010). "Retinol status of newborn infants is associated with congenital diaphragmatic hernia." Pediatrics **126**: 712-720.

Biben, C., & Harvey, R.P. (1997). "Homeodomain factor Nkx2-5 controls left/right asymmetric expression of bHLH gene eHand during murine heart development." Genes & Development **11**: 1357-1369.

Birney, E., Clamp, M., & Durbin, R. (2004). "GeneWise and Genomewise." Genome Research **14**: 988-995.

Boeve, M. H., van der Linde-Sipman, T., & Stades, F.C. (1988). "Early morphogenesis of persistent hyperplastic tunica vasculosa lentis and primary vitreous." Investigative Opthalmology & Visual Science **29**(7): 1076-1087.

Bouillet, P., Oulad-Abdelghani, M., Vicaire, S., Garnier, J-.M., Schuhbaur, B., Dolle, P., & Chambon, P. (1995). "Efficient cloning of cDNAs of retinoic acid-responsive genes in P19 embryonal carcinoma cells and characterization of a novel mouse gene, Stra1 (Mouse LERK-2/Elpg2)." Developmental Biology **170**: 420-433.

Bouillet, P., Sapin, V., Chazaud, C., Messaddeq, N., Decimo, D., Dolle, P., & Chambon, P. (1997). "Developmental expression pattern of Stra6, a retinoic acid-responsive gene encoding a new type of membrane protein." Mechanisms of Development **63**: 173-186.

Brand, N., Petkovich, M., Krust, A., Chambon, P., De The, H., Marchio, A., Tiollais, P., Dejean, A. (1988). "Identification of a second human retinoic acid receptor." Nature **332**: 850-853.

Casey, J., Kawaguchi, R., Morrissey, M., Sun, H., McGettigan, P., Nielsen, J.E., Conroy, J., Regan, R., Keny, E., Cormican, P., Morris, D.W., Tormey, P., Chronin, M.N., Kennedy, B.N., Lynch, S.A., Green, A., & Ennis, S. (2011). "First implication of STRA6 mutations in isolated anophthalmia, microphthalmia and coloboma: a new dimension to the STRA6 phenotype." Human Mutation **EPub**.

Chambon, P. (1996). "A decade of molecular biology of retinoic acid receptors." The FASEB Journal **10**(9): 940-954.

Chang, B.-E., Blader, P., Fischer, N., Ingham, P.W., & Strahle, U. (1997). "Axial (HNF3b) and retinoic acid receptors are regulators of the zebrafish sonic hedgehog promoter." The EMBO Journal **16**: 3955-3964.

Chassainq, N., Golzio, C., Odent, S., Lequeux, L., Vigouroux, A., Martinovic-Bouriel, J., Tiziano, F.D., Masini, L., Piro, F., Maragliano, G., Delezoide, A.L., Attie-Biatch, T., Manouvier-Hanu, S., Etchevers, H.C., & Calvas, P. (2009). "Phenotypic spectrum of STRA6 mutations: from Matthew-Wood syndrome to non-lethal anophthalmia." Human Mutation **30**(5): 673-681.

Chiba, H., Muramatsu, M., Nomoto, A. & Kato, H. (1994). "Two human homologues of Saccharomyces cerevisiae SWI2/SNF2 and Drosophila brahma are transcriptional coactivators cooperating with the estrogen receptor and the retinoic acid receptor." Nucleic Acids Research **22**(10): 1815-1820.

Chitayat, D., Sroka, H., Keating, S., Colby, R.S., Ryan, G., Toi, A., Blaser, S., Viero, S., Devisme, L., Boute-Benejean, O., Manouvrier-Hanu, S., Mortier, G., Loeys, B., Rauch, A., & Bitoun, P. (2007). "The PDAC syndrome (pulmonary hypoplasia/agenesis, diaphragmatic hernia/eventration, anophthalmia/microphthalmia, and cardiac defect) (Spear syndrome, Matthew-Wood syndrome): Report of eight cases including a living child and further evidence for autosomal recessive inheritance." American Journal of Medical Genetics Part A **143A**: 1268-1281.

Conway, S. J., Kruzynska-Frejtag, A., Kneer, P.L., Machnicki, M., & Koushik, S.V. (2003). "What cardiovascular defect does my prenatal mouse mutant have, and why?" Genesis **35**: 1-21.

Crow, J. A., & Ong, D.E. (1985). "Cell-specific immunohistochemical localization of a cellular retinol-binding protein (type two) in the small intestine of rat." Proceedings of National Academy of Sciences **82**(14): 4707-4711.

Cunningham, T. J., Chatzi, C., Dandell, L.L., Trainor, P.A., & Duester, G. (2011). "Rdh10 mutants deficient in limb field retinoic acid signalling exhibt normal limb patterning but display interdigital webbing." Developmental Biology **240**(5): 1142-1150.

D'Ambrosio, D., Clugston, R.D., & Blaner, W.S. (2011). "Vitamin A Metabolism: An update." Nutrients **3**: 63-103.

Dehal, P. B., J.L. (2005). "Two rounds of whole genome duplication in the ancestral vertebrate." PLoS Biology **3**: 1700-1708.

Depew, M. J., Lufkin, T., & Rubenstein, J.L. (2002). "Specification of jaw subdivisions by Dlx genes." Science **298**: 381-385.

Dickman, E. D., Thaller, C., & Smith, S.M. (1997). "Temporally-regulated retinoic acid depletion produces specific neural crest, ocular and nervous system defects." Development **124**: 3111-3121.

Donner, A. L., & Maas, R.L. (2004). "Conservation and non-conservation of genetic pathways in eye specification." International Journal of Developmental Biology **48**: 743-753.

Draper, B. W., Morcos, P.A., & Kimmel, C.B. (2001). "Inhibition of zebrafish fgf8 pre-mRNA splicing with morpholino oligos: A quantifiable method for gene knockdown." Genesis **30**(3): 154-156.

Drummond, A. J., & Rambaut, A. (2007). "BEAST: Bayesian evolutionary analysis by sampling trees." BMC Evolutionary Biology **7**: 214.

Dupe, V., Matt, N., Garnier, J-.M., Chambon, P., Mark, M., & Ghyselinck, N.B. (2003). "A newborn lethal defect due to inactivation of retinaldehyde dehydrogenase type 3 is prevented by maternal retinoic acid treatment." PNAS **100**(24): 14036-14041.

Ellies, D. L., Langille, R.M., Martin, C.C., Akimenko, M-.A., & Ekker, M. (1997). "Specific craniofacial cartilage dysmorphogenesis coincides with a loss of dlx gene expression in retinoic acid-treated zebrafish embryos." Mechanisms of Development **61**(1-2): 23-36.

Fan, X., Molotkov, A., Manabe, S-.T., Donmoyer, C.M., Deltour, L., Foglio, M.H., Cuenca, A.E., Blaner, W.S., Lipton, S.A., & Duester, G. (2003). "Targeted disruption of Aldh1a1 (Raldh1) provides evidence for a complex mechanism of retinoic acid synthesis in the developing retina." Molecular and Cell Biology **23**(13): 4637-4648.

Farjo, K. M., Sato, T., Kaneko, S., Gotoh, O., Fujii-Kuriyama, Y., Oswawa, K., Kato, S., & Hamada, H. (1997). "Metabolic inactivation of retinoic acid by a novel P450 differentially expressed in developing mouse embryos." The EMBO Journal **16**: 4163-4173.

Fujii, H., Sato, T., Kaneko, S., Gotoh, O., Fujii-Kuriyama, Y., Osawa, K., Kato, S., & Hamada, H. (1997). "Metabolic inactivation of retinoic acid by a novel P450 differentially expressed in developing mouse embryos." The EMBO Journal **16**: 4163-4173.

Gagon, I., Duester, G., & Bhat, P.V. (2003). "Enzymatic characterization of recombinant mouse retinal dehydrogenase type 1." Biochemical Pharmacology **65**(10): 1685-1690.

Garen, A., Kauver, L., & Lepesant, J-.A. (1977). "Roles of ecdysone in Drosophila development." Proceedings of the National Academy of Sciences **74**(11): 5099-5103.

Ghyselinck, N. B., Bavik, C., Sapin, V., Mark, M., Bonnier, D., Hindelang, C., Dierich, A., Nilsson, C.B., Hakansson, H., Sauvant, P., Azais-Braesco, V., Frasson, M., Picaud, S., & Chambon, P. (1999). "Cellular retinol-binding protein 1 is essential for vitamin A homeostasis." The EMBO Journal **18**: 4903-4914.

Ghyselinck, N. B., Dupe, V., Dierich, A., Messaddeq, N., Garnier, J-.M., Rochette-Egly, C., Chambon, P., & Mark, M. (1997). "Role of retinoic acid receptor beta (RARB) during mouse development." International Journal of Developmental Biology **41**: 425-447.

Ghyselinck, N. B., Vernet, N., Dennefeld, C., Giese, N., Nau, H., Chambon, P., Viville, S., & Mark, M. (2006). "Retinoids and spermatogenesis: Lessons from mutant mice lacking the plasma retinol binding protein." Developmental Dynamics **235**: 1608-1622.

Giguere, V., Ong, E.S., Segui, P., & Evans, R.M. (1987). "Identification of a receptor for the morphogen retinoic acid." Nature **330**: 624-629.

Giovannucci, D. R., & Stephenson, R.S. (1999). "Identification and distribution of dietary precursors of the Drosophila visual pigment chromophore: analysis of carotenoids in wild type and ninaD mutants by HPLC." Vision Research **39**(2): 219-229.

Golzio, C., Martinovic-Bouriel, J., Thomas, S., Mougou-Zrelli, S., Grattagliano-Bessieres, B., Bonniere, M., Delahaye, S., Munnich, A., Encha-Razavi, F., Lyonnet, S., Vekemans, M., Attie-Biatch, T., & Etchevers, H.C. (2007). "Matthew-Wood syndrome is caused by truncating mutations in the retinol binding protein receptor gene STRA6." The American Journal of Human Genetics **80**(6): 1179-1187.

Gottesman, M. E., Quandro, L., & Blaner, W.S. (2001). "Studies of vitamin A metabolism in mouse model systems." BioEssays **23**: 409-419.

Gregg, R. G., Willer, G.B., Fadool, J.M., Dowling, J.E., & Link, B.A. (2003). "Positional cloning of the young mutation identifies an essential role for the Brahma chromatin remodelling complex in mediating retinal cell differentiation." Proceedings of National Academy of Sciences **100**(11): 6535-6540.

Hale, F. (1935). "The relation of vitamin A to the eye development in the pig." The American Society of Animal Production **1935**(1): 126-128.

Hall, B. L., & Thummel, C.S. (1998). "The RXR homolog ultraspiracle is an essential component of the Drosophila ecdysone receptor. ." Development **125**: 4709-4717.

Han, J., Li, L., Zhang, Z., Xiao, Y., Lin, J., & Li, Y. (2006) "PDGF-C participates in branchial arch morphogenesis and is down-regulated by retinoic acid." Toxicology Letters **166** (3): 248-254.

Harrison, E. H. (2005). "Mechanisms of digestion and absorption of dietary vitamin A." Annual Review of Nutrition **25**: 87-103.

Heller, J. (1975). "Interactions of the plasma retinol-binding protein with its receptor. Specific binding of bovine and human retinol-binding protein to pigment epithelium cells from bovine eyes." The Journal of Biological Chemistry **250**(10): 3613-3619.

Higgins, D. G., Thompson, J.D., & Gibson, T.J. (1996). "Using CLUSTAL for multiple sequence alignments." Methods in Enzymology **266**: 383-402.

Hornby, S. J., Gilbert, C.E., Rahi, J., Sil, A.K., Xiao, Y., Dandona, L., & Foster, A. (2000). "Regional variation in blindness in children due to microphthalmos, anophthalmos and coloboma." Ophthalmic Epidemiology **7**(2): 127-138.

Hornby, S. J., Ward, S.J., Gilbert, C.E., Dandona, L., Foster, A., & Jones, R.B. (2002). "Environmental risk factors in congenital malformation of the eye." Annals of Tropical Paediatrics **22**: 67-77.

Hu, P., Tian, M., Bao, J., Xing, G., Gu, X., Gao, X., Linney, E., & Zhao, Q. (2008). "Retinoid regulation of the zebrafish cyp26a1 promoter." Developmental Dynamics **237**(12): 3798-3808.

Huang, J. K., Jarjour, A.A., Qumesmar, B.N., Kerninon, C., Williams, A., Krezel, W., Kagechika, H., Bauer, J., Zhao, C., Evercooren, A.B., Chambon, P., Ffrench-Constant, C., & Franklin, R.J.M. (2011). "Retinoid X receptor gamma signalling accelerates CNS remyelination." Nature Neuroscience **14**: 45-53.

Humphrey, J. H., West, K.P., & Sommer, A. (1992). "Vitamin A deficiency and attributable mortality among under-5-year-olds." Bulletin of the World Organization **70**(2): 225-232.

Hussey, G. D., & klein, M. (1990). "A randomized, controlled trial of vitamin A in children with severe measles." The New England Journal of Medicine **323**: 160-164.

Iipenberg, A., Jeannin, E., Wahli, W., & Desvergne, B. (1997). "Polarity and specific sequence requirements of peroxisome proliferator-activated receptor (PPAR)/retinoid X receptor heterodimer binding to DNA." The Journal of Biological Chemistry **272**: 20108-20117.

Ikeda, S., Hawes, N.L., Chang, B., Avery, C.S., Smith, R.S., & Nishina, P.M. (1999). "Severe ocular abnormalities in C57BL/6 but not 129/Sv p53-deficient mice." Investigative Opthalmology & Visual Science **40**(8): 1874-1878.

Isken, A., Golczak, M., Oberhauser, V., Hunzelmann, S., Driever, W., Imanshi, Y., Palczewski, K., & von LIntig, J. (2008). "RBP4 disrupts vitamin A uptake homeostasis in the STRA6-deficient animal model for Matthew-Wood syndrome." Cell Metabolism **7**(5): 258-268.

Isken, A., Holzschuh, J., Lampert, J.M., Fischer, L., Oberhauser, V., Palczewski, K., & von Lintig, J. (2007). "Sequestration of retinyl esters is essential for retinoid signalling in the zebrafish embryo." Journal of Biological Chemistry **282**: 1141-1151.

Joly, J.-S., Joly, C., Schulte-Merker, S., Boulekbache, H., & Condamine, H. (1993). "The ventral and posterior expression of the zebrafish homeobox gene eve1 is perturbed in dorsalized and mutant embryos." Development **119**: 1261-1275.

Kalter, H., & Warkany, J. (1961). "Experimental production of congenital malformations in the strains of inbred mice by maternal treatment with hypervitaminosis." The American Journal of Pathology **38**(1): 1-21.

Kamelle, S., Sienko, A., & Benbrook, D.M. (2002). "Retinoids and steroids regulate menstrual phase histological features in human endometrial organotypic cultures." Reproductive Biology **78**(3): 596-602.

Kanai, M., Raz, A., & Goodman, D.S. (1968). "Retinol-binding protein: the transport protein for vitamin A in human plasma." The Journal of Clinical Investigation **47**: 2025-2043.

Kastner, P., Grondona, J.M., Mark, M., Gansmuller, A., LeMeur, M., Decimo, D., Vonesch, J-.L., Dolle, P., & Chambon, P. (1994). "Genetic analysis of the RXRa development function: Convergence of RXR and RAR signalling pathways in heart and eye morphogenesis." Cell **78**: 987-1003.

Kastner, P., Mark, M., Ghyselinck, N., Krezel, W., Dupe, V., Grondona, J.M., & Chambon, P. (1997). "Genetic evidence that the retinoid signal is transduced by heterodimeric RXR/RAR functional units during muse development." Development **124**: 313-326.

Kastner, P., Mark, M., Leid, M., Gansmuller, A., Chin, W., Grondona, J.M., Decimo, D., Krezel, W., Dierich, A., & Chambon, P. (1996). "Abnormal spermatogenesis in the RXRB mutant mice." Genes & Development **10**: 80-92.

Kasus-Jocobi, A., Ou, J., Birch, D.G., Locke, K.G., Shelton, J.M., Richardson, J.A., Murphy, A.J., Valenzuela, D.M., Yancopoulos, G.D., & Edwards, A.O. (2005). "Functional characterization of mouse RDH11 as a retinol dehydrogenase involved in dark adpatation in vivo." The Journal of Biological Chemistry **280**: 20413-20420.

Kaufman, M. H., & Navaratnam, V. (1981). "Early differentiation of the heart in mouse embryos." Journal of Anatomy **133**(2): 235-246.

Kawaguchi, R., Yu, J., Honda, J., Hu, J., Whitelegge, J., Ping, P., Wiita, P., Bok, D., & Sun, H. (2007). "A membrane receptor for retinol binding protein mediates cellular uptake of vitamin A." Science **315**: 820-825.

Kawaguchi, R., Yu, J., Ter-Stepanian, M., Zhong, M., Cheng, G., Yuan, Q., Jin, M., Travis, G.H., Ong, D., & Sun, H. (2011). "Receptor-mediated cellular uptake mechanism that couples to intracellular storage." ACS Chemical Biology **EPub**.

Kawaguchi, R., Yu, J., Wiita, P., Honda, J., & Sun, H. (2008). "An essential ligand-binding domain in the membrane receptor for retinol-binding protein revealed by large-scale mutagenesis and a human polymorphism." The Journal of Biological Chemistry **283**: 15160-15168.

Khaliq, S., Hameed, A., Ismail, M., Anwar, K., Leroy, B., Payne, A.M., Bhattacharaya, S.S., & Mehdi, S.Q. (2001). "Locus for autosomal recessive nonsyndromic persistent hyperplastic primary vitreous." Investigative Opthalmology & Visual Science **42**(10): 2225-2228.

Krezel, W., Dupe, V., Mark, M., Dierich, A., Kastner, P., & Chambon, P. (1996). "RARy null mice are apparently normal and compound $RXRa^{+/-}/RXRb^{-/-}/RXRy^{-/-}$ mutant mice are viable." Proceedings of National Academy of Sciences **93**: 9010-9014.

Krust, A., Kastner, P., Petkovich, M., Zelent, A., & Chambon, P. (1989). "A third human retinoic acid receptor, hRAR-gamma." PNAS **86**(14): 5310-5314.

Krzyzosiak, A., Szyszka-Niagolov, M., Wietrzych, M., Gobaille, S., Muramatsu, S-.I., & Krezel, W. (2010). "Retinoid X receptor gamma control of affective behaviours involves dopaminergic signalling in mice." Neuron **66**(6): 908-920.

Kumar, S., Tamura, K & Nei, M. (1994). "MEGA: Molecular Evolutionary Genetics Analysis software for microcomputers." Computer Applications in Bioscience **10**: 189-191.

Lammer, E. J., Chen, D.T., Hoar, R.M., Agnish, N.D., Benke, P.J., Braun, J.T., Curry, C.J., Fernhoff, P.M., Grix, A.W., Lott, I.T., Richard, J.M., & Sun, S.C. (1985). "Retinoic acid embryopathy." The New England Journal of Medicine **313**: 837-841.

Laudy, J. A., M & Wladimiroff, J.W. (2000). "The fetal lung 2: pulmonary hypolplasia." Ultrasound in Obstetrics and Gynecology **16**: 482-494.

Lee, C. M., Boileau, A.C., Boileau, T.W.M., Williams, A.X., Swanson, K.S., Heintz, K.A., & Erdman, J.W., (1999). "Review of animal models in carotenoid research." Journal of Nutrition **129**: 2271-2277.

Li, L., & Wei, J. (2006). "A Newborn with anophthalmia and pulmonary hypoplasia (The Matthew-Wood syndrome)." American Journal of Medical Genetics Part A **140A**: 1564-1566.

Lietz, G., Lange, J., & Rimbach, G. (2010). "Molecular and dietary regulation of B,B-carotene15,15'-monoxygenase 1 (BCMO1)." Archives of Biochemistry and Biophysics **502**(1): 8-16.

Link, B. A., Fadool, J.M., Malicki, J., & Dowling, J.E. (2000). "The zebrafish young mutation acts non-cell-autonomously to uncouple differentiation from specification for all retinal cells." Development **127**: 2177-2188.

Liu, L., & Gudas, L.J. (2005). "Disruption of the lecithin:retinol acyltransferase gene makes mice more susceptible to vitamin A deficiency." The Journal of Biological Chemistry **280**(48): 40226-40234.

Lohnes, D., Kastner, P., Dierich, A., Mark, M., LeMeur, M., & Chambon, P. (1993). "Function of retinoic acid receptor y in the mouse." Cell **73**: 643-658.

Lohnes, D., Mark, M., Mendelsohn, C., Dolle, P., Dierich, A., Gorry, P., Gansmuller, A., & Chambon, P. (1994). "Function of the retinoic acid receptors (RARs) during development. (I) Craniofacial and skeletal abnormalities in RAR double mutants. ." Development **120**: 2723-2748.

Lufkin, T., Lohnes, D., Mark, M., Dierich, A., Gorry, P., Gaub, M-.P., LeMeur, M., & Chambon, P. (1993). "High postnatal lethality and testis degeneration in retinoic acid receptor a mutant mice." Proceedings of National Academy of Sciences **90**: 7225-7229.

Maeda, A., Maeda, T., Imanishi, Y., Kuska, V., Alekseev, A., Bronson, J.D., Zhang, H., Zhu, L., Sun, W., Saperstein, D.A., Rieke, F., Baehr, W., & palczewski, K. (2005). "Role of photoreceptor-specific retinol dehydrogenase in the retinoid cycle in vivo." The Journal of Biological Chemistry **280**: 18822-18832.

Maeda, A., Maeda, T., Sun, W., Zhang, H., Baehr, W., & Palczewski, K. (2007). "Redundant and unique roles of retinol dehydrogenase in the mouse retina." Proceedings of National Academy of Sciences **104**(49): 19565-19570.

Mangelsdorf, D. J., Borgmeyer, U., Heyman, R.A., Zhou, J.Y., Ong, E.S., Oro, A.E., Kakizuka, A., & Evans, R.M. (1992). "Characterization of three RXR genes that mediate the action of 9-cis retinoic acid." Genes & Development **6**: 329-344.

Marletaz, F., Holland, L.Z., Laudet, V., & Schubert, M. (2006). "Retinoic acid signalling and the evolution of chordates." International Journal of Biological Science **2**: 38-47.

Marmorstein, A. D. (2001). "The polarity of the retinal pigmented epithelium." Traffic **2**(12): 867-872.

Marshall, H., Morrison, A., Studer, M., Popperl, H., & Krumlauf, R. (1996). "Retinoids and Hox genes." The FASEB Journal **10**(9): 969-978.

Martinovic-Bourial, J., Bernabe-Dupont, C., Golzio, C., Grattagliano-Bessieres, B., Malan, V., Bonniere, M., Esculpavit, C., Fallet-Bianco, C., Mirlesse, V., Lebidois, J., Aubry, M-.C., Vekemans, M., Morichon, N., Etchevers, H., Attie-Biatch, T., Encha-Razavi, F., & Benachi, A. (2007). "Matthew-Wood syndrome: report of two new cases supporting autosomal inheritance and exclusion of FGF10 and FGFR2." American Journal of Medical Genetics Part A **143**(3): 219-228.

Matt, N., Dupe, V., Garnier, J-.M., Dennefeld, C., Chambon, P., Mark, M., & Ghyselinck, N.B. (2005). "Retinoic acid-dependent eye morphogenesis is orchesrated by neural crest cells." Development **132**: 4789-4800.

Matt, N., Ghyselinck, N.B., Pellerin, I., & Dupe, V. (2008). "Impairing retinoic acid signalling in the neural crest cells is sufficient to alter entire eye morphogenesis." Developmental Biology **320**(1): 140-148.

Matt, N., Schidt, C.K., Dupe, V., Dennefeld, C., Nau, H., Chambon, P., Mark, M., & Ghyselinck, N.B. (2005). "Contribution of cellular retinol-binding protein type 1 to retinol metabolism during mouse development." Developmental Dynamics **233**(167-176).

McCollum, E. V., & Davis, M. (1913). "The necessity of certain lipins in the diet during growth." The Journal of Biological Chemistry **15**: 167-175.

McKeller, R. N., Fowler, J.L., Cunningham, J.J., Warner, N., Smeyne, R.J., Zindy, F., & Skapek, S.X. (2002). "The Arf tumor suppressor gene promotes hyaloid vascular regression during mouse eye development." PNAS **99**(6): 3848-3853.

Mendelsohn, C., Lohnes, D., Decimo, D., Lufkin, T., LeMeur, M., Chambon, P., & Mark, M. (1994). "Function of the retinoic acid receptors (RARs) during development. (II) Multiple abnormalities at various stages of organogenesis in RAR double mutants." Development **120**: 2749-2771.

Mic, F. A., Haselbeck, R.J., Cuenca, A.E., & Duester, G. (2002). "Novel retinoic acid generating activities in the neural tube and heart identified by conditional rescue of *Raldh2* null mutant mice." Development **129**: 2271-2282.

Mic, F. A., Molotkov, A., Fan, X., Cuenca, A.E., & Duester, G. (2000). "RALDH3, a retinaldehyde dehydrogenase that generates retinoic acid, is expressed in the ventral retina, otic vesicle and olfactory pit during mouse development." Mechanisms of Development **97**(1-2): 227-230.

Moore, T. (1930). "Vitamin A and carotene. The absence of liver oil vitamin A from carotene. VI The conversion of carotene to vitamin A in vivo." Biochemical Journal **24**(3): 692-702.

Nair, A. K., Sugunan, D., Kumar, H., & Anilkumar, G. (2010). "Case-control analysis of SNPs in GLUT4, RBP4 and STRA6: Association of SNPs in STRA6 with type 2 diabetes in a South Indian population." PLoS One **5**(7): e11444.

Nicholas, K. B., Nicholas, H.B., & Deerfield, D.W. (1997). "GeneDoc: analysis and visualization of genetic variation." EMBNEW NEWS **4**: 14.

Niederreither, K., Subbarayan, V., Dolle, P., & Chambon, P. (1999). "Embryonic retinoic acid synthesis is essential for early mouse post-implantation development." Nature Genetics **21**: 444-448.

Niederreither, K., Vermot, J., Messaddeq, N., Schuhbaur, B., Chambon, P., & Dolle, P. (2001). "Embryonic retinoic acid synthesis is essential for heart morphogenesis in the mouse." Development **128**: 1019-1031.

Noy, N. (1999). Physical-chemical properties and action of retinoids. Retinoids: the biochemical and molecular basis of vitamin A and retinoid action. H. Nau, & Blaner, W.S. Berlin-Heidelberg, Springer-Verlag**:** 3-30.

Ostor, A. G., Stillwell, R., & Fortune, D.W. (1978). "Bilateral pulmonary agenesis." Pathology **10**(3): 243-248.

Ozeki, H., Shirai, S., & Ogura, Y. (1999). "Critical period for retinoic acid-induced developmental abnormalities of the vitreous in mouse fetuses." Experimental Eye Research **68**(2): 223-228.

Parker, R. O., & Crouch, R.K. (2010). "Retinol dehydrogenase(RDHs) in the visual cycle." Experimental Eye Research **91**(6): 788-792.

Pasutto, F., Sticht, H., Hammersen, G., Gillessen-Kaesbach, G., FitzPatrick, D.R., Nurnberg, G., Brasch, F., Schirmer-Zimmermann, H., Tolmie, J.L., Chitayat, D., Houge, G., Fernandez-Martinez, L., Keating, S., Mortier, G., Hennekam, R.C.M., von der Wense, A., Slovotinek, A., Meinecke, P., & Bitoun, P. (2007). "Mutations in STRA6 cause a broad spectrum of malformations including anophthalmia, congenital heart defects, diaphragmatic hernia, alveolar capillary dysplasia, lung hypoplasia, and mental retardation." The American Journal of Human Genetics **80**(3): 550-560.

Pei, Y. F., & Rhodin, J.A.G. (1970). "The prenatal development of the mouse eye." The Anatomical Record **168**(1): 105-126.

Petkovich, M., Brand, N.J., Krust, A., & Chambon, P. (1987). "A human retinoic acid receptor which belongs to the family of nuclear receptors." Nature **330**: 444-450.

Piantedosi, R., Ghyselinck, N.B., Blaner, W.S., & Vogel, S. (2005). "Cellular retinol-binding protein type III is needed for retinol incorporation into milk." The Journal of Biological Chemistry **280**: 24286-24292.

Quandro, L., Blaner, W.S., Salchow, D.J., Vogel, S., Piantedosi, R., Gouras, P., Freeman, S., Cosma, M.P., Colantuoni, V., & Gottesman, M.E. (1999). "Impaired

retinal function and vitamin A availability in mice lacking retinol-binding protein. ." The EMBO Journal **18**(17): 4633-4644.

Quandro, L., Hamberger, L., Gottesman, M.E., Wang, F., Colantuoni, V., Blaner, W.S., & Mendelsohn, C.L. (2005). "Pathways of vitmain A delivery to the embryo: insights from a new tunable model of vitamin A deficiency." Endocrinology **146**(10): 4479-4490.

Ray, W. J., Bain, G., Yao, M., & Gottlieb, D.I. (1997). "CYP26, a novel mammalian cytochrome P450, is induced by retinoic acid and defines a new family." The Journal of Biological Chemistry **272**: 18702-18708.

Reichel, M. M., Ali, R.R., D'Esposito, F., Clarke, A.R., Luthert, P.J., Bhattacharya, S.S., & Hunt, D.M. (1998). "High frequency of persistent hyperplastic primary vitreous and cataracts in p53-deficient mice." Cell Death & Differentiation **5**(2): 156-162.

Reijinjes, S., Zile, M.H., & Maden, M. (2010). "The expression of Stra6 and Rdh10 in the avian embryo and their contribution to the generation of retinoid signatures." International Journal of Developmental Biology **54**: 1267-1275.

Rice, P., Longden, I., & Bleasby, A. (2000). "EMBOSS: the European Molecular Biology Open Software Suite." Trends in Genetics **16**: 276-277.

Robu, M. E., Larson, J.D., Nasevicius, A., Beiraghi, S., Brenner, C., Farber, S.A., & Ekker, S.C. (2007). "p53 activation by knockdown technologies." PLoS Genetics **3**(5): e78.

Rossant, J., & Cross, J.C. (2001). "Placental development: Lessons from mouse mutants." Nature Reviews Genetics **2**: 538-548.

Rossant, J., Zirngibi, R., Cado, D., Shago, M., & Giguere, V. (1991). "Expression of a retinoic acid response element-hsplacZ transgene defines specific domains of transcriptional activity during mouse embryogenesis." Genes & Development **5**: 1333-1344.

Russell, R. B., Breed, J., & Barton, G.J. (1992). "Conservation analysis and structure prediction of the SH2 family of phosphotyrosine binding domains." Federation of European Biochemical Societies **304**(1): 15-20.

Ryckebusch, L., Wang, Z., Bertrand, N., Lin, S-.C., Chi, X., Schwartz, R., Zaffran, S., & Niederreither, K. (2008). "Retinoic acid deficiency alters second heart field formation." Proceedings of National Academy of Sciences **105**(8): 2913-2918.

Saari, J. C., Nawrot, M., Garwin, G.G., Kennedy, M.J., Hurley, J.B., Ghyselinck, N.B., & Chambon, P. (2002). "Analysis of the visual cycle in the cellular retinol-binding protein type I (CRBPI) knockout mice." Investigative Opthalmology & Visual Sciences **43**(6): 1730-1735.

Saitou, N., & Nei, M. (1987). "The neighbour-joining method: a new method for reconstructing phylogenetic trees." Molecular Biology and Evolution **4**: 406-425.

Sakai, Y., Meno, C., Fujii, H., Nishino, J., Shiratori, H., Saijoh, Y., Rossant, J., & Hamada, H. (2001). "The retinoic acid-inactivating enzyme CYP26 is essential for estabilishing an uneven distribution of retinoic acid along the antero-posterior axis within the mouse embryo." Genes & Development **21**: 213-225.

Sandell, L. L., Sanderson, B.W., Moiseyev, G., Johnson, T., Mushegian, A., Young, K., Rey, J-.P., Ma, J-.X., Straehling-Hampton, K., & Trainor, P.A. (2007). "Rdh10 is essential for synthesis of embryonic retinoic acid and is required for limb, craniofacial, and organ development." Genes & Development **21**: 1113-1124.

Seller, M. J., Davis, T.B., Fear, C.N., Flinter, F.A., Ellis, I., & Gibson, A.G. (1996). "Two sibs with anophthalmia and pulmonary hypoplasia (the Matthew-Wood syndrome)." American Journal of Medical Genetics **62**: 227-229.

Semba, R. D., Chiphangwi, J.D., Miotti, P.G., Dallabetta, G.A., Hoover, D.R., Canner, J.K., & Saah, A.J. (1994). "Maternal vitamin A deficiency and mother-to-child transmission of HIV-1." The Lancet **343**(8913): 1593-1597.

Senechal, A., Humbert, G., Surget, M-.O., Bazalgette, C., Arnaud, B., Arndt, C., Laurent, E., Brabet, P., & Hamel, C.P. (2006). "Screening genes of the gene of the retinoid metabolism: novel LRAT mutation in Leber cogenital amaurosis." American Journal of Ophthalmology **142**: 702-704.

Shiotsuga, J., Katsuyama, Y., Arima, K., Baxter, A., Koide, T., Song, J., Chandraratna, R.A.S., & Blumberg, B. (2004). "Multiple points of interaction between retinoic acid and FGF signalling during embryonic axis formation." Development **131**: 2653-2667.

Silbert, M., & Gurwood, A.S. (2000). "Persistent hyperplastic primary vitreous." Clinical Eye and Vision Care **12**(3-4): 131-137.

Silverman, A. K., Ellis, C.N., & Voorhees, J.J. (1987). "Hypervitaminosis A syndrome: A paradigm of retinoid side effects." Journal of the American Academy of Dermatology **16**: 1027-1039.

Smets, K. J., Barlow, T., & vanhaesebrouck, P. (2006). "Maternal vitamin A deficiency and neonatal microphthalmia: complications of biliopancreatic diversion? ." European Journal of Pediatrics **165**(7): 502-504.

Stafford, D., & Prince, V.E. (2002). "Retinoic acid signalling is required for a critical early step in zebrafish pancreatic development." Current Biology **12**(14): 1215-1220.

Sucov, H. M., Dyson, E., Gumeringer, C.L., Price, J., Chein, K.R., & Evans, R.M. (1994). "RXRa mutant mice estabilish a genetic basis for vitamin A signalling in heart morphogenesis." Genes & Development **8**: 1007-1018.

Sumanas, S., Kim, H.J., Hermanson, S., & Ekker, S.C. (2001). "Zebrafish frizzled-2 morphant displays defects in body axis elongation." Genesis **30**: 114-118.

Sumanas, S., Kim, H.J., Hermanson, S., & Ekker, S.C., (2001). "Zebrafish frizzled-2 morphants displays defects in body axis elongation." genesis **30**: 114-118.

Summerton, J. (1999). "Morpholino antisense oligomers: The case for an RNase-H independent structural type.
." Biochimica et Biophysica Acta **1489**(1): 141-158.

Sundaram, M., Sivaprasadarao, Z., DeSousa, M.M., & Findlay, J.B.C. (1998). "The transfer of retinol from serum retinol-binding protein to cellular retinol-binding protein is mediated by a membrane receptor." The Journal of Biological Chemistry **273**(6): 3336-3342.

Suzuki, R., Shintani, T., Sakuta, H., Kato, A., Ohkawara, T., Osumi, N., & noda, M. (2000). "Identification of RALDH-3, a novel retinaldehyde dehydrogenase, expressed in the ventral region of the retina." Mechanisms of Development **98**(1-2): 37-50.

Tanaka, M., Chen, Z., Bartunkova, S., Yamasaki, N., & Izumo, S. (1999). "The cardiac homeobox gene Csx/Nkx2.5 lies genetically upstream of multiple genes essential for heart development." Development **126**: 1269-1280.

Tatusova, T. A., & Madden, T.L. (1999). "Blast 2 sequences - a new tool for comparing protein and nucleotide sequences." FEMS Microbiology Letters **174**: 247-250.

Thaung, C., Arnold, K., Jackson, I.J., & Coffey, P.J. (2002). "Presence of visual head tracking differentiates normal sighted from retinal degenerate mice." Neurosciences Letters **325**(1): 21-24.

Thisse, B., & Thisse, T. (2005). "ZFIN." Retrieved 21/09, 2011, from http://zfin.org/action/marker/view/ZDB-GENE-980526-112.

Thompson, D. A., Janecke, A.R., Lange, J., Feathers, K.L., Hubner, C.A., McHenry, C.L., Stockton, D.W., Rammesmayer, G., Lupski, J.R., Antinolo, G., Avuso, C., Baiget, M., Gouras, P., Heckenlively, J.R., den Hollander, A., Jacobson, S.G., Lewis, R.A., Sieving, P.A., Wissinger, B., Yzer, S., Zrenner, E., Utermann, G., & Gal, A. (2005). "Retinal degeneration associated with RDH12 mutations results from decreased 11-cis-retinal synthesis due to disruption of the visual cycle." Human Molecular Genetics **14**(24): 3865-3875.

Thompson, D. A., Li, Y., McHenry, C.L., Carlson, T.J., Ding, X., Sieving, P.A., Apfelstedt-Sylla, E., & Gal, A. (2001). "Mutations in the gene encoding lecithin retinol acyltransferase are associated with early-onset severe retinal dystrophy." Nature Genetics **28**: 123-124.

Uehara, M., Yashiro, K., Takaoka, K., Yamamoto, M., & Hamada, H. (2009). "Removal of maternal retinoic acid by embryonic CYP26 is required for correct Nodal expression during early embryonic patterning." Genes & Development **23**: 1689-1698.

Underhill, C., Qutob, M.S., Yee, S-.P., & Torchia, J. (2000). "A novel nuclear receptor corepressor complex, N-CoR, contains components of the mammalian SWI/SNF complex and the corepressor KAP-1." The Journal of Biological Chemistry **275**: 40463-40470.

Verma, A. S., & FitzPatrick, D.R. (2007). "Anophthalmia and microphthalmia." Orphanet Journal of Rare Diseases **2**: 47.

Vogel, S., Mendelsohn, C.L., Mertz, J.R., Piantedosi, R., Waldburger, C., Gottesman, M.E., & Blaner, W.S. (2000). "Characterization of a new member of the fatty acid-binding protein family that binds all-trans-retinol." The Journal of Biological Chemistry **276**: 1353-1360.

Vogel, S., Piantedosi, R., O-Bryne, S.M., Kako, Y., Quandro, L., Gottesman, M.E., Goldberg, I.J., & Blaner, W.E. (2002). "Retinol-binding protein-deficient mice: Biochemical basis for impaired vision." Biochemistry **41**(51): 15360-15368.

Wang, X., Penzes, P., & Napoli, J.L. (1996). "Cloning of a cDNA encoding an aldehyde dehydrogenase and its expression Escherichia coli. Recognition of retinal as a substrate." The Journal of Biological Chemistry **271**: 16288-16293.

Wason, I. M. (1921). "Ophthalmis, associated with a dietary deficiency in fat soluble A." Journal of the American Medical Association **76**(14): 908-912.

Wentworth, J. M., Schoenfeld, V., Meek, S., Elgar, G., Brenner, S., & Chatterjee, V.K.K. (1999). "Isolation and characterisation of the retinoic acid receptor-a gene in the pufferfish, F.rubripes." Gene **236**(2): 315-323.

West, K. P., Katz, J., Khatry, S.K., LeClerq, S.C., Pradhan, E.K., Shrestha, S.R., Connor, P.B., Dali, S.M., Christian, P., Pokhrel, R.P., & Sommer, A. (1999). "Double blind, cluster randomised trial of low dose supplementation with vitamin A or beta carotene on mortality related to pregnancy in Nepal." BMJ **318**: 570-575.

White, J. A., Guo, Y-.D., Baetz, K., Beckett-Jones, B., Bonasoro, J., Hsu, K.E., Dilworth, F.J., Jones, G., & Petkovich, M. (1996). "Identification of the retinoic acid-inducible all-trans-retinoic acid 4-hydrolase." The Journal of Biological Chemistry **271**: 29922-29927.

Wietyrch, M., Meziane, H., Sutter, A., Ghyselinck, N.B., Chapman, P.F., Chambon, P., & Krezel, W. (2005). "Working memory deficits in retinoid X receptory-deficient mice." Learning & Memory **12**: 318-326.

Wikipedia. (2011). "Morpholino." Retrieved 26/09, 2011, from http://en.wikipedia.org/wiki/Morpholino.

Wilson, J. G., Roth, C.B., & Warkany, J. (1953). "An analysis of the syndrome of malformations induced by maternal vitamin A at various times during gestation." The American Journal of Anatomy **92**(2): 189-217.

Wingert, R. A., Selleck, R., Yu, J., Song, H-.D., Zhou, Y., Thisse, C., McMahon, A.P., & Davidson, A.J. (2007). "The cdx genes and retinoic acid control the positioning and segmantation of the zebrafish pronephros." PLoS Genetics **3**(10): 1922-1938.

Wolf, G. (2001). Discovery of vitamin A., eLS.

Wolf, G. (2006). "Is 9-cis-retinoic acid the endogenous ligand for the retinoic-acid-X receptor?" Nutrition Reviews **64**(12): 532-538.

Wu, K. H. C., Madigan, M.C., Billson, F.A., & Penfold, P.L. (2003). "Diffential expression of GFAP in early v late AMD: a quantitative analysis." British Journal of Opthalmology **87**: 1159-1166.

Xueping, E., Zhang, L., Lu, J., Tso, P., Blaner, W.S., Levin, M.S., & Li, E. (2002). "Increased neonatal mortality in mice lacking cellular retinol-binding protein II." The Journal of Biological Chemistry **277**: 36617-36623.

Yamagishi, H., Yamagishi, C., Nakagawa, O., Harvey, R.P., Olson, E.N., & Srivastava, D. (2001). "The combinatorial activities of Nkx2.5 and dHAND are essential for cardiac ventricle formation." Developmental Biology **239**(2): 190-203.

Yamamoto, H., Simon, A., Eriksson, U., Harris, E., Berson, E.L., & Dryja, T.P. (1999). "Mutations in the gene encoding 11-cis-retinol dehydrogenase cause delayed dark adaptation and fundus albipunctatus." Nature Genetics **22**: 188-191.

Yan, J., Tanaka, S., Oda, M., Makino, T., Ohgane, J., & Shiota, K. (2001). "Retinoic acid promotes differentiation of trophoblast stem cells to a giant cell fate." Developmental Biology **23**(2): 422-432.

Yang, Q., Graham, T.E., Mody, N., Preitner, F., Peroni, O.D., Zabolotny, J.M., Kotani, K., Quandro, L., & kahn, B.B. (2005). "Serum retinol binding protein 4 contributes to insulin resistance in obesity and type 2 diabetes." Nature **436**: 356-362.

Yu, V. C., Delsert, C., Andersen, B., Holloway. J.M., Devary, O.V., Naar, A.M., Kim, S.Y., Boutin, J-.M., Glass, C.K., & Rosenfeld, M.G. (1991). "RXRb: A

coregulator that enhances binding of retinoic acid, thyroid hormone, and vitmain D receptors to their cognate response elements." Cell **67**(6): 1251-1266.

Zhang, M., Hu, P., Krois, C.R., Kane, M.A., & Napoli, J.A. (2007). "Altered vitamin A homeostasis and increased size and adiposity in the rdh1-null mouse." The FASEB Journal **21**: 2886-2896.

Zhao, D., McCaffery, P., Ivins, K.J., Neve, R.L., Hogan, P., Chin, W.W., & Drager, U.C. (1996). "Molecular identification of a major retinoic-acid-synthesizing enzyme, a retinaldehyde-specific dehydrogenase." European Journal of Biochemistry **240**: 15-22.

Zile, M. H. (2001). "Function of vitamin A in vertebrate embryonic development." The Journal of Nutrition **131**(3): 705-708.

Zolfaghari, R., & Ross, A.C. (2000). "Lecithin:retinol acyltransferase from mouse and rat liver: cDNA cloning and liver-specific regulation by dietary vitamin A and retinoic acid." Journal of Lipid Research **41**: 2024-2034.